The petrology and chemistry of the Setberg volcanic region and of the intermediate and acid rocks of Iceland

Haraldur Sigurdsson

THE PETROLOGY AND CHEMISTRY OF THE SETBERG VOLCANIC REGION AND OF THE INTERMEDIATE AND ACID ROCKS OF ICELAND

by

Haraldur Sigurdsson, B.Sc. (Belfast),
Graduate Society, Durham.

A THESIS SUBMITTED FOR THE DEGREE OF DOCTOR OF PHILOSOPHY, UNIVERSITY OF DURHAM.

JANUARY, 1970.

The petrology and chemistry of the Setberg volcanic region and of the intermediate and acid rocks of Iceland

by

Haraldur Sigurdsson

Abstract

The Tertiary to Mid-Quaternary Setberg volcano in western Iceland consists of two centres. The northern, Centre 1 is tholeiitic and defined by cone sheets, a caldera and a gabbro intrusion. The southern, Centre 2 is chemically transitional between a tholeiitic and an alkalic basalt series, and contains a cone sheet swarm, gabbroic ring features and a major granophyric cone sheet. Each centre can be related to a minor magma chamber at a depth of 2-3 km. General hydrothermal alteration around both centres has resulted in aureoles of epidotization and the development of greenstones, containing garnet in the central areas.

Late-Quaternary volcanism in the Setberg area has produced an alkalic basalt succession, ranging from alkalic olivine basalts to benmoreites. This activity is related to the E-W Snaefellsnes volcanic zone and its causes are explained in terms of Icelandic plate tectonics.

The tholeiitic series of Centre 1 form a differentiated sequence from olivine tholeiites to rhyolites, containing a Ca-poor pyroxene and augite in the basic and intermediate rocks, and a large compositional interval devoid of olivine. Plagioclase is the sole feldspar phase. The transitional series of Centre 2 is olivine-bearing throughout, with augite and rare phenocrysts of orthopyroxene in the basalts. Two lineages of differentiated rocks of this series are typified either by iron-enrichment (to icelandites) or by alkali-enrichment (to rhyodacites and alkalic-rhyolites). The latter contains anorthoclase and potassic oligoclase or sanidine, as well as sodic pyroxene. Rocks of the alkalic series are olivine and pyroxene-bearing, with anorthoclase appearing in the benmoreites, while phlogopite and hornblende have been found in some of the lavas. Apatite occurs as a phenocryst in members of both the transitional and alkalic series.

The origin of the transitional basalt magma is discussed according to two hypotheses. Its formation is accounted for by solidification from above in a magma reservoir of great vertical dimensions, leading to confinement of the magma to depths where orthopyroxene replaces olivine on the liquidus, resulting in a trend towards undersaturation. The chemistry of the Late-Quaternary alkalic basalts of Setberg and Snaefellsnes is related to magma generation at greater depths than in the case of the tholeiitic basalts of the Icelandic central volcanic zone.

The volume, bimodal distribution and diversity of acid and intermediate magmas in Iceland are discussed. The high proportion of acid to basic volcanic rocks in eastern Iceland is contrasted with 3-4% in the rest of the country. Two types of acid centres are identified: centres of Thingmuli type, where tholeiitic basalts are associated with low-alkalic rhyolites; and alkalic centres, containing comendites, quartz-trachytes, alkalic-rhyolites and associated alkalic basalts or transitional basalts. Peralkaline acid rocks are identified and described from Iceland for the first time. Their genesis is discussed and related to fractionation from alkalic-rhyolites and trachytes by the "plagioclase effect". No evidence has been unearthed in this study which contravenes the hypothesis that the Icelandic acid rocks are a product of fractionation from basic magma.

Til

Áshildar og Bergljótar

Table of Contents

List of Figures

List of Tables

CHAPTER I: INTRODUCTION

A. Scope of Research.

This research is essentially two-fold as implied by the title, although the two themes are closely inter-related. The investigation has involved a detailed field study of an area covering 300 km^2, enclosing the Setberg volcanic centre, some description of which has already been published (Sigurdsson, 1966). To aid understanding of the petrology of the Setberg volcano, particularly when dealing with the younger basaltic lavas, a study of the volcano-tectonics of western Iceland or, more precisely, the Snaefellsnes Quaternary to Recent volcanic zone, proved necessary. Hence an area adjacent to and east of Setberg, covering 600 km^2, was mapped in reconnaissance style. Sampling and general studies of several other acid volcanic centres in Iceland were also carried out.

Each summer, from 1963 to 1968, fieldwork has been carried out in Snaefellsnes, varying from a few weeks to several months, and totalling 9 months. Very detailed stratigraphic mapping is difficult if not impossible to achieve in this entirely volcanic succession, and of doubtful value when secondary alteration and a large number of minor intrusions are present. Instead, a fairly large area was

covered and sampled thoroughly, but mapping was carried out with the aid of aerial photographs on the scale 1:35000.

As fieldwork progressed and radiated outwards from the Setberg centre, so the geological interest was channelled into the pursuit of a more defined line of research, and during the summers of 1967 and 1968 the overriding interest in the nature of acid and intermediate rocks of Iceland led the writer further afield and outside Snaefellsnes. It is to this aspect that the latter part of the thesis is devoted, making use of samples and field evidence from seven volcanic centres.

B. Acknowledgements:

The writer is indebted to many persons and institutions for help during the six years since work on the geology of western Iceland was first started, and only a few can be mentioned here. In Iceland the guidance and encouragement in the early stages of this work by Dr. Thorleifur Einarsson and Dr. Gudmundur E. Sigvaldason at the University Research Institute in Reykjavik is gratefully acknowledged. Dr. John Preston in Belfast also had great influence on my early work in geology.

Professor G. M. Brown in Durham has shown a welcome enthusiasm and given constructive supervision throughout the

two years in Durham. The author is greatly indebted to him and his staff in the Department of Geology at the University of Durham. Dr. C. H. Emeleus and Dr. J. W. Aucott gave invaluable help in the early stages of my work on the Geoscan electron probe. I am equally grateful to Dr. J. G. Holland for his efficient supervision of the use of the X-ray fluorescent spectrometer. The author wishes to thank Mr. Gunnbjörn Egilsson in Iceland and Mr. L. MacGregor and Mr. G. Randall in Durham, who cut and polished the thin sections with great skill. I am also grateful to Mr. G. Dresser for photographic work executed with great patience.

The award of a grant from the Icelandic Science Fund (Visindasjodur) made this research possible, and additional financial support, received in the form of a Foundation Studentship from the Academic Council of the Queen's University of Belfast, is also gratefully acknowledged.

C. Methods of Study

The analytical work, which forms the bulk of this research, was started in the laboratories of the University Research Institute in Reykjavik, Iceland (1965-67), but the majority of analyses were performed in the Geology Department at Durham, where all previous analyses were repeated to ensure conformity and standardisation of results. Much of

the routine thin section studies were completed in Iceland.

The access to automatic X-ray fluorescence equipment (Philips PW 1212) and methods at Durham made it possible to analyse 281 whole-rock samples for major and trace element constituents, while access to an electron microprobe (Geoscan Mk. 2) permitted analysis of the major mineral components in a representative, selected suite of rocks. Computing of X-ray output data and its translation into meaningful concentration values was achieved by the use of data-processing facilities at Durham and Newcastle. Without these computing facilities the handling of information for the relatively large number of samples would not have been possible.

In all, 429 rock and mineral samples were collected for this study. These include 246 rock samples from the Setberg region and 95 rock samples from other centres in Iceland. In addition, 88 specimens of minerals, mainly "secondary" minerals from hydrothermal aureoles, were collected. 466 thin sections were cut in connection with this research, 132 in Iceland and 334 in Durham, 112 of which are polished and carbon-coated sections for electron microprobe study.

Electron microprobe analyses were carried out on 547 minerals. The minerals analysed were 248 feldspars, 185

pyroxenes and 114 olivines. The following elements were determined: in feldspars: Si, Fe, Al, Ca, Na, K, in pyroxenes: Si, Fe, Mg, Ca, Ti, Na, Mn, in olivines: Si, Fe, Mg, Mn. The method of probe analysis and subsequent computation is stated in Section 1 of the Appendix.

The geochemistry of 281 whole-rock samples investigated by X-ray fluorescence spectrometry, included 186 samples from the Setberg area and 95 samples from other regions of Iceland. Concentrations of the following 16 elements were determined, where present: Si, Al, Fe, Mg, Ca, Na, K, Ti, Mn (major elements), Sr, Rb, Zr, Zn, Ba, Cu, Ni (trace elements). The operating conditions and computing procedures used in the X-ray fluorescence analyses are described in Section 2 of the Appendix.

Ferrous iron was determined by the metavanadate method (see Section 3 of the Appendix).

Routine petrographic studies were rarely supplemented by optical measurements, in view of the emphasis on probe data. However, detailed optical, X-ray and wet chemical studies were carried out on a restricted sample of minerals in order to compare with the analytical results of the electron probe study.

Examination of iron-titanium oxides and other opaque minerals was only cursory and no quantitative data on these

minerals is presented here, but such a study is the logical continuation of the present research.

D. Petrogenetic significance of Iceland

The great interest among earth scientists in Mid-Ocean Ridges and processes in the Upper Mantle has recently focussed much attention on oceanic islands and the deep ocean floor as sources of new data, most notably in studies of crustal spreading and on the nature and origin of basaltic and other mantle-derived magmas. It is demonstrable, for several reasons, that Iceland is bisected by a basalt-producing Mid-Ocean Ridge; nevertheless, Iceland's role has been small in research on these world-wide features until recently. The emphasis is clearly changing, as marked by the publication of an Icelandic symposium volume devoted entirely to Icelandic geology in the light of the Ocean-Ridge environment (Björnsson, 1967). Hopefully, the present interest in Icelandic geology will be maintained, as the country possesses the unusual distinction not only of containing an extensive exposed segment of a Mid-Ocean Ridge system, but also of offering a more-or-less unbroken stratigraphic succession of volcanic rocks throughout the past 15-20 million years.

In addition to the obvious geological links with the Mid-Atlantic Ridge, Iceland forms part of an older

geological feature: the Wyville-Thompson Ridge, probably representing an expression of Tertiary igneous activity in the Thulean province. Essentially two views have been put forward on the origin of the Wyville-Thompson Ridge. Noe-Nygaard (1966) envisages an early oceanic fissure system running SE-NW from NW Scotland to Greeland, giving rise to the Wyville-Thompson Ridge in early Tertiary times and unrelated to present-day activity in Iceland, which he considers a restricted phenomenon. Another view more in keeping with recent evidence, is that the Wyville-Thompson Ridge is a "branch"-ridge (Wilson 1965, Moorbath, Sigurdsson and Goodwin 1968) created by a process of crustal spreading at a mid-oceanic ridge, such as is actively going on in Iceland today.

In spite of the geological association with the Mid-Atlantic Ridge, Iceland does not show close similarities to the Ridge as a petrographic province, particularly in regard to the Tertiary volcanics. However, Icelandic petrography has distinct affinities with the Tertiary Thulean (Brito-Arctic) petrographic province, as borne out particularly by the iron-rich character of its Tertiary basalts.

Problems of petrogenesis in Iceland are various. The above-mentioned apparent paradox of a close geological

association between Iceland and the Mid-Atlantic Ridge, but lack of a petrographic association may be a function of the relatively thick crust in the Iceland region or in some way it may be connected with the presence of the Wyville-Thompson Ridge. Recently in Iceland, as in many other volcanic regions, the problem of association of alkalic and tholeiitic basalts has arisen. Attempts will be made here to view the petrogenesis of these rock-types in Iceland in the light of their geographical position as well as according to the evidence suggesting variable depth of origin of the two magma types.

The basaltic rocks present a variety of petrological problems, but the very interesting and perhaps most difficult question is the origin of the rather abundant acid rocks and the apparent scarcity of intermediate magmas in Iceland.

E. Previous investigations:

The very early petrographic work in Iceland of W. S. von Waltershausen, R. Bunsen, A. Penck, K. W. Schmith and H. Bäckström is now superseded and is chiefly of historic interest. A new spate of research on Icelandic petrology started with Holmes (1918), but more particularly with an ambitious project begun by M. A. Peacock on the "Petrology

of Iceland", of which only two publications appeared (Peacock, 1925 and 1926). Holmes published the first silica-variation diagram of Icelandic rocks and pointed out that the basalts are neither of an "Atlantic" nor "Pacific" type, i.e. neither alkalic nor calc-alkalic, thus heralding the concept of a third group, the tholeiitic basalts. Holmes also recognised the outstanding feature of the basalts of the Thulean province, i.e. high Fe and Ti content and a saturated character.

Peacock's interest in Icelandic petrology was fired by the collections of Sir George S. Mackenzie, but an expedition with G. W. Tyrrell to Iceland in 1924 was the basis of Peacock's work. He recognised there a great number of rock-types, some of which he analysed and arranged in two principal series, "an earlier calc-alkali series and a later series of mildly alkalic character", and furthermore: "There is no doubt that the Iceland series lie in the transitional zone between alkalic and sub-alkalic" (Peacock, 1931). He describes truly alkalic basalts with trachytic differentiates and a "calc-alkalic" series with rhyolitic differentiates, and makes the very interesting suggestion that "pre-glacial" (Tertiary) rocks are oversaturated but that inter- and post-glacial rocks tend to be just-saturated or even under-saturated. Peacock was possibly on the brink of making a

breakthrough in petrology with his Icelandic material at hand, but due to unknown circumstances his work in Iceland and on his Icelandic collection was abruptly terminated and, regrettably, much data never got published.

Little or no petrological research was carried out for a number of years on Icelandic rocks after Peacock's important contribution and some of his work was apparently ignored or unknown to subsequent workers.

Barth (1962) held the view that, petrographically, Iceland was transitional into a continental province and consisted essentially of a tholeiitic series, perhaps contaminated and not unrelated to supposed "patches of sialic continental crust underneath the Thulean basalt plateaux". Noe-Nygaard (1966) re-emphasises the characteristic features of the Thulean basalts (as first noted by Holmes, 1918), i.e. a high Fe and Ti content, and calls attention to their dissimilarity to oceanic tholeiites. He regards Iceland as made up of two geologically distinct provinces, the Tertiary basalt formation, associated with the Wyville-Thompson Ridge, and the Quaternary formation, associated with the mid-Atlantic Ridge. Recent work, however, suggests that all the Icelandic lava pile has been formed in a more-or-less continuous process of crustal spreading (Böðvarsson and Walker, 1964) and furthermore, that all petrographic types of lavas

found in the Tertiary are also represented in the Quaternary and Recent volcanics, although the latter are much more diverse according to our present state of knowledge.

Alkalic basalts were finally re-discovered in Iceland by Muir and Tilley (1964) who commented on data of Robson and Spector (1962) on the Eldgja-Katla fissure zone, some 40 years after Peacock's initial recognition of alkalic rocks in Iceland.

The Icelandic acid rocks have gained more attention than the basalts, dating back to R. Bunsen's visit to Iceland in 1851 when he became so impressed with the abundance of rhyolites that he proposed the existence of two primary magma types: one basic and one acid. Hawkes and his co-workers (1928) mapped and carried out petrographic descriptions of the major intrusions in south-eastern Iceland, as well as a number of smaller occurrences of acid lavas and minor intrusions elsewhere in eastern Iceland. They were impressed with the subordinate bulk of intermediate rocks and while favouring a "process of differentiation for the formation of the extreme magmas", they suggest rather ambiguously "that the lighter supporting substratum which isostasy demands for Iceland is built up of acid rocks, and the intrusion of acid magma beneath it has saved it from the

general collapse of the North-Atlantic plateaux".

Walker (1963, 1964, 1966) gave the first quantitative data on the abundance and distribution of acid rocks in eastern Iceland, after ten years of detailed field mapping. He concludes that in eastern Iceland alone, acid rocks occupy 9% by volume, that is that some 800 km^3 of acid rocks occur above sea level in an area covering only 8% of Iceland. Walker was so impressed by the truly great volume of acid magma that he considers it "unlikely to have originated by crystal fractionation of basalt magma, and a sialic crust seems a more likely source", and he also observes (1964) "the fact that Iceland stands above the sea, the only landmass astride the Mid-Atlantic Ridge, would seem to be difficult to reconcile with the absence of a sialic layer". Similar views, favouring sial, were expressed by van Bemmelen and Rutten (1955) and Tryggvason (1965). Noe-Nygaard also states (1956): "The most likely explanation (for the formation of Icelandic liparites) is to assume that they are, through transfusion, regenerated sialic material from a sub-basaltic substratum".

The outstanding and by far the largest contribution to Icelandic petrology is the work of I.S.E. Carmichael (1960, 1961, 1962, 1963), particularly on the acid rocks. He

conducted a systematic mineralogical and chemical study of 14 acid glasses, both of residual glass and of separated phenocryst phases. He showed that the eastern Icelandic pitchstones have a relatively simple mineralogy. They are devoid of quartz phenocrysts and the feldspar is either anorthoclase or high-temperature plagioclase, no sanidine being ever recorded. The eastern Icelandic pitchstones were clearly distinguished from the Scottish Tertiary pitchstones through the former being richer in Na relative to K, as well as through significant differences in trace-element geochemistry.

Carmichael (1963) concluded that one-feldspar rhyolites, such as the Icelandic acid rocks, are the product of fractionation of tholeiitic magma, unlike the Scottish Tertiary two-feldspar pitchstones which he considered either the result of sialic fusion or contamination of fractionation products with sial. It must be stressed here, that Carmichael dealt only with 14 samples from a relatively restricted part of the stratigraphic succession in eastern Iceland, spanning a part of the sequence ranging in age from 12 to 8 million years. His results and petrogenetic conclusions are quite valid for this part of the Icelandic stratigraphic column and probably for the eastern Iceland

Tertiary rocks in general. However, they should only be applied with caution to the rest of the Icelandic acid rocks, particularly to the Quaternary and Recent volcanics where quite different petrography has been encountered by the writer in certain areas.

The work by Carmichael (1964) on the now-classic Thingmúli Tertiary central volcano in eastern Iceland demonstrated, perhaps more than does any other line of evidence, that there exists a continuous line of descent of magmas from olivine-tholeiite to rhyolitic compositions, and it strongly indicates that the origin of eastern Iceland's acid magmas lies in the fractionation of tholeiite magmas.

Unfortunately, Carmichael's work on the Thingmúli basalts is the only modern petrological account of Icelandic Tertiary basalts to date, and as his samples were derived from only a single, tholeiite-producing volcano, few generalisations can be made about the petrography of the basalt succession in eastern Iceland from these data.

Walker (1959) proposed a useful field classification of Tertiary basalt lavas, consisting of "tholeiites", "olivine-basalts" and "porphyritic basalts", making up 48%, 23% and 12% of the volcanic pile in eastern Iceland, respectively. This field classification has evidently been

mis-interpreted by Turner and Verhoogen (1960) who state: "Typical of the Brito-Arctic region in general is close association of alkaline olivine basalts and of tholeiite lavas ..... In eastern Iceland both types of basaltic lavas are present." Walker (personal communication, 1969) denies any genetic significance for his term olivine basalt and is of the opinion that none of the "olivine basalts" occurring in eastern Iceland are true alkalic basalts.

Some 28 chemical analyses exist in the previous literature on Icelandic Tertiary basalts and are plotted on an alkalis/silica diagram in Fig. 1. All these analyses fall into the field of tholeiites and we can only conclude, from this scanty evidence and from Walker's opinion, that alkalic basalts are unknown from the Icelandic Tertiary areas. Peacock's claim is therefore amplified, that the Tertiary ("pre-glacial") basalts are tholeiitic ("over-saturated") whereas alkalic basalts, as well as tholeiites, are found in the Quaternary and Recent succession. This

---

Fig. 1: Alkalis/silica diagram of Tertiary basaltic rocks from Iceland, outside the Setberg area, compiled from the following sources: Friedrich (1966), Holmes (1918), Peacock (1925), Tyrrell (1948), Carmichael (1964), Tyrrell (1949), Walker (1963), Rutten (1964). The diagonal line represents the boundary between the alkalic and tholeiitic fields as based on Hawaiian rocks (Macdonald and Katsura, 1964).

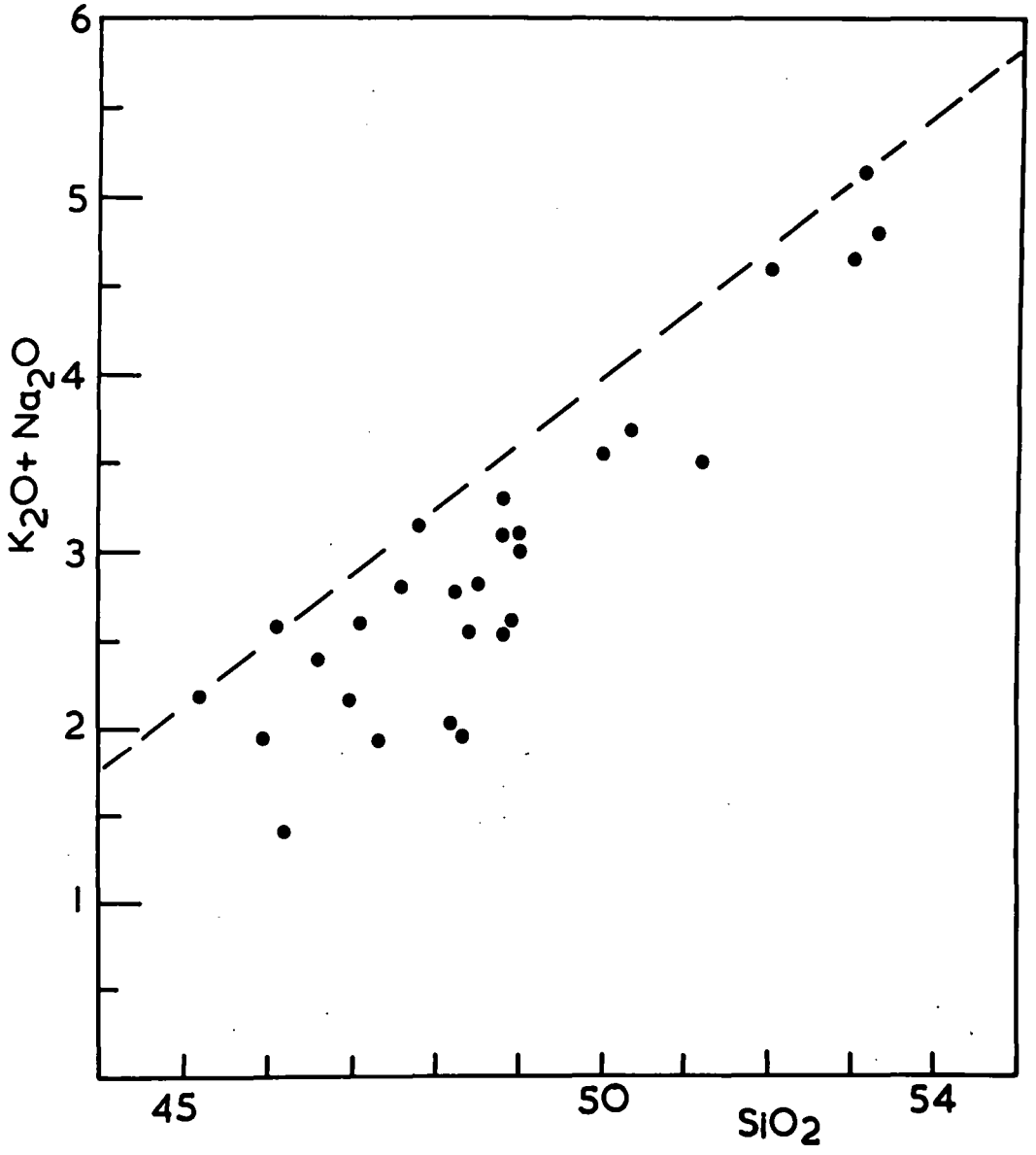
6
5
4
3
2
1
$K_2O + Na_2O$
45
50
54
SiO_2

basic difference in petrology between the Tertiary and post-Tertiary basalts, if valid, must be considered one of the fundamental problems in Icelandic petrogenesis.

Heier et al. (1966) studied the geochemistry of four Icelandic Recent basalts. They agree with previous workers that the Icelandic basalts resemble most the Hebridean basalts in major element chemistry and conclude that no crustal contamination has affected their geochemistry. Sigvaldason (1969) compiled analyses of basalts from the central rift zone and points out that in addition to alkalic and tholeiitic series, there exist several sub-groups of basalts, in each of which a group of lavas appear to have fractionated along a similar path. He concludes that each group of lavas is a product of a batch of primary magma and that no unique, primary liquid exists for the Icelandic basalts as a whole.

Strontium and lead isotope investigations on igneous rocks from Iceland by Moorbath and others (1965, 1968) have given the most illuminating evidence so far available on the petrogenesis of the acid rocks. Initial $^{87}Sr/^{86}Sr$ ratios for Icelandic acid and basic rocks are virtually identical and the results clearly indicate that the acid rocks investigated were derived from the same source region as the basic rocks, i.e. the Upper Mantle, either by fractional

crystallization of basic magma or by some process of partial melting of basic rocks. The lead isotope studies (Welke et al. 1968) support these conclusions on the origin of the acid rocks and rule out the possibility of ancient sialic crust beneath Iceland as an important source of the acid rocks investigated so far.

CHAPTER II: GENERAL GEOLOGY OF THE SETBERG AREA AND SNAEFELLSNES

A. Introduction

Snaefellsnes is an 80 km-long peninsula that extends into the North Atlantic from the central western part of Iceland, accentuated at its western tip by the snow-capped Snaefellsjökull central volcano. General aspects of the geology of Snaefellsnes have been dealt with elsewhere (Sigurdsson, 1966, 1967) and only a brief account is presented here. The Snaefellsnes peninsula consists of a wide variety of geological formations, ranging from Tertiary to Recent. The Tertiary plateau basalts are the oldest known formation and of unknown thickness, consisting essentially of olivine basalts and tholeiites (approximately 90%). Broadly speaking, Snaefellsnes is on the northern limb of an anticlinal structure, the axis of which runs NNE-SSW in the Borgarnes region, with dips of 10-15° on either side. A synclinal axis with a NE-SW trend runs through Breidifjördur, immediately north of the Snaefellsnes peninsula, where a gentle 5-10° north-westerly dip is predominant (Figure 2).

Although made up chiefly of basaltic lavas, the Tertiary formation on Snaefellsnes contains at least three

volcanic centres typified by acid and intermediate rocks, minor intrusions, and propylitization products. These centres are, from east to west: Alftafjörður, Setberg and Froda and in addition, a layered anorthosite body associated with minor acid and basic intrusions is exposed in the island of Hrappsey and neighbouring islands, just north of Snaefellsnes.

Two major dyke swarms have been found on the peninsula, one associated with the Setberg centre, another in Aftafjörður, both trending ENE-WSW. Dykes are generally closely associated with volcanic activity in Iceland and dyke swarms are believed to be the hypabyssal manifestation of a volcanic zone. The Tertiary Snaefellsnes volcanic zone, already in Tertiary time, thus had a trend almost at right angles to the northerly trend of the east and north Iceland Tertiary volcanic zones and possibly other Tertiary volcanic zones outside western Iceland.

Throughout the Pleistocene, the Tertiary plateau on Snaefellsnes was planed and cut by glacial erosion, and an irregular surface, dipping gently W or NW, underlies the Pleistocene formations. In eastern Snaefellsnes the Tertiary volcanics out-crop on the mountain tops, but the unconformity drops to the west and at Olafsvik, near the western end of

Snaefellsnes, the Tertiary/Quaternary unconformity is at sea level.

In western Iceland, volcanic activity had ceased everywhere by the end of the Tertiary. In Snaefellsnes, however, eruptions continued within an east-westerly zone, especially in late-Pleistocene to Recent times (Figure 2). The Quaternary rocks represent a very complex picture due to a number of local unconformities, rapid accumulation of subglacial and subaerial volcanics, and a great variety of rock-types including basalt lavas, palagonite tuffs, breccias and pillow lavas.

In early Pleistocene, subsidence took place in western Snaefellsnes and the Tertiary basalts were transgressed by the sea. During the period of submergence, tillites and shallow-water sediments were deposited in the north-western part of the peninsula, containing an Arctic shelly fauna.

Fig. 2: A diagrammatic geological map of the Snaefellsnes region, showing the distribution of mid- to late-Quaternary lavas (cross-hatched), late-Quaternary basic tuffs (stippled) and Recent lavas (horse-shoe pattern). The Tertiary areas are blank, with arrows indicating the amount and direction of dip. Note the Borgarnes anticlinal axis in the south-eastern part. Black dots indicate Recent craters or Quaternary volcanic plugs, defining the WNW-trending volcanic line of Snaefellsnes. Coinciding with this line are three shallow-depth cones in Breidafjördur to the north-west (depth in metres). The areas covered by Figs. 4 and 10 are indicated.

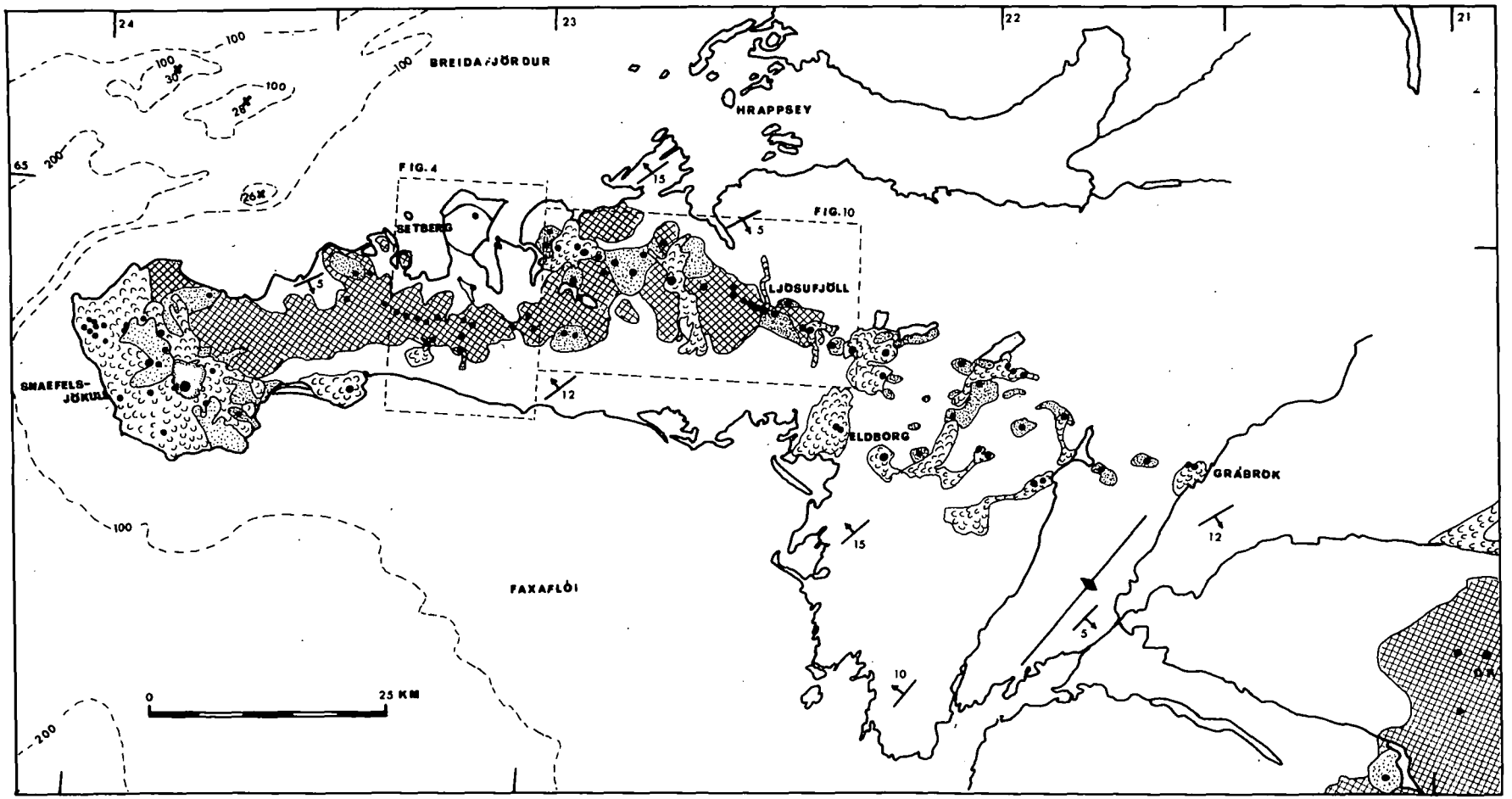
24
23
22
21
BREIDAFJÖRDUR
HRAPPSEY
FIG. 4
FIG. 10
SETBERG
LJÓSUFJÖLL
SNAEFELS-
JÖKULL
ELDBORG
GRÁBROK
FAXAFLÓI
100
200
26M
30M
28M
15
5
12
10
0
25 KM

These are overlain by marine sediments with boreal fauna and deltaic sediments with leaves of Alnus and other plants, indicating a temperate climate (Askelsson, 1938). The sediments and intercalated lava flows indicate that several extreme climatic fluctuations took place during the Pleistocene, resulting in the retreat of glaciers and permitting subaerial lavas to flow, in contrast to the characteristic sub-glacial products. Subsidence only affected the western or perhaps the north-western part of Snaefellsnes and for some time the shoreline was on the western margin of the Setberg area. Uplift took place before the end of the Pleistocene and the sediments are now found up to 150 m above sea level.

Pleistocene volcanicity was largely confined to the E-W trending crestal ridge of Snaefellsnes. Recent volcanicity is also widespread but not voluminous. Snaefellsjökull is the most noteworthy volcano and the only Recent strato- or central volcano on Snaefellsnes. It is a central volcano par excellence with products ranging from basalts and andesites to rhyolitic tuffs. Two rhyolitic explosive eruptions took place in Snaefellsjökull approximately 1800 and 4000 years ago (Steinthorsson, 1967), but younger lava flows of unknown age have been erupted, although none in historic[1)] time. Most of the Recent volcanic activity on

---

[1)] Historic time in Iceland is the last 1100 years.

Snaefellsnes is concentrated in a narrow, WNW-ESE trending fault zone in the north-eastern part of the peninsula. The basaltic eruption of Eldborg is the only historic volcanic activity in Snaefellsnes (Askelsson, 1955).

B. The Tertiary centre of the Setberg area (Centre 1)

The oldest rocks in the Setberg area are Tertiary flood basalts, generally exposed everywhere at sea level. Tholeiites, olivine-tholeiites and porphyritic basalts are all represented. The basalts have been poured over a relatively flat and featureless surface and no stratigraphic breaks have been observed. Regionally, the basalts are flat-lying or dip 3-5° NNW, but higher dips near the volcanic centre must be attributed to downwarping of the base of the volcano.

A Tertiary dyke swarm runs through the Setberg area and dykes are generally abundant in the Tertiary basalts. They are 1-2 m wide on the average, and trend E or ENE. This swarm may be correlated with an easterly trending dyke swarm in Alftafjörður, some 30 km to the east. The Setberg swarm

---

Fig. 3: An outline geological map of Iceland, defining the areas of Recent volcanic activity (within heavy broken lines), distribution of Quaternary lavas (cross-hatching) and silicic centres (stippled patches), many of which represent central volcanoes (Sigurdsson, 1967).

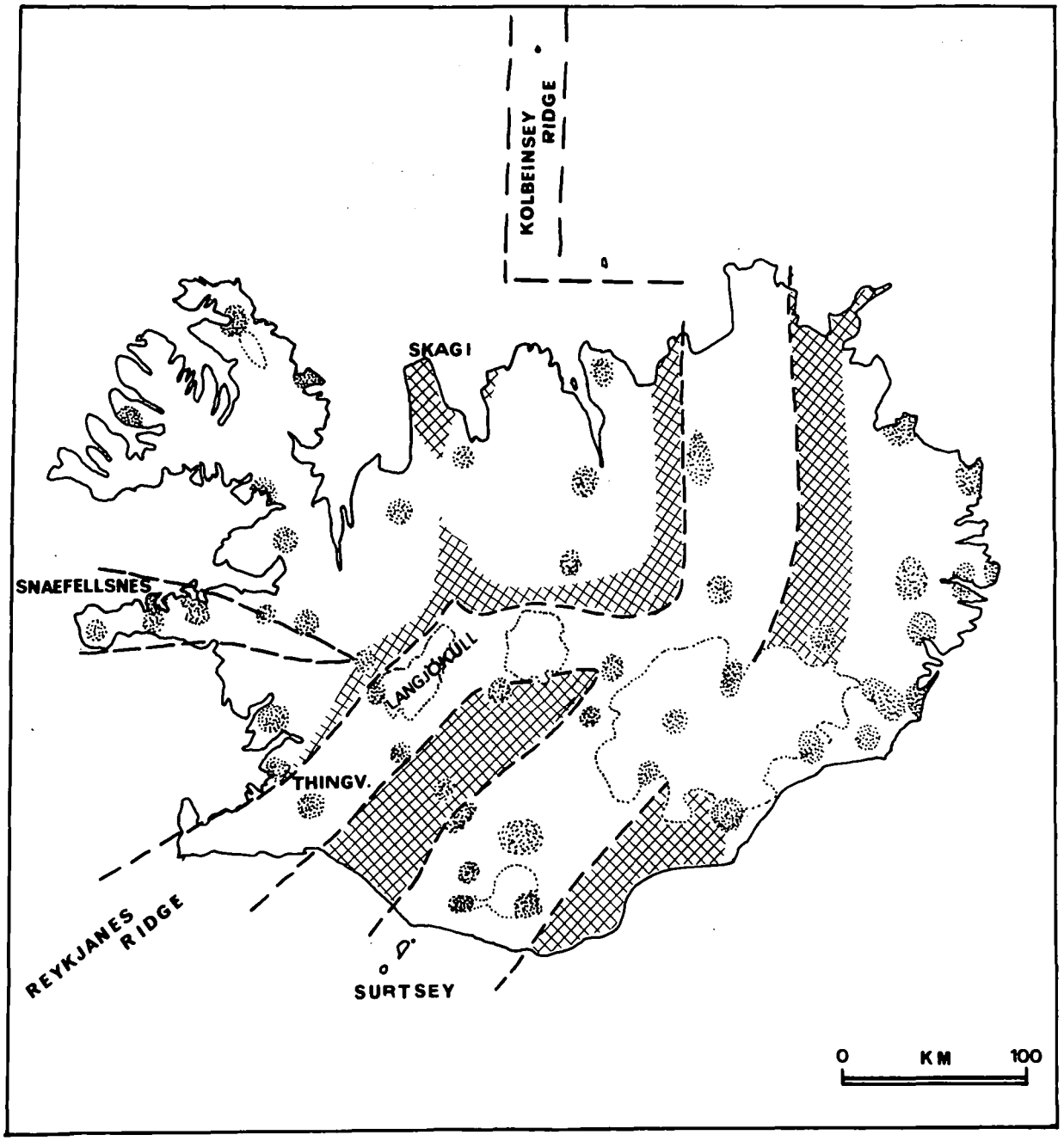
KOLBEINSEY RIDGE
SKAGI
SNAEFELLSNES
LANGJOKULL
THINGV.
REYKJANES RIDGE
SURTSEY
0 KM 100

is well exposed in Hraunsfjördur, where in a 1 km-long cross section the aggregate thickness of dykes is 65 m, i.e. representing 6.5% stretch of the basalt pile in a north-southerly direction. Dyke intrusion has been considered to be a mechanism of crustal drift in Iceland (Böðvarsson and Walker, 1964) and the many northerly trending dyke swarms in eastern Iceland, and indeed in other parts of the country (Sigurdsson, 1967), are supporting evidence for this hypothesis. Crustal stretch in a north-south direction in the Tertiary of Snaefellsnes cannot be fitted into the simple hypothesis of east-west crustal drift about the Mid-Atlantic Ridge, and similar problems are encountered when trying to account for the structure of the Quaternary and Recent volcanics on Snaefellsnes, as discussed at the end of this chapter.

In late Tertiary a central volcano became active in the northern half of the Setberg area, built on the regional basalt plateau. Not much is known of the early effusive products of this volcano, which have generally been eroded away during the many glaciations of the area. In Bjarnarhafnarfjall, however, in the north-eastern part of the area, a 350 m-thick succession of andesitic basalts, icelandites[1)], dacites and acid tuffs is exposed, believed

---

1) The term icelandite is used according to the definition of Carmichael (1964) for lavas with SiO_2 59-65%, low in Al and high in Fe.

to represent some of the earliest products of the Setberg central volcano. The age of one of the Bjarnarhafnarfjall icelandites has been determined by the K-Ar method (Moorbath, Sigurdsson and Goodwin, 1968), and gave an age of 6.7 ± 0.4 m.y., providing a good idea of the age of the earliest activity in the Setberg centre, i.e. Early Pliocene.

The Bjarnarhafnarfjall succession contains 6 acid tuff layers, one of which reaches 45 metres in thickness, but andesitic basalts predominate. The layers dip north-westerly, from 15 to 40°. Some of this dip may be of a primary depositional nature, but it seems likely that the sequence was tilted, due either to downwarping under the load of the central volcano or to tilting caused by the intrusion of the gabbro body of Kolgrafamuli to the south.

Apart from the Bjarnarhafnarfjall succession, no lavas in the area can be attributed with certainty to the early activity of the volcano. There are two reasons for this state of affairs. Firstly, very extensive erosion took place repeatedly in the area in Quaternary times and removed most of the evidence for the effusive activity in the early stages of the volcano. Secondly, extreme hydrothermal alteration in the volcano has made identification of rock types and stratigraphic mapping very difficult. Thus some of the

Fig. 4: Distribution of petrographic types in the Setberg area.

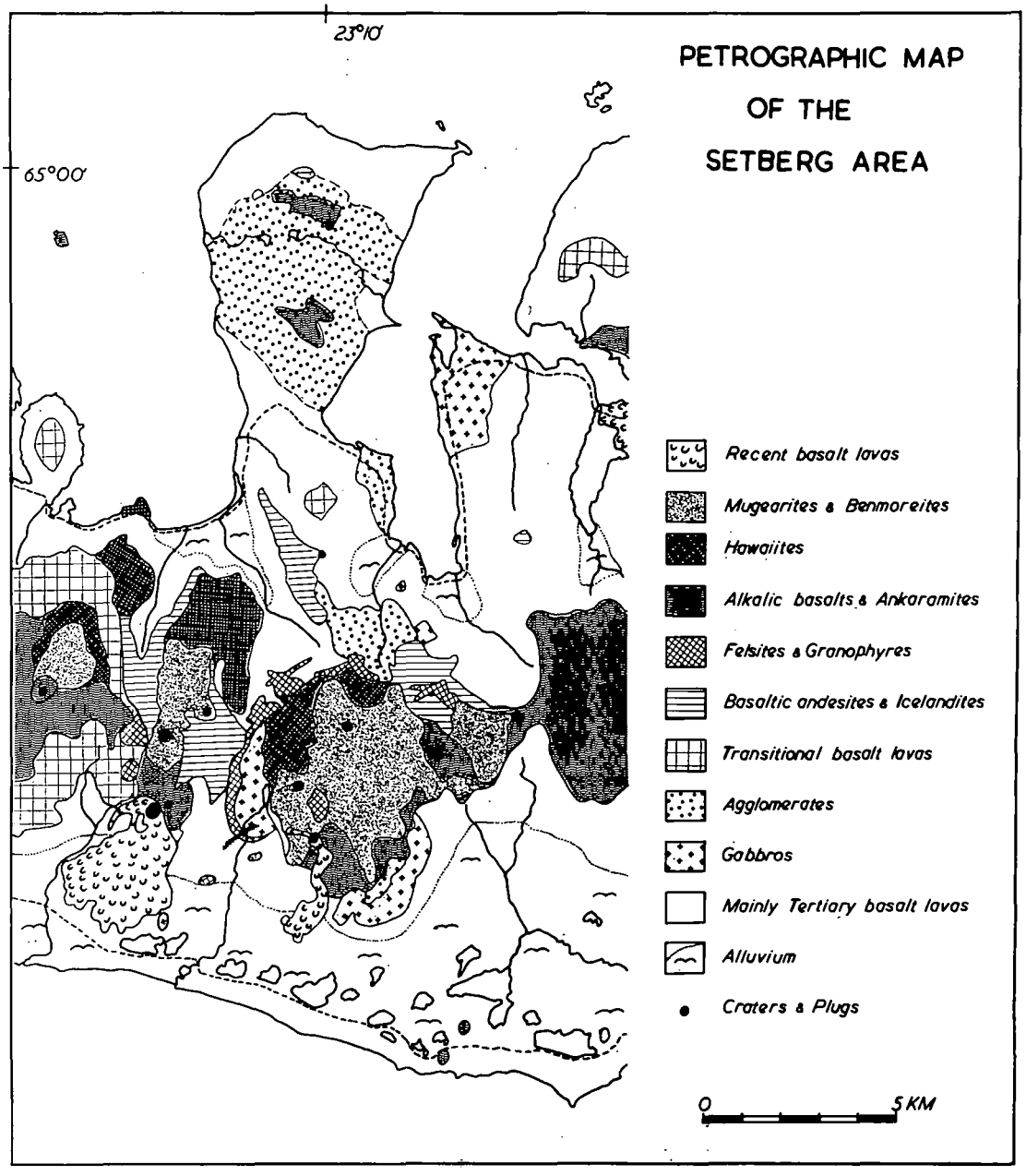
23°10'
65°00'
PETROGRAPHIC MAP
OF THE
SETBERG AREA
Recent basalt lavas
Mugearites & Benmoreites
Hawaiites
Alkalic basalts & Ankaramites
Felsites & Granophyres
Basaltic andesites & Icelandites
Transitional basalt lavas
Agglomerates
Gabbros
Mainly Tertiary basalt lavas
Alluvium
Craters & Plugs
0
5 KM

Fig. 25: A diagrammatic geological section of the Setberg area, from south to north. Crosses: Thorgeirsfell gabbro in Centre 2; dots: agglomerates and breccias (from south to north) in the Thorgeirsfell and Grenjadalur vents of Centre 2, and the Hjardarbol caldera of Centre 1; horizontal lining indicates the basaltic series of Centre 2; vertical lining: alkalic series of the Late-Quaternary; unit no. 1 is the Midhyrna obsidian dome and unit no. 2 the Lysuskard granophyric cone sheet. The cone sheet swarms of Centres 1 and 2 are shown diagrammatically. Feeders of the alkalic and transitional lavas shown black, while Tertiary lavas are blank.

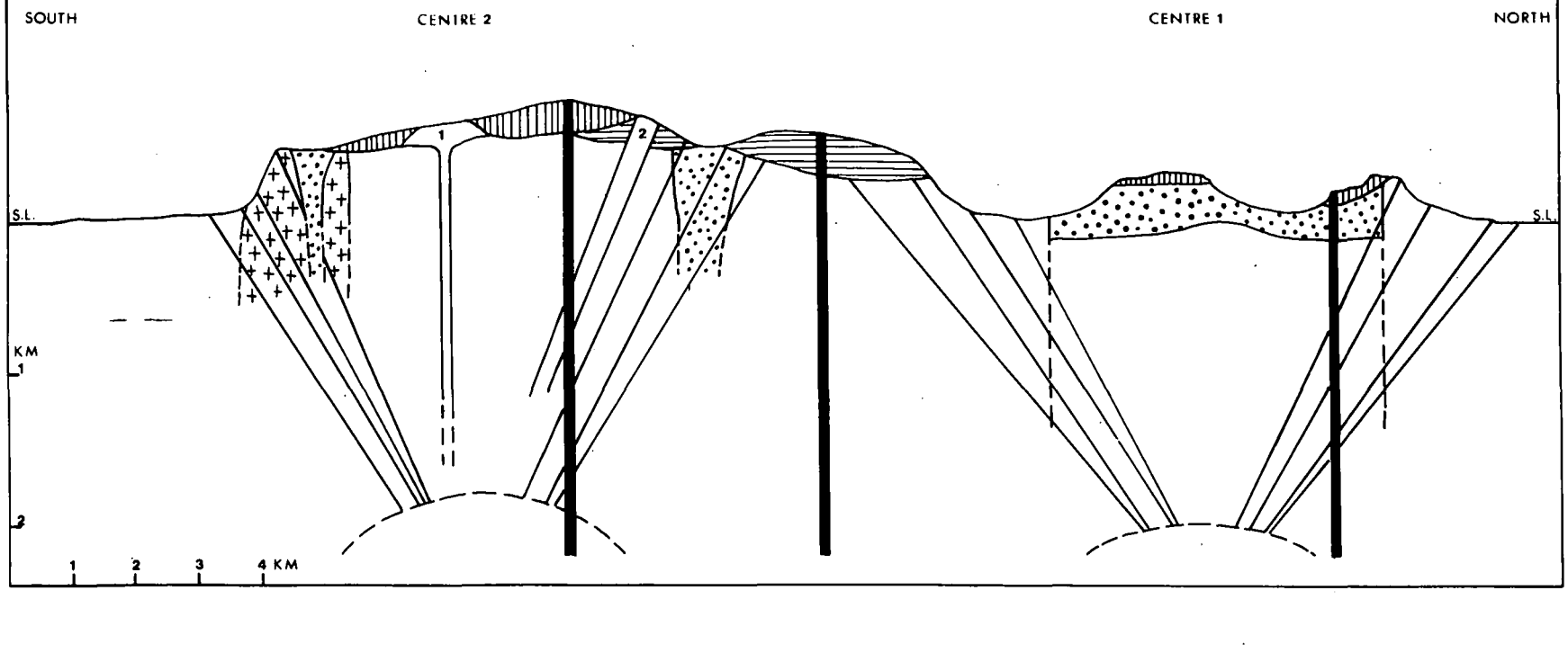
THORGEIRSFELL
GRUNDARMÓN
KLAKKUR
EYRARFJALL
SOUTH
CENTRE 2
CENTRE 1
NORTH
S.L.
S.L.
1
2
KM
1
2
1
2
3
4 KM

propylitized lavas, regarded as part of the Tertiary flood basalt succession, might in fact belong to this early phase.

1. Caldera and acid breccias

After outpouring of tholeiites and their differentiates, a caldera was formed in the first Setberg centre, 5 km in diameter. The caldera is now filled by a pile of miscellaneous acid breccias, tuffs, minor acid intrusions and rhyolite lavas, over 300 m in thickness. The acid pyroclastics contained within the caldera are floored by altered basalt lavas, as seen near Hjardarbol, and probably represent the down-thrown block that gave rise to the caldera. The minimum established depth in the caldera is 350 m.

Acid breccias form the vast majority of the caldera infilling. They are, on the whole, an unlayered pile of rhyolite fragments, generally a few centimetres in diameter, but rhyolitic blocks up to 2 m across are recorded. The breccia matrix is a finely comminuted rhyolitic dust. The absence of bedding or other depositional structures and lack of unconformities suggests that the breccias were erupted largely during a single episode. It is logical to associate this great magmatic event with the formation of the Setberg caldera

itself. The breccias and other acid rocks within the caldera are approximately 5 km^3 by volume and the outpouring of such great quantities in a relatively short time is bound to have caused partial emptying of a high-level magma chamber, assumed to be present under the Setberg centre. By the development of a ring fracture, a block of country rock could have subsided into the void and given rise to the caldera.

The Setberg caldera is of the Krakatoan type (McBirney, 1969), where collapse resulted from copious eruptions of magma as acid pyroclastics, mainly from vents within the region defined by the caldera itself.

Near Hrafnkelsstadir, south of the caldera, an explosive vent is exposed, 1500 m in diameter. The vent is probably of similar age as the caldera and is filled by acid breccias, welded tuffs and dacitic breccias.

The above description of the effusive phase of the first Setberg centre is limited by the fragmentary field evidence, which is restricted to the occurrence of scattered outliers and often masked by severe hydrothermal alteration. Clearly the volcano must have had an eventful history between the outpouring of the Bjarnarhafnarfjall lavas and the explosive activity of acid magma which culminated in the formation of the Setberg caldera.

2. Kolgrafamuli gabbro

The Tertiary basalts in the eastern part of the centre were intruded by a quartz-gabbro, over 3 km. from north to south and 1500 m wide, referred to as the Kolgrafamuli gabbro. A chilled doleritic margin has been found in contact with the basalt lavas north-east of Kolgrafamuli and the contacts along the eastern margin of the gabbro are generally steep to vertical, suggesting a stock-like intrusion. The gabbro pre-dates the dense cone-sheet swarm of the first Setberg centre, but is at the same topographic level as the Setberg caldera. The rock is remarkably coarse grained and must have solidified at considerable depth, i.e. after the Setberg caldera had been covered by 500 to 1000 m of lavas. The gabbro intrusion is therefore placed temporally between the caldera formation and the intrusion of the first Setberg cone-sheet swarm.

3. Cone-sheet swarm of first centre

An intense cone-sheet swarm encircles the Setberg caldera, in a 2 km-wide band with a diameter of 9 km. (Figure 6). The cone-sheet density, or the percentage of sheets in the country rock, is frequently 70-75% in one-kilometre sections. The majority of the sheets are basaltic

1-2 m thick with a dip of 30-35° on the average. Acid sheets are fewer in number, but much thicker and up to several hundred metres in some cases. Both acid and basic, and sheets of intermediate composition, dip to a common centre under the Setberg caldera. By assuming a constant dip of the cone sheets, a hypothetical point of origin or apex lies 2600 m below the present surface of the caldera, contrasted with a 5 km depth for the centres of Mull, Skye and Ardnamurchan (Richey, 1930). The relative paucity of larger intrusions exposed in the Setberg centre and evidence from secondary minerals suggest that the area exhibits a relatively shallow level of erosion as compared with the Scottish Tertiary centres. The differences in depth to cone-sheet apices may also be more apparent than real if we take into account the possibility that cone fractures curve with depth and become steeper, as is suggested by the experimental work of Field (1964). The Scottish cone sheets are, in fact, steeper than the Setberg ones, with dips of 45° on the average and in keeping with an hypothesis of a trumpet-shaped cone fracture. The Setberg cone sheet swarm has an apparent apical cone angle of 120°, as compared with 90° for the Scottish swarms. By adopting a trumpet-shaped

cone angle it is possible to account for all these differences of dip, depth of erosion, cone angle, and depth to magma chamber as being, in fact, an expression of the level of intersection of the cone by the present-day erosion surface.

A trumpet-shaped cone fracture would give a deeper point of intersection of opposite cone sheets than would be arrived at by direct extrapolation from measured dips of cone sheets exposed at the surface. It can, however, be assumed that the hypothetical point of intersection (cone apex) does not lie in the roof of a magma chamber but rather within it, and hence 2500 to 3000 m from the present surface is a realistic depth to the roof of a magma chamber beneath the Setberg caldera. To this may be added 500 to 1000 m thickness of volcanics, eroded since emplacement of the cone-sheet swarm and after cessation of activity in the first Setberg centre, giving 3 to 4 km as a probable depth to the Setberg magma chamber from the original volcano surface. Some idea of the horizontal dimensions of this magma chamber may be gained from the fact that the Setberg caldera has a diameter of

---

Fig. 6: The cone-sheet swarm of Centre 1. Only a small percentage of the sheets actually present is drawn on this map. The northern margin of the cone-sheet swarm of Centre 2 is seen in the southern part of the map.

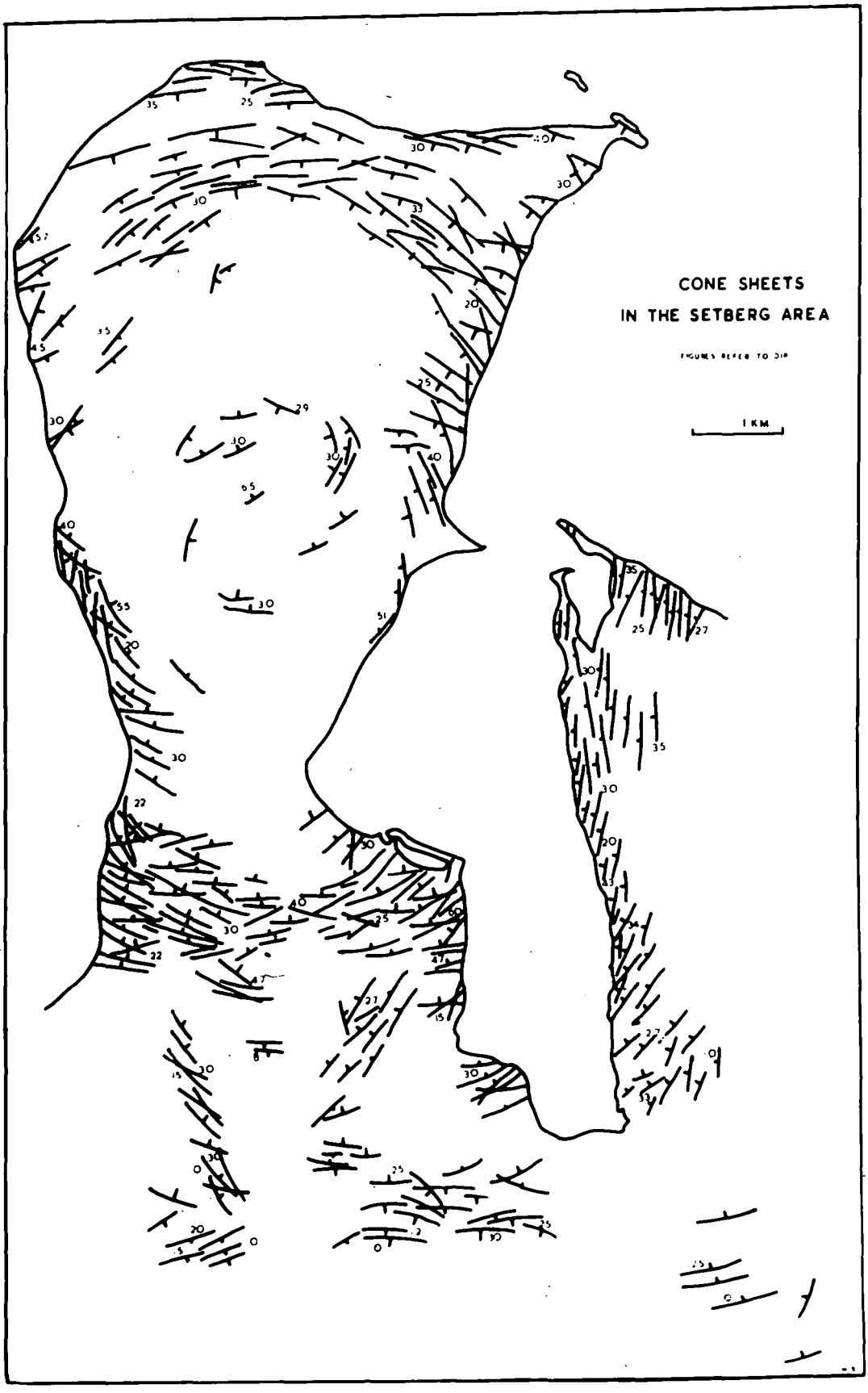
CONE SHEETS
IN THE SETBERG AREA
FIGURES REFER TO DIP
1 KM

5 km and is most probably the result of collapse. The diameter of this high-level magma chamber is most likely of the same order.

Basaltic, intermediate and acid magmas have been available throughout the intrusive history of the Setberg cone-sheet swarm. No systematic order of intrusion of magma types can be observed and, indeed, the contemporaneous availability of the magmas is best demonstrated by the numerous composite sheets, where both basic and acid magma have often been intruded simultaneously in the fluid state.

C. The Mid-Quaternary centre of the Setberg Area (Centre 2)

1. Introduction.

In Iceland the Tertiary/Pleistocene boundary is usually identified easily in the field as a marked unconformity between regularly layered flood basalts below and pillow lavas, palagonite breccias or irregular lava flows above. These dissimilar formations are frequently separated by a tillite or a boulder bed. In the Setberg area, however, this significant stratigraphic break is often harder to locate. Many of the basalts in the region, particularly those on lower ground, were initially considered of Tertiary age because of their trap features and the fact that they had

suffered propylitization, sometimes so extreme that garnet and epidote are found as secondary minerals. Further mapping and K-Ar age dating have cleared the status of these basalts and made possible their correct placing in the Pleistocene stratigraphy.

The erosion surface, on which the lavas of Centre 2 rest, has been constructed from the elevations of the various outliers. The lavas of the second centre preserve only one of the many erosion surfaces of the Quaternary, but this mid-Quaternary landscape has a north-westerly slope, from 600 m in the south-east (Thorgeirsfell) to 150 to 200 m above sea-level in the Kirkjufell region. It was on this surface that the extrusive activity of the second volcanic centre took place, after glacial erosion had removed some 500 to 1000 metres from the first Setberg centre. The mid-Quaternary erosion surface is marked by a conglomerate or tillite layer, ranging in thickness from 60 m at lower levels, to 2-3 m of hardened tillite in the south and east.

The similarity of lavas, and their small lateral extent when compared with sediments, makes stratigraphic mapping difficult in volcanic terranes. In the Setberg area this is further complicated by a very large number of unconformities due to several glaciations during the volcanic history of the second centre, and there is evidence for at least five glacial

advances in the area. A great aid in mapping out the two main Quaternary volcanic series was the concept of stratigraphic correlation by the polarity method, i.e. determining the magnetic polarity of each outcrop visited as "normal" (with the same polarity as that of the present magnetic field) or "reversed". For this purpose a light-weight, portable, fluxgate magnetometer was carried as an essential field tool and the sense of polarity determined on oriented rock samples at the outcrop.

Through palaeomagnetic mapping a relatively simple, overall stratigraphic picture of the Setberg Quaternary emerged: of a lower series of "reverse" magnetized lavas, and an upper series with "normal" polarity (Figure 7). The Quaternary geomagnetic time scale of the Earth is now well established through geomagnetic work in conjunction with K-Ar dating in several volcanic regions throughout the world (Doell et al. 1966), but to place the Setberg sequence into that scale required K-Ar dating. Three K-Ar analyses of "reverse" magnetized rocks from the area range in age from 1.1 to 1.7 m.y., all within the limits of the Matuyama polarity epoch during which the Earth's magnetic field was reversed. The upper, "normally" magnetized series dates therefore from the Brunhes polarity epoch, which spans over

the period from 0.7 m.y. ago to the present day. The "reverse" magnetized Quaternary series of the Setberg area are associated with Centre 2 and described here, whereas the younger, "normally" magnetized lavas of the Late-Quaternary form a distinct petrographic group.

The second Setberg centre consists of explosive vents, lavas ranging from basalts to rhyolites, gabbro and granophyre intrusions, and a later cone-sheet swarm. Thus the same structural elements are present as in the first centre, except that the presence of a caldera has not been established in the second centre. This may, however, exist below the late-Quaternary alkalic basalt lavas that lie unconformably on part of this centre (Figure 4).

2. Explosive vents.

Two agglomerate vents are associated with the second centre. The Grenjadalur vent in the northern part is 2 km in diameter and filled by acid breccia with a minimum thickness of 500 metres. On the eastern side the vent agglomerate has vertical contacts with the Tertiary basalts, but on the northern side the basalt-lava wall of the vent is at an angle

---

Fig. 7: A stratigraphic column of the Setberg area, showing the relationship between the volcanic history and the geomagnetic time-scale. Shaded parts of time-scale represent periods of normal polarity, and arrows on time-scale indicate positions of K-Ar dates from the Setberg area.

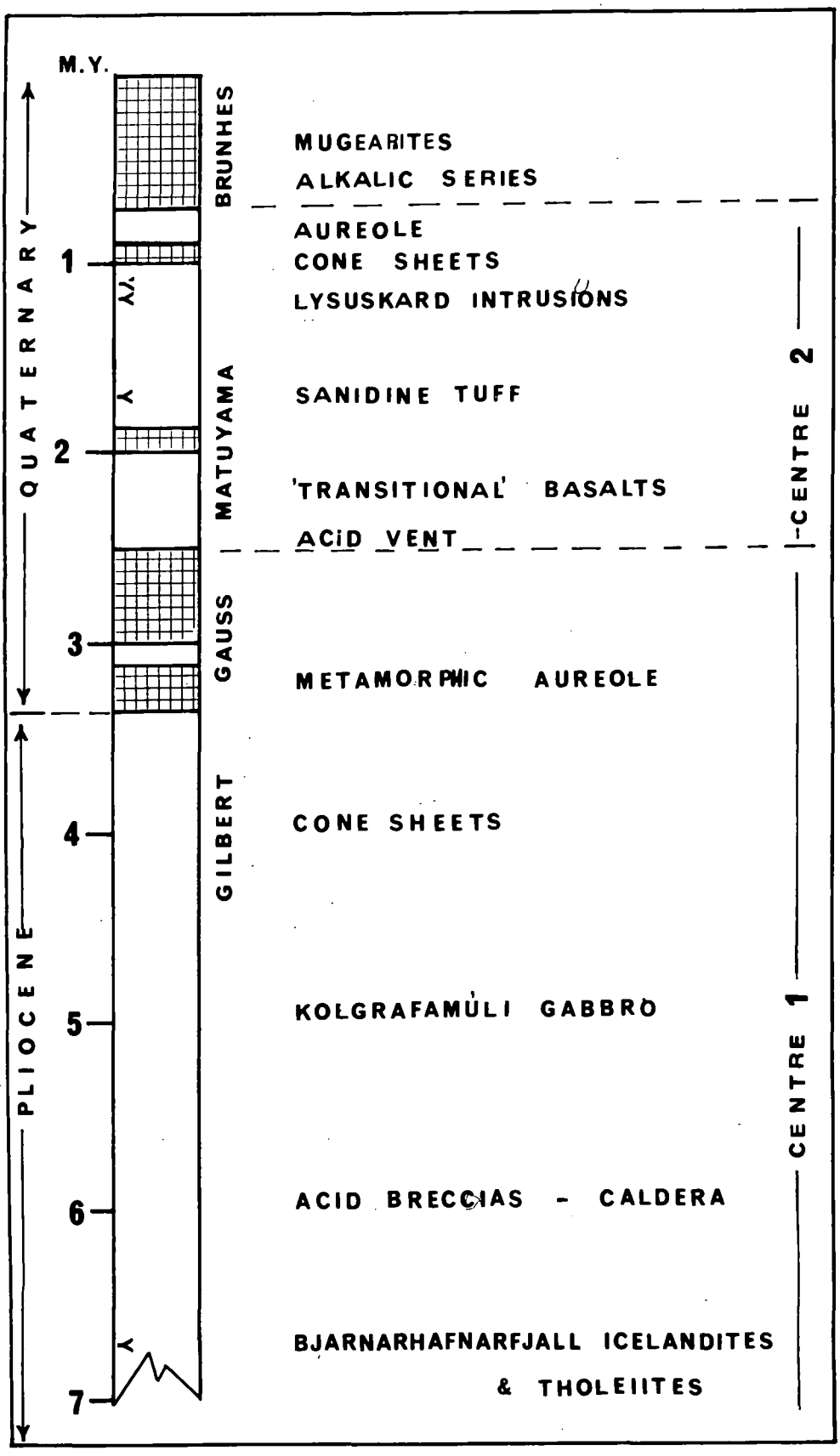
M.Y.
QUATERNARY
PLIOCENE
1
2
3
4
5
6
7
BRUNHES
MATUYAMA
GAUSS
GILBERT
MUGEARITES
ALKALIC SERIES
AUREOLE
CONE SHEETS
LYSUSKARD INTRUSIONS
SANIDINE TUFF
'TRANSITIONAL' BASALTS
ACID VENT
METAMORPHIC AUREOLE
CONE SHEETS
KOLGRAFAMULI GABBRO
ACID BRECCIAS - CALDERA
BJARNARHAFNARFJALL ICELANDITES
& THOLEIITES
CENTRE 2
CENTRE 1

of 40°. The acid breccias are purplish in colour, with rhyolite fragments dominant (2-4 cm in diameter) but fragments of granophyre, basalt and granite occur. A granite fragment from this vent has been described in detail elsewhere (Sigurdsson, 1968). The breccia matrix consists of a very fine-grained rhyolitic material, probably of devitrified glass shards which, together with the homogeneity of the larger rhyolitic fragments, indicates that the majority of the vent breccia originated from a rhyolite magma. Its explosive activity may have been responsible for the formation of the vent, as suggested in connection with the acid breccias of the Setberg caldera (Centre 1).

A tongue of the breccia extends over the northern lip of the vent and is exposed in the succession of Grundarmön mountain, where it is found at the base of the Quaternary lava pile. The stratigraphic position of this breccia layer is the criterion for placing the explosive vent among the earliest products of the second centre of the Setberg volcano.

A second vent is exposed in cross section in the gabbro face of Thorgeirsfell in the southern part of the centre. The south-eastern sector of this vent is exposed, but the rest is overlain unconformably by late-Quaternary olivine

basalts. The portion exposed is just over 1 km long, and entirely within the Thorgeirsfell gabbro. The vent walls are inclined inwards or are vertical and confine a heterogenous agglomerate of basalt, gabbro and rhyolite blocks in a green to pale-greenish matrix of intermediate composition. Gabbroic blocks are dominant in the agglomerate and are clearly derived from the enclosing intrusion which is highly fractured around the vent. Gradation from massive gabbro to gabbro-agglomerate with blocks up to 2 m in diameter is seen in the field.

Acid and basic cone sheets are abundant in the gabbro enclosing the vent, but within the vent they are absent and believed to make up most of the basaltic and rhyolitic fragments in the agglomerate. One rhyolite dyke post-dates the vent formation and cuts the agglomerate.

The presence of a few scoriaceous, fine grained or almost glassy andesitic fragments, and the fact that the agglomerate matrix is very homogenous, suggests that some primary magmatic material was erupted as pyroclastics during the formation of the vent. Although formed relatively late in the history of the centre, the vent did not escape the general hydrothermal alteration of the area. The agglomerate has a chloritized matrix and abundant calcite and quartz as a cementing agent, as well as sulphide minerals, mainly chalcopyrite and pyrite, in the vugs.

3. Eruptive products

Volcanic activity in the Setberg second centre extended over approximately 0.5 m.y., during which at least four glaciations took place in the area (Sigurdsson, 1966). Consequently the habit of the volcanic products is varied, as subglacial eruptions were frequent. In the northern part, the earliest lavas form a 70 m-thick series of icelandites and basaltic andesites in Grundarmön. Basaltic andesite lavas also occur 4 km to the west, at a similar level in Arnardalur, and these two outliers may probably be correlated. These subaerial lavas are typically very fine grained, dark coloured rocks, sometimes almost glassy, and with platy jointing along the planes of flow as well as superimposed columnar jointing. Similar lavas occur further up in the succession and on the summit of Grundamön, 40 m in thickness.

On top of the lower basaltic andesite series in Grundarmön rests a 150 m-thick succession of highly plagioclase-phyric basalt lavas. These thin (1-2 m) pahoehoe lavas can be traced to a plug in eastern Grundarmön, but similar plagioclase-phyric lavas occur on top of Gjafakollur to the east and in Kirkjufell, 6 km to the west, where phyric lavas occur about 200 to 250 m above sea level. These phyric lavas are usually somewhat vesicular and tend to weather easily to spheroidal forms. Associated with the phyric lavas in

Grundarmön is an overlying formation of subglacial, plagioclase- and pyroxene-phyric, basaltic, palagonite breccia.

The basaltic andesites in Arnardalur and Grundarmön, as well as in Bjarnarhafnarfjall in the northeast, are interbedded with tholeiitic basalts. All gradations of rock types from tholeiites to icelandites are presented in these successions, but no regular sequence of eruption of compositional types can be established. As in the Tertiary Centre 1 of the Setberg area, magmas of all compositions, from acid to basic, have been available for eruption in the second centre during its known period of activity.

The most voluminous remnants of eruptive products from the centre are basaltic andesite and tholeiite breccias and lavas. In Tindar and Smjörhnukur, where these occur, the thicknesses are 400 m and 300 m respectively. The Smjörhnukur formation has suffered propylitization in the lower part and the presence of chlorite, epidote and even garnet as secondary minerals in the lower part of this formation led to its original mis-identification as belonging to the Tertiary. The tholeiitic and intermediate rocks in Smjörhnukur and Tindar have been intruded by later acid and basic minor intrusions and clearly belong to the earlier products of the centre. The rocks are very fine grained and

almost glassy in some cases, and often occur as basaltic depositional breccias. The presence of pillow structures, in some cases, indicates a subaqueous or subglacial volcanic environment for part of the series, but lavas are predominant. A similar basaltic breccia rests on the basaltic andesite lavas in the eastern part of Arnardalur, probably of the same age. Only two layers of acid volcanic material from Centre 2 are preserved in the area. One is a glassy, rhyolitic lava outlier on Gjafakollur, 45 m thick; the other is an acid tuff, rich in sanidine and quartz phenocrysts, reaching 50 m in maximum thickness. The acid tuff lies between the upper basaltic andesites (above) and the porphyritic basalt series in Grundarmön but has not been found elsewhere in the area, in spite of its great thickness. The sanidine-tuff is welded in the lowermost part, and devitrified throughout. Granitic and granophyric fragments are common constituents, reminiscent of the Grenjadalur breccia. K-Ar determination on sanidines separated from the tuff gave an age of 1.7 ± 0.3 m.y. (Moorbath, Sigurdsson and Goodwin, 1968).

Fig. 8: Generalized geological map of the Setberg area, showing the cone-sheet swarms of Centres 1 and 2. Spot heights are in metres.


SETBERG VOLCANIC CENTRE
CENTRE 1
CENTRE 2
360
568
613
609
850
840
748
930
874
918
934
897
420
680
646
648
610
BLÁFELDARHRAUN
HRAUNSMÚLAHRAUN
RECENT LAVA
QUATERNARY
AGGLOMERATE
CONE SHEETS
GABBRO
GRANOPHYRE
0 1 2 4
KM
HSig

4. The Thorgeirsfell gabbro.

Gabbroic and granophyre intrusions occur in the southern and western part of the second centre, and some of their features have been briefly described by Upton and Wright (1961). The most prominent of these intrusions is the Thorgeirsfell gabbro, over 3 km in length, exposed in cliffs and screes over 500 m high. The north-western boundary of the gabbro is concealed below the unconformably overlying, Late-Quaternary basalts, and the central area of the gabbro is punctured by an agglomerate vent, already described (p. 36). The exposed width of the intrusion is 1 km. Contacts with basaltic country rock are steep to vertical everywhere.

The gabbro has a highly porphyritic, doleritic marginal facies, with plagioclase phenocrysts dominant but augite and, more rarely, olivine are also present. The marginal facies is up to 20 cm wide, but grades into normal gabbro. In some outcrops, well away from the contacts, very faint and discontinuous banding can be seen, with darker pyroxene-rich bands less than $\frac{1}{2}$ cm thick and 5-8 cm long, in more-or-less horizontal attitude. This feature is more reminiscent of fluxion banding than igneous layering, but in the interior of the intrusion some layered, sub-horizontal units 0.5 to 1 m thick are found, consisting of a lower pyroxene-rich band and an upper, paler coloured plagioclase-rich layer, often

with interstitial granophyric patches. Igneous layering is by no means a distinct feature of the intrusion, but undoubtedly present. Olivine is found in the darker bands, but rarely.

In an outcrop in the north-western part of the intrusion a very coarse-grained, plagioclase cumulate rock is exposed, consisting essentially of 2 to 4 cm long, euhedral plagioclase laths with intercumulus augite.

An important feature of the Thorgeirsfell intrusion is the present attitude of the layers. Although generally horizontal in the interior parts, the igneous layers tend to become outward dipping as the contacts are approached, and dips near to vertical have been observed close to the contact. Considerable disruption of layers and irregular, small-scale faulting, along with the frequently observed outward dip, suggest that the gabbro was intruded upwards as a semi-solid body whose outer margins were dragged downwards relative to the centre.

In a number of localities, granophyric patches, veins and minor intrusions occur within the gabbro, particularly near the western contact. The later granophyric magma may either be interpreted as representing the still-fluid component of the gabbroic mush that was squeezed out and

segregated near the margins during emplacement or, alternatively, as an independent series of acid intrusions. The first view is favoured because the contacts between gabbro and granophyre are both irregular and gradational.

On the geological map (Figures 4 and 8) the Thorgeirsfell gabbro has an arcuate form, suggestive of a ring intrusion. The northern contacts are, however, concealed and the available field evidence suggests a stock-like intrusion. The intrusion may have taken advantage of a structural weakness associated with circular fracture in the second centre, judging from the location of the intrusion relative to other elements of the centre.

5. The Lysuskard intrusions

The Lysuskard valley is floored by an elongate, biotite-gabbro intrusion, measuring 3 km from north to south (Figure 8). In the south, west and north, a granophyric sheet forms a screen, 200 to 400 m wide, between the gabbro and the basaltic country rock. The Lysuskard gabbro is overlapped by unconformable, Late-Quaternary basalts in the east and the only visible intrusive contacts with the country rocks are in the southern part, where the contact is steep or vertical. Contacts are badly exposed but, like the Thorgeirsfell intrusion, the Lysuskard gabbro may have a stock-like form.

A variety of rock-types occur within this intrusion. In the southern part, a very pale-coloured, plagioclase-rich and often drusy gabbroic rock, with granophyric patches, grades into the more common, biotite-bearing, dark-green gabbro. Some 300 m thickness of gabbro are exposed in Lysuskard, composed chiefly of thick, horizontal sheets of biotite-gabbro but with at least three thinner sheets or screens, also horizontal, of gabbro rich in basalt xenoliths. The sequence suggests an intrusive mechanism whereby successive gabbroic sheets were emplaced near the roof where active stopping of the basalt country-rock was taking place, resulting in a lower part of each sheet rich in basalt xenoliths and a thicker, upper, homogenous gabbroic part. The Lysuskard granophyre, which envelopes much of the gabbro intrusion, is roofed in the western and southern part by the basalts of Smjörhnukur. The basalt/granophyre contact is here approximately horizontal, or gently dipping westerly. Contacts between the gabbro and granophyre are complicated by a gradational relationship that often exists between the two main rock-types, particularly in the southern part where a dioritic gabbro, pale in colour, separates the two. Chilling of granophyre against gabbro has been found in one case and the evidence indicates that the granophyre is a later intrusion. In the northern and northwestern parts of the centre, the outer

contacts of the granophyre are well exposed and here the hornfelsed basalts dip at 45 to 60° southerly and under the granophyre. The arcuate outcrop of the relatively thin granophyre intrusion, together with the inward dipping contact, suggest the form of a cone sheet. It was mentioned above that the granophyre in Smjörhnukur was partly roofed by basalts. Similarly the basalt lava roof of this cone sheet is partly preserved in the northern part, and it is clear that the present erosion level is very near the roof of the intrusion. In this context the Tindar felsite sheet, to the north-east (Figures 4 and 8) may be considered a further continuation of this cone sheet. The distinct chemical and mineralogical similarities of all samples from this arcuate series of outcrops of granophyre and felsite, from Lysuskard in the south to Tindar in the north-east, are additional evidence for considering them as parts of the same cone-sheet intrusion. The Tindar felsite sheet intrudes the Mid-Quaternary basalts and is inclined 25 to 40° southwesterly. Further south this sheet is overlapped by Late-Quaternary alkalic basalts.

In the west, near Arnarskard, two small outcrops of acid rocks occur, intruded into the Mid-Quaternary basalts (Figure 4). The felsitic or microgranophyric intrusion has obsidian margins and has presumably been intruded at small depth below

the volcanic surface.

Four small gabbro outcrops, believed to be associated with the second centre, occur in Gunnungsfell and Holahlid in the north and Stekkholl and Tradir in the southern part. The northern intrusions have a plug-like form with vertical contacts, whereas contacts of the smaller olivine gabbro bodies in the south are concealed.

The small hill of Lysuholl, on the plain west of Lysuskard, consists entirely of granophyre but no contacts are visible and the outcrop is surrounded entirely by alluvium. Slightly east of this intrusion, a borehole in the Lysuholl thermal field encountered granophyre at a depth of 38 metres, after passing through metamorphosed basalt lavas and thin basaltic intrusive sheets (cone sheets?). Granophyre persists to the bottom of the hole at 100 m. K-Ar determinations have been carried out on samples from this granophyre core (Gale et al. 1966) and four independent analyses gave an average age of 2.6 $\pm$ 0.3 m.y.. In mineralogy and chemistry this granophyre is comparable to the Lysuskard granophyre cone sheet, although apparently 1 m.y. older.

Four K-Ar determinations are available on the Lysuskard

intrusions (Gale et al. 1966; Moorbath et al. 1968). A biotite from the gabbro gave an age of 1.1 ± 0.3 m.y., while three samples from the granophyric intrusion gave the following ages: 1.2 ± 0.6 m.y., 1.6 ± 0.7 m.y. and 2.1 ± 0.7 m.y.. The age differences between the intrusions are not significant, judging by the available K-Ar data, and a probable age for the intrusions of biotite-gabbro and granophyre in Lysuskard is about 1.3 m.y., or shortly after the succession of lavas in Grundarmön was erupted, but a sanidine-bearing acid tuff from that succession gave an age of 1.7 m.y. (p. 40).

These ages provide evidence for the very rapid sequence of events in the history of this volcanic centre: only 0.5 m.y. after the Grundarmön lavas were erupted, major intrusions were emplaced at the same level, presumably under a cover of some 500 to 1000m of lavas. The Lysuskard intrusions were exposed at the surface approximately 0.7 m.y. ago, that is, no more than 1 m.y. after their emplacement into the base of the second centre. This is good testimony to the very rapid erosion processes characteristic of the Icelandic Quaternary period.

6. Cone-sheet swarm:

A great number of inclined sheets intrude the Tertiary and Mid-Quaternary basalts in Centre 2, forming a well-developed cone-sheet swarm (Figure 8). The vast majority of the sheets are basaltic, but rhyolitic and intermediate sheets are also present and usually thicker. The swarm cuts the major intrusions, and Grenjadalur agglomerate and the Mid-Quaternary breccias and lavas. It post-dates all the known formations of the centre, except for the Thorgeirsfell agglomerate vent (p. 36). All determinations on the magnetic polarity of the cone sheets have shown them to be "reverse" magnetized, thus belonging, like the lavas, to the Matuyama polarity epoch.

The average thickness of 100 cone sheets is between 0.5 and 1 metre and very few sheets are more than 2 m thick. The average dip of 216 sheets is 35°. The diameter of the cone-sheet swarm is 7 km and, by projecting the sheets to a common focal point, their hypothetical point of origin is calculated to lie at 2.5 km depth, similar to that of Centre 1 (2.6 km).

The concentric arrangement of major intrusions and the cone-sheet swarm indicate a common centre underneath the unconformable pile of Late-Quaternary lavas north of Thorgeirsfell. It is possible that a caldera, analogous to the features of the first centre, lies hidden under this cover and in the middle

of the second centre.

The cone-sheet swarms of the two centres in the Setberg area have contributed significantly to the crustal pile by volume. In both centres the swarms occupy an area at least 1 km in width, in which approximately 50% of the rock consists of cone sheets, i.e. a width of some 500 metres. Intrusion of such magnitude would result in an uplift of over 500 metres of the central cone, if no subsidence occurred in order to accommodate the vast number of sheets. Some downwarping has been observed in the first centre, but it is probable that significant uplift occurred during the emplacement of the swarms.

Tumescence of larger active volcanoes is a well-documented phenomenon, i.e. the up-arching or swelling of a volcano during the periods when rising magma preceded an eruption (Stearns and Macdonald, 1946), but usually this is a short-lived event and associated with a rise of magma in the central region. Prolonged uplift of the entire volcano has not been documented anywhere, to the writer's knowledge, but it seems an inescapable conclusion in cases where intense cone-sheet swarms have been intruded.

D. Metamorphic aureoles of the Setberg centres:

An extensive region of propylitization envelopes both centres of the Setberg area, characterized by the occurrence of chlorites, epidote, calcite, quartz and laumontite, as well as albite and garnet (grossular-andradite series). The secondary minerals frequently occur in vesicles and cavities of the altered lavas, either alone or in varying combinations. The distribution of the three most characteristic minerals, laumontite, epidote and garnet, has been mapped out and is presented in Figure 9.

Several other minerals are also present but in less abundance, including fluorite, prehnite, pyrite, chalcopyrite, reyerite, dolomite, actinolite, yugawaralite and many of the more common zeolites. In Figure 11 the variation of secondary minerals in vesicles and cavities of the greenstones is shown diagrammatically against distance from the centres, based on data from over 200 localities. The sequence garnet - albite - epidote - laumontite is well demonstrated, as is the antipathy between quartz and laumontite, and the small overlap between epidote and laumontite and between laumontite and other zeolites.

The present mineral assemblage in the greenstone cavities is unlikely to represent an equilibrium assemblage, but the scarcity of incompatible phases occurring together

suggests that equilibrium was approached in some parts of the aureole.

Evidence of a previous regional, low-temperature, secondary mineral assemblage has only been found within the aureole in some of the Tertiary basalts of pre-Setberg age, which contain relict analcime in their cavities. Analcime and its associated zeolites (chabazite, thomsonite and sometimes mesolite) occur frequently in the upper part of the Snaefellsnes Tertiary succession (Sigurdsson, 1966). These minerals characterize the analcime-zone of Walker (1960), considered to have formed at a depth of approximately 800 metres in the original lava pile. The lower part of the Snaefellsnes Tertiary contains abundant mesolite and scolecite, placing it in Walker's mesolite zone.

The hourglass form of the aureole (Figure 9) indicates its close connection with the two centres. The form is that of two over-lapping aureoles, the southern one being the younger. Within the epidote zone, most of the basalts have a greenish colour due to the presence of chlorite and epidote. Similar greenstones have been observed in numerous other

---

Fig. 9: The distribution of laumontite, epidote and garnet in the hydrothermal aureole of the Setberg area. The dash-lines mark the outer limits of occurrence of the respective secondary mineral zones enveloping Centres 1 and 2.

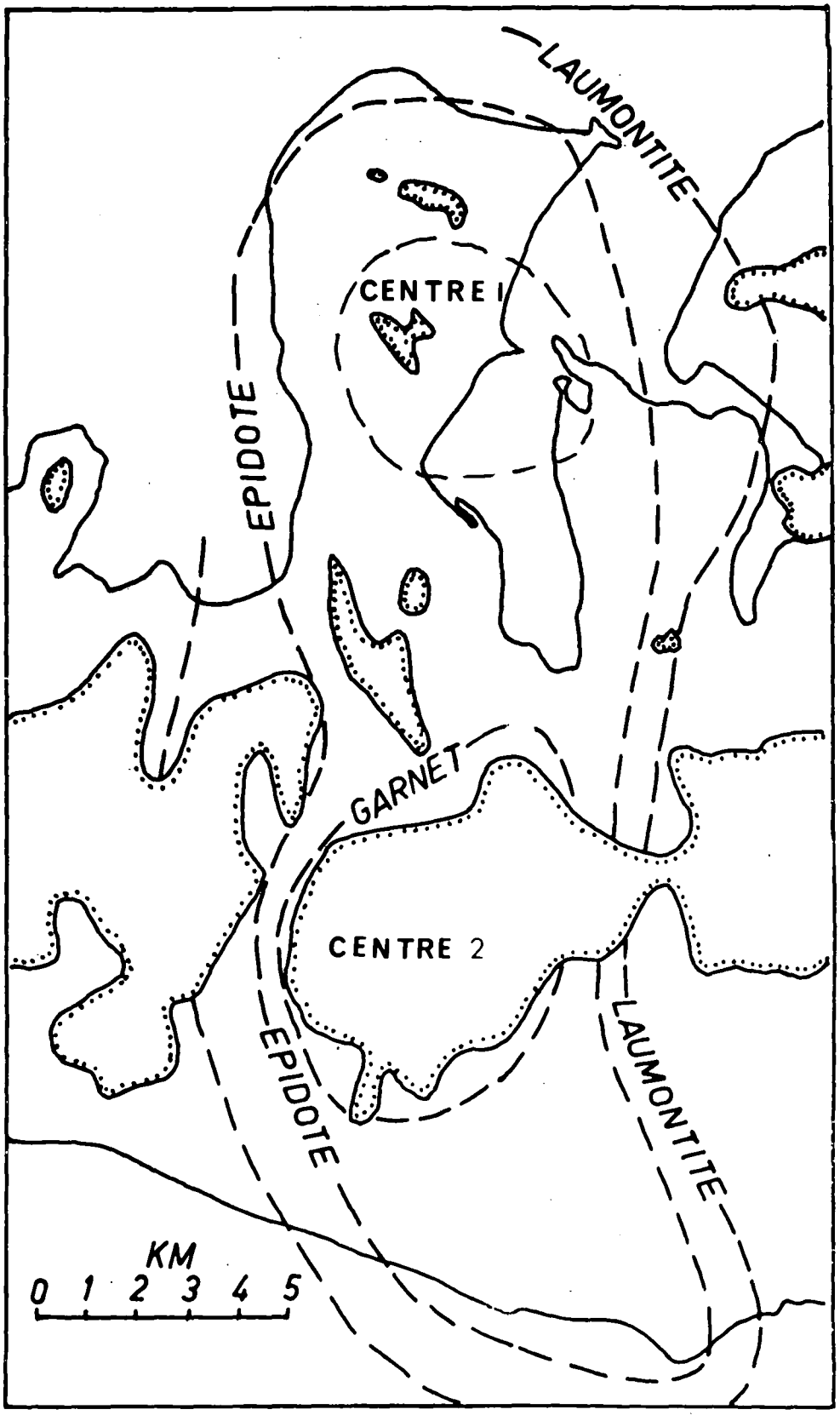
LAUMONTITE
CENTRE 1
EPIDOTE
GARNET
CENTRE 2
EPIDOTE
LAUMONTITE
KM
0 1 2 3 4 5

volcanic centres in Iceland and described from the Breiddalur volcano (Walker, 1963). The origin of the Setberg aureoles is considered to be associated with high-temperature hydrothermal activity in the root region of the volcanic centre. It is too widespread to be attributed to the intrusions in the area, which are themselves affected by the alteration process. No doubt the major intrusions and cone sheets have contributed towards the alteration, but its major source probably lies deeper.

From the evidence of the cone-sheet swarms, it has been concluded that two shallow-level magma reservoirs were present at 2-3 km depth under both centres. The cooling and de-gassing of large quantities of magma in these magma chambers, aided by convective circulation of groundwater, is believed to be the main agent in the transformation of the lava pile to greenstones, often approaching greenschist facies in their mineralogy. The role of exothermic hydration reactions, such as the formation of chlorites from the ferro-magnesian minerals, may have contributed some heat to the system, once the initial heat had been supplied by the cooling

---

Fig. 10: A geological map of the central portion of the Snaefellsnes volcanic zone, covering the area indicated in Fig. 2. The map brings out the striking linearity of craters and plugs of Quaternary and Recent age, and their coincidence with a WNW-ESE tectonic trend.

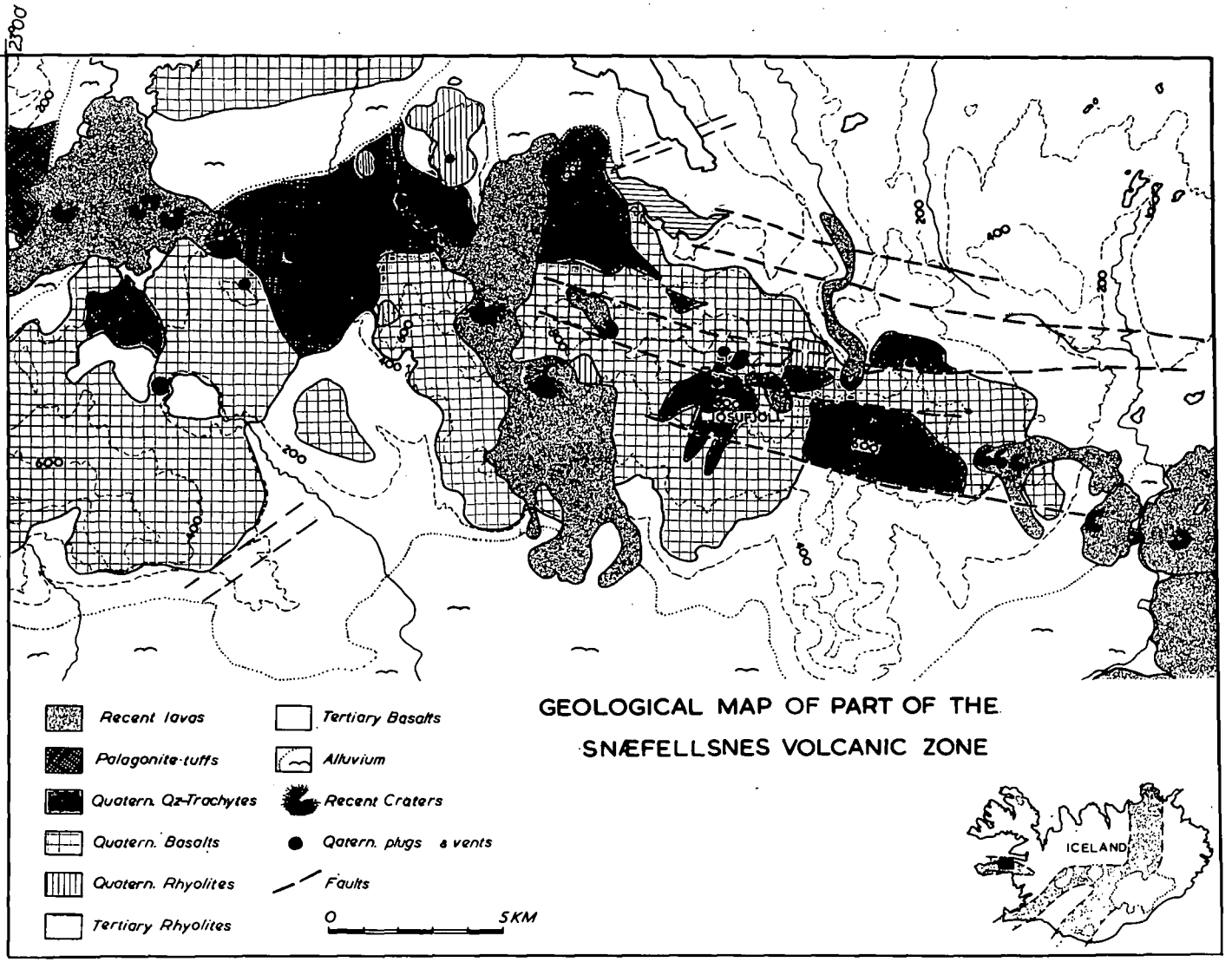

GEOLOGICAL MAP OF PART OF THE SNÆFELLSNES VOLCANIC ZONE

at depth. However, the relatively small volume of hydrous minerals in the inner parts of the aureole exclude this as a significant source of heat.

Active central volcanoes in Iceland are also the areas of most intense hot-spring activity today. In such areas as Torfajökull, Hengill and Myvatn we are probably witnessing the surface manifestation of deep-seated hydrothermal activity, stemming from large volumes of magma in the roots of a volcano. Deep drilling in one such area has demonstrated the presence of an epidote-rich mineral assemblage at 400 m depth below the surface, in a region of hot-spring activity (Sigvaldason, 1963), but temperatures up to 270°C have been recorded in thermal areas in Iceland at depths of 1.5 km or less. Tertiary basalt outcrops on the south coast of the Setberg area are greenstones, containing epidote and associated minerals. It is debatable whether this alteration is part of the Setberg aureole, as indicated on the map (Figure 9), or an independent aureole, possibly associated with the intense dyke swarm in that part of the area. A wide belt of alluvium and vegetative cover conceals the relationships between the second centre and these coastal outcrops.

Fig. 11: A diagrammatic representation of the relative abundances of secondary minerals in the Setberg hydrothermal aureole, and variations in their abundance with distance from the volcanic centres. Distributions at a distance of 2 km or less from the centres are not shown, as intrusions, caderas and

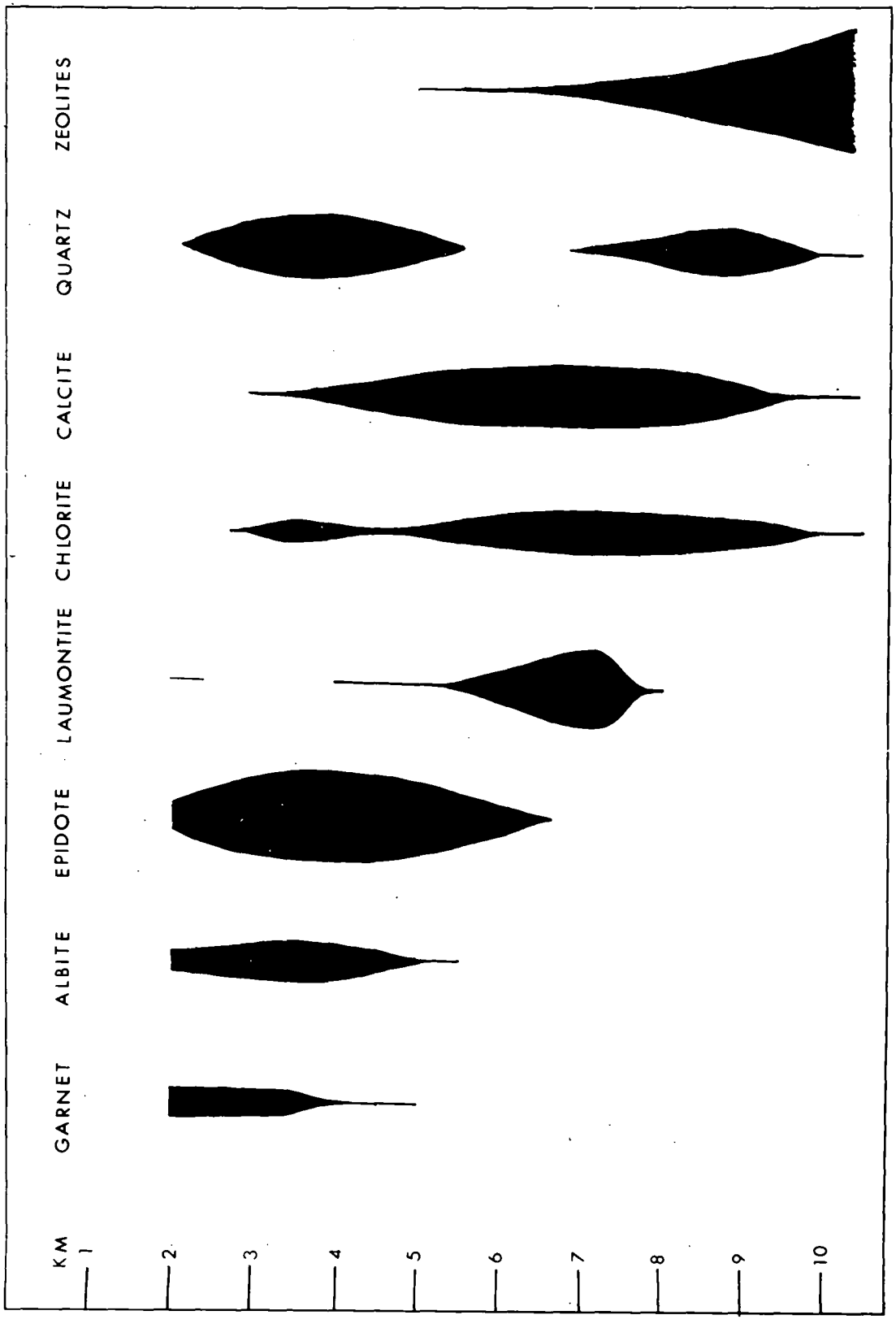
KM
1
2
3
4
5
6
7
8
9
10
GARNET
ALBITE
EPIDOTE
LAUMONTITE
CHLORITE
CALCITE
QUARTZ
ZEOLITES

E. Late-Quaternary alkalic basalt series

On higher ground in the Setberg area an alkalic basalt series often overlies unconformably the Mid-Quaternary lavas (Figure 4). The younger lavas are generally somewhat more coarse grained and paler in colour than the fine grained, extrusive rocks of Centre 2 and resemble other Interglacial and Recent lavas found elsewhere in the Snaefellsnes volcanic zone.

The alkalic basalt series reaches a maximum thickness of 400 m north of Thorgeirsfell, where it overlies unconformably the intrusions and lavas on Centre 2, and is abundant in the mountain ridges east and west of the area (Figure 4).

The unconformity below the alkalic basalt series represents a major period of erosion, which removed the volcanic edifice from Centre 2 and exposed its major intrusions, probably emplaced at 500 to 1000 metres depth. K-Ar evidence (p. 48) indicates that this interval was less than 1 m.y. in duration, before the alkalic basalts were erupted. The underlying unconformity is highly irregular, resembling the present-day topography, with deep valleys and steep scarps. This is unlike the relatively gentle landscape onto which the Centre 2 lavas were erupted.

The vast majority of the alkalic basalts consist of sub-aerial lava flows, but sub-glacially erupted palagonite

breccias and pillow lavas occur at the base of the Late-Quaternary succession in Thorgeirsfell, above Blafeldur, and in Klakkur and Axarhamar (Sigurdsson, 1966, p. 105 and 111). Although dominantly on higher ground, i.e. over 300 above sea-level, alkalic basalts of this age have been found as small outliers in Kirkjuholl on the south coast and on the island Melrakkaey in the north-western part of the region (Figure 4).

The alkalic basalt series is "normally" magnetized, i.e. with the same polarity as the present-day geomagnetic field, and belongs to the Brunhes geomagnetic epoch which spans the last 0.7 m.y.. These Late-Quaternary lavas are often only lightly affected by glacial erosion, and a crater at 900 m above sea-level in Helgrindur has completely escaped glaciation, presumably because it projected above the ice cover as a nunatak, owing to its great elevation. The interpretation is advanced that the alkalic suite was erupted during the last Interglacial of the Quaternary period, and the two Recent lava flows in the area, which are also alkalic (Figure 8), support the view that the alkalic series was formed at the very end of the Quaternary.

The largest region of the alkalic series is north of Thorgeirsfell, where olivine basaltic palagonite breccia

at the base is followed by ankaramites and olivine-phyric basalts. These in turn are overlain by coarser grained, relatively lighter-grey coloured mugearites and benmoreites. In the northern part of this area, plagioclase-phyric hawaiites occur at the base, underneath the mugearites. Two crater remnants occur on top of this sequence; a 20 m wide, glacially scoured crater in the southwestern part, built up of thick lava aprons of benmoreite, and a plug-like remnant of mugearite in the northern part.

Within this region of alkalic lavas, an alkali-rhyolite inlier is exposed near Midhyrna. This dome of rhyolite is 1 km long and bordered by obsidian. The youthfulness of this rhyolite suggests a Late-Quaternary age, and its peralkaline affinities support this association with the alkalic series. The Midhyrna alkali-rhyolite is the only acid rock which can be associated with the alkalic basalt series on field evidence, but an isolated obsidian dyke within the Tertiary to the north has also tentatively been included with the Late-Quaternary lavas on account of its high degree of peralkalinity.

East of the Thorgeirsfell area, ankaramites and porphyritic olivine basalts occur at the base of the alkalic series, again overlain by mugearites which here overlap the Mid-Quaternary tholeiitic basalt breccias of Tindar. An

olivine basalt plug occurs in the alkalic series at Klakkur to the east.

West of the Thorgeirsfell area a gap exists in the outcrop, but the Late-Quaternary alkalic series is found again in Arnardalsskard to the west (Figure 4), where two crater remnants are preserved. The general sequence is the same here as in the eastern region: olivine basalts and ankaramites or hawaiites at the base, overlain by mugearites.

The alkalic series has been mapped to a point slightly west of the beautifully preserved Helgrindur crater. Below and to the west of the crater, some E-W trending olivine basalt dykes are exposed which are probably feeder dykes to the olivine basalts. Here olivine basalts are again at the base, overlain by hawaiites and finally by mugearites.

Outside the Setberg area the alkalic series extends in an E-W direction along the mountainous crest of Snaefellsnes for some 5 to 10 km in either direction (Figure 2). Alkalic basalts do, however, occur in other parts of Snaefellsnes and are of similar age to the Setberg alkalic series. However, they are associated with the Ljosufjöll and Snaefellsjökull volcanoes (Figure 2), as will be discussed later.

The two Recent lava flows in the Setberg area are Blafeldarhraun[1)] in the south-west and Hraunsmulahraun in the

---

[1)] Hraun is Icelandic for lava.

south (Figure 8). Both these lavas are very small by Icelandic standards: 0.1km^3 and 0.02 km^3, respectively. The eruptions which gave rise to them were not fissure eruptions sensu stricto but, instead, the lavas issued from single craters which, like other Recent craters in the Snaefellsnes volcanic zone, are relatively large cinder cones.

The Late-Quaternary lavas in the area are very fresh and youthful rocks. The basal palagonite breccias and pillow lavas do, however, occasionally contain large clusters of well-formed, radiating aragonite in vesicles.

F. Structural origin of the Snaefellsnes volcanic zone and Icelandic plate tectonics

The Late-Quaternary Setberg alkalic series have a close relationship with other Late-Quaternary and Recent lavas on Snaefellsnes both in chemistry, time and tectonic setting. The ten craters and plugs found within the Setberg Late-Quaternary series, as well as the rare dykes, are arranged in an east-westerly direction in common with the rest of the Snaefellsnes volcanic zone (Figures 2 and 4).

Volcanic fissures are rare in the Snaefellsnes zone, but the alignment of craters in the northern and eastern part is of striking regularity (Sigurdsson, 1967). Thirty-five craters occur on Snaefellsnes, outside the domain of Snaefellsjokull, and 24 of these fall on or near a line trending 108°, or 18° south of east, and two fissure eruptions on the line have the same trend (Figure 2). A parallel fault zone, running from Ljosufjoll in the western part (Figures 2 and 10) to Grabrok in the eastern part, coincides with the volcanic line. Many of the faults in the Ljosufjoll-Raudimelur region are post-glacial and post-date some of the younger lavas.

On continuation of this volcanic and tectonic line into the bay of Breidafjordur to the north-west, two shallow-depth cones rise to within 26 metres of the ocean surface (Figure 2).

The coincidence of these youthful submarine features with the Snaefellsnes volcanic zone may indicate former submarine activity in the WNW part of the volcanic zone. Snaefellsnes is generally regarded an aseismic region, but at least six events have been recorded in the eastern part, although of a magnitude less than 5 in the period from 1912 to 1962 (Tryggvason, quoted in: Ward et al. 1969).

During the last glacial a number of sub-glacial eruptions occurred on Snaefellsnes, giving rise to palagonite tuff and basalt breccia mountains and, in one case, a table mountain (Grimsfjall) where volcanic action was sufficiently vigorous to extend the vent well above the glacial surface. Distribution of volcanoes from the last glacial is very close to the volcanic line followed by many of the Recent eruptions and clearly the same tectonic control was active (Figure 2).

Going deeper down the succession we find that lavas from the last interglacial were also erupted from this zone in northern and eastern Snaefellsnes, but are more abundant in the central and western part of the peninsula, notably in an area from Ellidatindar in the east to Hofdakulur in the WNW, including also the Setberg Late-Quaternary basalts. Evidence from the Setberg area (p. 61) and preliminary work in nearby regions indicates that here another line of craters or plugs

stretches in a WNW or westerly direction, forming a predominantly Late-Quaternary volcanic line parallel to the active volcanic line in the north-eastern part of Snaefellsnes and spaced 10 km apart (Figure 2). A considerable overlap exists in the period of activity of the two lines: a large amount of Quaternary rocks is associated with the eastern and younger line, and likewise the Recent lavas of Blafeldarhraun and Hraunsmulahraun are probably associated with the predominantly Late-Quaternary volcanic line of central Snaefellsnes. Generally speaking, however, Quaternary volcanism in central Snaefellsnes is older and includes some "reverse" magnetized lavas of the Brunhes geomagnetic period.

The active central volcano Snaefellsjokull dominates the structure of western Snaefellsnes and no systematic distribution of the many craters around this volcano is evident, but further work now in progress by Sigurdur Steinthorsson will clarify the picture in that part of the peninsula.

We are now able to relate the Quaternary and Recent volcanic activity on Snaefellsnes, outside the Snaefellsjokull area, to two major volcanic fractures striking WNW. Further fieldwork may confirm the presence of such fractures

in the western part of Snaefellsnes also, and establish the apparent en echelon pattern of the fractures, but from the available evidence we shall attempt to account for the hitherto problematical westerly trend of the Snaefellsnes volcanic zone, striking at right angles to the major rift zones of Iceland.

The concept of crustal spreading as applied to the evolution of the Icelandic lava pile (Bodvarsson and Walker, 1964) has done much to revitalize geological thinking in Iceland - pro and contra. The simple hypothesis of an east-west spreading due to dyke injection in a north-south trending volcanic zone (part 1 in Figure 12) is probably valid for much of the Mid- to Late-Tertiary as indicated by the predominant northerly trend of dykes and dyke swarms in almost all parts of Iceland except Snaefellsnes (Sigurdsson, 1967).

At some stage near the very end of the Tertiary or in early Quaternary time the major north-south trending volcanic zone was joined by, or even partly replaced by, another north-south zone approximately 100 km to the west. For a while the western zone was active along its entire length from Thingvellir to Skagi (Figure 3), producing in the northern part the Quaternary formation of Skagi and

Skagafjordur, Maelifellshnukur, etc., ranging in age from 1.5 to 0.5 m.y. (Th. Einarsson, 1968). North of Iceland the Kolbeinsey ridge forms a continuation of the active volcanic zone, although displaced by a transform fault 100 km to the west (Sigurdsson and Brown, 1970). In Skagi the western volcanic zone strikes north towards the Kolbeinsey ridge, probably a fair indication that these zones were united when the Skagi area was an active part of the western volcanic zone (part 2, Figure 12).

In Late-Quaternary the northern half of the western zone, from Langjokull to Skagi, became inactive, probably near the end of the Pleistocene, whereas the southern half, from Langjokull to Thingvellir, continued activity to Recent time but no historic eruptions have taken place in this half (Figure 3).

Numerous open fissures and considerable volcanicity in the Thingvellir-Langjokull volcanic zone indicate that crustal spreading has been significant here after termination of all activity directly to the north, in the Langjokull-Skagi area. The fact that no spreading was taking part in the north of this western zone at the time of activity in the south, indicates that crustal movement effected by the volcanicity and dyke injection in the Langjokull-Thingvellir zone must have been dissipated by other means, either by a transform

fault eastward to the main central volcanic belt, or by transcurrent faulting westwards, through the Snaefellsnes region, to the western edge of the Icelandic shelf. The effect of an east-west trending transform fault would be to translate spreading from the Langjokull-Thingvellir zone to the northern part of the eastern volcanic zone. Evidence for such an east-west structure, running between the two main volcanic zones, may lie in the presence of small craters of Recent age. These are scattered in an east-westerly direction in this region, including the E-W trending fissure eruption of Dvergar, and run at right angles to the fissures of the volcanic belts, to the west and east (Figures 3 and 12).

In Late-Quaternary and Recent time we thus had a state of affairs where the entire eastern zone was active, plus the southern limb of the western volcanic zone, from Thingvellir to Langjokull, as well as the Reykjanes zone. Thus two parallel zones were, in effect, active in the south and only one in the north. The total spreading rate of these

---

Fig. 12: A diagrammatic reconstruction of the proposed evolutionary pattern of the Icelandic rift zones. 1 represents the relatively simple structural framework of Tertiary times, while in 3 the complex relationship of the central volcanic zones (see text) is considered to propagate a transcurrent fault into Snaefellsnes.

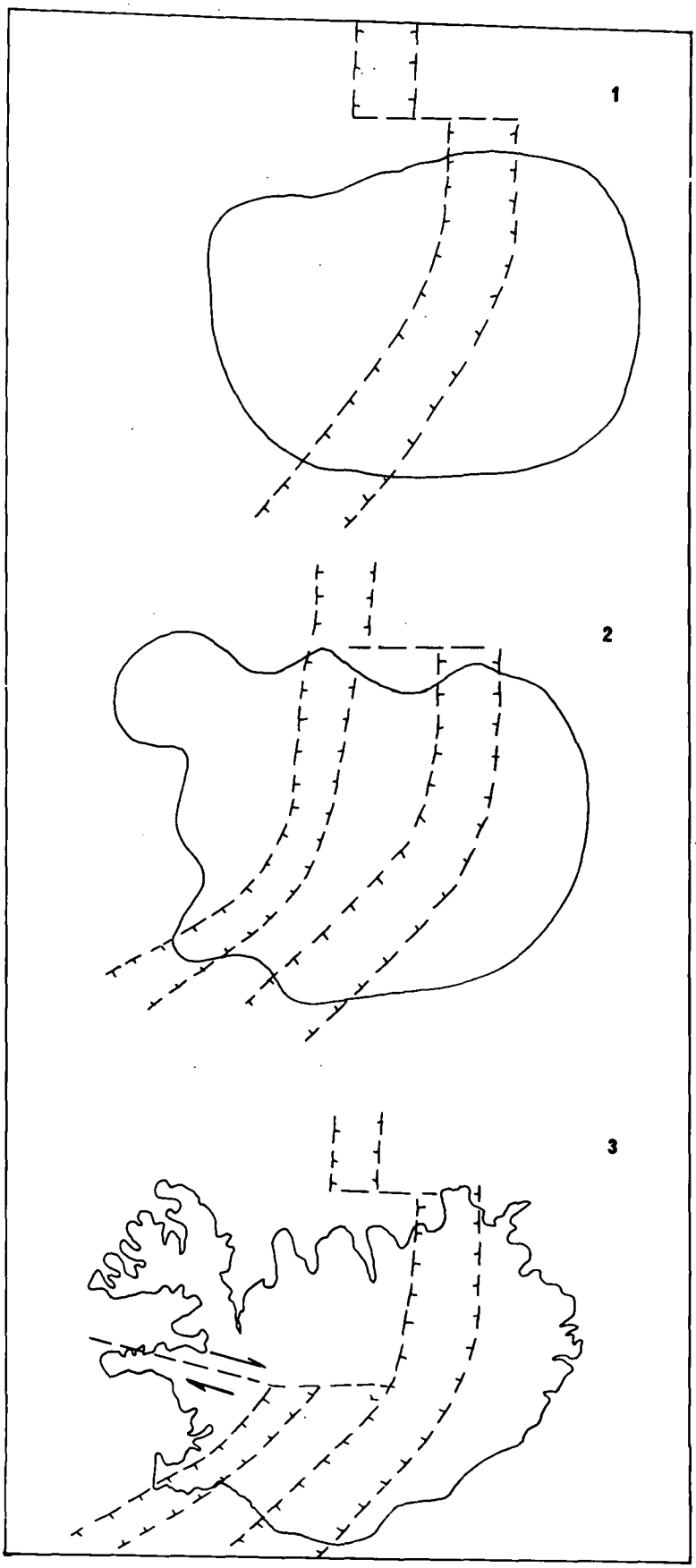
1
2
3

two southern zones in relation to the single northern volcanic zone is very important to our hypothesis regarding the origin of the Snaefellsnes zone, running at right angles to them.

Firstly, if we assume that the two southern zones, east and west, were behaving more-or-less as a single volcanic zone, in direct continuation of the northern zone, an equal spreading rate prevailed throughout Iceland. If, on the other hand, the western zone (Thingvellir-Langjokull) was active independently of the eastern zone, then spreading in the Thingvellir-Langjokull region would be in excess of that in the northern part and this would result in dis-equilibrium of spreading rates for north and south Iceland (Figure 12).

Viewing eastern Iceland as a single stable plate, such dis-equilibrium of spreading rates in south and north Iceland could only result in a breaking-up of the western part of the Icelandic crust into two plates, thus propagating the transform fault of central Iceland in a westerly direction and resulting in a transcurrent fault through the Snaefellsnes peninsula, from east to west. The presence of such a fault in Snaefellsnes, as has been established in the discussion above (p. 63), must be viewed as very suggestive evidence in support of this hypothesis for the crustal tectonic evolution of Iceland.

The two main volcano-tectonic lines on Snaefellsnes have been interpreted above as WNW en echelon fractures and it is encouraging to note that transcurrent faulting with a left-lateral movement would produce such fractures, e.g. when a southern plate is moved westerly in relation to a more slowly moving northern plate.

According to the hypothesis presented here, the Snaefellsnes volcanic zone is not a primary volcanic zone in the classical sense of a tensional rift about a mid-oceanic ridge axis, such as is envisaged for the central zones of Iceland (Bodvarsson and Walker, 1964), but principally a transcurrent-fault zone generated by differential spreading rates in north and south Iceland. The presence of deep lying faults in the area has made the rise of small amounts of magma possible in the fault zone, with unusual chemistry and of small quantity as compared with the primarily tholeiitic volcanism of the central Icelandic volcanic zones.

In comparing the Snaefellsnes volcanic province with the provinces of the central rift zone, the following points are important:-

(a) Non-dilatory strike-slip faulting in Snaefellsnes contrasts with the E-W tensional tectonic framework of the central zone.

(b) Rate of volcanicity and heat flow is high in the central zone, whereas the Snaefellsnes province is relatively "cold".

(c) The alkalic basalt volcanism of Snaefellsnes is in contrast to the dominantly tholeiitic volcanism in the central zone.

These observations have an important bearing on hypotheses of magma generation in these areas. The high heat flow and voluminous tholeiitic volcanicity of the tensional central zone reflects a steep thermal gradient and possibly melting in the mantle at shallower level than in areas of low heat flow. Kushiro (1965) and many other authors have suggested that the composition of magmas, produced by partial melting in the mantle, becomes more silica-poor with increase in pressure at which melting occurs. Fall-off of heat flow, and consequently of mantle isotherms, with distance from the central zone will constrain partial melting to deeper levels of the mantle in outlying areas, such as the Snaefellsnes province, some 200 km west of the central zone, resulting in more silica-poor parental magmas.

CHAPTER III: PETROGRAPHY OF THE SETBERG AREA

A. Rock classification

"Terminology is a matter of language and has little to do with scientific thought," writes A. Streckeisen (1967) who then proceeds to construct a highly elaborate scheme of classification and nomenclature of igneous rocks. Any classification imposes arbitrary and usually unnatural boundaries on analytical data, particularly when such a scheme is not based upon some petrogenetic aspects. Such a genetic classification is not yet available, however, and the increasing abundance of analytical data makes the shortcomings of existing schemes all the more evident, particularly as transitional types have to be reckoned with, illustrating all gradations between the main, long-recognized rock series.

A classification scheme for the rocks of the Setberg area must serve to identify and separate the two basaltic series, alkalic basalts on the one hand and tholeiites on the other, each with their close differentiates, and furthermore such a classification would serve the purpose of dividing the group of acid rocks into characterisable units. To this end a chemical classification is adopted, based on a number of factors. The main factors employed are the differentiation index (D.I.) of Thornton and Tuttle (1960), the weight

percentage of various oxides, the CIPW-normative mineralogy, and the trace element data - particularly the concentration of strontium. The solidification index (S.I.) of Kuno (1968) has been used to divide the various types of basaltic rocks within each rock series.

1. Classification of basalts

Considerable difficulty is encountered when attempting a simple basalt classification for the Setberg lavas. The widely used CIPW-normative classification of Yoder and Tilley (1962) is an indirect chemical classification in the "basalt tetrahedron". By virtue of their position within this tetrahedron, basalts are termed tholeiites, olivine-tholeiites or alkalic basalts. The objective grouping of this classification is desirable, but tends to create artificial clarity, particularly in the case of "olivine-tholeiites". The effect of oxidation has, in particular, a critical influence on the normative mineralogy of lavas lying near the "critical plane of silica undersaturation", and a weakly Ne-normative magma may plot in the tetrahedron as a Hy-normative rock if it has suffered slight post-magmatic oxidation.

Poldervaart (1964) showed that some Hy-normative basalts do not possess olivine reaction relationships,

i.e. those falling in the volume Di-Fo-Pl-X in the basalt tetrahedron, where X is the point of intersection between the join Pl-Opx and the line from Fo to the peritectic point in the system SiO_2-Pl-Fo. The volume Di-Fo-Pl-SiO_2 should be, according to Yoder and Tilley (op. cit.), alien to alkalic basalts at low pressures, and is indeed so to Ne-normative basalts, when these are plotted in the basalt tetrahedron. But here also an area exists where there is no reaction relationship between olivine and pyroxene; the area between the Fo-Di join and a line drawn from the Fo corner to the thermal divide on the Di-Opx join. Basalts plotting in this region are petrographically alkalic basalts, as shown by Poldervaart (op. cit.), although Hy-normative. The presence of such basalts and other transitional types is not accounted for in the classification of Yoder and Tilley, where they would be lumped under the heading "olivine-tholeiites" (containing normative Ol and Hy), thus often giving the false impression of a tholeiitic parentage. The term olivine basalt, which formerly spanned a considerable range of basalt compositions, as applied in common usage, was allocated by Yoder and Tilley to basalts with normative Ol only. As pointed out by Macdonald and Katsura (1964), this reduces the olivine basalts almost to a vanishing point, as very few olivine basalts indeed have

neither Hy nor Ne in the norm.

In this account we shall follow broadly the classification of Yoder and Tilley (1962), based on the basalt tetrahedron, but for the definition of olivine basalts, which here is expanded on the basis suggested by Poldervaart (1964), where some of the volume of olivine-tholeiites is included. The following terms are used to define the principal basaltic rock types in the Setberg area:-

Quartz tholeiite: basalts with normative Hy and Qz. Lavas lying close to the plane of silica saturation, i.e. with Di, Hy and Pl as the principal normative components and very little Qz or Ol, are termed tholeiites.

Olivine tholeiites: normative Ol and Hy, but where $Ab-2En(Hy)-1.5Fs(Hy)<0$. This value, taken from Poldervaart (1964), serves to demarcate the olivine tholeiites and the olivine basalts, and is referred to as the Poldervaart Index (P.I.) in the following discussion. Ab is the normative content of Albite, En and Fs are the normative contents of Enstatite and Ferrosilite in Hypersthene. The Poldervaart Index is positive for olivine basalts but negative for olivine tholeiites.

Olivine basalt: normative Ol and Hy, but Poldervaart Index $Ab-2En(Hy)-1.5Fs(Hy)>0$.

Alkalic basalt: basalts with normative Ol and Ne, but with the latter less than 5%.

The main pitfall of a normative classification like the one outlined above is the question of oxidation, which will of course shift a rock-composition towards the silica corner in the normative basalt tetrahedron. Oxidation is common among the rocks of the Setberg area, and some oxidation has even demonstrably taken place during the fine grinding of the samples. It is therefore necessary to adjust the ferrous/ferric iron ratio of many of the analyses of older basalts from the Setberg area in order to achieve a meaningful normative composition. It is unfortunate that an exact knowledge of the oxidation state of the iron in these magmas is not obtainable from our data, as this knowledge is very critical when dealing with transitional basalts where a slight change in oxidation state results in a very significant difference in normative mineralogy.

The division of the basaltic types within each rock-series is facilitated by the value of MgO x 100 / MgO + Fe_2O_3 + FeO + Na_2O + K_2O, or Solidification Index (S.I.) (Kuno, 1968) corresponding to the value of "M" in the AFM triangular plot. The Solidification Index is a much more sensitive measure of the chemical variation in basaltic

rocks than the differentiation index of Thornton and Tuttle, which is better suited to intermediate and acid rocks. The solidification Index is perhaps most useful when dealing with the transitional basalt types, neither distinctly alkalic nor tholeiitic, and where oxidation has a critical influence on the normative mineralogy. Consequently this parameter (S.I.) has been employed in the basalt classification along with the normative classification.

2. Classification of differentiated rocks

The so-called differentiated rocks, i.e. lavas of intermediate and acid composition, present fewer problems of classification due to the dichotomy of the alkalic and tholeiitic basalt trends on differentiation.

The intermediate types of the alkalic rock series are classified, with increasing alkalinity, into hawaiites, mugearites and benmoreites, broadly following Tilley and Muir (1964) and Macdonald and Katsura (1964). Details of this scheme are given in Table 1.

The same terminology and chemical definitions are used for the tholeiitic differentiates as Carmichael (1964) applied to the intermediate rocks of the Thingmuli central volcano in Eastern Iceland, and are also laid down in detail in Table 1 where the boundaries assigned to each

Table 1: Chemical Classification of Differentiated Rocks

	ALKALIC SERIES					THOLEIITIC SERIES			
	Hawaiiite	Mugearite	Benmoreite	Quartz-Trachyte	Comendite	Basaltic Andesite	Icelandite	Rhyo-Dacite	Rhyolite
D.I.	35-45	47-57	60-70	80	90	45-60	60-75	85-90	90-95
Na_2O+K_2O	5.0-6.0	6-7.5	7.5-10	10	9	4-6	6-7	7.5-8.5	8-9
Ab (norm)	30-35	35-45	45-55	57	35-45	29	37	38	35-45
Or (norm)	7-10	10-15	15-20	24	25-30	7	11	25	25
Sr (ppm)	425	500	500	100	10	350	320	150	50
SiO_2	48-50	50-55	53-57	63	70-75	53-57	60-67	66-70	68-75
Fe total	12	10	5-8	4	3-5	10-15	9	3-5	2-3
Na_2O/K_2O	2.8	2.5	2.0	1.5	1.0	3.0	2.0	1.3	1
Feldspar	An>Or	Or≥An	Or>An	Or≫An	Ac	Ab>Or	Ab≥Or	An=Or	Or>An
S.I.	23-16.5	16.5-12.5	10-7		2	20-10	10-5	5	

rock-type are indicated. A certain amount of overlap is unavoidable when dealing with many parameters, but the differentiation index (sum of normative Qz, Ab, Or and Ne, when present) is a convenient scale for classification.

The amount of strontium present in a rock has turned out to be a good indicator of rock-type, particularly in the alkalic series, and observed ranges of strontium concentration in the various rock types are included in Table 1.

The term ankaramite, as used here, refers to highly olivine- and augite-phyric basalt lavas with 10 to 16% MgO, often Ne-normative. They do, however, contain 40-50% normative feldspar and up to 47% SiO_2, whereas Hawaiian ankaramites sensu stricto have approximately 30% normative feldspar and about 44-46% SiO_2 (Macdonald and Katsura, 1964). The augite-olivine-phyric lavas of the Setberg alkalic series are thus not strictly analogous to the Hawaiian ankaramites but will be referred to as such, owing to their close association with the alkalic series and for the want of a better name.

The chemical classification scheme used here, and particularly the distinction between the various basaltic types, is further reinforced by mineralogical criteria,

particularly the pyroxene mineralogy as discussed in a later chapter.

B. Petrography of Tertiary and Mid-Quaternary rocks of Tholeiitic and Transitional series

Petrographic descriptions of the main rock types in the Setberg area are given in this chapter, but whole-rock chemistry and analytical data on individual mineral phases are discussed in subsequent chapters.

The petrography of igneous rocks from Centres 1 and 2 (Tertiary and Mid-Quaternary, respectively) is discussed under a joint heading due to many similarities of these two rock suites, while the Late-Quaternary alkalic series is treated separately. The term "transitional" series is used here in a sense similar to that employed by Coombs (1963), who thus designated the mildly alkaline basalts of Ascension, Reunion, Easter Island and Mauritius, all characterized by high normative Hy and Ol, and a general lack of calcium-poor pyroxenes.

1. Gabbros of Centre 1

The Kolgrafamuli gabbro is by far the largest gabbroic intrusion in the Setberg area, with over 6 km^2 exposed at the surface. The gabbro is a coarse grained rock (107, 115, 233, 234, 235, 236, 238)[1], with euhedral to subhedral

---

[1] Numbers in brackets are specimen numbers, and refer to analyses in Appendix

plagioclase laths and ophitic to poikilitic augites which reach up to 2 cm in diameter, giving a distinct mottled appearance to the rock in hand specimen. Plagioclase constitutes over 60% of the rock in rare cases, but on the whole the modal proportions of the main constituents are: 48% plagioclase, 30% augite, and 16% iron oxides. Plagioclase ranges in composition from An_{40} (margins) to An_{60} (cores), but An_{49-53} is the predominant composition. The pyroxenes are invariably augites, with very thin exsolution lamellae of another pyroxene present in rare cases. A determination of β refractive index (1.693 $\pm$ 0.001) and optic axial angle ($2V_{\gamma}$ 45°) indicates a composition of $Ca_{42}Mg_{44}Fe_{14}$ atom % (Brown and Vincent, 1963).

Iron ore is very abundant in the gabbro and forms 20% by volume in some parts of the intrusion. Typically it is in globular or irregularly rounded 1-4 mm patches that are interstitial to plagioclase and augite. Biotite is associated with the iron ore, often occurring as very small crystals in embayments or among silicate inclusions of the iron ore grains.

A characteristic feature of all rocks of this intrusion is the presence of residual areas of quartz-feldspar graphic intergrowths which in some localities, particularly on the beach north of Berserkseyri, develop into granophyric

segregations, 15 to 25 cm in diameter. These felsic residual patches contain alkali feldspar and quartz intergrowths, around sodic plagioclase laths mantled by alkali feldspar. The granophyric segregations contain euhedral, elongated crystals of ferro-augite (faint green pleochroism), up to 5 mm in length, and apatite as accessory needles. Subhedral to euhedral grains of iron ore occur alongside or within the ferroaugites in these granophyric patches.

The Kolgrafamuli gabbro is an iron-rich rock (15-18% FeO + Fe_2O_3) and it is significant that most of this must be contained in the iron oxides, which form about 16% of the rock by volume. This is reflected in the normative mineralogy, as the molecular ratio of MgO/MgO + FeO in the ferromagnesian minerals is 0.75 - 0.82, indicating the iron-poor nature of the augites, as borne out by the data on the pyroxenes.

The relatively high iron-oxidation ratio (Fe_2O_3/FeO + Fe_2O_3) of 38 to 45% displayed in chemical analyses of the gabbro can be regarded as a primary feature and not due to subsequent post-magmatic processes, and the common acid granophyric patches and segregation veins within the gabbro may thus owe their origin and abundance to the silica enrichment resulting from an early oxidation of a basic magma. Further evidence of high oxygen pressure in the original Kolgrafamuli

magma is the presence of biotite in association with the iron oxides.

The absence of olivine, and abundance of interstitial acid material indicate the quartz-tholeiite nature of the magma.

2. Gabbros of Centre 2

The Thorgeirsfell intrusion forms an arcuate body in the southern periphery of Centre 2 (254, 417, 447). The rock ranges in texture from a plagioclase-augite-olivine-phyric doleritic marginal facies to a very coarse grained, plagioclase-cumulate rock. Plagioclase forms 3-10 mm long, euhedral laths of bytownite, zoned from An_{80} cores to narrow An_{60} margins in the cumulate facies. Phenocrysts in the doleritic marginal facies are continuously zoned from An_{80} cores to An_{40} margins.

The gabbro contains only one type of pyroxene, an augite forming intercumulus poikilitic regions up to 5 cm in diameter in the cumulative gabbro. Olivine, pseudomorphed by serpentine, forms discrete grains and iron ore is present but much less abundant than in the Kolgrafamuli intrusion. The gabbro has suffered considerable alteration and epidote, chlorite, calcite and pyrite are frequently present in substantial amounts. Analyses of the freshest available material reveal an olivine basaltic composition,

but an analysis of a "bytownite gabbro" from this intrusion, by Tyrrell (1949), is Ne-normative (3.3% Ne) and otherwise very comparable. The Mid-Quaternary age of the Thorgeirsfell intrusion was discussed on p.44 and the olivine basaltic composition of the gabbroic magma gives a further link with the transitional rock series of Centre 2.

The Lysuskard gabbroic rocks are unusual in many respects (248, 249, 218). The ubiquitous presence of biotite and frequent presence of hornblende as well, characterize their mineralogy. Most voluminous are euhedral to subhedral plagioclase laths 2-4 mm long, ranging in composition from An_{55} cores to An_{40} margins in the main gabbro and to An_{30} margins in the more feldspathic facies of the gabbro, where alkali feldspar and quartz interstitially form graphic intergrowths.

Diopsidic augite forms 1-2 mm granules in the gabbro, occasionally rimmed by hornblende, but augite occurs less commonly as ophitic patches enclosing plagioclase laths. Hornblende and biotite are important constituents, the former rimming pyroxene or replacing the augites, giving a sieve-texture. The biotite occurs as large, irregular flakes in the interstitial areas, up to 4 mm in diameter. Quartz and alkali feldspar are present interstitially in

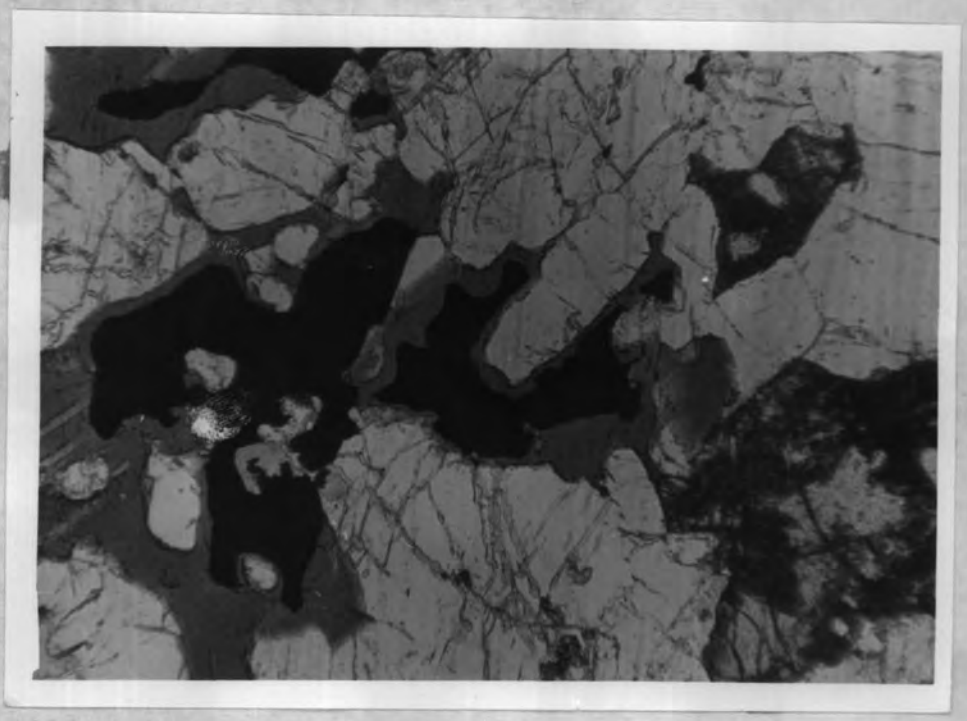

Fig. 13: Biotite (rimming iron ore), plagioclase and augite in the Lysuskard gabbro (249), x 60.

Fig. 14: Ophitic texture in the Stekkholl gabbro (252), x 60.

all samples from the Lysuskard gabbro, although in varying amount. Apatite needles are an abundant accessory.

Chemically the Lysuskard gabbro shows some unusual features, the most striking being a low iron enrichment ratio (FeO/MgO + FeO) of 0.54, combined with a low TiO_2 content (1.5%). Normative features are a high Hy content (15-19%) and a tendency to straddle the Qz-Ol boundary in the basalt tetrahedron, one sample containing 0.2% normative Qz and another, 0.5% normative Ol.

The Lysuskard gabbro, like other basic rocks of Centre 2, falls between typical tholeiitic and alkalic rock series with respect to chemistry, as is illustrated by the alkalis/SiO_2 plot. The gabbro is differentiated with respect to alkalis, titania and silica, but not magnesium. The chemistry and mineralogy is thus indicative of the differentiation process of a relatively "wet" basic magma which, instead of producing an iron enrichment trend, resulted in the early separation of iron-titanium oxides. Mineralogically and chemically the gabbro has affinities with the calc-alkaline rocks and compares with the average Cascades basalt (Carmichael, 1964) in low TiO_2 and low iron ratio, but is unlike the basaltic rocks associated with orogenic series in having a low Al_2O_3 content (15.1-15.9%).

Carmichael (op. cit.) has emphasized the contrast between the tholeiitic Thingmuli series of eastern Iceland, where an early low, constant oxygen content led to iron enrichment, and the orogenic series of Cascades lavas where a constant partial pressure of oxygen led to early separation of the magnetite phase. The presence of hydrous minerals (biotite and hornblende) in the Lysuskard gabbro is clear evidence of a volatile-rich magma, leading to high oxygen fugacity during crystallization. Thus a high and rather constant oxygen pressure would lead to a low iron ratio.

Minor gabbroic intrusions occur in four localities in the Setberg area. The outcrops at Tradir (242) and Stekkholl (252) in the south consist of olivine-bearing rocks, with 1-2 mm long, subhedral laths of plagioclase ranging from An_{70} to An_{55} in composition. Augite is the sole pyroxene phase, forming ophitic patches in the Stekkholl gabbro but of granular habit in Tradir. Chemically the olivine gabbros resemble the Thorgeirsfell olivine gabbro intrusion, although tending towards a more olivine-tholeiitic composition, in keeping with the transitional nature of the basaltic rocks in Centre 2.

Gabbroic xenoliths have been found in three localities within the Setberg area, all within the Late-Quaternary alkalic series. A very coarse-grained (1-2 cm)

plagioclase-rich gabbro (213)[1] was found in an olivine-basalt pillow lava at Axarhamar. The xenolith consists predominantly of subhedral plagioclase (An_{80-60}) with intergranular pyroxenes. Augite is the predominant ferromagnesian mineral, of the composition $Wo_{42}En_{43}Fs_{15}$[2], accompanied by a faintly pleochroic bronzite, En_{70}. Olivine grains, up to 4 mm in diameter, are often rimmed by bronzite granules.

No iron-oxides are present in this rock, which is considered a fragment of a coarse grained, plagioclase cumulate. The chemistry of the xenolith faithfully reflects the mineralogy, and the norm includes 3% Ol and 8% Hy, suggesting tholeiitic affinities.

Two other xenoliths, petrographically related to the above-described, two-pyroxene xenolith from Axarhamar, have been found in Horn (1208) and Helgrindur (405), some 4 and 14 km directly east and west of Axarhamar respectively. The Horn fragment is a granular gabbro with 1-2 mm plagioclase grains (An_{50-55}) and two pyroxenes: an augite and smaller, less abundant grains of bronzite. The

---

1) Numbers in brackets are specimen numbers, and refer to analyses in Appendix

2) Pyroxene analyses are expressed in molecular weight per cent, unless otherwise stated, and are derived from electron microprobe analysis.

Helgrindur xenolith is similar in texture, with plagioclase of An_{60} composition, large subhedral to euhedral augite (2-3 cm) containing narrow exsolution lamellae of ortho-pyroxene parallel to 100, and smaller granular aggregates of faintly pleochroic bronzite.

All three xenoliths show the type of pyroxene relations usually associated with tholeiitic magmas, but were carried to the surface by alkalic or olivine basalt lavas in all cases. We therefore do not interpret them as cognate inclusions but rather as fragments of pre-Mid-Quaternary gabbroic bodies associated with the predominantly tholeiitic magmatic activity on Snaefellsnes in late-Tertiary and Mid-Quaternary times.

3. Granophyres of Centre 2

The Lysuskard cone sheet is by far the most extensive granophyric or acid body in the Setberg area, and has been sampled extensively. The rock is very fresh and typically made up of 1-3 mm, euhedral to subhedral, strongly zoned plagioclase (An_{25-40}) rimmed by alkali feldspar, which also occurs independently as subhedral grains. Intergranular, graphic intergrowths of quartz and alkali feldspar make up a large proportion of the rock, except in some textural varieties, which lack the graphic texture and consist of granular aggregates of quartz and alkali

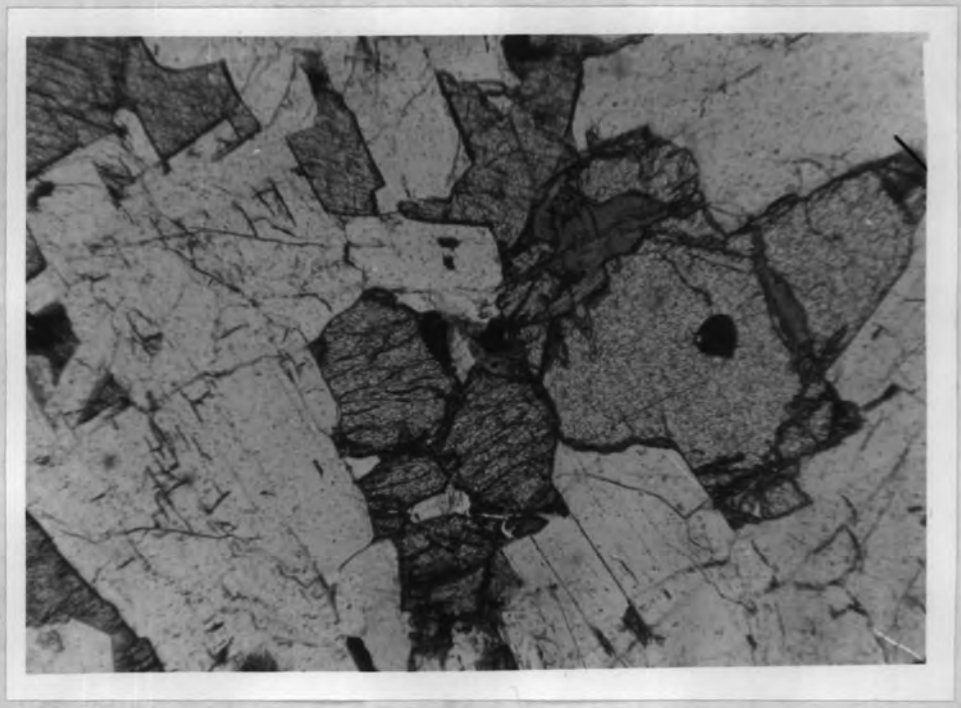

Fig. 15: Granular olivine in the Tradir gabbro (242), x 60.

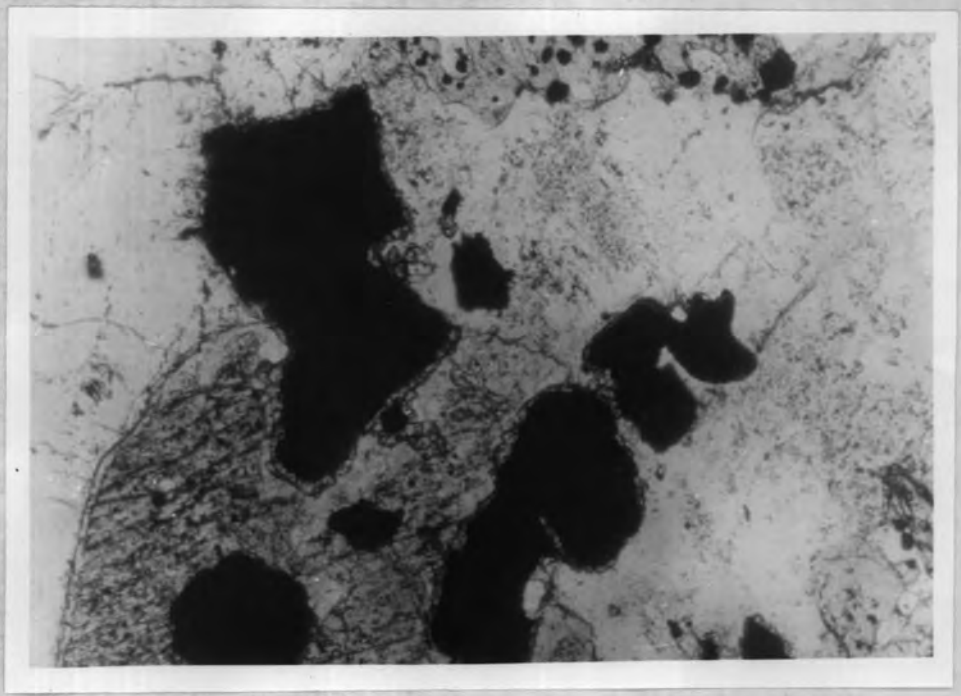

Fig. 16: Photomicrograph of the Lysuskard cone sheet, showing fayalitic olivine rims on iron ore and ferroaugite rimmed and penetrated by hornblende, giving a sieve-texture (221), x 110.

feldspar, tending towards a granitic texture.

Greenish, faintly pleochroic ferroaugite crystals are elongated and up to 2 mm in length. They range in composition from $Ac_2Wo_{39}Fs_{30}En_{29}$ to $Ac_{22}Wo_{29}Fs_{23}En_{26}$, showing a complete range from large greyish augite phenocrysts, to aegirine-augites of greenish colour occurring as groundmass constituents or as rims to the augitic crystals. The felsitic marginal facies of the cone sheet contains the most acmitic pyroxenes encountered in the intrusion, showing strong pleochroism from green to pale-green and very small extinction angle.

Olivine is present, although somewhat rare, and forms 1-1.5 mm long, pale-yellow crystals, often pseudomorphed by brown-coloured mineraloids. Fresh olivines have the composition Fo_{16-20} [1]. Iron ore grains are common throughout the granophyric cone sheet.

The six specimens from the Lysuskard granophyre which have been analyzed (221, 223, 226, 227, 228, 229) show a small compositional range. They are characterized by a high total iron content ($FeO + Fe_2O_3 = 4.7 - 6.0\%$), SiO_2 = 66 to 69% and rather high total alkalis (8.5 - 9.8%). In

---

[1] Olivine compositions were determined with the microprobe and are quoted as mol. %.

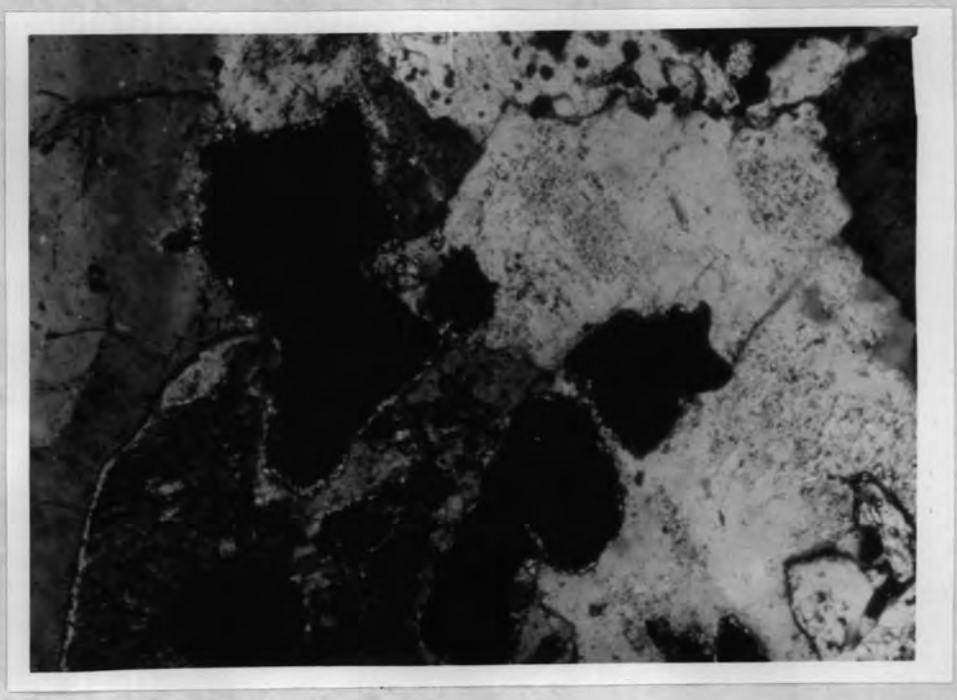

Fig: 17: Lysuskard granophyric cone sheet, as Fig. 16, but crossed nicols, x 110.

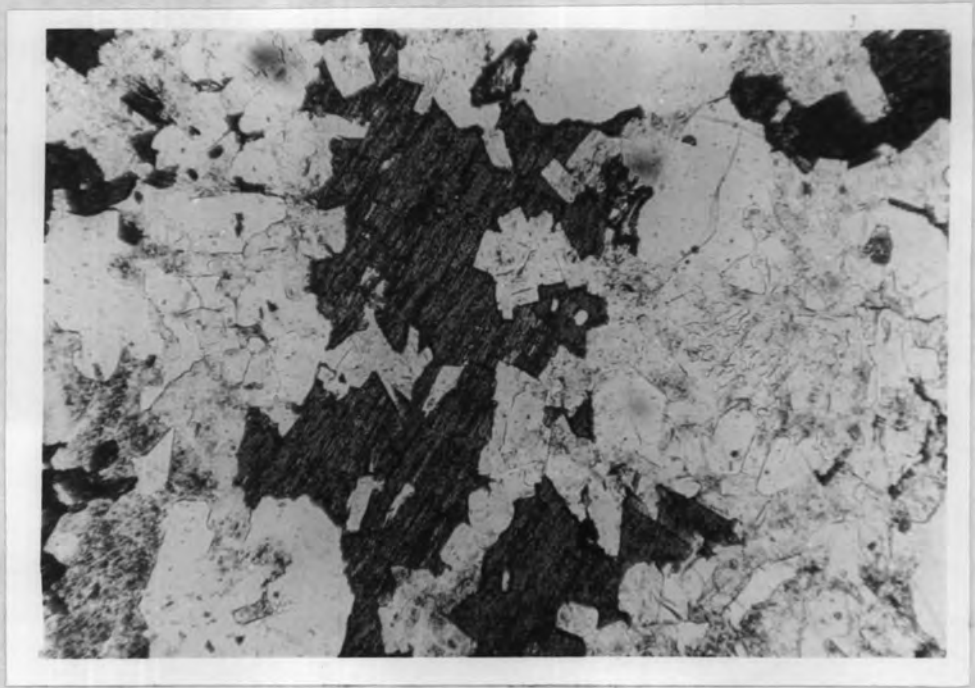

Fig. 18: Arnardalsskard granophyre, showing large, ophitic areas of sodic amphibole (505C), x 60.

order to distinguish this rock of somewhat intermediate composition from the rhyolites proper, the Lysuskard granophyre is referred to as a rhyodacitic granophyre, although normative Or is greater than normative An and not equal, as is the case with rhyodacites sensu stricto.

A pleochroic, yellowish-brown to pale-brown hornblende occurs in some parts of the Lysuskard granophyre, as small interstitial grains or, more commonly, as rims around the ferroaugites, penetrating deep into the augite host in an irregular manner to give a "sieve texture", (Figure 16). The iron-titanium oxides in the hornblende-bearing varieties of the granophyre are frequently mantled by a thin rim of olivine of fayalitic composition.

Arnardalsskard granophyre: a small outcrop of granophyre on the south slope of Arnardalsskard forms an intrusion of considerable similarity to the Lysuskard cone sheet, in chemistry and mineralogy. It is Mid-Quaternary and thus forms the westernmost occurrence of acid rocks in Centre 2.

The intrusion consists of two textural facies (505): a felsitic rock in the outer part and a granophyric, more coarse grained rock in the interior. The felsite is a slightly porphyritic rock, with 3-5 mm long, euhedral laths of plagioclase (An_{20-30}) rimmed by an alkali feldspar.

Phenocrysts of anorthoclase are also present, although less abundant. Pyroxene forms elongated crystals of ferroaugite, showing faint pleochroism and more intense pale green to green colours on grain margins.

The granophyric variety is made up of subhedral anorthoclase-oligoclase laths, 2-3 mm long, surrounded by smaller anhedral grains of quartz and sodic feldspar, with interstitial granophyric or graphic frets. A strongly green- to brown-pleochroic amphibole forms subophitic patches interstitially (Figure 18), reaching up to 3 mm in length. The amphibole is probably of the ferrohastingsite variety, and is associated with small grains of aegirine-augite. Iron-oxides are absent from this rock.

4. Felsites of Centre 1

Several of the acid cone sheets in Centre 1 of the Setberg area, notably in Gerdishamrar and Lambahnukur, consist of a distinctive, rather dark-coloured felsite (303, 101, 255) containing scattered, 2-4 mm long, euhedral plagioclase phenocrysts. In thin section the feathery areas surrounding the phenocrysts are a striking textural feature (Figure 19), resulting from a rapid growth of a continuously zoned plagioclase, containing abundant stringers of glass inclusions. The plagioclases range in

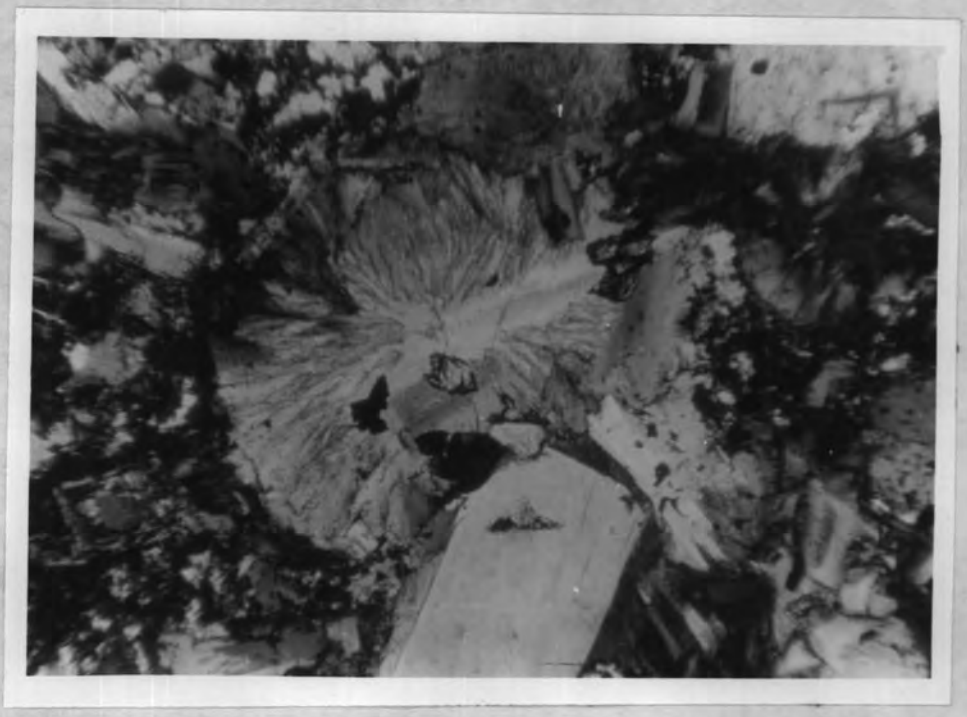

Fig. 19: Feathery growth around plagioclase in the Gerdishamrar felsite of Centre 1 (255), x 60, crossed nicols.

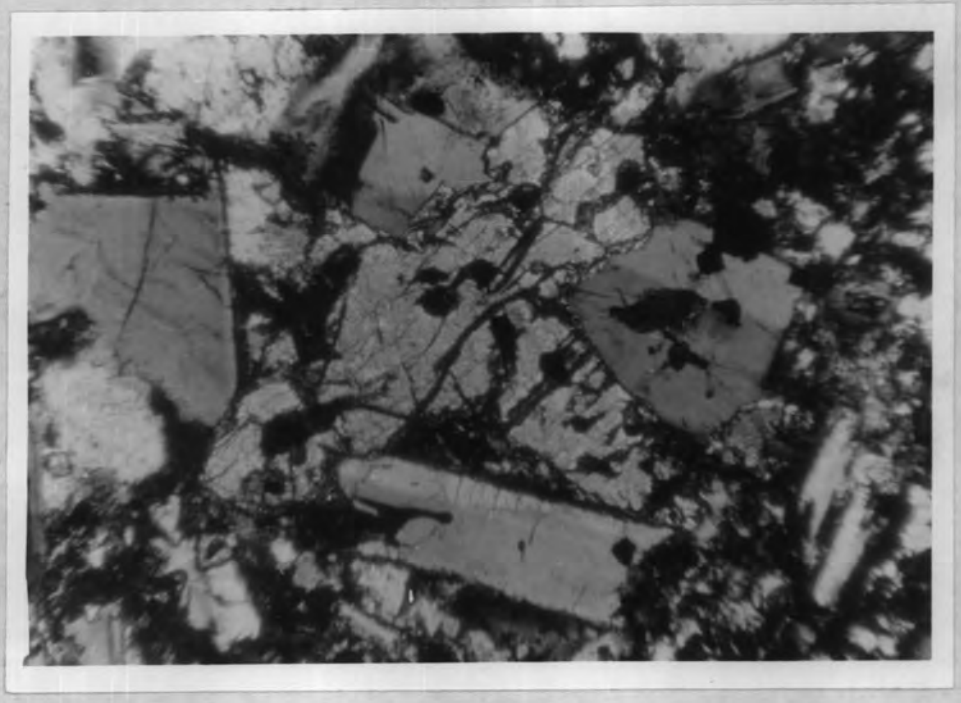

Fig. 20: Fayalite phenocryst, partly enclosed by plagioclase, in the Gerdishamrar felsite (255), x 60, crossed nicols.

composition[1] from An_{30} to An_{15}, but alkali feldspar and quartz occur in the micrographic groundmass. Up to a quarter of the felsites consists of brown glass, finely distributed throughout the interstitial areas and often enclosing small, swallow-tail oligoclase laths.

Pyroxenes form pale-green, elongated phenocrysts up to 3 mm long, consisting of ferrohedenbergite which ranges in composition from $Wo_{38}En_{14}Fs_{48}$ to $Wo_{40}En_{3}Fs_{57}$. They form up to 7% by volume of the rock, and range in size to minute groundmass crystals. Pale-yellow, subhedral to euhedral olivine crystals, 1-3 mm in diameter, are often pseudomorphed by brown mineraloids, but when fresh the olivine shows an almost pure fayalite composition (Fa_{98-99}). Apatite and zircon are common accessories, as well as tiny, hexagonal, reddish and translucent plates of ilmenite or rutile. Larger iron oxide grains make up to 3% of the rock by volume.

Chemically the fayalite-hedenbergite felsites are distinctive rocks. For an acid rock containing 69-70% SiO_2 they are very iron-rich (6-7% FeO + Fe_2O_3), as reflected in their mineralogy and an iron ratio of 0.98

---

1) Composition of feldspars were determined on the electron microprobe in most cases, and are given in weight per cent An in the discussion, but detailed feldspar analyses are presented in Chapter IV.

but rather low in alkalis (7%). In many respects these felsites of the Setberg area resemble the Sydtoppen transitional granophyre of the Skaergaard intrusion (Wager and Brown, 1968), particularly in the high degree of iron enrichment.

Kolgrafir felsite

A westerly-dipping cone sheet, some 5 m thick, occurs at Kolgrafir and bears strong resemblance to the iron-rich felsites described above. The Kolgrafir felsite (509) contains 7.6% total iron, 68.2% SiO_2 and has a differentiation index of 81%. Mineralogically and texturally, however, this rock is quite different from the Gerdishamrar and Lambahnukur felsite sheets. It contains 9% of phenocrysts, set in a very fine (<0.2 mm) groundmass consisting of alkali feldspar, quartz and clino-pyroxene. The phenocrysts are of two distinct types and fall into two compositional groups. Plagioclase forms either small euhedral laths of An_{25} composition, zoned to An_{20} margins, or larger (1-2 mm) subhedral, sometimes corroded crystals of An_{45-50} composition. Many of the more calcic plagioclase grains are in a state of disintegration but others have thin overgrowths of An_{25} composition, giving euhedral form (Figure 21).

Two types of pyroxene occur in the felsite: larger

Fig. 21: Xenocryst of calcic plagioclase with thin overgrowth of sodic plagioclase, from the Kolgrafir composite felsite sheet (509), x 60, crossed nicols.

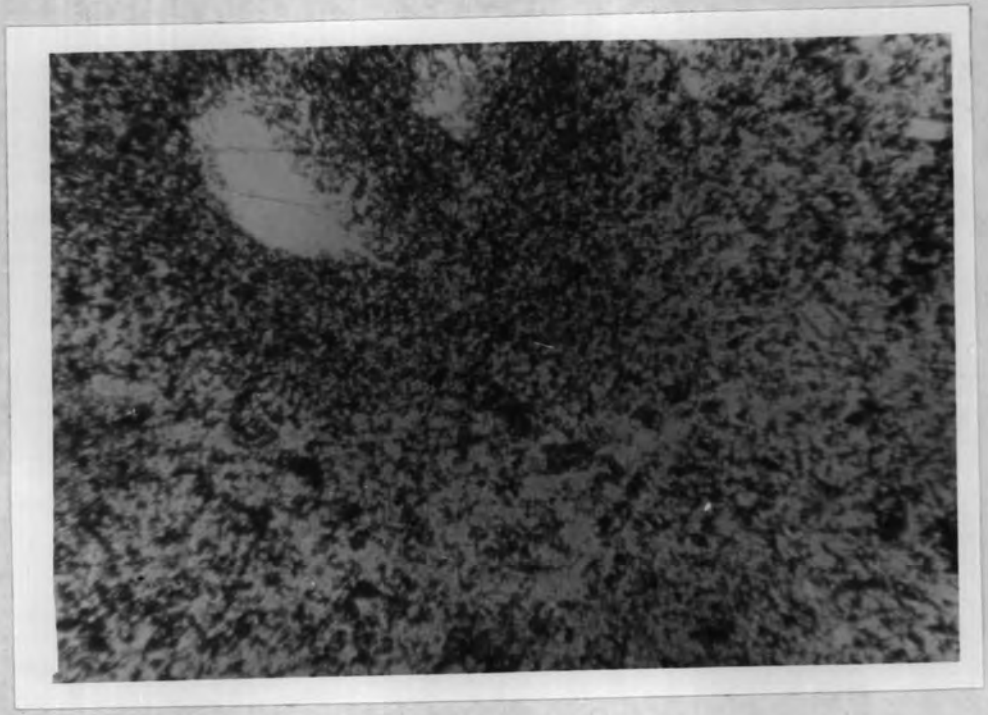

Fig. 22: Basic patch surrounding calcic plagioclase xenocryst, in the Kolgrafir composite sheet (509), x 60.

phenocrysts of greenish hedenbergite ($Wo_{39}En_2Fs_{59}$) and small brownish phenocrysts of ferroaugite, ranging from $Wo_{36}En_{40}Fs_{24}$ to $Wo_{34}En_{31}Fs_{35}$, characteristically associated with the corroded, more calcic plagioclases in glomero-porphyritic clusters. A fayalitic olivine also occurs as a phenocryst phase, forming subhedral grains up to 2 mm in diameter. Small, octahedral microphenocrysts of iron ore are present.

A distinctly mottled appearance characterizes the Kolgrafir felsite and darker, irregular areas of groundmass, 2-4 mm in diameter, occur within this generally leucocratic rock. The darker fields, which occur typically around the andesine and ferroaugite assemblages, are interpreted as the remnants of a more basic or intermediate magma which has intermingled with and been partially mixed with the acid magma making up the main body of the cone sheet. The two distinct generations of augite and plagioclase phenocrysts and the strong corrosion features suggest that the Kolgrafir felsite represents the mixture of an acid magma with a magma of basaltic andesite composition.

5. Felsites of Centre 2

The Tindar felsite

A rather fine grained, porphyritic felsite occurs as a cone sheet near the summit of Tindar, in the eastern part

of Centre 2. It has been interpreted as a possible roof facies or high-level apophysis of the Lysuskard cone sheet, which lies on the same strike (p. 46).

The Tindar felsite (259, 260) is a porphyritic rock containing 15-20% anorthoclase and oligoclase in a very fine groundmass, which varies from a trachytic texture, caused by the tabular 0.1-0.2 mm long sodic feldspar laths, to an extremely fine grained, ill-defined matrix which may be partly devitrified. Anorthoclase forms 2-4 mm long, subhedral phenocrysts with very fine quadrille structure and a medium 2V angle. Euhedral, small plagioclase laths (An_{20-25}) are less abundant. Clinopyroxene phenocrysts make up to 3% by volume and display pale-greenish to pale-brown pleochroism. Olivine phenocrysts are entirely pseudomorphed by a mineraloid, probably chlorophaeite. Microphenocrysts of iron-oxides tend to be elongated and up to 1 mm long.

The Tindar felsite is very similar in composition to the Lysuskard granophyre, in relatively low SiO_2 content (66-69%) and high total alkalis (8.5-9.1%) as well as high $FeO + Fe_2O_3$ (4.7-6.0%). If our correlation of the Tindar felsite and the Lysuskard cone sheet is valid, then some 180° of arc of this sheet is exposed at the surface in Centre 2.

6. Composite intrusions

Instances of composite intrusion are numerous in the Setberg area, and indeed in Iceland as a whole (Gibson and Walker, 1963; Blake et al., 1965). The coming together of acid and basic magma is observed in both dykes and cone sheets, particularly in Centre 1, but the rocks are highly altered in many instances and some of the mineralogical features obliterated. The Kolgrafir felsite described above (p. 98) is one example of composite intrusion, but two other occurrences will be described here.

A 7 m wide cone sheet is exposed on the beach north of Kolgrafir, stemming from Centre 1 and dipping 30° westerly. The sheet has basaltic margins, and a felsitic interior which makes up the main body of the rock. The felsite is characterised by a great abundance of basic clots and lobate bodies, a few mm to tens of cm in length, becoming more numerous towards the basaltic margins. An intimate mixing of the basic envelope and the felsic magma occurs in places, with stringers and irregular appphyses running from one rock type into the other. At the time of solidification the result of this mixing was a rather basified felsite, littered with basaltic clots. Thin sections of the felsite show a porphyritic rock, with up to 25% of plagioclase phenocrysts in a matrix of alkali feldspar and

quartz intergrowths. Plagioclase xenocrysts are subhedral, often corroded, 4 mm in length, and most often found within basified areas of the felsite. As a rule they are albitized due to later alteration, but presumably they represent former calcic plagioclase that has suffered post-magmatic alteration, in common with other rocks in the vicinity, being within the hydrothermal aureole of Centre 1. Augite xenocrysts in the felsite are up to 6 mm in length, sub-ophitic and free of corrosion.

Slender greenish ferroaugite crystals and a generation of smaller euhedral plagioclase laths are considered indigenous to the felsite.

An unusual example of composite intrusion is found near Gjafakollur where an irregular, plug-like body of highly porphyritic, brownish felsite intrudes the Tertiary basalts and the Mid-Quaternary porphyritic basalts of Centre 2. The plug is thus of probable Centre 2 age but deserves more than a cursory petrographic examination because of its unusual mineralogy. The very fresh rock (211) contains 15% oligoclase phenocrysts, 2-3 mm long and set in a fine groundmass of anorthoclase crystals, 0.1-0.2 mm long and euhedral or swallow-tailed to dendritic in habit. Brownish glass is abundant interstitially. Greenish clinopyroxene phenocrysts form 2% of the rock by

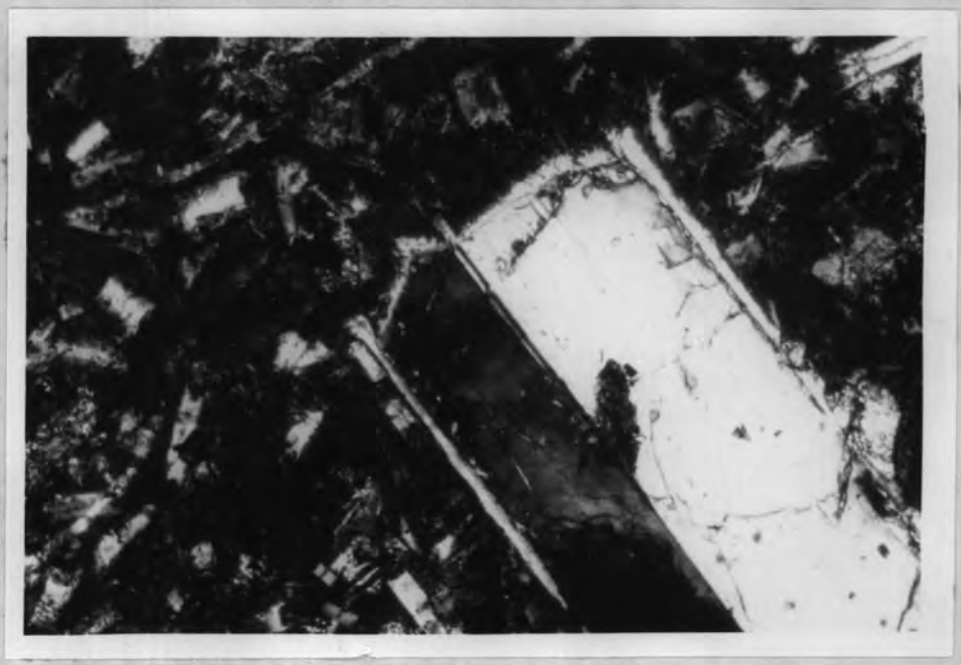

Fig. 23: Gjafakollur composite intrusion. Xenocryst of bytownite with thin outer rim of oligoclase (211), x 110, crossed nicols.

Fig. 24: Finger-print texture on margin of oligoclase phenocryst in the Gjafakollur felsite, with an outer rim of sodic anorthoclase (211), x 110.

volume. They range in size from 0.5 to 1 mm long grains, with the composition $Wo_{38}En_{28}Fs_{34}$. Iron oxide grains form microphenocrysts which are approximately 1% by volume of the rock and are typically associated with the ferroaugites.

The Gjafakollur felsite is a composite rock and although predominantly made up of acid material, basaltic patches occur, containing 2-3 mm long phenocrysts of euhedral plagioclase and augite which both form xenocrysts in the felsitic component. The basaltic plagioclase phenocrysts and xenocrysts are bytownites (An_{85}), generally euhedral to subhedral and with no signs of corrosion or resorption by the felsite, but frequently exhibiting very thin overgrowths of oligoclase ($An_{26}Ab_{66}Or_{8}$)(Figure 23). Basaltic augite xenocrysts are also unaffected by the felsite magma and have the composition $Wo_{42}En_{37}Fs_{21}$.

The abundant, indigenous plagioclase phenocrysts of the acid magma show a very striking corrosion feature (Figure 24). A rim of partial fusion, 0.1-0.2 mm wide, surrounds the entire crystal and consists of minute, irregular fragments of the original oligoclase phenocryst, enclosed by glass which ramifies the entire rim. This has given rise to a "finger-print" texture in the fused crystal margins, identical to that described by Guppy and Hawkes (1925) in phenocrysts from a composite dyke from eastern

Iceland. Similar spongy, marginal "finger-print" textures have been observed in the alkali feldspars of a partially fused granite in the vicinity of an andesite plug, by Al-Rawi and Carmichael (1967). The association of finger-print texture in sodic plagioclase phenocrysts with composite magmas is thus well documented, and such association is indeed to be expected if one considers the rise in temperature likely to occur within the acid magma as a result of intimate mixing with a much hotter basaltic magma. The temperature difference between the two magmas may be as much as 200°C.

The oligoclase phenocrysts have the composition $An_{29}Ab_{65}Or_6$ but a thin overgrowth, exterior to the fused rim, has the composition $An_{19}Ab_{67}Or_{14}$ (anorthoclase). Groundmass anorthoclase grains approach this latter composition but contain up to 17% of the Or molecule.

Feldspar compositions in the Gjafakollur felsite are shown in Figure 25, based on electron microprobe analyses.

Fig. 25: The composition of feldspars in the composite rock from Gjafakollur (211). The limit of ternary solid solution in ternary feldspars is taken from Tuttle and Bowen (1958). Point S represents the bulk analysis of the composite felsite, in terms of normative feldspars, and point T is the calculated composition of the acid liquid, after subtraction of 15% oligoclase and 3% of "basaltic" material. Oligoclase phenocrysts marked by circles, and the extent of zoning is indicated by an arrow. Groundmass anorthoclase or "potassic oligoclase" shown as filled circles. The line X - X is the compositional trend of feldspars from Icelandic acid glasses (Carmichael, 1963).

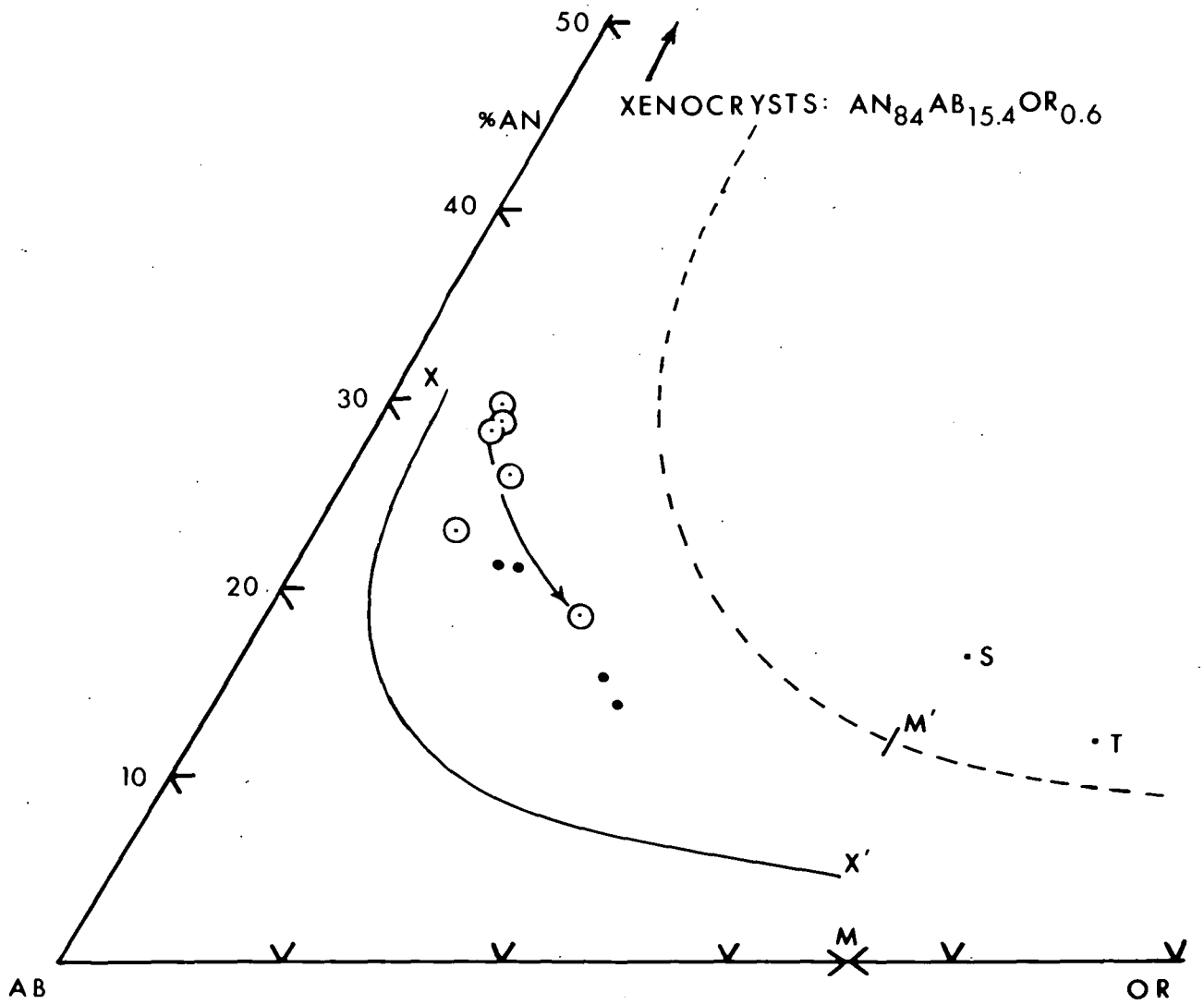
50
%AN
40
30
20
10
XENOCRYSTS: $AN_{84}AB_{15.4}OR_{0.6}$
X
X'
M'
M
S
T
AB
OR

The initial oligoclase phenocrysts contain twice as much of the Or molecule in solid solution as do oligoclase phenocrysts from eastern Iceland (Carmichael, 1963). The compositional trend of the felsite feldspars is also significantly different from that of feldspars from the eastern Iceland pitchstones, notably in the much higher K/Ca ratio of the Gjafakollur feldspars. The high degree of solid solution of the three end-members shown by the late-forming Gjafakollur feldspars may perhaps be linked with the temperature increase which was a direct result of the coming together of the two magmas. The extent of ternary solid solution among the feldspars depends upon the temperature and composition of the parental liquid (Tuttle and Bowen, 1958). The effect of composition is mainly that of a depression of liquidus and solidus in silica-rich rocks, such as the eastern Iceland pitchstones, while relatively silica-poor and feldspathic magmas, such as trachytic rocks, show a greater degree of solid solution and precipitate feldspars in an expanded solubility field. The Gjafakollur composite magma was a rather silica-poor and probably somewhat superheated magma, and both of these factors are believed to have contributed to the high degree of ternary solid solution shown by the late-stage feldspars.

Bulk analysis of the felsite shows a rhyodacitic

composition, but this includes a significant quantity of basaltic material as well as 15% of oligoclase phenocrysts. An attempt has been made to estimate the composition of the original acid liquid, by subtracting 15% of oligoclase and an arbitrary amount of 3% of "basaltic" material from the bulk composition of the composite rock. The bulk composition of the Gjafakollur felsite and calculated composition of the original acid magma are plotted in Figure 25 as S and T respectively. They fall near the minimum for calcium-bearing alkali feldspars (M') in the ternary feldspar diagram, and when plotted in the system Qz-Ab-Or the Gjafakollur felsite falls near the feldspar "thermal valley", in a region close to the two-feldspar boundary surface of the quaternary system An-Ab-Or-SiO_2.

7. Basaltic and intermediate rocks of Centre 1

Due to the considerable alteration of the Tertiary lava pile in the Setberg area a restricted number of good quality samples is available, but nevertheless a number of petrographic basalt-varieties can be identified.

Olivine basalt

With the exception of this single lava (121), all the basalts of Tertiary age examined within the Setberg area show tholeiitic affinities. This is a basalt from Eyraroddi, north-east of the caldera of Centre 1, containing normative

olivine and falling into the olivine basalt group of our classification by virtue of having a Poldervaart Index (p. 76) of + 16. The rock is intergranular to sub-ophitic in texture, with 0.1-0.5 mm long labradorite laths and a colourless augite. Round or oval patches of serpentine are probably the pseudomorphs of olivine microphenocrysts. The common microphenocrysts of iron oxide are up to 0.5 mm in diameter. An interstitial mineral with low birefiringence and relief may be an alkali feldspar.

Olivine tholeiites

Only three Tertiary basalts from the Setberg area can be placed among the olivine tholeiites. One of these is a lava from the succession in Straumhlid, east of Centre 1, which carries euhedral hypersthene phenocrysts, up to 2 mm in diameter (290). This is the first occurrence in Iceland, known to the author, of a hypersthene basalt. The hypersthene phenocrysts tentatively identified in the Askja tholeiite lavas from 1961 (Thorarinsson and Sigvaldason, 1962) are now considered to be augite (G. E. Sigvaldason, pers. comm.).

The hypersthene phenocrysts are strongly pleochroic, with γ green, α and β yellow to pale-yellow. The 2V angle (-ve)(measured on the universal stage) is 55°, indicating a composition near En_{60} (Deer et al. 1963). Most of the

hypersthene phenocrysts show varying degrees of alteration to serpentine, which pseudomorphs the pyroxene entirely in many cases.

Augite phenocrysts are also present, but smaller and less common than the hypersthene, and plagioclase phenocrysts, 2-3 mm in length, are of An_{60-70} composition.

The groundmass consists of intergranular augite and andesine, with interstitial ore and chlorite. Ovoidal, serpentinous areas may represent pseudomorphs after olivine microphenocrysts, whereas smaller serpentine pseudomorphs in the groundmass may be remnants of hypersthene.

The hypersthene basalt from Staumhlid (290) and other examined olivine tholeiites from the Setberg area (286, 301) are rocks typically low in K_2O (0.13-0.15%) and TiO_2 (1.88-1.93%), but high in CaO (10.1-12.7%), resembling in this respect the so-called "primitive" olivine tholeiites from ocean floors. With the exception of the hypersthene-porphyritic lava described above, the Setberg olivine tholeiites contain only a single pyroxene phase: an augite, generally confined to the groundmass. Plagioclase phenocrysts are characteristically present and range in composition from An_{65-70}, but groundmass plagioclase is An_{50}. Iron oxides are found in the groundmass only and do not form a microphenocryst phase, as they commonly do in the

basaltic rocks of Centres 1 and 2.

Quartz tholeiites

The majority of the cone sheets (109,210) in Centre 1 are quartz tholeiite dolerites, 0.2-0.5 mm in grain size. They are sub-ophitic in texture, with euhedral labradorite laths partly enclosed by slightly purplish augite, the latter frequently showing hour-glass zoning and wavy extinction. Pigeonite has not been found in these dolerites, nor olivine, but quartz occurs interstitially. Iron oxides form abundant euhedral octahedra, 0.5 mm in diameter, often enclosed by the augites. The iron oxides are clearly an important and rather early crystallizing phase in the quartz-tholeiitic dolerites, as contrasted with the olivine tholeiites. Apatite needles are a common accessory.

Quartz tholeiite lavas (291, 212) are either aphyric or contain scattered phenocrysts of plagioclase, An_{59-52}, zoned to An_{47} margins. Groundmass plagioclase has a composition in the range An_{40-50}. Thus the feldspars are significantly less calcic than those of the olivine tholeiites. Clinopyroxene forms microphenocrysts in one lava, $<$ 0.5 mm in diameter and with variable 2V angle, down to 30°. Electron microprobe analyses of 8 grains from this rock show a range from $Wo_{38}En_{35}Fs_{27}$ to $Wo_{27}En_{35}Fs_{38}$.

While they do not bridge the miscibility gap between co-existing calcium-rich and calcium-poor pyroxenes (Brown, 1957), these pyroxenes tend towards a subcalcic augite composition, as also is indicated by the low 2V angle. Euhedral microphenocrysts of iron oxide are abundant, while ore occurs also in the groundmass, along with intergranular pyroxene and plagioclase.

Basaltic andesites

Several dykes and cone sheets of basaltic andesite composition occur among the Tertiary rocks of Centre 1, as well as with the sequence of basaltic and intermediate lavas in Bjarnarhafnarfjall which also originated from Centre 1 (p. 23). Although less abundant than the quartz tholeiites, the basaltic andesites are completely gradational to the more basic rocks.

The basaltic andesites have a differentiation index in the range 45 to 60%, SiO_2 of 53-57%, and typically very high total iron ($FeO + Fe_2O_3$ = 10-15%). They range in texture from medium-grained (1 mm) sub-ophitic cone sheets (275) with labradorite and very faintly pleochroic greenish to purplish ferroaugite and interstitial quartz, to very fine grained, intergranular dyke rocks (412), with plagioclase of An_{45-50} composition, a pigeonite in the groundmass, and traces of brown glass. One of the Bjarnarhafnarfjall

basaltic andesite lavas (413) is a devitrified, slightly porphyritic rock, with rounded phenocrysts of plagioclase showing reverse zoning from An_{27} cores to An_{35} margins. The pyroxenes in this lava are predominantly augites ($Wo_{36}En_{33}Fs_{31}$), but pigeonite with the composition $Wo_{12}En_{53}Fs_{35}$, and sub-calcic augite, form rare microphenocrysts. As would be expected from the high total iron content, magnetite forms very common microphenocrysts in the basaltic andesites.

Icelandites

Very fine grained and partly glassy lavas in the Bjarnarhafnarfjall succession of Centre 1 (363) may be termed icelandites owing to their position intermediate between basaltic andesites and rhyolitic rocks (SiO_2 63.9%), and a high iron content. They contain occasional plagioclase laths as phenocrysts, zoned from An_{45} cores to An_{35} margins, and small, euhedral ferroaugite grains ($Wo_{37}En_{20}Fs_{43}$). Fayalitic olivine occurs as microphenocrysts, which are more associated with the intergranular groundmass generation of crystals. There are rare phenocrysts of euhedral magnetite but iron ore, with plagioclase and pyroxene, also forms microlites in the microcrystalline groundmass.

8. Basaltic and intermediate rocks of Centre 2

The Mid-Quaternary basalts of Centre 2 are divisible into two types, olivine tholeiites and tholeiites, which are olivine-normative and just-saturated basalts, respectively.

The basalt lavas of Centre 2 are, however, distinguished by their rather high alkalis content when compared with tholeiitic basalts in general, the persistence of olivine, and the occurrence of hypersthene phenocrysts (although very rare). The first two characters indicate their transitional nature, between the tholeiitic basalts of Centre 1 and the alkalic series of the Late-Quaternary. The absence of an appropriate terminology has resulted, however, in the use of the term "tholeiite" in the following descriptions.

Olivine tholeiites

These are fine grained rocks (339,346, 349, 502) with intergranular texture in a groundmass consisting of augite granules, plagioclase laths and magnetite. Plagioclase phenocrysts are generally present as large, euhedral and calcic grains (An_{70-85}), whereas groundmass plagioclase is An_{50-70}. Xenocrysts of andesine (An_{45}) are common in one of the lavas (349), and much affected by resorption. While augite is the predominant pyroxene phase in all the olivine

tholeiites of Centre 2, large hypersthene phenocrysts are also present in some of the lavas but exceedingly rare. Hypersthene occurs in up to 3 mm long, euhedral crystals which are invariably much altered, often to the extent of being entirely replaced by serpentinous material. On the average, only one or two hypersthene grains can be found in each slide but when present, the strong greenish to yellowish or pink pleochroism makes for easy identification. Probe analysis in one lava gave the composition $En_{41}Fs_{58}Wo_1$.

Olivine and augite phenocrysts occur together with plagioclase in one of the lavas (502), where hypersthene is rare and largely replaced by serpentine. Magnetite is characteristically confined to the groundmass of the hypersthene-bearing olivine tholeiites and does not form the euhedral microphenocrysts so characteristic of the more differentiated lavas of Centre 2.

The olivine tholeiites of Centre 2 are, like the olivine tholeiites of Centre 1, "primitive" in some respects, notably in showing little enrichment in iron and in being poor in alkalis and titania. They are, however, more differentiated than the olivine tholeiites in Centre 1, as borne out by higher alkalis and lower magnesia in the Mid-Quaternary olivine tholeiites.

Fig. 26: Phenocryst of hypersthene in transitional basalt from Centre 2 (339), x 110.

Fig. 27: Xenocryst of quartz, rimmed by clinopyroxene, in basaltic andesite of Centre 2 (501), x 110.

Tholeiites

More differentiated than the olivine tholeiites, the tholeiites have differentiation indices ranging from 35 to 38% and are either slightly Qz-normative or neither Qz nor Ol-normative. There is an increase in alkalis and TiO_2 going from the olivine tholeiites to the tholeiites of Centre 2, and a decrease in MgO. Both these basalt types are equally abundant in the Setberg area, but tholeiites (277, 309, 360, 366, 390) are particularly abundant in Grundarmúli.

Plagioclase phenocrysts are usually present with cores of An_{60-75}, zoned to An_{50-56} margins, while groundmass plagioclase laths are of An_{50} composition. Augite forms rare phenocrysts, with the composition $Wo_{42}En_{37}Fs_{21}$ in one lava (309). While hypersthene has not been found with certainty in any of the more differentiated tholeiites of Centre 2, several of the lavas contain brownish-coloured pseudomorphs, which may well be after hypersthene. Microphenocrysts of olivine occur in one of the lavas (360) but show no reaction relationships. Serpentine pseudomorphs in other tholeiite lavas may represent former olivines.

Magnetite is abundant in all the differentiated tholeiites of Centre 2, forming euhedral, seriate microphenocrysts which range in size down to a groundmass

fraction and are more abundant here than in the olivine tholeiite lavas.

Porphyritic transitional basalts

Highly porphyritic basalt lavas are associated with the tholeiitic lavas of Centre 2. Most voluminous are the plagioclase-phyric lavas of Grundarmon (308), totalling 150 metres in thickness. These rather vesicular and thin, pahoehoe lavas contain up to 50% of 2-5 mm long, stout plagioclase phenocrysts, zoned from An_{60} cores to An_{50} margins.

Rare, partly pseudomorphed phenocrysts of hypersthene are present, up to 2 mm in diameter, but augite granules form the sole pyroxene phase of the groundmass.

Basalts from an upper porphyritic series in Grundarmon (393) contain up to 40% of augite, olivine and plagioclase phenocrysts in roughly equal proportions. Euhedral plagioclase forms grains up to 20 mm in diameter, zoned from An_{80} cores to An_{70} margins. Olivines are invariably highly altered to serpentine around the margins, but remnants of a pleochroic, brownish-yellow to greenish-brown mineral in the marginal area of the olivine phenocrysts may be the remains of hypersthene rims to the olivines.

Augite phenocrysts range in composition from diopsidic augite ($Wo_{48}En_{42}Fs_{10}$) cores to $Wo_{42}En_{38}Fs_{20}$ margins. A

highly corroded xenocryst of augite has the composition $Wo_{41}En_{29}Fs_{30}$. The groundmass contains a single pyroxene phase ($Wo_{41}En_{41}Fs_{18}$) and a calcic plagioclase (An_{55-60}). Olivine phenocrysts are zoned from Fo_{86} cores to Fo_{70} margins.

Basaltic andesites

Most of the basaltic succession in Grundarmon, Arnardalur and Smjorhnukur is composed of basaltic andesites from Centre 2 (336, 340, 347, 352, 358, 361, 362, 501). These exceedingly fine grained, almost black and flinty rocks are largely aphyric, but scattered phenocrysts of plagioclase (An_{40-45}) and microphenocrysts of augite are often present in small amount, the latter ranging from $Wo_{42}En_{35}Fs_{23}$ to $Wo_{39}En_{26}Fs_{35}$ in composition.

Many of the basaltic andesites contain phenocrysts of olivine, up to 1 mm in diameter, but more generally as scattered and rare microphenocrysts, with 2V angle of 60 to 70°, suggesting a rather iron-rich composition.

A basaltic andesite from the Arnardalur succession is devoid of olivine (501) but contains occasional pigeonite microphenocrysts as well as augite. Xenocrysts of quartz are very common in this lava, 2-4 mm in diameter, highly corroded and invariably rimmed by prismatic clinopyroxene grains. The absence of olivine and presence of Ca-poor

pyroxene in this lava is adequately accounted for by the assimilation of quartz by the "normal" basaltic andesite magma. (Figure 27).

Magnetite forms euhedral microphenocrysts in all the basaltic andesites of Centre 2, as well as occurring in the groundmass. Small hornblende laths occur in druses in one of the more siliceous of the basaltic andesites (361). Apatite is an ubiquitous accessory and in one lava (347), euhedral phenocrysts of apatite occur, up to 0.5 mm in diameter (Figure 28). Chlorophaeite is abundant in the lavas, both in vesicles and groundmass, but glass is present in some.

The basaltic andesites are high in alkalis when compared with other rocks of similar silica content. The average of eight analyses contains 5.95% K_2O + Na_2O (SiO_2 54.2%), whereas the average of Thingmuli basaltic andesites (Carmichael, 1964) contains 4.76% K_2O + Na_2O (SiO_2 54.9%).

The alkaline nature of these lavas, the occurrence of olivine and apatite, and the absence of a calcium-poor pyroxene (except in a contaminated lava) suggest affinities with the trachy-basalts of some oceanic islands, while the general silica-enrichment of the suite shows their tholeiitic affinities. Again we come across the

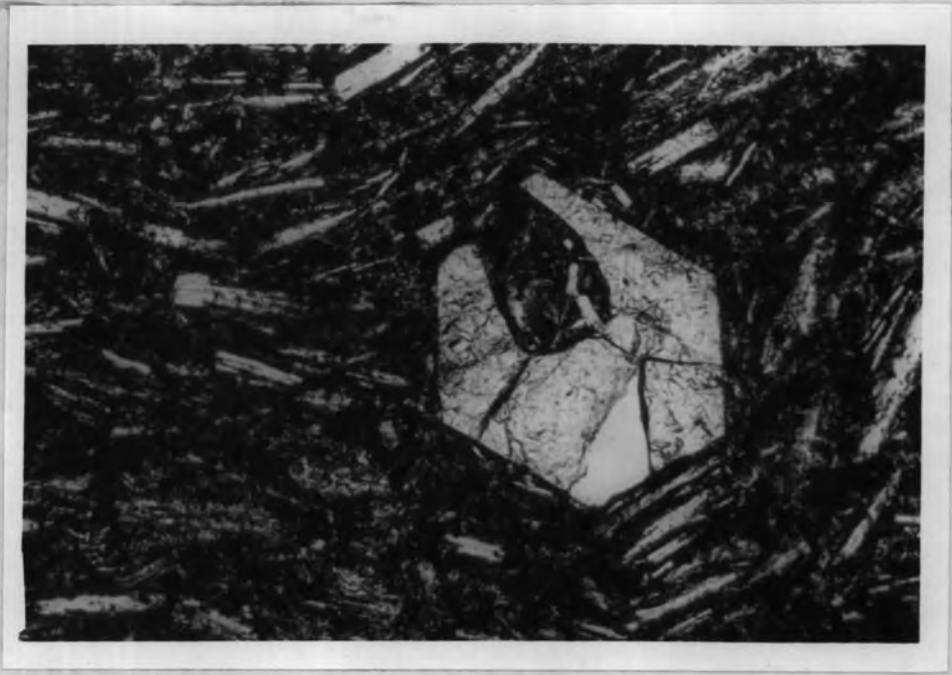

Fig. 28: Apatite phenocryst in basaltic andesite lava from Centre 2 (347), x 110.

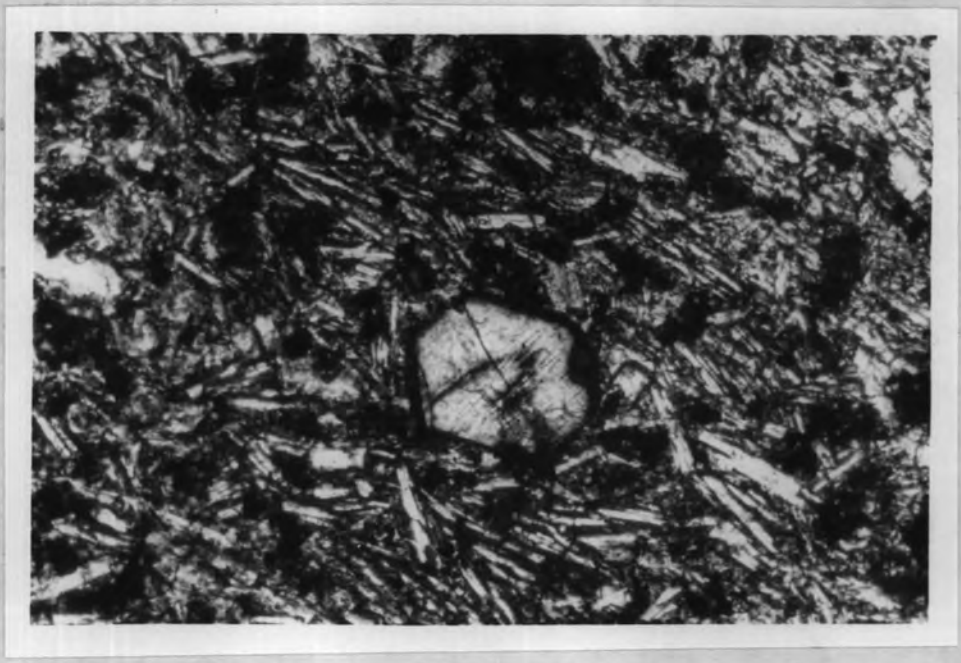

Fig. 29: Apatite phenocryst in icelandite from Centre 2 (506), x 110.

transitional nature of the lavas of Centre 2 (as noted on p.115).

Icelandites

At the base of the Mid-Quaternary succession in Grundarmon, a thick sequence (some 70 m) of very fine grained to glassy rocks of intermediate composition make up the most voluminous occurrence of icelandites in the Setberg area. The icelandites of Centre 2 (306, 307, 364, 365, 367, 476, 506) are invariably intergranular and sparsely porphyritic, with subhedral to euhedral phenocrysts of plagioclase ranging from An_{36} cores to An_{30} margins, although relatively homogenous phenocrysts of An_{14-20} composition are present in one lava (307).

Euhedral augite phenocrysts have the compositional range $Wo_{40}En_{25}Fs_{35}$ to $Wo_{42}En_{5}Fs_{53}$, covering ferroaugites to ferrohedenbergites. Pigeonites have not been observed. Pseudomorphs after olivine microphenocrysts are common in some lavas and fresh fayalitic olivine has been found in one rock (476). Hypersthene phenocrysts occur as very sporadic grains, 0.5 mm in diameter, in a lava from Smjorhnukur (506). They show the typical strong pleochroism from green to pink.

A characteristic feature of all the icelandites of Centre 2 is the presence of euhedral apatite phenocrysts,

up to 0.5 mm in diameter. The apatites show faint reddish brown pleochroism, with O< E. Magnetite phenocrysts are present in the icelandites but much less abundant than in the basaltic andesites of this series. Chlorophaeite is particularly abundant in the Grundarmon icelandites, but its occurrence has been described in detail elsewhere (Sigurdsson, 1966).

9. Rhyolitic rocks of Centre 1

Rhyolitic rocks are very common in Centre 1 but occur not as lavas but predominantly as cone sheets, dykes or irregular shallow-level intrusions. In the northern part of the caldera of Centre 1, however, some large bodies of acid rocks have been interpreted as probable rhyolitic lava flows, erupted within the acid breccias.

Rhyodacites

Two chemical types of "rhyolite" occur in Centre 1: firstly, less differentiated rocks with relatively low SiO_2 content, high in CaO, MnO and Fe_2O_3 + FeO. These are the most common acid rock-type among the cone sheets and dykes and are here referred to as rhyodacites. Secondly, more siliceous rhyolites such as the caldera-lavas, low in CaO, MnO and Fe_2O_3 + FeO. These are the rhyolites proper.

The rhyodacites are sparsely prophyritic rocks (272, 302, 303, 304, 475), either spherulitic or with a very fine

groundmass, and probably devitrified in most cases. Plagioclase phenocrysts are invariably in the An_{25-30} range but an alkali feldspar, with a variable 2V angle, forms rare phenocrysts in one cone sheet (303). The ferromagnesian minerals are distinctive of these acid rocks, and both ferrohedenbergite and fayalitic olivine are usually present. The pyroxene phenocrysts are variable in form, from stout, euhedral grains to smaller, needle-shaped crystals which are slightly pleochroic greenish to yellow, and of the composition $Wo_{38}En_{3}Fs_{59}$. Olivine phenocrysts are much less common and frequently pseudomorphed by a brown isotropic substance, but a medium 2V angle and the yellow colour suggests a fayalitic composition. Magnetite microphenocrysts occur in most of the rhyodacites of Centre 1 and zircon is a common accessory.

The obsidian margin of an acid cone sheet in Arnarhyrna (296) displays important mineralogical features. The rock contains 8.4% of feldspar phenocrysts, consisting of euhedral plagioclase (An_{25-30}) and less abundant, larger corroded phenocrysts of alkali feldspar with a variable 2V angle, probably ranging from anorthoclase to low sanidine composition.

While olivine is entirely absent, the pyroxene phases are of two types: augite ($Wo_{35}En_{33}Fs_{32}$) and pigeonite

($Wo_8En_{41}Fs_{51}$), both occurring as subhedral to euhedral crystals. The pyroxenes form 1.5% of the rocks, which are predominantly glassy with delicate, feathery microlites of pyroxene in the glass (Figure 30). Magnetite phenocrysts make up to 1% of the rock by volume.

The rhyodacites are identical to the felsitic cone sheets of Centre 1, both in their mineralogy and chemistry (p. 95), and both are characterized by an iron-rich nature.

Rhyolites

The calderan rhyolite lavas are more silicic rocks (104, 110, 112, 262, 323, 510), generally aphyric or very sparsely porphyritic with oligoclase phenocrysts in a very fine to glassy groundmass. Greenish hedenbergite phenocrysts are rare and olivine and magnetite microphenocrysts are only present in one specimen. Tridymite needles occur in the microcrystalline groundmass and zircon is an accessory. Rhyolites of this group are frequently slightly altered, due to their location within the caldera of Centre 1, and albitization of the plagioclase phenocrysts is sometimes observed. One lava (112) contains phenocrysts which have been completely replaced by albite, $An_1Ab_{98}Or_1$. Such samples have, of course, been rejected from the collection of analyses which make up the average of these acid rocks (Table 9).

10. Rhyolitic rocks of Centre 2

The acid lavas, dykes and cone sheets of Centre 2 fall into two petrological and chemical groups. The less siliceous (SiO_2 66.6-68.8%) and more calcic rocks are termed rhyodacites, although they do not fulfil the rigid definition of rhyodacites sensu stricto. The more differentiated rhyolites are characterized by the presence of sanidine or anorthoclase phenocrysts.

Rhyodacites

These occur as thin cone sheets and dykes, and also form a lava flow on Gjafakollur (261, 263, 342, 505). They are either microcrystalline or glassy, and porphyritic. Euhedral plagioclase phenocrysts show little range in composition, zoned from An_{30} to An_{25}. Small, corroded phenocrysts of sanidine-anorthoclase have been found in two lavas, but are rare and clearly unstable (342, 505).

These rather iron-rich rocks contain pyroxene phenocrysts ranging in composition from $Wo_{41}En_{20}Fs_{39}$ (ferroaugite) to $Wo_{42}En_2Fs_{56}$; The almost pure hedenbergite forms strongly pleochroic green to yellowish green crystals.

Olivine accompanies the ferroaugite phenocrysts (Fs_{39}) in one obsidian (505), forming large but scattered, yellow crystals of good habit with the composition Fo_{18}. Magnetite grains occur in all the rhyodacites but is not abundant.

Fig. 30: Microlites and dendrites of pyroxene in obsidian margin of a cone sheet from Centre 1 (296), x 60.

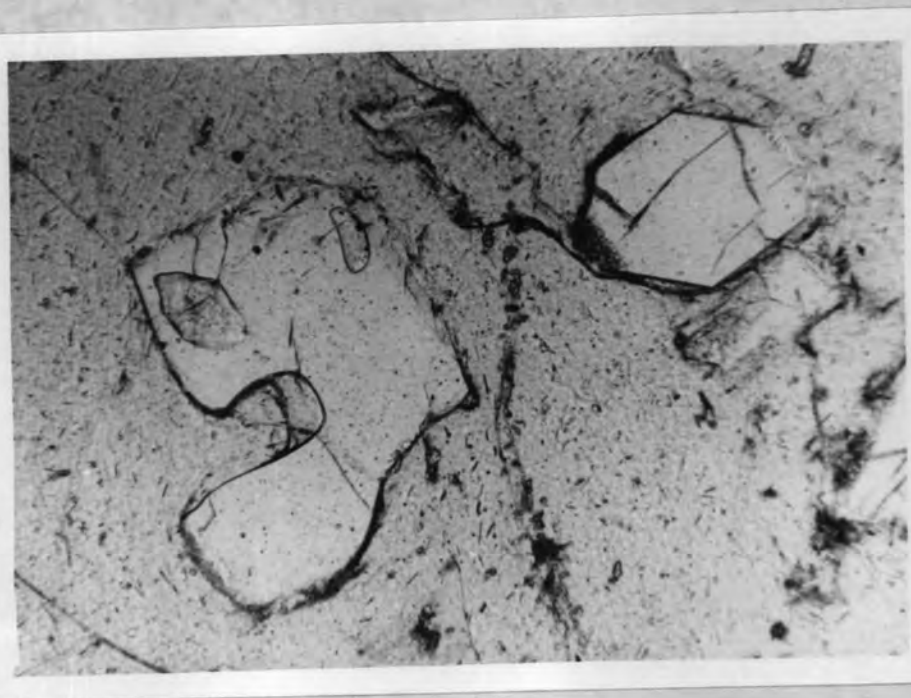

Fig. 31: Phenocrysts of quartz (corroded) and sanidine in comenditic obsidian (331), x 60.

The rhyodacites of Centre 2 are similar in mineralogy and chemistry to the Lysuskard granophyric cone sheet and the Tindar felsite (p. 100).

Rhyolites

The glassy lavas, dykes and tuffs included in this section are the most differentiated and siliceous rocks encountered within the Setberg area (335, 311, 295, 331). All contain sanidine-anorthoclase and frequently quartz in varying proportions. While two of these rhyolites are of definite Mid-Quaternary age (311 and 335) and hence related to Centre 2, the age of the two rhyolites showing peralkaline affinities (295 and 331) is problematical, as discussed on p. 60 .

The acid tuff in Grundamon (311) is sandwiched within the basaltic andesites of Centre 2. It is packed with fractured crystals of sanidine and quartz, totalling 36% by volume, set in a matrix of devitrified shards. No other minerals occur in this rock. The sanidine is a cryptoperthite which ranges in composition from $Or_{35.0}$ to $Or_{36.6}$, and the average of eight electron probe analyses is $Or_{35.9}$. In all cases the anorthite molecule is less than 0.5 weight per cent. It is of interest to note that this is virtually identical to the composition (Or_{35}) of the temperature minimum in the system $NaAlSi_3O_8$-$KAlSi_3O_8$ under "dry"

conditions (Tuttle and Bowen, 1958, p.41).

The bulk composition of the Grundarmon acid tuff, expressed in terms of normative weight per cent Qz-Ab-Or, plots on the cotectic boundary curve separating the silica and feldspar fields in the system SiO_2-Ab-Or-H_2O at 2000kg/cm^2 ($Qz_{35}Ab_{35}Or_{30}$). This composition is not, however, that of the acid liquid, and by subtracting from this the appropriate amount of solid phases (22% sanidine and 14% quartz) we approach the true composition of liquid ($Qz_{37}Ab_{32}Or_{31}$) which plots near the experimentally determined boundary curve for the system Ab-Or-SiO_2-H_2O at 1000kg/cm^2 (Tuttle and Bowen, 1958).

The abundance of quartz and feldspar crystal phases in this tuff speaks clearly for our contention that the liquids had reached such a boundary curve before eruption, suggesting an immediate derivation for this acid magma from a depth of the order of 3 to 4 km.

Similar relationships are shown by the mineral phases in a pitchstone from the margin of a cone sheet in Arnarhyrna (335). This residual glass contains euhedral sanidine (1.3% by volume) and quartz phenocrysts (2.1%), as well as a trace of green pyroxene grains enclosed by a strongly flow-banded glass. Elongated phenocrysts of an opaque mineral are rare and show strong anisotropy in

reflected light, suggesting pyrrhotite.

Rhyolites with peralkaline affinities

Two obsidians from the Setberg area are of distinct peralkaline character. One of these (295) is the obsidian dome near Midhyrna (p. 60), whose age is problematical but probably Late-Quaternary. This rock has a peralkalinity ratio of 0.91 (mol % Na_2O+K_2O/Al_2O_3) and is thus, strictly speaking, not peralkaline in the sense of having acmite or sodium metasilicate in the norm, but approaches closely a comendite composition.

The other occurrence is an obsidian dyke (331) north of Lysuskard, whose emplacement within the Tertiary rocks does not allow for a better age estimate than to call it post-Tertiary. The dyke post-dates the metamorphic aureole associated with Centre 2, and is thus probably Mid-- to Late-Quaternary in age. (Figure 31).

The Midhyrna obsidian dome (295) consists almost entirely of glass, with small phenocrysts totalling only 0.6% by volume. Phenocrysts of alkali feldspar, clinopyroxene and iron oxides occur in roughly equal proportions. The euhedral sanidine phenocrysts range from Or_{35} to Or_{41} and contain less than 1% of the An molecule. Very small and rare feldspar crystals of a more sodic composition occur in the glass, of the composition Or_{25} to Or_{30}, with

An content of approximately 2%. The clinopyroxene phenocrysts have not yet been analyzed, but the strong green colour suggests a rather sodic pyroxene.

Figure 32 illustrates the relationship of the feldspar phases with regard to the position of the bulk liquid composition of this residual glass in the system $NaAlSi_3O_8$-$KAlSi_3O_8$-SiO_2-H_2O at 2000 kg/cm^2 (Tuttle and Bowen, op. cit.), but 95.7% of the composition of the Midhyrna obsidian is represented by this system, as the rock contains only 0.2% CaO.

The absence of a silica phase suggests that this liquid had not reached the boundary curve separating the silica and feldspar volumes, and the presence of sanidine testifies to crystallization (early) on the potassic feldspar side of the "thermal valley" of the feldspar volume. These criteria indicate that during the early crystallization of sanidine the liquid was held at water pressures in excess of 1000 kg/cm^2, and probably near 2000 kg/cm^2. By fortunate coincidence the Midhyrna obsidian is virtually identical to one of the mixtures used by Tuttle and Bowen in their experimental runs at 2000 kg/cm^2 (Q1 - 13H, Table 10, p.60). This charge gave glass only at 700°C, but when quenched at 680°C it contained a feldspar of the composition Or_{42}. Similarly the Midhyrna obsidian contains

feldspar with up to Or_{41} but ranging to Or_{35}, i.e. approaching the minimum in the binary system $NaAlSi_3O_8$-$KAlSi_3O_8$.

The smaller anorthoclase crystals in the obsidian are interpreted as the product of crystallization at very much lower pressure or at the surface. The decrease of pressure, caused by the ascent of magma or on extrusion, results in a shift of the temperature minimum on the quartz-feldspar boundary line to the right (Figure 32), thus placing the Midhyrna acid liquid in the trace of the thermal valley, or possibly on the plagioclase-side of it. Crystallization at progressively lower pressures resulted in precipitation of feldspars ranging in composition from Or_{31} to Or_{25}.

The considerable water pressures invoked here to account for the phase relations in the Midhyrna obsidian

---

Fig. 32: The normative salic constituents (less anorthite) of the Midhyrna obsidian (295) and the peralkaline obsidian dyke (331) plotted in the system $NaAlSi_3O_8$-$KAlSi_3O_8$-SiO_2. The experimental boundary curve and minimum at 2000 kg/cm^2 are after Tuttle and Bowen (1958). Filled squares are acid residual glasses from eastern Iceland (p.128, 19, 18, Carmichael, 1963 and 1964). The dotted line joining the two crosses shows the position of the minimum on the quartz-feldspar boundary from 500 kg/cm^2 to 3000 kg/cm^2. Filled circles represent feldspar and whole-rock compositions of obsidian 331, open circles those of 295.

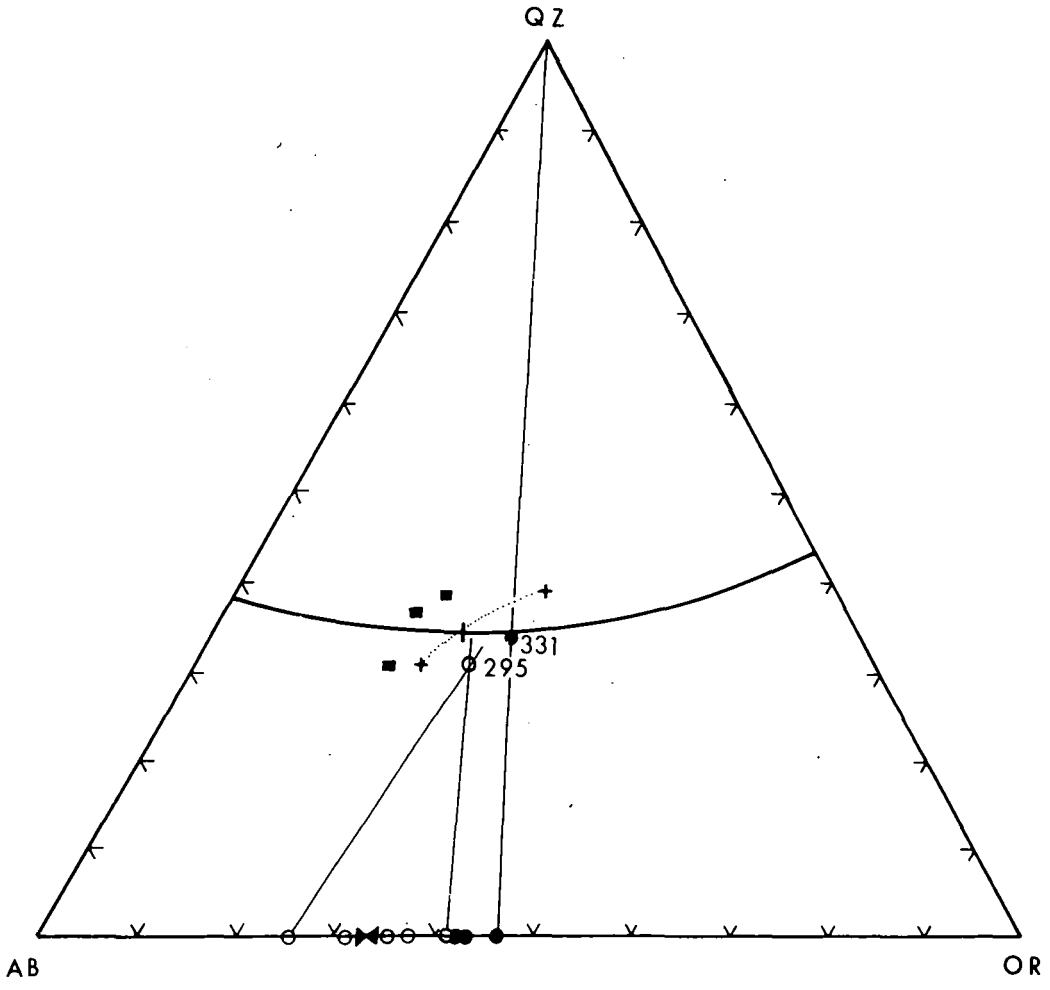
QZ
331
295
AB
OR

would correspond to a depth of the order of 3 to 4 km; not in excess of that expected on geological grounds. More unusual is the position of this acid rock in the system Ab-Or-SiO_2-H_2O with respect to acid liquids associated with an origin by fractionation of basaltic magmas, such as the pitchstones of eastern Iceland, also plotted in Figure 32 (Carmichael, 1963). The petrogenetic significance of the Midhyrna obsidian will be discussed later (Ch. VI).

The comenditic obsidian dyke north of the Lysuskard valley (331) has a peralkalinity ratio of 1.33 (mol % Na_2O+K_2O/Al_2O_3), and thus has the distinction of being the first peralkaline acid rock ever reported from Iceland. (Figure 31).

The glass contains 1.4% of sanidine phenocrysts, subhedral and 1-2 mm in diameter, ranging in composition from Or_{47} to Or_{41}. Quartz forms larger, often slightly embayed grains, constituting 0.8% of the rock by volume. Elongated crystals of a deep red or brown, translucent mineral, up to 1 mm in length, are rare phenocrysts and are probably of aenigmatite, but this awaits electron microprobe confirmation.

The obsidian contains over 8% acmite in the norm and 2% sodium metasilicate. The composition of this glass and

would correspond to a depth of the order of 3 to 4 km; not in excess of that expected on geological grounds. More unusual is the position of this acid rock in the system Ab-Or-SiO_2-H_2O with respect to acid liquids associated with an origin by fractionation of basaltic magmas, such as the pitchstones of eastern Iceland, also plotted in Figure 32 (Carmichael, 1963). The petrogenetic significance of the Midhyrna obsidian will be discussed later (Ch. VI).

The comenditic obsidian dyke north of the Lysuskard valley (331) has a peralkalinity ratio of 1.33 (mol % Na_2O+K_2O/Al_2O_3), and thus has the distinction of being the first peralkaline acid rock ever reported from Iceland. (Figure 31).

The glass contains 1.4% of sanidine phenocrysts, subhedral and 1-2 mm in diameter, ranging in composition from Or_{47} to Or_{41}. Quartz forms larger, often slightly embayed grains, constituting 0.8% of the rock by volume. Elongated crystals of a deep red or brown, translucent mineral, up to 1 mm in length, are rare phenocrysts and are probably of aenigmatite, but this awaits electron microprobe confirmation.

The obsidian contains over 8% acmite in the norm and 2% sodium metasilicate. The composition of this glass and

its feldspars is plotted in Figure 32. The obsidian falls on the cotectic boundary line separating the quartz and feldspar fields at 2000 kg/cm^2, and the presence of quartz and alkali feldspar phenocrysts in the glass supports our hypothesis that the liquid was equilibrated at this pressure and probably derived from a depth of approximately seven kilometers.

C. Petrography of the Late-Quaternary Alkalic Series

The holocrystalline lavas of the alkalic series tend to be somewhat lighter in colour than the dark, fine-grained basaltic rocks of Centre 2. The latter also show a well developed columnar jointing which is lacking or poorly developed in the alkalic series, but the distinction between the two series is by no means an easy task in the field. The coarser grain and often somewhat porous or miarolitic texture of the alkalic series is, however, a characteristic feature in thin section.

1. Alkalic basalts

The basaltic lavas of the alkalic series will be dealt with under the headings corresponding to the classification scheme outlined on p.76. The alkalic basalts are olivine-phyric rocks containing up to 3.5%

normative nepheline, in which olivine occurs invariably as a groundmass phase. They range in solidification index from 43 to 35 and have differentiation indices of 22 to 28 (372, 399, 344, 402, 446, 385, 400, 389, 384, 383).

Texturally they are intergranular porphyritic lavas, often miarolitic and medium to fine grained. The euhedral olivine phenocrysts are predominantly Fo_{78-71}, but larger phenocrysts have more magnesian cores of up to Fo_{90}. Strong compositional zoning is characteristic as indicated by the increase in birefringence towards crystal margins for which probe analyses indicate a composition of Fo_{65-52}. Analyses of olivine microphenocrysts and groundmass phases give a composition of Fo_{62-44}.

The strong zoning and the occurrence of highly magnesian cores of the olivine phenocrysts in the alkalic basalts is an important feature, and an indication of a strong fractionation of magnesium in these lavas. The normative composition of olivine (Fo_{59}) in the average alkalic basalt (Table 11) and the groundmass crystals of similar composition indicate the extent of fractionation of the alkalic basalt magma which, although the most basic member and hence a likely parent of the alkalic series, must itself be regarded as a fractionation product of a still more primitive liquid.

Plagioclase phenocrysts are present in some of the alkalic basalts but are by no means common and are always corroded. They range from An_{60-70}, but calcic cores occur in some cases, up to An_{75-81} in one lava. Groundmass plagioclase is generally of An_{50-30} composition.

Augite forms scattered, large phenocrysts in some of the alkalic basalts but is always the major ferromagnesian mineral in the groundmass, forming purplish-tinted crystals which are invariably more abundant than the groundmass olivine. Alkali feldspar forms an interstitial phase in coarse grained varieties, but nepheline has not been positively identified in any of the lavas in spite of its presence in the norm. Magnetite is usually restricted to the groundmass, but forms microphenocrysts in one lava. Brown, euhedral inclusions of picotite occur in most of the larger olivine phenocrysts.

Biotite occurs in some of the more coarse grained alkalic basalts as interstitial flakes of irregular outline, but it is not as prominent as in many of the olivine basalts. The term biotite is used here rather loosely; the appreciable 2V (-ve) of these interstitial grains suggests a phlogopitic composition, as shown by electron probe analysis for similar interstitial and drusy micas in one of the mugearites (p.150).

The alkalic basalts are typified by a high content of MgO (the average of ten lavas is 8.88%) and consequently a high solidification index, which is combined with relatively low total iron and total alkalis contents compared with the olivine basalts.

2. Olivine basalts [1)]

The olivine basalts comprise a group of olivine phyric lavas, invariably intergranular and rather fine grained. They are slightly Hy-normative on the whole, but the average value for nine olivine basalt analyses shows only 0.01% hypersthene in the norm. Many are thus true olivine basalts in the classical sense, having neither normative Ne nor Hy in appreciable quantity except where oxidation is significant. The olivine basalts are less magnesian than the alkalic basalts (MgO 6.06% for the average of nine) and have a solidification index of 35 to 22, but a differentiation index of 29 to 35. The division of alkalic basalts and olivine basalts has been based on the solidification index, as well as on the normative characters. These two parameters are not always in total agreement and thus our grouping must inevitably cut across the normative classification in some cases. Thus four lavas that are just Ne-normative and low-magnesian are included among the olivine basalts. The normative parameters of

---

1) The following samples are classified as olivine basalts: 202, 373, 371, 398, 318, 391, 368, 382, 319.

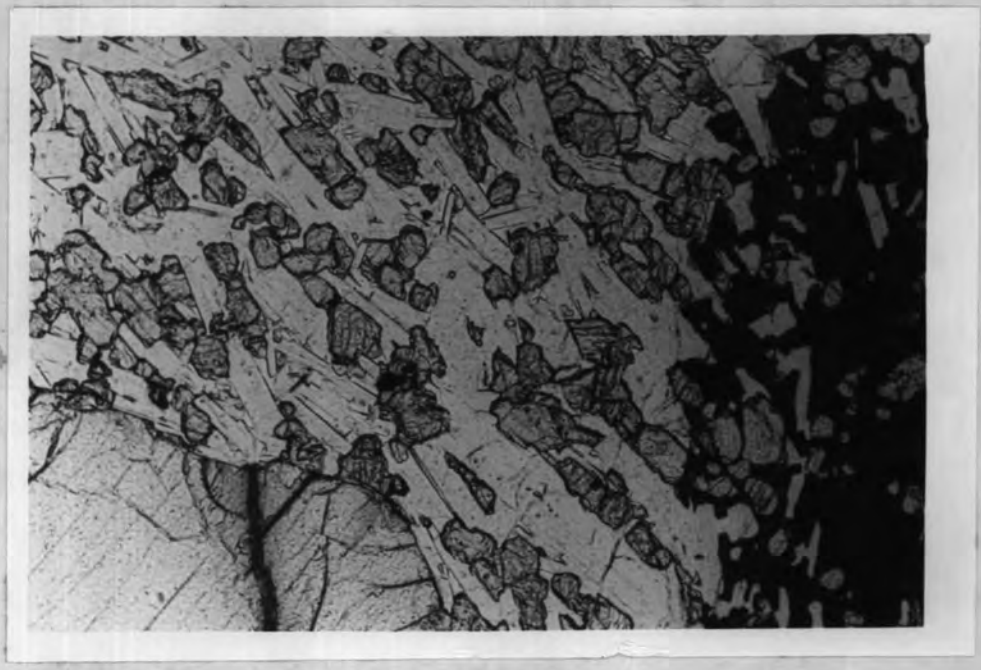

Fig. 33: Textural features of an olivine basalt, with intergranular texture, showing olivine phenocrysts and sub-ophitic iron ore, (202), x 110.

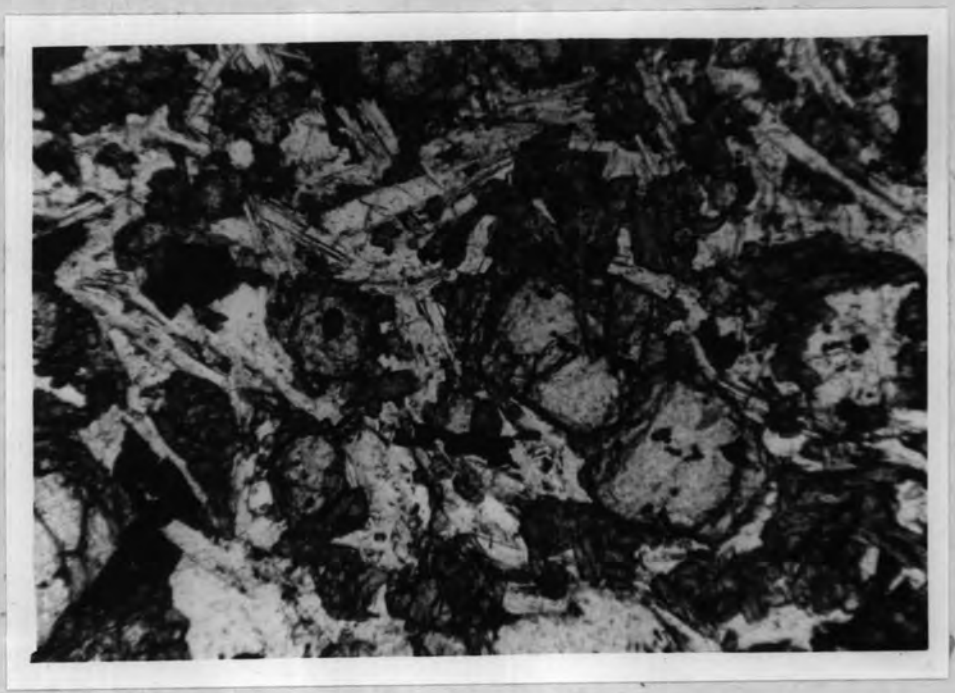

Fig. 34: Olivine basalt from Kirkjuholl (Setberg alkalic series), showing miarolitic texture (371), x 110.

the two groups indicate how closely the alkalic series follow the critical plane of silica undersaturation during early fractionation of the series.

Olivine phenocrysts are ubiquitous in the olivine basalts, commonly of Fo_{60-61} composition, while microphenocrysts and groundmass olivines are Fo_{53-51}. Plagioclase forms phenocrysts but is usually rare and always highly corroded. The crystals are zoned from An_{70} cores to An_{50-45} margins and groundmass plagioclase is An_{45-40}. Purplish augite is a phenocryst phase in some lavas, and is the major ferromagnesian groundmass mineral. Magnetite is more abundant than in the alkalic basalts, forming irregular microphenocrysts. Alkali feldspar, with a moderate 2V, occurs interstitially, mantling some plagioclase laths in the groundmass. Characteristic of most of the olivine basalts is the presence of interstitial biotite flakes in the groundmass, up to 0.2 mm in diameter, showing strong pale-brown to brown pleochroism. Picotite forms a common accessory, particularly in larger olivine phenocrysts.

3. Ankaramites and porphyritic basalts

Many of the basaltic lavas of the alkalic series contain very abundant phenocrysts of olivine and augite, but only in one eruption has ankaramite *sensu stricto* been

produced, as total feldspar in most of the phyric lavas of the Setberg area is in excess of the 30% permitted for true ankaramites (Macdonald and Katsura, 1964).

The field relations of the ankaramitic pillow basalts (111, 114, 394, 395, 396) and the palagonite tuff layer of the Setberg area have been described in some detail in a previous publication (Sigurdsson, 1966). Briefly, this sub-glacial basaltic eruption started with an explosive phase, presumably due to the initial interaction of melt-water with the magma, resulting in the deposition of a glassy tuff in the vicinity of the crater. Outpouring of pillow lava followed, which in a number of localities shows signs of primary flow brecciation produced as pillows or lava tongues cascaded down slopes, and the semi-solid magma became fragmented and acquired a foreset bedding. The Klakkur and Eyrarfjall subglacial basalt formation is up to 80 metres in thickness and can be traced back to an adjoining, cylindrical plug of perfect proportions, 15 m in diameter.

All the facies of basaltic material erupted from this plug are highly porphyritic, with olivine and clinopyroxene as 1 to 2 cm long, euhedral crystals. Plagioclase phenocrysts are common in the early basic tuff and some part of the pillow lava, but are absent from most of the lavas,

particularly those erupted later. There is thus a significant change from the early erupted liquid, moderately abundant in phenocrysts of olivine and pyroxene as well as plagioclase, to the last lava erupted, almost devoid of plagioclase phenocrysts and containing up to 50% of olivine and clinopyroxene phenocrysts in equal proportions. Floating of the plagioclase and some accumulation of the ferromagnesian minerals has clearly occurred prior to eruption.

The early plagioclase phenocrysts are calcic bytownites and range in composition from An_{85} to An_{92}, with margins of An_{70} in the subophitic, holocrystalline lavas. Groundmass plagioclase forms laths up to 0.3 mm long, ranging from An_{73} to An_{41}. Olivine phenocrysts are euhedral, and generally 0.5 cm long. Compositions of olivine cores, as determined by 2V measurements and refractive index, are Fo_{95} and Fo_{94} respectively, whereas electron probe analyses indicate a Fo_{89} composition, with phenocryst margins as low as Fo_{52}. Groundmass olivines range from Fo_{63} to Fo_{44}.

Clinopyroxene forms euhedral, large diopsidic phenocrysts ($Wo_{46}En_{46}Fs_{8}$), whereas augite granules occur in the groundmass ($Wo_{41}En_{33}Fs_{26}$). Rare, euhedral phenocrysts of dark-brown spinel, up to 1 mm in diameter, are present in

the ankaramitic facies but spinel commonly forms small inclusions in many of the olivine phenocrysts. Biotite is rare interstitially, but an alkali feldspar is frequently found in the residuum.

4. Hawaiites

The most voluminous rock-type of the Late-Quaternary alkalic series in the Setberg area are low-magnesian basalts with groundmass andesine, here termed hawaiites. Apart from being generally finer grained than the alkalic and olivine basalts, the hawaiites do not differ significantly in their field characters from the more basic members of the series. However, they are readily identified in thin section by the characteristic sub-trachytic texture and the presence of plagioclase phenocrysts, generally rare in the less differentiated lavas of the alkalic series.

The hawaiites are Ol-Hy-normative rocks on the whole, but two lavas (379 and 401) contain Ne in the norm and the group as a whole does not deviate far from the critical plane of silica undersaturation, as shown by the high Poldervaart index of + 17.6 for the average of 15 hawaiites. In this account hawaiites include rocks with solidification indices in the range 23 to 16.5 and differentiation indices of 35 to 45, but the presence of

andesine in the groundmass provides a convenient means of distinction (Macdonald and Katsura, 1964).

The Setberg hawaiites include the following samples: 410, 404, 403, 401, 392, 379, 345, 321, 320, 207, 397, 498, 499, 387, 348. Plagioclase phenocrysts in these lavas are either large corroded grains, with cores of An_{58-60} showing oscillatory zoning to An_{35-40} margins, or euhedral microphenocrysts of An_{35} composition. Groundmass plagioclase forms slender laths of An_{35} to An_{40}, but more rarely as low as An_{30}. The abundant plagioclase in the groundmass frequently renders a sub-trachytic texture. Olivine is always present as euhedral phenocrysts but is rarely identified in the very fine groundmass. Phenocrysts range usually from Fo_{68-59} cores, but rare cores of up to Fo_{83} have been recorded. Two electron probe analyses of phenocryst margins gave Fo_{44} and Fo_{45}. Olivine to hypersthene reaction relationships have never been observed in the hawaiites.

Augite forms microphenocrysts in only four of the 15 hawaiites examined, always showing a slight purplish tint. They range in composition from $Wo_{43}En_{36}Fs_{21}$ to $Wo_{35}En_{29}Fs_{36}$, the latter being also the composition of groundmass pyroxenes.

Magnetite forms euhedral microphenocrysts or phenocrysts in two thirds of the lavas, as well as being an important groundmass phase. Ilmenite is also present in the groundmass, in keeping with the fact that the hawaiites are the most titaniferous group of the alkalic series, with an average TiO_2 content of 2.71% for 15 hawaiites. The ilmenite crystals form slender, slightly translucent, reddish rods in the groundmass.

Biotite is present interstitially but is much less abundant than in the olivine basalts. Apatite forms minute needles in the groundmass.

Due to the very small grain size of the Setberg hawaiites the nature of the interstitial residuum is as yet unknown. Pale brown glass is present in some lavas but a low-birefringent, low relief, interstitial material found in more coarse grained varieties may be alkali feldspar.

5. Mugearites

Next to hawaiites, the mugearitic lavas are the most common rock type of the alkalic series (350, 416, 507, 503, 500, 487, 479, 405, 381, 380, 375, 370, 369, 359, 357, 356, 343). They occur typically near the top of the succession, always resting on olivine basalts or alkalic basalt lavas. In spite of a great difference from basalts in chemistry,

the mugearites are not easily identified as such in the field. This is partly due to the subglacial environment in which some of these lavas were erupted, resulting in rapid chilling of the magma. Consequently the dark, very fine grained pillow lavas and flow breccias of mugearitic composition can only be positively identified in thin section or by chemical analysis. Subaerial mugearitic lavas are greyish rocks, which commonly display a platy jointing parallel to the planes of flow.

Mugearites are primarily lavas of basaltic habit, but containing groundmass oligoclase. The Setberg lavas are further classified by their solidification index (16.5 to 12.5) and show a range in differentiation index from 47 to 57. They are subtrachytic in texture (Figure 35), displaying good alignment of the elongated plagioclase laths which make most of the rock. Very fine grained, intergranular types also occur.

The mugearites are sparsely porphyritic, but generally contain 2 to 3% of small phenocrysts of olivine and plagioclase as well as magnetite of variable size. Plagioclase ranges in core composition from An_{55} to An_{44}, zoned to An_{25} or An_{22} margins. Oscillatory zoning is common, and corrosion is evident in calcic xenocrysts. One lava contains numerous xenocrysts of anorthoclase, 2 to 4 mm in

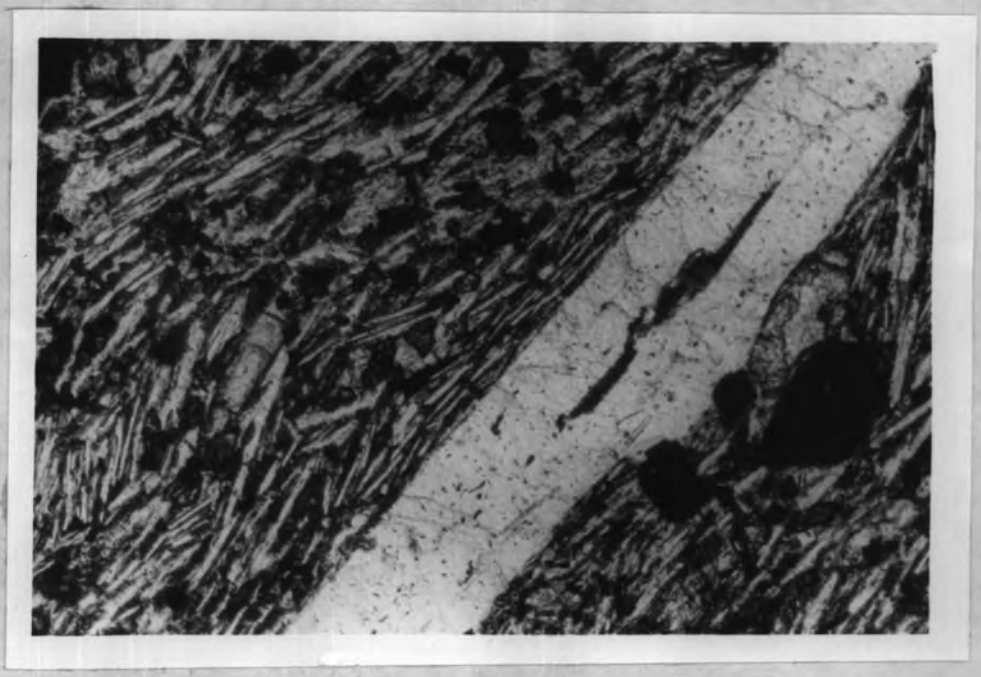

Fig. 35: Mugearite, displaying sub-trachytic texture (343), x 110.

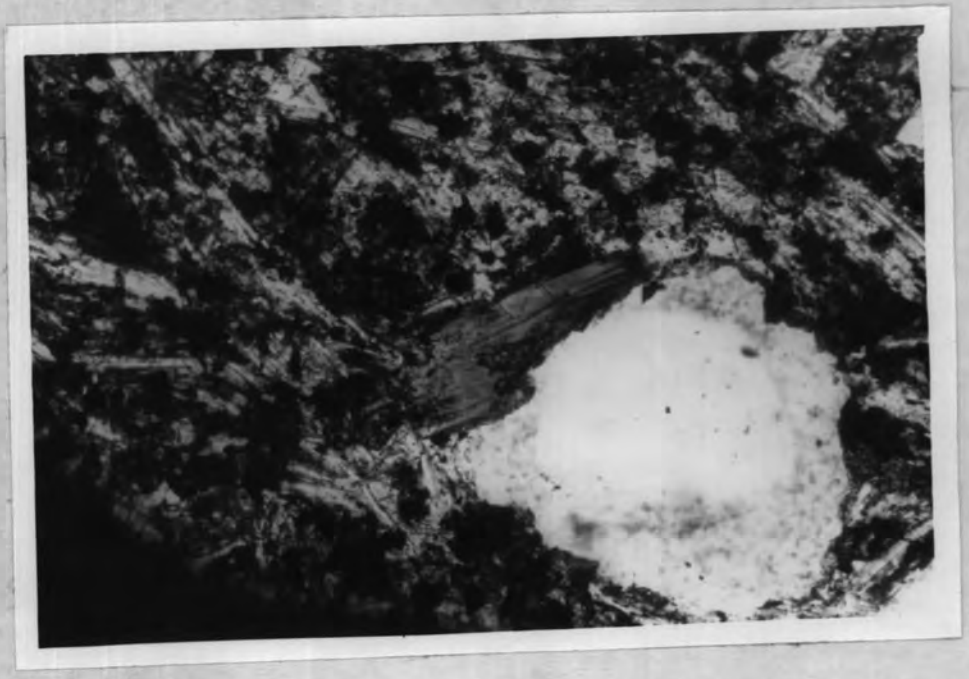

Fig. 36: Phlogopite crystal in the cavity of a mugearite lava (369), x 110.

diameter, with moderate to small 2V angle. Quartz xenocrysts, rimmed by a clinopyroxene, have been found in another rock (487).

Plagioclase laths in the groundmass are chiefly An_{25} to An_{30}, and rarely may be as sodic as An_{20}.

Olivine forms euhedral crystals, ranging from 1 to 2 mm long phenocrysts of Fo_{66-70} to microphenocrysts of Fo_{54} to Fo_{45} composition. Groundmass olivines are too minute for probe analysis, but the margin of a microphenocryst yielded a composition of Fo_{34}.

Pyroxene microphenocrysts have been found in only four of the 20 mugearites examined. They form euhedral, purplish grains with moderate to rather small 2V angle, while in lavas transitional to benmoreite the pyroxenes show a faint greenish colour. Euhedral octahedra of magnetite, up to 0.5 mm in diameter, are ubiquitous phenocrysts.

Apatite forms stout (0.4 mm) but rare phenocrysts in many of the lavas, notably in those containing at least 1% P_2O_5. The euhedral hexagonal crystals are slightly pleochroic (reddish with O < E) and identical to the apatite phenocrysts of the icelandites of Centre 2. The basaltic members of the alkalic series show a gradual increase in P_2O_5 content with decreasing solidification index (Figure 46),

culminating at about 1% in the mugearites. It is probable that this value approaches the saturation point of phosphorus in the magma, at which level apatite becomes a cumulus phase. In their discussion of phosphorus-enrichment in rocks of the Upper Zone of the Skaergaard intrusion, Wager and Brown (1968) indicate that apatite precipitates when 97% of the initial liquid is solid, from a residual liquid with 1.75% P_2O_5. The lower phosphorus concentration required for apatite-saturation in the Setberg alkalic series may be a function of the considerable differences in major element chemistry between the tholeiitic and alkalic magma types.

The unusually varied ferromagnesian mineral assemblage in one of the Setberg mugearites (369) has been examined in some detail by means of the electron microprobe. In addition to olivine phenocrysts, zoned from Fo_{63} to Fo_{54}, microphenocrysts of olivine (Fo_{34}) are present. The groundmass surprisingly contains small grains of a calcium-poor pyroxene, approximating to pigeonite in composition ($Wo_6En_{39}Fs_{55}$), as well as an augite. A strongly pleochroic, brown to light-brown phlogopite forms crystals up to 0.3 mm in diameter in druses and vesicles, accompanied by euhedral, edenitic hornblende crystals with weak pale-brown to yellow

pleochroism. The phlogopite is transitional to biotite, with Mg:Fe in the proportions 2:1.(Figures 36 and 37).

The mugearite is an entirely fresh rock, and a secondary origin for these hydrous minerals is out of the question. The drusy character of the rock suggests a high volatile component in the magma, and it was probably during the escape of this phase that these minerals crystallized, at a late stage of solidification of the magma.

6. Benmoreites

At the very top of the succession of the Setberg alkalic series in the Midhyrna, Arnardalsskard and Torfahlid successions, one encounters vesicular, grey coloured lavas of basaltic habit. These rocks are distinguished chemically by a very low solidification index (7-10) and a high differentiation index (60-70) reflecting their high content of modal feldspar. We have named these intermediate rocks benmoreites, following the definition by Tilley and Muir (1964) of sodic lavas intermediate between mugearite and trachyte, hitherto best known from the alkalic basalt series of Hawaii and the Hebridean region.

In the Setberg area the benmoreites (504, 406, 376, 337) are most voluminous in and around the Late-Quaternary

Fig. 37: Hornblende showing basal cleavage, in the cavity of a mugearite lava (369), x 110.

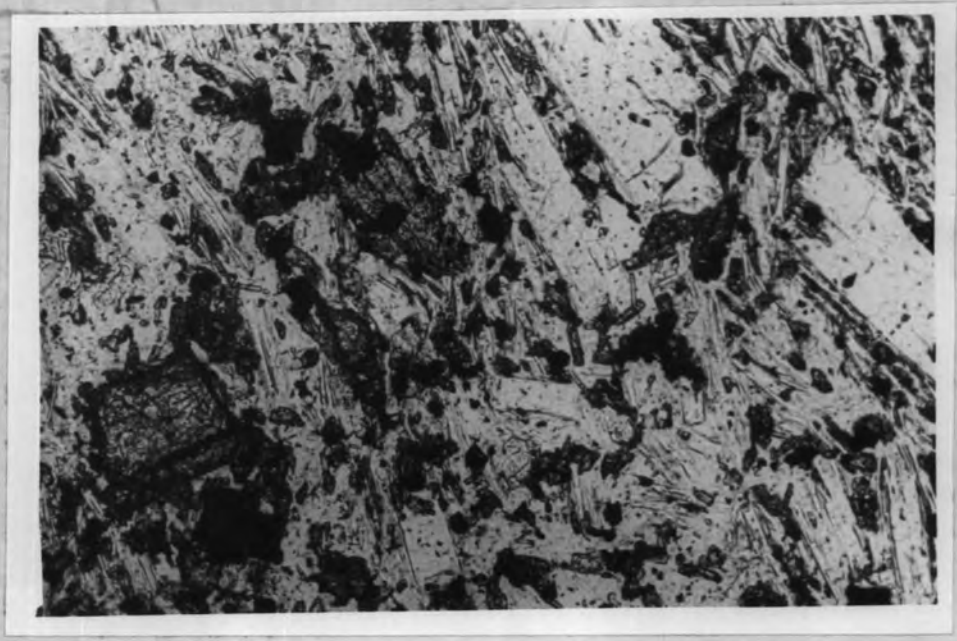

Fig. 38: Trachytic texture in benmoreite (376), containing microphenocrysts of olivine and plagioclase, x 110.

crater north of Midhyrna, and clearly represent the last effusive products of that vent. In thin section the lavas are microporphyritic, rather vesicular and fine grained rocks, with sub-trachytic to trachytic texture (Figure 38). Microphenocrysts of plagioclase, olivine and magnetite are present in all the lavas, but augite is rare. Plagioclase xenocrysts of labradorite composition occur in one lava, but most of the euhedral feldspar laths are in the compositional range An_{45} to An_{30}, with crystal margins of An_{15} to An_{20}. Anorthoclase is present in the groundmass, but subordinate to oligoclase. Olivine phenocrysts have cores of Fo_{56-53}, zoned to margins of an iron-rich composition and often surrounded by small granules of iron ore.

Microphenocrysts of augite are tinted by a purplish-brown colour, and range from $Wo_{40}En_{36}Fs_{24}$ to $Wo_{42}En_{34}Fs_{24}$. One of the lavas (376) also contains microphenocrysts with a small 2V angle, and significantly lower in wollastonite content. Probe analysis of this sub-calcic augite gave the composition $Wo_{30}En_{41}Fs_{29}$. Olivine microphenocrysts in the same lava range from Fo_{46} to $Fo_{55.5}$ and show no signs of reaction with the liquid.

Magnetite forms common, euhedral phenocrysts, up to 1 mm in diameter, often enclosing small crystals of apatite

which also occurs independently as rare microphenocrysts, but much less commonly than in the mugearites.

Anorthoclase occurs in the very fine grained groundmass, while cristobalite and hornblende are common in druses of one lava (504).

No trachytes have been found in association with the alkalic series of the Setberg area, but two alkali-rich rhyolites may be associated with this series. These are the Midhyrna obsidian (295) and the peralkaline obsidian dyke from north of Lysuskard (331). The petrography of these unusual rocks has been dealt with on pages 131–136.

CHAPTER IV: MINERALOGY

This chapter deals with the chemical variation within the three principal mineral groups which make up the Setberg lavas, as well as analytical data on some of the accessory minerals. The electron probe was utilized, permitting analyses to be carried out on both phenocrysts and groundmass phases in a large number of rocks. Complete analyses were carried out in most instances, using closely comparable standards when possible. The analytical techniques and subsequent correction procedures are dealt with in Appendix.

A. Feldspars

Plagioclase, anorthoclase and sanidine are present in the Setberg series as a whole. The former two occur either as phenocrysts or groundmass constituents, whereas sanidine is found solely as phenocrysts in the glassy acid rocks.

A total of 248 feldspars were analysed with the electron microprobe. The presentation of all the data is impracticable here, and instead a selection of 43 feldspar compositions from the three rock series of the Setberg area is presented in Table 2. Simple optical studies have been carried out in a number of cases and a comprehensive analytical study was carried out on the plagioclase phenocrysts in a palagonite tuff from the basal facies of the Late-Quaternary ankaramitic

TABLE 2

FELDSPAR ANALYSES

	WEIGHT PER CENT								NUMBER OF IONS (32 O)		
	SiO_2	Al_2O_3	CaO	Na_2O	K_2O	Ab	Or	An	Z-site	Y-site	X-site
TERTIARY THOLEIITIC SERIES (CENTRE 1):											
213, GABBRO XENOLITH:											
An-rich	46.8	33.8	16.7	2.15	0.12	17.9	0.7	81.4	16.000	0.001	4.089
Ab-rich	47.2	33.1	16.7	2.30	0.17	18.8	1.0	80.2	15.950	0.000	4.164
NORM	-	-	-	-	-	18.1	1.0	80.9	-	-	-
212, THOLEIITE:											
PHEN.	53.3	28.6	12.0	4.88	0.20	40.5	1.2	58.3	15.963	0.000	4.098
GMSS.	56.0	27.4	9.5	7.19	0.52	54.8	2.8	42.4	15.939	0.000	4.527
NORM	-	-	-	-	-	55.4	6.9	37.8	-	-	-
412, BASALTIC ANDESITE:											
XENOCRYST	47.5	33.4	16.8	1.75	0.01	15.1	0.1	84.8	16.000	0.015	3.931
PHEN.	55.7	27.9	10.0	5.72	0.22	48.6	1.3	50.1	16.000	0.015	3.988
GMSS.	56.2	27.2	9.3	6.33	0.26	52.9	1.5	45.6	16.000	0.002	4.073
NORM	-	-	-	-	-	60.6	12.8	26.6	-	-	-

TABLE 2 (continued)

	WEIGHT PER CENT								NUMBER OF IONS (320)		
	SiO_2	Al_2O_3	CaO	Na_2O	K_2O	Ab	Or	An	Z-site	Y-site	X-site
413, ICELANDITE:											
XENOCRYST	55.9	27.4	10.2	5.31	0.25	46.3	1.5	52.2	16.000	0.021	3.891
PHEN.	62.8	24.5	6.2	6.87	0.67	62.6	4.3	33.1	16.000	0.092	3.702
GMSS.	67.0	24.8	4.8	7.41	0.53	70.0	3.5	26.5	16.000	0.200	3.568
NORM	-	-	-	-	-	58.7	13.2	28.1	-	-	-
222, RHYODACITE:											
PHEN.	65.0	25.3	6.2	8.25	0.74	66.4	4.2	29.4	15.993	0.000	4.234
GMSS.	63.8	22.3	2.5	9.26	1.78	77.3	10.4	12.3	16.000	0.040	4.072
NORM	-	-	-	-	-	54.4	31.6	14.0	-	-	-
255, RHYODACITE:											
PHEN.	60.4	24.6	6.2	7.94	0.56	66.4	3.3	30.3	15.992	0.000	4.058
GMSS.	64.3	22.1	2.7	9.57	1.05	80.7	6.2	13.1	16.000	0.032	4.023
NORM	-	-	-	-	-	56.7	27.4	15.8	-	-	-

TABLE 2a

FELDSPAR ANALYSES

	WEIGHT PER CENT								NUMBER OF IONS (320)		
	SiO_2	Al_2O_3	CaO	Na_2O	K_2O	Ab	Or	An	Z-site	Y-site	X-site
MID-QUATERNARY TRANSITIONAL SERIES (CENTRE 2):											
349, OLIVINE THOLEIITE:											
PHENOCRYST	49.2	31.8	16.0	2.45	0.07	20.6	0.4	79.0	15.938	0.000	4.032
XENOCRYST	57.0	26.5	9.3	6.79	0.05	55.2	0.3	44.5	15.923	0.000	4.180
GMSS.	58.2	25.9	8.6	6.47	0.33	55.0	2.0	43.0	15.977	0.000	3.983
NORM	-	-	-	-	-	50.2	4.4	45.3	-	-	-
360, THOLEIITE:											
PHEN.	49.0	31.6	14.1	3.50	0.14	29.6	0.8	69.6	16.000	0.067	4.044
GMSS.	53.7	28.3	10.2	6.17	0.43	49.6	2.4	48.0	15.999	0.000	4.258
NORM	-	-	-	-	-	52.4	11.2	36.4	-	-	-
340, BASALTIC ANDESITE:											
PHEN.	55.1	27.7	10.2	5.61	0.47	47.2	2.8	50.0	16.000	0.006	4.044
GMSS.	56.8	27.0	8.5	6.31	0.68	53.5	4.1	42.4	16.000	0.042	4.006
NORM	-	-	-	-	-	58.8	17.7	23.5	-	-	-
211, COMPOSITE INTRUSION:											
XENOCRYST	46.7	33.0	18.1	1.71	0.09	13.8	0.5	85.7	15.866	0.000	4.210
PHEN.	59.2	25.1	6.3	8.38	1.02	65.7	5.6	28.7	15.942	0.000	4.354
GMSS.	62.9	20.8	3.4	8.85	3.14	68.0	16.9	15.1	15.862	0.000	4.458
NORM	-	-	-	-	-	51.1	32.5	16.3	-	-	-

TABLE 2a (continued)

	WEIGHT PER CENT								NUMBER OF IONS (320)		
	SiO_2	Al_2O_3	CaO	Na_2O	K_2O	Ab	Or	An	Z-site	Y-site	X-site
311, ACID TUFF:											
SANIDINE	66.5	19.4	0.03	7.59	5.83	64.9	35.0	0.1	16.000	0.051	3.964
SANIDINE	66.7	19.1	n.d.	7.36	6.07	63.4	36.6	0.0	16.000	0.049	3.935
NORM	-	-	-	-	-	53.7	46.2	0.1	-	-	-
295, OBSIDIAN:											
SANIDINE	65.6	19.2	0.14	7.45	7.47	58.4	41.0	0.6	15.932	0.000	4.353
ANORTHOCLASE	65.8	19.9	0.25	8.50	5.43	68.2	30.6	1.2	15.982	0.000	4.236
NORM	-	-	-	-	-	59.5	38.9	1.6	-	-	-
331, COMENDITE DYKE:											
SANIDINE	66.2	18.8	0.04	6.24	7.68	53.6	46.2	0.2	16.000	0.046	3.950
SANIDINE	66.0	18.5	0.03	7.34	7.29	58.9	41.0	0.1	15.949	0.000	4.249
NORM	-	-	-	-	-	53.7	46.3	0.0	-	-	-

TABLE 2b

FELDSPAR ANALYSES

	WEIGHT PER CENT								NUMBER OF IONS (320)		
	SiO_2	Al_2O_3	CaO	Na_2O	K_2O	Ab	Or	An	Z-site	Y-site	X-site
LATE-QUATERNARY ALKALIC SERIES:											
111, PORPHYRITIC ALKALIC BASALT:											
PHEN.	49.8	31.6	14.7	3.13	0.16	26.3	1.0	72.7	15.992	0.000	4.035
GMSS.	55.6	28.5	8.1	6.29	0.66	54.6	4.0	41.4	16.000	0.168	3.916
NORM	-	-	-	-	-	38.4	10.0	51.6	-	-	-
371, OLIVINE BASALT:											
PHEN.	49.5	31.5	14.5	3.42	0.21	28.4	1.2	70.4	15.992	0.000	4.108
GMSS.	51.4	30.4	12.8	4.16	0.25	35.2	1.5	63.3	16.000	0.039	4.026
NORM	-	-	-	-	-	39.3	7.8	52.9	-	-	-
348, HAWAIITE:											
XENOCRYST	48.0	30.5	16.8	0.82	0.02	7.7	0.1	92.2	15.935	0.000	3.572
PHEN.	54.0	28.9	13.5	3.03	0.11	27.6	0.7	71.7	15.981	0.000	3.692
GMSS.	58.6	26.1	9.1	5.12	0.44	47.7	2.9	49.4	16.000	0.062	3.612
NORM	-	-	-	-	-	48.1	13.7	38.2	-	-	-

TABLE 2b (continued)

	WEIGHT PER CENT								NUMBER OF IONS (320)		
	SiO_2	Al_2O_3	CaO	Na_2O	K_2O	Ab	Or	An	Z-site	Y-site	X-site
381, MUGEARITE:											
XENOCRYST	48.7	32.2	15.9	2.91	0.06	23.8	0.4	75.8	15.929	0.000	4.166
PHEN.	53.5	28.6	11.6	5.16	0.28	42.5	1.6	55.9	15.967	0.000	4.132
GMSS.	56.1	27.0	8.5	6.71	0.61	55.4	3.5	41.1	16.000	0.030	4.133
NORM	-	-	-	-	-	52.4	17.0	30.6	-	-	-
376, BENMOREITE:											
PHEN.	55.9	27.4	10.1	5.95	0.34	49.1	2.0	48.9	15.949	0.000	4.117
GMSS.	57.9	28.9	4.7	7.60	0.39	71.6	2.6	25.8	16.000	0.409	3.598
GMSS.	-	-	-	7.14	4.87	60.5	29.0	10.5	-	-	-
NORM	-	-	-	-	-	57.4	20.4	22.1	-	-	-

TABLE 3 ANALYTICAL DATA ON PLAGIOCLASE PHENOCRYSTS FROM KLAKKUR PALAGONITE TUFF (394)

	1 ("CLASSICAL")	2 (ELECTRON PROBE ANALYSES)	3	4
SiO_2	47.00	47.47	45.85	47.39
Al_2O_3	33.74	34.44	35.84	34.57
Fe_2O_3	0.57	0.66	0.61	0.65
MnO	0.01	-	-	-
MgO	0.14	-	-	-
CaO	17.70	15.55	16.10	15.62
Na_2O	1.44	1.87	1.61	1.77
K_2O	0.06	n.d.	n.d.	n.d.
TiO_2	0.02	-	-	-
SrO	0.08	-	-	-
	100.76			
mol. %				
Ab	13.0	17.9	15.3	17.0
Or	0.5	-	-	-
An	86.5	82.1	84.7	83.0
Qz	(0.2)	(3.3)	(2.0)	(3.6)
Wt. %				
Ab	12.2	17.0	14.6	16.2
Or	0.4	-	-	-
An	87.4	83.0	85.4	83.8

R.I. glass (Schairer et al. 1956) 1.563 An 87
1.564 An 89
R.I. β 1.580 An 91
Optic orientation (Burri et al. 1965) An 85,85,90,85,85.
$2V\alpha$: 82°, 84°, 80° and 82°.
X-Ray determination (2θ(131-2θ(131), Smith and Yoder, 1956) An 85,85,90,92.
Trace elements (p.p.m.): Sr 660, Rb 7, Zr 68, Ba 1300.

series on Klakkur (p. 59). The results are given in Table 3, including a "wet" chemical analysis of separated, hand-picked material, compared with the microprobe analyses of phenocrysts from the same tuff. Unfortunately, these crystals are inhomogenous and hence a direct comparison between the wet chemical analysis, representing the composition of a collection of crystals, and the microprobe data cannot be made. The chemical analysis calculates well in terms of mol. % An, Ab and Or, whereas the probe analyses show a consistent silica excess (2-3% in terms of normative quartz). Whether this is a function of the quality of the analysis of the particular probe standard employed, or inherent in the correction methods applied to the probe data or, thirdly, a real silica excess in the plagioclases is not known. The optical and X-ray diffraction data for the tuff plagioclase show a range in composition from An_{85} to An_{92} but An_{85} is the most frequent value, in fair agreement with the probe and chemical data.

Figure 39 is a histogram of the totals of all the feldspar analyses carried out for this work, representing the

---

Fig. 39: (Upper) A frequency histogram of total oxide content in analyzed feldspars. (Lower) Fe_2O_3 content in feldspars, plotted against Wt.% anorthite. Circles are phenocrysts, dots represent groundmass and microphenocrysts. Three circles marked Y are analyses of secondary albite (112), but points marked X are sanidine and anorthoclase phenocrysts from the acid rocks of Centre 2.

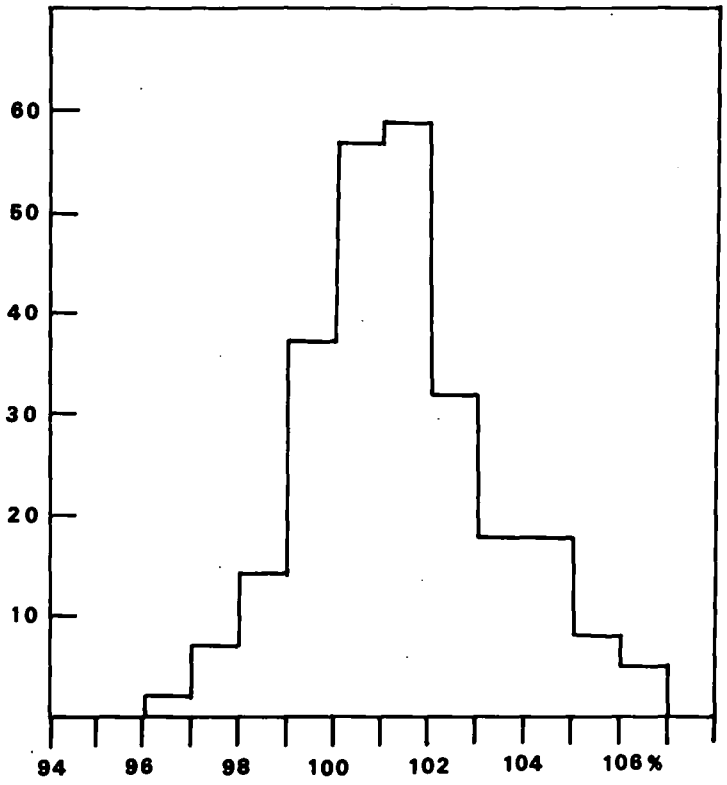
60
50
40
30
20
10
94
96
98
100
102
104
106%

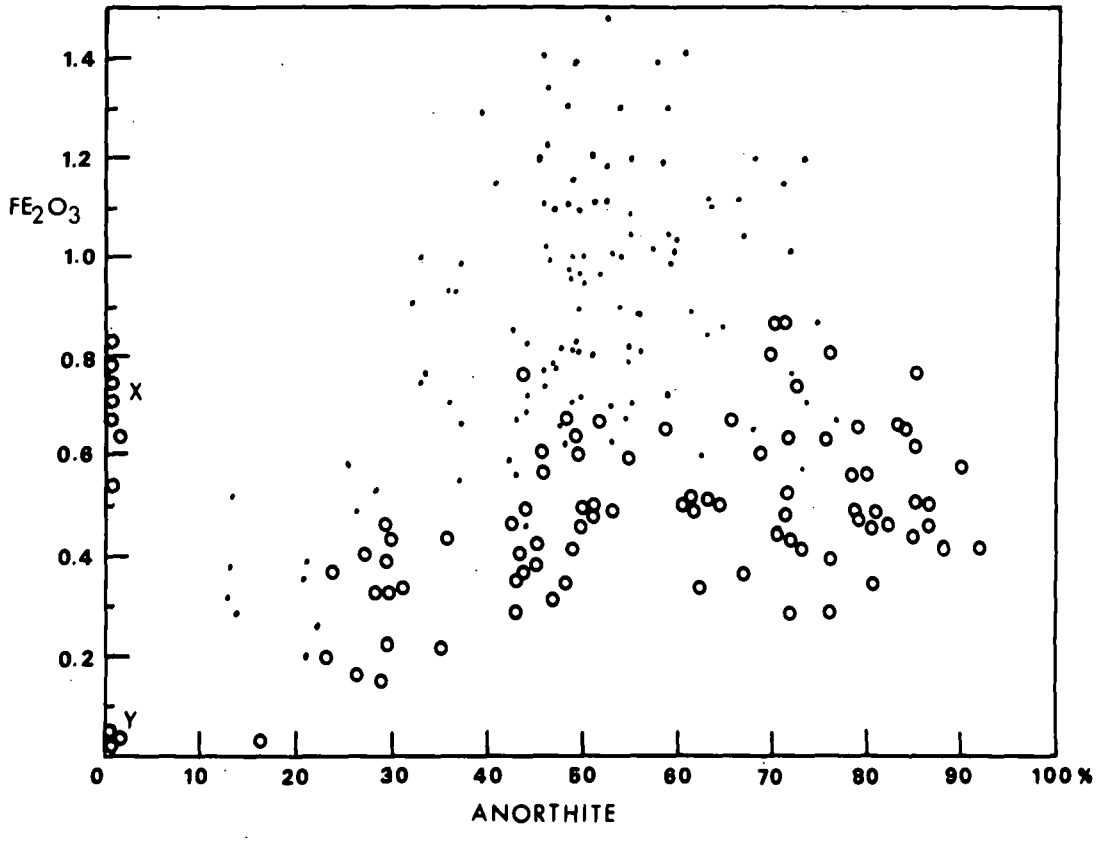
1.4
1.2
FE2O3
1.0
0.8
X
0.6
0.4
0.2
Y
0
10
20
30
40
50
60
70
80
90
100%
ANORTHITE

total of oxides prior to correction for fluorescence, atomic number effect and absorption. The totals show an almost normal distribution about a mean of 101%. Most of the analyses show excess silica when recalculated in terms of molecular proportions of the three feldspar end members, and the high original totals are probably related to a small, constant analytical error in the probe determination of SiO_2.

1. Iron content

The concentration of iron has been determined in the majority of analysed feldspars. In keeping with conventions and the evidence from chemically analyzed feldspars, we have assumed that all the iron is in the trivalent state and consequently have expressed it as weight % Fe_2O_3.

In Figure 39 the Fe_2O_3-content is plotted against wt. % Anorthite in groundmass feldspars (dots) and phenocrysts (circles). Several important points emerge from this figure. Firstly, a gradual increase in iron-content is observed with increasing An in the plagioclase phenocrysts. Secondary albite is very low in iron, as shown by three analyses of albitized plagioclase phenocrysts within the metamorphic aureole of Centre 1 (112). Sanidine and anorthoclase phenocrysts on the other hand are iron-rich, and contain up to 0.8% Fe_2O_3, equal to that

of some of the ferriferous orthoclases from Madagaskar (Kracek and Neuvonen, 1952). The replacement of Al by Fe^{3+} is commonly observed in the alkali feldspars, but the extremely low concentration observed in the secondary albites is an interesting contrast.

The oligoclase-andesine phenocrysts contain 0.2 to 0.4% Fe_2O_3, whereas iron in the bytownite phenocrysts is of the order of 0.4 to 0.6% Fe_2O_3. This slight but significant increase in iron content towards the calcic end of the plagioclase series may be related to the sympathetic variation in Al_2O_3, considering the diadochy of Al and Fe^{3+}.

The plagioclase grains of the groundmass show consistently higher Fe_2O_3 when compared with phenocrysts of corresponding An content. In some extreme cases the high iron content may be due to the diameter of the electron beam excitation area being greater than the diameter of the groundmass crystal, in which case the excitation of iron-bearing groundmass phases or glass will give erroneously high values. Analyses in which this effect has been suspected have been omitted from Figure 39.

Bearing in mind that the groundmass grains are quench products, whereas the phenocrysts have grown under rather stable equilibrium conditions, a greater structural

disordering will inevitably prevail in the groundmass plagioclase. The incorporation of Fe^{3+} into such a disordered high-albite structure to a greater extent than into a more ordered structure of the phenocrysts could well account for the observed differences in iron content.

2. Plagioclase compositions

The compositions of all the analysed feldspars have been recalculated to weight per cent of the three feldspar components and plotted in Figure 40. The detailed feldspar analyses for a representative suite of rocks are presented in Table 2, together with the normative feldspar of the host rock.

A continuous range of plagioclase compositions exists in each of the three rock series of the Setberg area, from bytownite to sodic andesine, with a small but significant increase in Or content towards the sodic end of the feldspar trend.

The trend of plagioclase compositions in the Tertiary tholeiitic series of Centre 1 is identical to that of the

---

Fig. 40 : The variation in composition of feldspars in the three Setberg rock series represented in terms of the components albite, anorthite and orthoclase (weight per cent). Microprobe analyses of feldspars are represented by dots, but the normative feldspar of the Setberg host rocks by a circle. Sections 1, 2 and 3 refer to the tholeiitic, transitional and alkalic rock series, respectively.

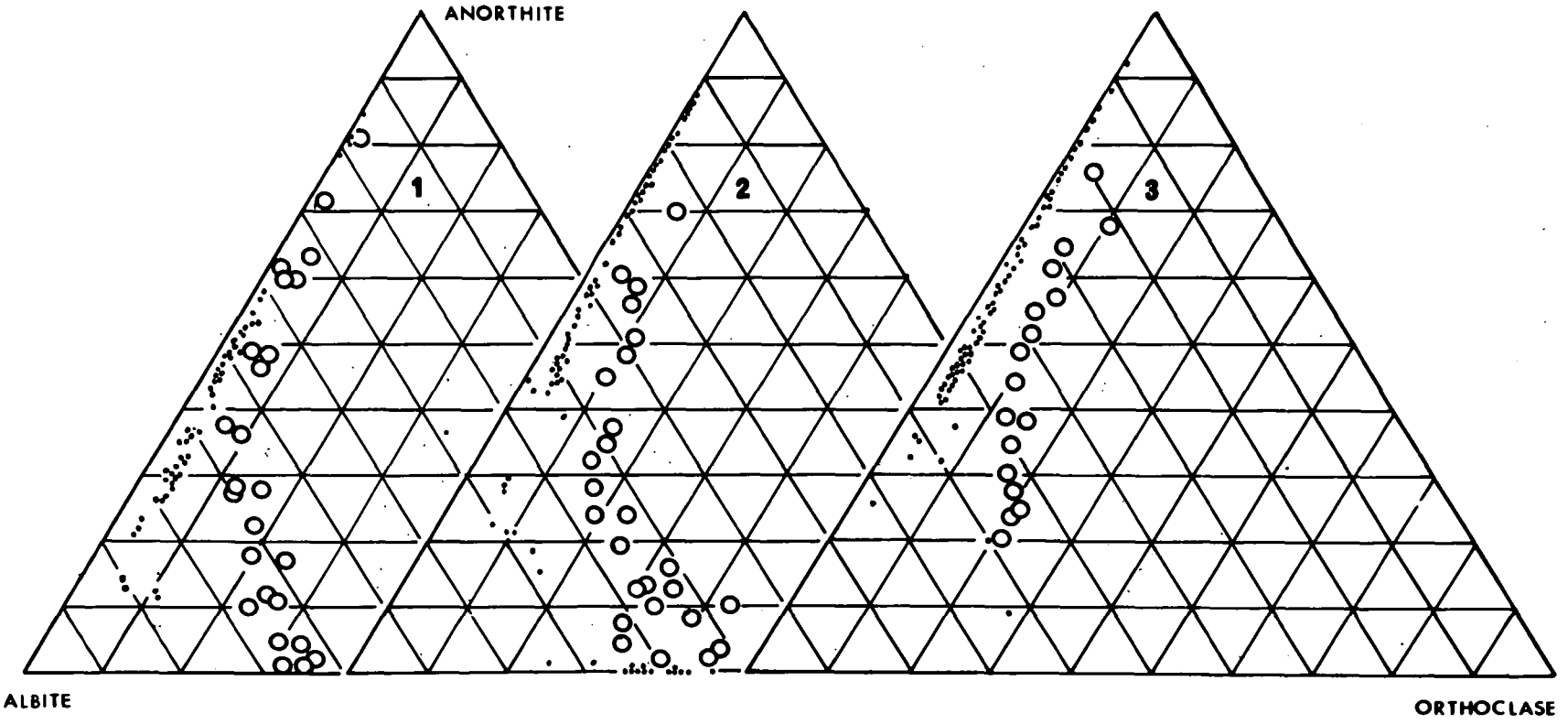
ANORTHITE
1
2
3
ALBITE
ORTHOCLASE

Thingmuli series from eastern Iceland (Carmichael, 1967). The basalts of Centre 1 contain calcic phenocrysts (An_{80}) with K_2O at or below detection limit, but a gradual increase in the Or molecule takes place with increasing Ab content, with 2 and 4% Or in feldspars of An_{45} and An_{30}, respectively. Only in the groundmass feldspars of the rhyodacites (222, 255) does the Or content reach 10%, at An_{12}.

Plagioclases of the transitional basalt series of Centre 2 (Figure 40 , no. 2) show significantly greater solid solution of the Or molecule than those of Centre 1. For crystals of An_{45} composition the Or content is 3%, and 6% in grains of An_{30} composition. Furthermore, the rhyodacites of Centre 2 contain groundmass anorthoclase or potash-oligoclase, with up to 17% Or.

The basaltic rocks of the alkalic series show similar feldspar relations as do the lavas of Centre 2, but the benmoreites contain groundmass feldspars of potash-oligoclase with up to 20% of the Or molecule, and anorthoclase.

The normative feldspar content of rocks in the three series (Figure 40) shows a successive increase in normative Or from the Tertiary tholeiitic series, low in alkalis, to the mildly alkaline series of Centre 2 and

the Late-Quaternary alkalic series.

The extent of solid solution of the three feldspar components in the oligoclase-anorthoclase range was discussed on p.168, with reference to the effect of temperature and composition of the magma. The data of Figure 40 further amplify the view of Tuttle and Bowen (1958), Carmichael (1963) and others, that the solubility volume of ternary feldspars is expanded in magmas rich in the feldspathic component, as opposed to highly siliceous magmas.

3. Alkali feldspar compositions

In addition to the groundmass anorthoclase in the rhyodacites of Centre 2 and the Late-Quaternary benmoreites, sodic sanidine and anorthoclase phenocrysts occur in the rhyolites of Centre 2 and the comenditic obsidians (p.127). The most potassic of these is a sanidine from a comendite dyke (331), containing 46% of the Or molecule, while the majority of the potassic feldspars in the rocks of Centre 2 group around Or_{35} to Or_{40}. All the sanidines analysed contain less than 1% of the An molecule, whereas co-existing anorthoclase in one obsidian (295) contains up to 2% of An. Feldspar relations in the sanidine-bearing comenditic rocks are discussed on p.132.

Five examples of two-feldspar rhyolites have been found in the Setberg area, all of which belong to Centre 2 (505, 259, 260, 342, 295). One of these is the obsidian dome north of Midhyrna (295, p.131), which contains early phenocrysts of sanidine and small laths of anorthoclase. The two-fold feldspar assemblage in this rock has been explained in terms of polybaric crystallization (p.133). The other two-feldspar rocks contain phenocrysts of oligoclase (An_{25-30}) which is accompanied by very rare and corroded grains of sanidine (342 and 505) or by anorthoclase (259 and 260). In none of these cases is equilibrium crystallization of a liquid on the two-feldspar boundary surface in the quaternary system $CaAl_2Si_2O_8$ - $NaAlSi_3O_8$ - $KAlSi_3O_8$ - SiO_2 a likely explanation. In one case the sanidines are clearly xenocrysts (342), but in the case of anorthoclase-oligoclase rocks we suggest that early crystallization of oligoclase was followed by formation of anorthoclase through the liquid reaching the feldspar thermal valley before reaching the feldspar-silica boundary surface. This path resembles initially that taken by trachytic rocks and other alkaline differentiates. Technically, the rocks are thus one-feldspar rhyolites, and our evidence of feldspar crystallization does not contradict Carmichael's (1963)

placing of the Icelandic acid rocks among the one-feldspar (plagioclase or anorthoclase) rhyolites, as opposed to the group of potassic two-feldspar rhyolites. Our evidence does, however, expand the spectrum of Icelandic acid rocks to include also the third type, characterized by the presence of anorthoclase phenocrysts and sometimes undersaturation of alumina with respect to soda, i.e. the alkaline and peralkaline acid rocks.

B. Olivines

In the Tertiary tholeiitic rocks of Centre 1 olivine is present only as sporadic phenocrysts in the olivine-tholeiite lavas and as fayalite phenocrysts in the rhyodacite cone sheets. There is thus a considerable range of magma compositions in which olivine was not precipitated and its place was taken by pigeonite, analogous to the behaviour of olivine in the Thingmuli series and the "Middle Zone" of the Skaergaard intrusion (Wager and Brown, 1968). In marked contrast to this is the presence of olivine throughout the differentiation sequence of the Transitional basalt series of Centre 2 and in the Alkalic series.

The olivine analyses presented here are of two types: "complete" microprobe analyses, where SiO_2, FeO, MgO, MnO and CaO were determined and partial analyses, including

TABLE 4 OLIVINE ANALYSES

COMPLETE ANALYSES[1)]

	369	376	228	229	505A	255	471	394
SiO_2	34.89	32.93	30.68	30.43	30.40	29.76	30.60	39.81
FeO	33.15	43.36	56.33	58.16	56.77	65.47	59.44	11.56
MgO	32.31	20.88	7.69	6.02	7.01	0.41	6.34	48.36
CaO	0.13	0.26	0.19	0.18	0.32	0.30	0.39	0.37
MnO	1.09	2.54	4.16	4.09	4.07	3.11	3.03	0.20
	101.57	99.98	99.05	98.88	98.57	99.05	99.80	100.68[2)]
Weight %								
Fa	47.4	61.8	80.0	83.6	80.9	93.0	84.5	16.4
Fo	56.5	36.6	13.5	10.6	12.2	0.7	11.1	84.5
Tp	1.6	3.6	6.0	5.9	5.8	4.5	4.3	0.3
La	0.2	0.4	0.3	0.3	0.5	0.5	0.6	0.6
	105.7	102.4	99.8	100.4	99.4	98.7	100.5	101.8
mol. %								
Fa	36.1	51.7	75.5	79.5	76.9	94.0	80.1	11.7
Fo	62.5	44.9	18.5	14.6	17.0	1.0	15.2	87.7
Tp	1.2	3.1	5.7	5.7	5.5	4.5	4.0	0.4
La	0.2	0.3	0.3	0.2	0.6	0.5	0.7	0.2

1)Numbers refer to specimen numbers in Table 14 of Appendix.

2)Includes 0.35% Al_2O_3 and 0.03% TiO_2.

TABLE 4a

OLIVINE ANALYSES

PARTIAL ANALYSES

	383	111	371	207	385	371	392	207
SiO_2	40.44	39.63	38.76	36.91	35.50	35.48	33.82	33.34
FeO	9.93	11.18	17.68	28.37	36.99	39.41	42.68	55.21
MgO	49.24	48.59	42.28	34.76	25.25	22.64	18.97	12.83
	99.61	99.40	98.73	100.04	97.73	97.53	95.47	101.38
Weight %								
Fo	86.0	85.1	74.0	60.8	44.2	39.5	33.2	22.4
Fa	14.1	15.9	25.3	40.5	52.5	56.0	60.8	78.7
	100.1	101.0	99.3	101.3	96.5	95.5	94.0	101.1
mol. %								
Fo	89.7	88.5	80.9	68.6	55.0	50.5	44.2	31.5
Fa	10.3	11.5	19.1	31.4	45.0	49.5	55.8	68.5

SiO_2, FeO and MgO only. A selection of analyses is presented in Table 4. The summation in terms of wt. % of the four olivine end-members is a good indicator of the quality of the analyses.

A systematic variation in CaO and MnO contents with increasing fayalite is demonstrated, and illustrated in Figure 41. The CaO content, expressed as the Larnite molecule, shows a small but significant increase from 0.2% in the forsteritic olivines to a maximum of 0.9% in fayalites. A much greater increase is observed in MnO with fayalite content, reaching 6% Tephroite in the olivine phenocrysts of some acid rocks.

The low amount of Ca-substitution in the forsteritic olivines is a reflection of the much greater ionic radius of Ca^{2+} (0.99) relative to the Mg^{2+} ion (0.66). With increasing iron content, increasing substitution or admission of Ca^{2+} and Mn^{2+} becomes possible. The preferential uptake of Mn^{2+} over Ca^{2+}, as demonstrated in Figure 41, takes place in spite of the much higher electronegativity of Mn^{2+} (1.4). The ionic radius of Fe^{2+} (0.74) and Mn^{2+} (0.88) are however, very

---

Fig. 41: (Upper) Fayalite content in analysed olivines plotted against the solidification index (MgO x 100/MgO+ Fe_2O_3+FeO+Na_2O+K_2O) of the host rock. The vertical bar shows the Fo range of olivines within each rock. (Lower) Calcium and manganese in olivines, expressed as wt. % Larnite and Tephroite, plotted against Fayalite content of olivine. Tie-lines join core and margin of zoned crystals.

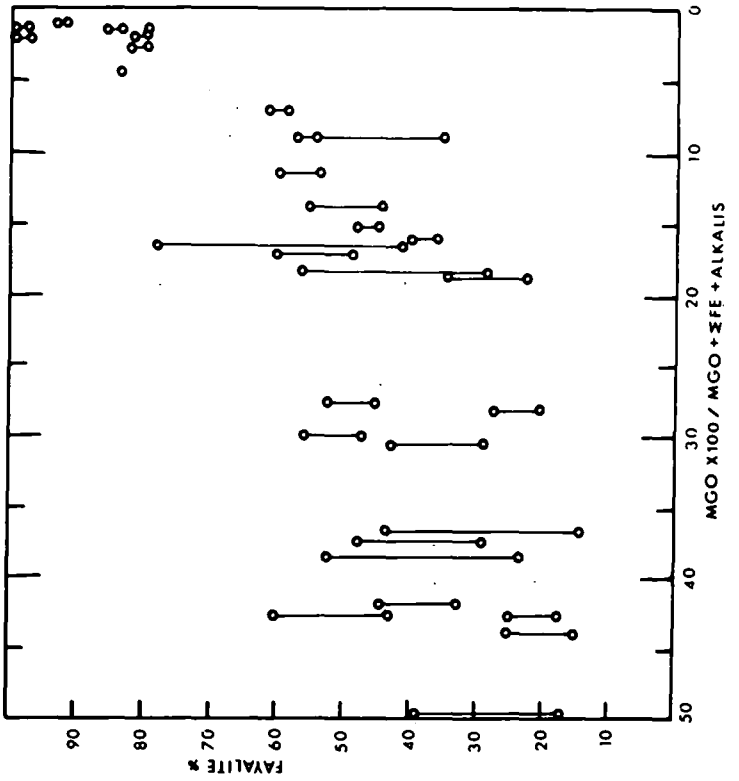
MGO X100 / MGO + ΣFE + ALKALIS
FAYALITE %

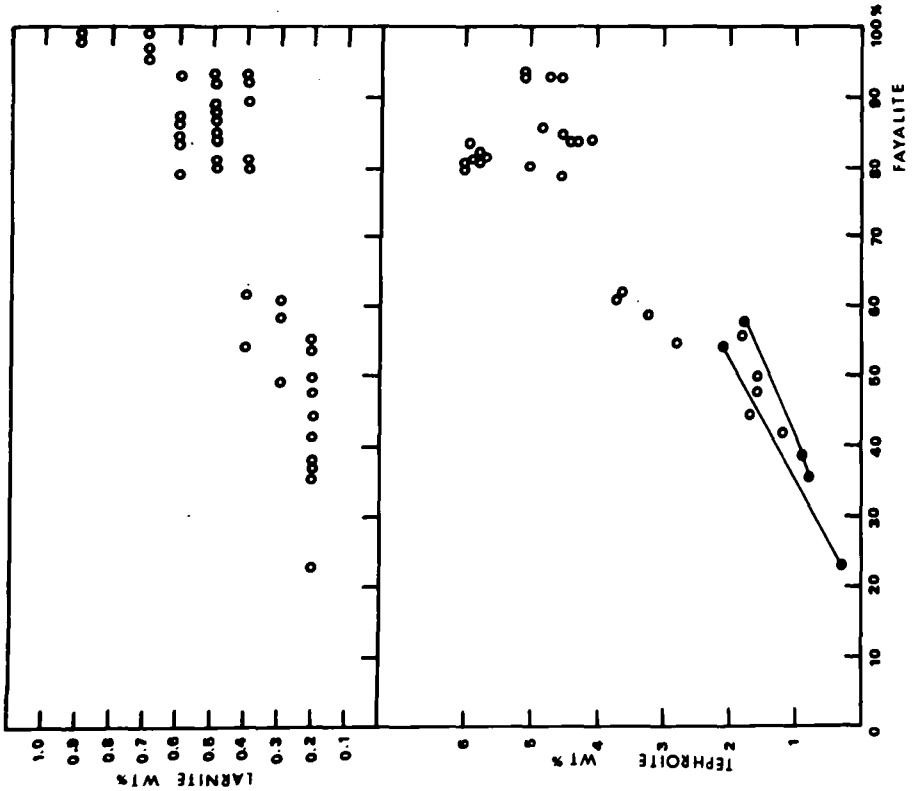
FAYALITE
TEPHROITE WT %
LARNITE WT %

similar and preferential admission of Mn^{2+} over Ca^{2+} into fayalite is thus accounted for.

It was emphasised in the discussion on petrology of the alkalic series that olivines show a great compositional range within one rock, and extensive zoning is observed within one grain. The compositional range of olivines observed in a number of rocks is plotted against solidification index of the host rocks in Figure 41. The magnitude of compositional variation is maintained in the basaltic and intermediate rocks, (S.I.$<$10), but is small in the fayalites. The relationship between co-existing olivines and pyroxenes is shown in Figure 42. The olivines have always a higher Fe/Mg ratio than associated clinopyroxenes, and the orientation of their tie-lines is similar to comparable phases in the Thingmuli series (Carmichael, 1967).

C. Pyroxenes

The pyroxenes are the most varied mineral group in the lavas of the Setberg area and characterize each of the three rock series. The tholeiitic series of Centre 1 contains rare hypersthene phenocrysts in the olivine tholeiites and bronzite in gabbroic xenoliths, in addition to the ubiquitous augite. Although a sub-calcic augite or pigeonite are not important constituents by volume, the former does occur in a

tholeiite (212) and the latter either as rare phenocrysts in the basaltic andesites (e.g. 413) or quite commonly in one of the icelandites (296). Most of the icelandites and rhyodacites of Centre 1 contain a fayalitic olivine instead of a calcium-poor pyroxene, along with ferroaugite or ferrohedenbergite.

Pyroxenes in the transitional basalt series of Centre 2 show less variety, but augite is present throughout. Very rare hypersthene phenocrysts are present in many lavas of this series, from tholeiitic lavas to icelandites (e.g. 339), but olivine is the dominant magnesium-bearing mineral in this series, instead of a Ca-poor pyroxene. The presence of pigeonite in one of the basaltic andesites of Centre 2 (501) has been attributed to contamination, as evidenced by the presence of quartz xenocrysts in this rock (p.120), favouring a reaction analogous to $Fo + SiO_2 = En$.

The acid rocks of Centre 2 are fayalite-ferroaugite or ferrohedenbergite-bearing, but a trend to sodic augite and aegirine-augite is observed in the Lysuskard rhyodacitic cone sheet (p. 90).

Augite is the sole pyroxene in the Late-Quaternary alkalic series, with one exception: the occurrence of pigeonite in the groundmass of an augite-olivine micro-porphyritic mugearite (369).

TABLE 5 PYROXENE ANALYSES

A: THOLEIITIC SERIES, CENTRE 1

	213a	213b	212	413a	413b	296a	296b	255	255	509
SiO_2	51.24	53.66	51.14	49.95	61.00	52.27	50.81	49.08	51.62	49.14
FeO	8.92	15.26	17.46	15.12	13.12	13.22	23.61	25.66	27.36	29.69
Fe_2O_3	0.24	0.13	0.83	0.62	-	0.34	0.39	0.73	0.79	0.75
MgO	16.15	27.55	12.95	12.74	16.01	13.27	15.71	3.96	1.90	0.80
CaO	19.42	1.26	14.83	16.56	4.50	16.17	3.88	17.57	19.40	17.69
MnO	0.37	0.52	0.63	0.71	1.03	-	-	1.09	-	-
TiO_2	0.50	0.26	0.79	1.04	0.46	0.58	0.30	0.54	0.79	-
Na_2O	0.09	0.05	0.32	0.24	-	0.13	0.15	0.28	0.86	0.29
Al_2O_3	3.21	1.33	1.15	3.09	0.86	3.48	0.99	1.17	-	-
mol. %										
En	41.3	68.5	33.5	33.4	53.0	33.6	41.1	10.3	5.0	2.1
Fs	17.5	28.9	34.6	30.6	34.6	32.3	50.5	51.5	52.8	58.5
Wo	41.2	2.6	31.9	36.0	12.4	34.1	8.4	38.2	42.2	39.4
Atom %										
Mg	45.7	73.8	38.4	38.0	58.9	38.4	47.3	12.5	6.1	2.7
Fe	14.8	23.7	30.1	26.5	29.2	28.1	44.3	47.5	49.2	55.2
Ca	39.5	2.4	31.5	35.5	11.9	33.5	8.4	40.0	44.7	42.1
FORMULAE OF PYROXENES ON THE BASIS OF 6 OXYGENS										
Z-site	2.000	2.000	2.000	2.000	2.150	2.000	2.000	2.000	2.008	2.043
Y-site	1.240	1.972	1.320	1.310	1.303	1.348	1.815	1.204	1.088	1.105
X-site	0.779	0.053	0.643	0.693	0.170	0.645	0.174	0.779	0.874	0.812

TABLE 5a PYROXENE ANALYSES

B: TRANSITIONAL SERIES, CENTRE 2

	393	393	340	309c	211	339b	306	505	364	342
SiO_2	54.04	48.39	51.83	49.62	52.33	54.00	51.10	51.95	49.96	48.46
FeO	4.61	8.42	14.58	10.21	14.99	24.84	19.67	17.89	26.86	29.60
Fe_2O_3	0.80	0.86	0.88	0.96	0.96	-	-	0.78	0.70	0.75
MgO	14.68	15.65	11.48	13.57	11.61	12.99	8.24	8.46	1.64	0.74
CaO	20.47	19.51	17.75	18.45	17.06	0.44	18.57	17.74	18.70	18.80
MnO	0.14	0.21	0.70	0.45	-	-	-	-	-	-
TiO_2	0.74	-	0.84	1.66	0.56	-	-	-	-	-
Na_2O	0.31	0.33	0.34	0.37	0.37	-	-	0.30	0.27	0.29
Al_2O_3	4.29	3.86	1.69	4.81	1.07	0.39	-	-	-	-
mol. %										
En	41.7	40.9	30.6	36.9	30.8	41.0	21.6	23.2	44	1.9
Fs	9.9	16.6	30.0	21.4	31.6	57.8	38.0	36.2	53.5	57.1
Wo	48.8	42.4	39.4	41.7	37.6	1.2	40.4	40.6	42.1	41.0
Atom %										
Mg	45.8	45.3	35.0	41.4	35.3	47.7	25.3	27.1	5.4	2.4
Fe	8.3	14.0	26.1	18.2	27.5	51.2	33.8	32.1	50.0	53.8
Ca	45.9	40.7	38.9	40.4	37.2	1.1	40.9	40.8	44.6	43.8
FORMULAE OF PYROXENES ON THE BASIS OF 6 OXYGENS										
Z-site	2.000	2.000	2.000	2.000	2.000	2.145	2.033	2.056	2.055	2.019
Y-site	1.117	1.223	1.226	1.228	1.250	1.486	1.143	1.114	1.046	1.101
X-site	0.816	0.805	0.747	0.766	0.722	0.018	0.792	0.776	0.846	0.863

TABLE 5b PYROXENE ANALYSES

C: ALKALIC SERIES

	111	111	111c	392	207	207c	337c	369b	376	394
SiO_2	53.25	50.68	52.20	52.75	49.87	45.50	50.90	52.07	51.08	50.31
FeO	3.34	7.51	12.50	9.79	10.85	19.47	11.49	28.19	11.76	3.72
Fe_2O_3	0.62	1.19	0.75	1.16	0.67	1.01	1.22	0.29	1.27	1.86
MgO	16.62	14.22	12.20	13.22	15.13	11.78	11.53	14.75	13.48	17.08
CaO	19.88	19.22	17.83	18.28	18.79	15.58	18.20	2.51	17.48	20.67
MnO	0.13	0.32	0.39	0.42	0.34	0.29	0.46	0.95	0.51	0.11
TiO_2	0.36	1.20	1.05	1.00	1.14	-	-	0.26	-	0.58
Na_2O	0.24	0.46	0.29	0.45	0.26	0.39	0.47	0.11	0.49	0.22
Al_2O_3	5.62	5.27	2.88	2.87	3.03	4.37	3.74	0.60	2.73	5.65
mol. %										
En	46.5	39.5	33.4	36.8	38.8	30.0	32.5	38.3	36.4	48.6
Fs	7.2	16.1	26.0	21.0	21.2	37.1	24.8	56.4	24.4	7.4
Wo	46.3	44.4	40.6	42.2	40.0	32.9	42.7	5.4	39.2	44.0
										100.24[1]
Atom %										
Mg	50.6	43.9	37.8	41.2	43.3	34.6	36.8	44.6	40.9	48.4
Fe	5.9	13.6	22.4	17.9	18.0	32.6	21.4	50.0	20.9	8.1
Ca	43.5	42.6	39.8	40.9	38.7	32.8	41.8	5.4	38.2	43.5

FORMULAE OF PYROXENES ON THE BASIS OF 6 OXYGENS

Z-site	2.000	2.000	2.000	2.000	2.000	2.000	2.000	2.012	2.000
Y-site	1.174	1.189	1.217	1.192	1.255	1.390	1.186	1.845	1.249
X-site	0.783	0.793	0.737	0.759	0.775	0.682	0.765	0.113	0.739

[1] Chemically analyzed

1. Pyroxene compositions and crystallization history

The analyzed pyroxenes are plotted in Figure 42, in terms of En, Fs and Wo mol. %, and a selection of analyses is presented in Table 5. In addition to the major elements, the concentrations of MnO, TiO_2 and Na_2O were determined in most of the analyzed pyroxenes. Al_2O_3 was determined in many, but after all the microprobe work had been completed it was discovered that the Al spectral peak or line is positioned on a sloping background with respect to 2θ, i.e. the intensity values on either side of the Al spectral peak are significantly different. As this effect was not taken into account at the time, all Al_2O_3 values reported here may be very slightly in excess of true, by as much as 0.2% Al_2O_3. However, a comparison of a pyroxene analysis carried out by chemical methods (394 in Table 5), and a microprobe analysis of pyroxene from the same rock (111, Table 5), reveals remarkably good agreement in Al-contents. However the alumina determinations in the former were by atomic absorption methods.

The analyses are calculated according to the general formula X Y Z_2 O_6, where X = Ca, Na, Y = Mg, Fe^{2+}, Mn, Al, Ti, Fe^{3+}, and Z = Si, Al Fe^{3+}. The valency of iron is, of course, unknown in the case of microprobe analyses and all Fe is taken as FeO. However, in the case of pyroxenes with

appreciable Na_2O, Fe_2O_3 is calculated by allotting equivalent molecular amounts of Fe_2O_3 to Na_2O, in making up the acmite molecule.

The compositional trends of the pyroxenes from the three rock series are shown in Figure 42. The tholeiitic series of Centre 1 follow broadly the Skaergaard pyroxene trend of progressive iron enrichment (Brown and Vincent, 1963), as well as showing a comparable orientation of tie lines between co-existing pyroxenes. A somewhat sub-calcic augite (Wo_{27}) and calcic pigeonite (Wo_{12}) in a basaltic andesite (413) are the only analyzed pyroxenes having affinities with sub-calcic augites, such as those reported from many Hawaiian tholeiitic lavas (Muir and Tilley, 1963). The Setberg Tertiary augites do, however, show a greater decrease in Ca as Fe replaces Mg than the Skaergaard augites, particularly in the range of basaltic andesites and icelandites. Co-existing diopsidic augite and bronzite from a Tertiary gabbroic xenolith (213), also plotted in Figure 42, may represent the early stages of this

---

Fig. 42: Variation in the composition of pyroxenes from the Setberg area, expressed by the components En, Fs and Wo in molecular per cent. Microprobe analyses of pyroxenes are indicated by circles and associated olivines by filled circles.

Dotted lines indicate the Skaergaard trend (Brown and Vincent, 1963). Parts 1, 2 and 3 refer to the Tholeiitic, Transitional and Alkalic rock series, respectively.

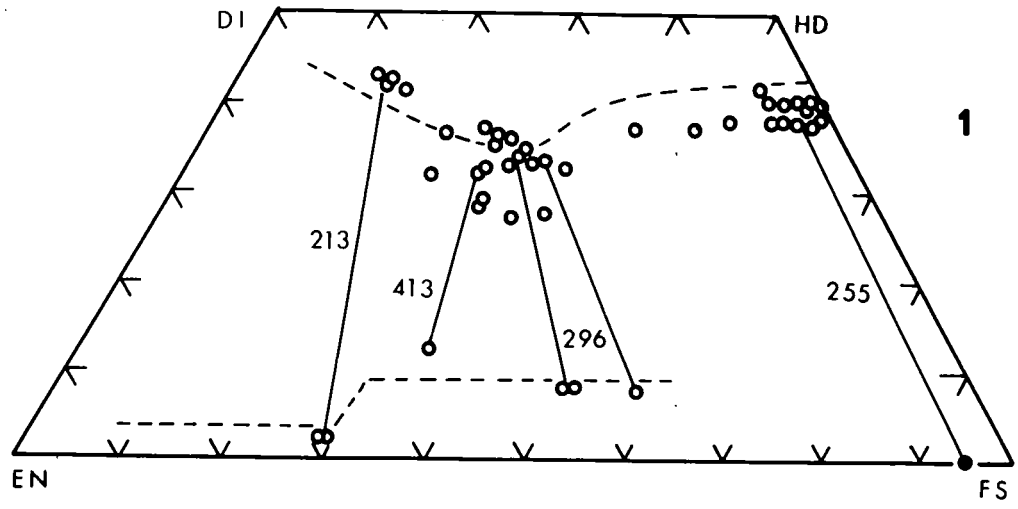
DI
HD
1
213
413
296
255
EN
FS

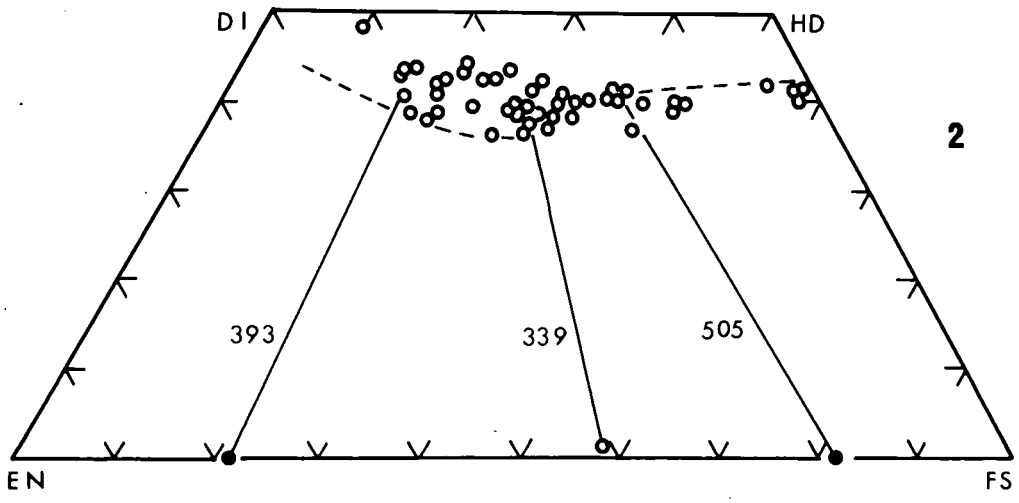
DI
HD
2
393
339
505
EN
FS

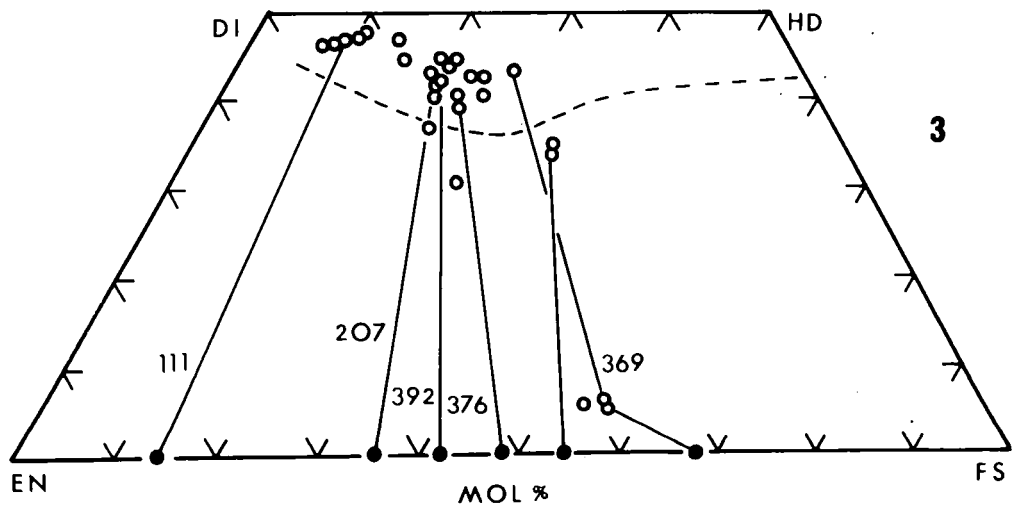
DI
HD
3
111
207
392
376
369
EN
MOL %
FS

fractionation series. The common bronzite-pigeonite trend of tholeiitic rocks is shown by the Tertiary series, but calcium-poor pyroxenes are rare in the Setberg Tertiary as compared with the Thingmuli lavas (Carmichael, 1967). The pigeonite trend does not reach the icelandites, which contain a ferroaugite and fayalitic olivine, with the exception of one icelandite obsidian (296) which contains phenocrysts of iron-rich pigeonite and ferroaugite. The Fe/Mg ratio in the average icelandite is 20, whereas this anomalous rock has an Fe/Mg ratio of 9. The stability of a Ca-poor pyroxene may be enhanced in such an iron-deficient liquid, resulting in the precipitation of pigeonite instead of a fayalitic olivine.

The augites of the transitional lavas of Centre 2 show a general iron-enrichment trend but are significantly richer in the Wo molecule than augites of the Tertiary series (Figure 42), and tend towards a calcic augite trend (characteristic of alkalic series) in the early stages of fractionation. The occurrence of both olivine and hypersthene phenocrysts, albeit rare, in the basalts and basaltic andesites of Centre 2 is an equally good indicator of the transitional nature of this rock-series.

If this assemblage of olivine, clinopyroxene and ortho-pyroxene is viewed in relation to the system

Fo-Di-SiO_2 at 1 atm. (Kushiro and Schairer, 1963; Kushiro, 1969), magmas of the transitional basalts can be thought of as liquids alternatively in equilibrium with Di and Fo, or Di and En. Two models can conceivably account for the triple ferromagnesian mineral assemblage in the transitional basalts. Early crystallization of the orthopyroxenes from a liquid on the Fo_{ss}-Pr_{ss} boundary curve in the system Fo-Di-SiO_2 (Kushiro, op.cit. Figure 6) would lead to a shift in composition of the liquid towards the Di corner, giving a liquid in equilibrium with Di and Fo, subsequently crystallizing olivine along with augite. On fractionation, such a liquid migrates to the reaction point Fo-Di-En (A in Figure 25, Kushiro and Schairer, op.cit.), a condition which has been observed only in one case in the transitional rock series of the Setberg area, namely in a basaltic andesite (501) precipitating pigeonite, in which case some silica contamination by quartz xenocrysts was operative.

Alternatively, the olivine-hypersthene-augite assemblage in the transitional basalts may reflect early crystallization at pressures sufficiently high to suppress the incongruent melting of enstatite, which at atmospheric pressure leads to formation of forsterite and liquid over-saturated in silica. Above pressures of about 6 kb,

melting of $MgSiO_3$ is congruent (Boyd and England, 1963), and Kushiro (1964) has demonstrated that the reaction point Fo-Di-En (Fo+liquid=Di+En) in the system Fo-Di-SiO_2 at atmospheric pressure lies within the Fo volume at 20 kb pressure in the dry system, and is probably the locus of the reaction En+liquid=Di+Fo. The average olivine-tholeiite and tholeiite of the transitional series (Table 10) fall on either side of the Fo_{ss} - Pr_{ss} boundary curve at 20 kb when plotted in the system Fo - Di - SiO_2. Early crystallization of such magmas at this pressure, or indeed any pressure above 6 kb (approx. 20 km depth) would result in initial precipitation of Fo and En, until the liquid reaches the reaction point Fo-Di-En (point P in Figure 6, Kushiro, 1969), where the three ferromagnesian phases can co-exist. The nature of this point is not yet clear from experimental work (Kushiro, 1969), but the career of such a magma in the volcanic environment would be drastically affected by ascent in the crust. Decrease in pressure expands the Fo field, leading to precipitation of olivine as the dominant fractionation control. The two alternatives suggested here, to account for the unusual mineralogy in the transitional basalts are equally plausible in the light of data available to us at present, but future work, such as determination of Al-content in the orthopyroxenes,

may help in discriminating between the two models.

Augites in the alkalic series show a typical calcic-augite trend, with a small degree of ferrous iron enrichment accompanied by slight fall in the Ca-content with differentiation (Figure 42). This is comparable to the trend of pyroxenes in the alkalic olivine basalt magma of the Gunnedah Sill (Wilkinson, 1956). Calcium-poor pyroxenes are absent from the Late-Quaternary alkalic series of the Setberg area, with the notable exception of a mugearite flow (369) containing augite, iron-rich pigeonite and fayalitic olivine, not unlike the assemblage in a Thingmuli icelandite (Carmichael, 1967) in which the fayalite has been considered a xenocryst phase. In the Setberg mugearite the ferromagnesian minerals are microphenocryst or groundmass phases, and a xenocryst origin is unlikely.

The Ca-rich nature of augites from undersaturated basalts, the absence of Ca-poor pyroxenes and the abrupt termination of the augite trend has been discussed by Brown (1968). As undersaturated liquids in the system Fo-Di-SiO_2 (Kushiro and Schairer, 1963) are in equilibrium with Di and Fo only, more calcium will be taken up by the clinopyroxenes. Distribution of calcium in liquids in

equilibrium with Di and En (augite and pigeonite in natural systems) accounts for the lower Ca-content of tholeiitic augites. The short trend is usually attributed to departure from the Wo-En-Fs plane with acmite enrichment, but no notable increase in Na was detected in the Setberg alkalic series pyroxenes.

2. Minor elements

The concentration of TiO_2, MnO and Al_2O_3 in the Setberg clinopyroxenes is shown in Figure 43, where weight per cent oxides is plotted against mol. per cent ferrosilite (as a convenient parameter of the fractionation trend). The distribution of minor elements between coexisting Ca-rich and Ca-poor pyroxenes follows the pattern

---

Fig. 43: Part 1: Variation in TiO_2 and MnO of pyroxenes, plotted against mol. % Ferrosilite. Filled circles are orthopyroxene analyses.

Part 2: Sodic clinopyroxenes from the Lysuskard cone sheet of Centre 2 plotted in terms of atom % Di, Hd and Ac. Two tie lines join sodic pyroxene margins with augite host. Dotted line marked A is the trend of pyroxenes from alkalic plutons in East Africa (Tyler and King, 1967), and line marked B is the trend of pyroxenes from alkalic lavas from Mount Suswa, Kenya (Nash et al., 1969).

Part 3: Variation in Al_2O_3 of pyroxenes plotted against mol. % Ferrosilite.

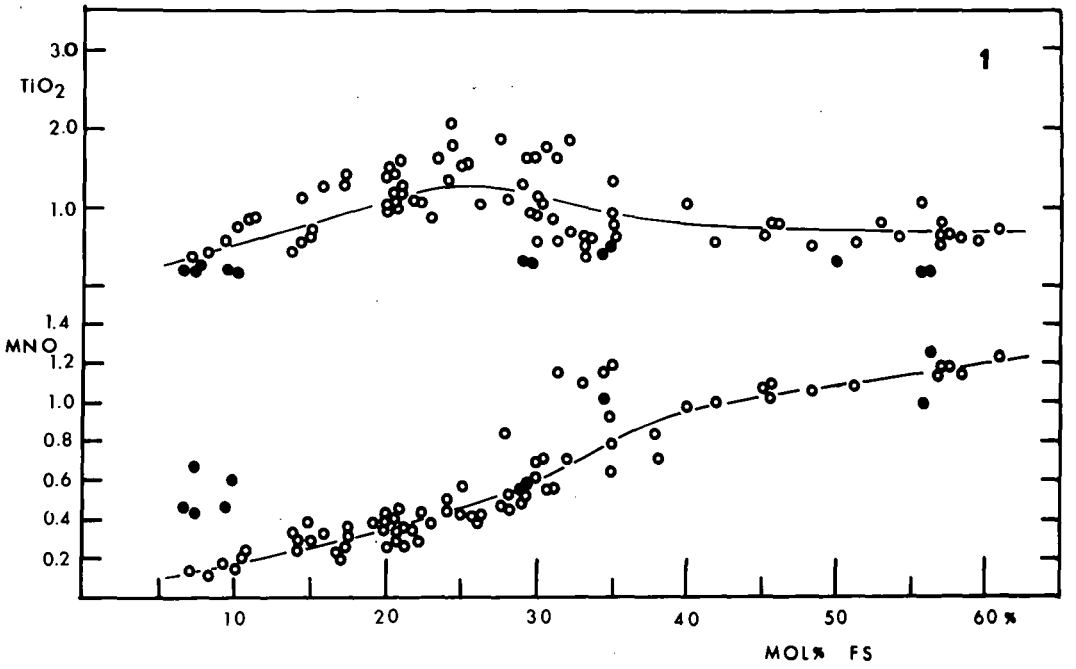
1
TiO2
3.0
2.0
1.0
MNO
1.4
1.2
1.0
0.8
0.6
0.4
0.2
10
20
30
40
50
60 %
MOL% FS

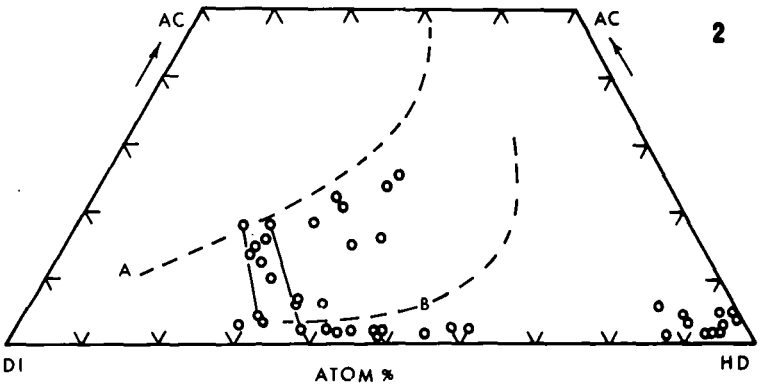
2
AC
AC
A
B
DI
ATOM %
HD

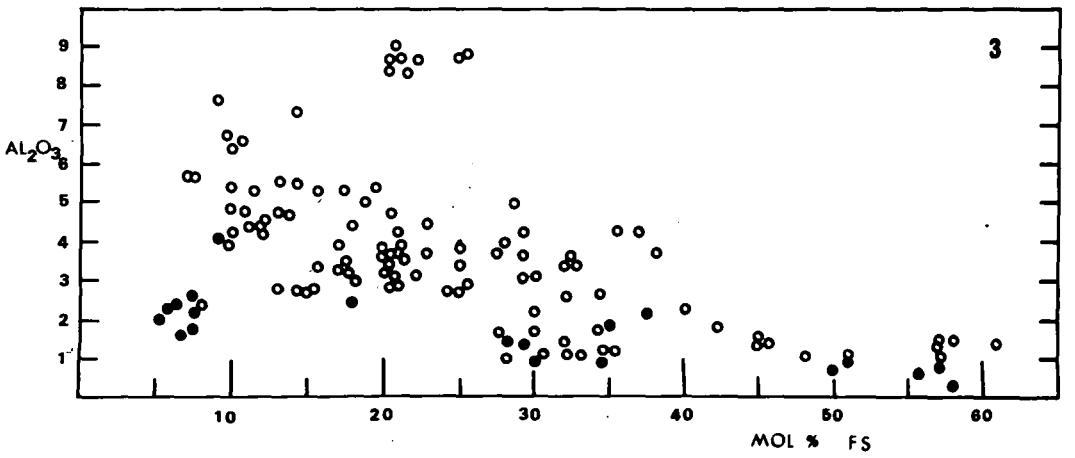
3
Al2O3
9
8
7
6
5
4
3
2
1
10
20
30
40
50
60
MOL % FS

of the Skaergaard intrusion (Brown, 1957) and the Thingmuli lavas (Carmichael, 1967). Augites are enriched in TiO_2 and Al_2O_3, whereas the Ca-poor pyroxenes show a higher Mn-content. The increase in MnO with iron enrichment is stepped, comparable to the MnO variation curve of the Thingmuli pyroxenes. Inspection of Carmichael's data (1964, 1967) shows that this step coincides with the appearance of magnetite as a microphenocryst in the lavas (specim. 6 to 13, Carmichael, 1964). The variation curve for TiO_2 is rather diffuse, but shows a broad hump in the range of basaltic lavas, decreasing antipathetically with the MnO-increase. Ti is clearly taken up by the titano-magnetites, which appear as a microphenocryst phase in the more differentiated basalts, and it becomes more scarce for incorporation into co-existing pyroxenes. Mn is, however, not greatly enriched in magnetites and ilmenites, with respect to the liquid, being only four times more abundant in the iron-titanium oxides than in the bulk rock (Carmichael, 1964, 1967), and thus Mn continues to be available for incorporation into the pyroxene network and, to a greater extent, into fayalitic olivines (p.175).

The Al_2O_3-content decreases, presumably with crystallization temperature, from 4-5% in diopsidic augites from the

undersaturated basalts, to approximately 1% in the ferrohedenbergites. The variation in Al content is also related to Ca and the very high Al_2O_3-values observed in the phenocrysts of certain undersaturated lavas from the Late-Quaternary series may possibly be due to formation of the Ca-Tschermak's molecule ($CaAl_2SiO_6$) in place of the anorthite molecule. As Al frequently makes up 6 to 10% of the Z-site in augites of the undersaturated lavas, it is probable that the low silica content of these magmas has favoured the formation of Ca-Tschermak's molecule, as suggested by Brown (1968).

The solubility of Al_2O_3 in enstatite increases with pressure (Boyd and England, 1963) and the high Al_2O_3-contents of orthopyroxenes and augites in basaltic nodules has generally been ascribed to high pressures of crystallization. Whether or not some of the augites and diopsidic augites of the Setberg alkalic lavas, containing 6 to 9% Al_2O_3, are inherited from such an event of high-pressure crystallization at depth is a matter of speculation, particularly in view of the high solubility of Al_2O_3 in diopside at 1 atm., as shown by Hytönen and Schairer (1961).

3. Sodic pyroxenes

Pyroxenes in the Lysuskard granophyre of Centre 2

(p. 90) exhibit a colour and pleochroism in various shades of green, and contain up to 27% of the Acmite molecule. The dominant pyroxene in the granophyric cone sheet is a greenish calcic augite of moderate iron content, typically near $Wo_{40}En_{30}Fs_{30}$ in composition and frequently zoned to lush green, sodic rims of aegirine-augite, which also forms an independent phase in some parts of the cone sheet (e.g. 223).

Analyses of several sodic pyroxenes are given in Table 6 and their compositions have been plotted in Figure 43, in terms of the end-members Ac - Di - Hd conventionally employed to represent pyroxenes of this composition (Tyler and King, 1967). The Setberg sodic pyroxenes are, however, badly represented by this plot owing to their transitional position between the augite trend and a true aegirine-augite composition. Their compositions lie on the En-Fs side of the Di-Ac-Hd plane in the pyroxene tetrahedron Wo-Ac-Fs-En, as is illustrated by the Wo-deficiency of the analyses when cast in this compositional plane (see Wo-balance in Table 6).

Ferrous iron enrichment, without appreciable sodium enrichment, is characteristic of pyroxenes in most acid rocks of the Setberg area, particularly those of Centre 1 and most of the rhyolitic rocks of Centre 2. The

TABLE 6 SODIC PYROXENE ANALYSES

	227A	227B	228	223A	223B	223C
SiO_2	51.84	52.00	45.01	52.00	51.94	53.21
FeO	12.29	10.31	16.83	9.57	10.00	8.84
Fe_2O_3	2.43	6.40	6.88	3.56	6.96	9.18
MgO	11.43	13.91	9.76	11.14	9.73	8.27
CaO	18.31	9.56	8.98	21.06	17.71	16.54
Na_2O	0.94	2.48	2.67	1.38[1]	2.70[2]	3.56[3]
mol. %						
Hn	29.7	37.7	25.9	27.7	24.1	21.0
Fs	23.5	20.6	33.0	18.4	19.5	17.1
Wo	39.5	21.6	19.9	43.6	36.4	34.9
Ac	7.3	20.1	21.2	10.3	20.0	27.0
Atom %						
Di	58.5	60.7	43.0	60.1	50.6	45.9
Hd	35.3	25.2	41.7	30.3	31.1	28.4
Ac	6.2	14.1	15.3	9.7	18.3	25.7
Wo Balance	-15	-37	-37	-5	-8	-4

FORMULAE OF SODIC PYROXENES ON THE BASIS OF 6 OXYGENS

Z-site	2.017	2.037	2.000	2.000	2.000	2.001
Y-site	1.134	1.338	1.412	1.056	1.093	1.050
X-site	0.835	0.590	0.641	0.953	0.918	0.926

KEY TO TABLE 6

227A: Pyroxene in rhyodacitic cone sheet of Lysuskard, Centre 2.

227B: Margin of 227A.

228 : Pyroxene in granophyric facies of Lysuskard cone sheet.

223A: Pyroxene in marginal facies of Lysuskard cone sheet, centre of grain.

223B: Pyroxene in marginal facies of Lysuskard cone sheet, margin of grain.

223C: Pyroxene in marginal facies of Lysuskard cone sheet, discrete grain of groundmass.

1) Contains 0.97% Al_2O_3, 0.27% TiO_2, 0.43% MnO.

2) Contains 0.70% Al_2O_3, 0.27% TiO_2, 0.68% MnO.

3) Contains 0.68% Al_2O_3, 0.33% TiO_2, 0.31% MnO.

deviation of the Lysuskard pyroxenes from this trend at an early stage of iron enrichment (Fs_{30} to Fs_{40}) and the formation of an $NaFe^{3+}$-enrichment trend, is a feature in common with the younger peralkaline obsidians only (p.130).

The soda-enrichment trend of the Lysuskard pyroxenes is intermediate betweenthat of pyroxenes from plutonic rocks of East Africa (Tyler and King, 1967), where soda-enrichment starts near the diposide corner (line A in Figure 43), and the trend of sodic pyroxenes from Mount Suswa, Kenya (Nash et al., 1969) shown by the line B in Figure 43. The Lysuskard granophyre is intermediate in habit and occurrence between the East African granites on the one hand and E. Africanlavas on the other and it is believed that the magma oxygen fugacity is the main controlling factor in determining the extent of $NaFe^{3+}$ enrichment.

Ferroaugites and ferrohedenbergites from other acid rocks in the Setberg area are also plotted in Figure 43. Some of these show a very slight increase in soda at the hedenbergite end, but clearly the two trends of clinopyroxene compositions are well separated and no intermediate types have been encountered.

D. Other minerals

In view of the extensive data presented on the main rock-forming minerals in the Setberg rocks, the shortage of data on the iron-titanium oxides is a serious omission, particularly with regard of the potential of these minerals as indicators of physical conditions in the magmas at the time of crystallization. Examination and analysis of the iron-titanium oxides is planned for the next stage in the investigation of the Setberg area.

1. Hornblende

The hornblende and phlogopite found in vugs and cavities of one of the Late-Quaternary mugearites (369, p.151) have been partially analysed with the microprobe. The analyses are presented in Table 7, together with partial analyses of apatite phenocrysts from an icelandite of Centre 2 (307) and from a Late-Quaternary benmoreite (337).

The hornblende has a composition close to that of an edenitic hornblende (e.g. analyses no. 4, Table 41, Deer et al., 1963), but the high SiO_2 and low Al_2O_3 are noteworthy. Hornblendes of late crystallization are frequently low in Al and there is little doubt that substitution of Si by Al in the Z-site is mainly controlled by the temperature at the time of crystallization. This is in keeping with

TABLE 7 ANALYSES OF MISCELLANEOUS MINERALS

	HORNBLENDE		PHLOGOPITE		APATITE	
	1	2	3	4	5	6
SiO_2	48.52	48.35	40.67	40.10	-	0.09
Al_2O_3	8.19	10.00	-	12.02	0.48	0.24
TiO_2	1.49	0.61	-	6.15	0.13	0.45
FeO	15.40	10.69	10.79	8.84	3.76	1.24
MgO	14.03	14.09	21.33	17.40	-	0.06
CaO	9.45	10.78	nil	nil	50.50	49.18
Na_2O	2.70	2.29	0.80	1.00	0.08	1.73
MnO	0.37	0.18	-	0.82	0.26	0.86
	100.15	100.37[1]		99.02[2]		

FORMULAE ON THE BASIS OF 24 OXYGEN ATOMS

Z-site	7.778	8.000
Y-site	5.205	5.15
X-site	1.706	2.36

KEY TO TABLE 7

1: Edenitic hornblende from vesicle in mugearite lava 369.

2: Hornblende, amphibole schist. (Table 41, p.282, Deer et al., 1963).

3: Phlogopite from vesicle in mugearite 369.

4: Phlogopite from vesicle in Jan Mayen lava (Flower, 1969).

5: Apatite phenocryst from icelandite of Centre 2 (307).

6: Apatite phenocryst from benmoreite of the Setberg alkalic series (337).

1) Includes 0.94% Fe_2O_3, 0.30% K_2O, 0.20% H_2O^- and 1.93% H_2O^+.

2) Includes 0.63% Fe_2O_3, 8.36% K_2O and 3.70% H_2O.

the occurrence of the Setberg edenitic hornblendes in druses and cavities of the lava.(Figures 36 and 37).

2. Phlogopite

Phlogopite grains, up to 0.5 mm in diameter, also occur in vugs of this mugearite. They form pleochroic yellow to fox-brown crystals, with a 2V(-ve) near zero. The average of two partial analyses is given in Table 7, along with an analysis of a phlogopite from vesicles in a lava flow from Jan Mayen island (Flower, 1969).

The occurrence of biotite (sensu lato) in the groundmass of many of the Late-Quaternary olivine basalts, hawaiites and mugearites has been referred to in Chapter 3. These biotites have, however, not yet been analysed, but their general similarity to the analysed phlogopite suggests a magnesian composition. Trioctahedral micas, commonly referred to as biotites, are rare in basaltic lavas but have been reported from Jan Mayen trachybasalts and trachyandesites (Roberts and Hawkins, 1965) where they occur as ragged plates and mossy aggregates in the groundmass. They have also been described as groundmass constituents of certain olivine basalts and trachybasalts from St. Helena (I. Baker, 1969) and Tristan da Cunha (P. Baker et al., 1964). A dark mica is reported in hawaiites of the upper series of Mauna Kea (Macdonald and Katsura, 1964).

The relative scarcity of biotites (s.l.) in extrusive basaltic rocks is commonly attributed to their breakdown at low pressures and magmatic temperatures. Yoder and Eugster (1954) have shown experimentally that the phlogopite stability curve lies above the minimum melting curve of basalt at intermediate pressures ($> 2 \times 10^{-3}$ atm.) but becomes unstable above 800 to 900°C at very low pressures in basaltic magmas.

Data derived from studies on the join $K_2O.6MgO.Al_2O_3.6SiO_2$-H_2O are, however, perhaps not directly related to the stability of a trioctahedral mica in a basaltic liquid. Further evidence on the stability of dark micas came from the experiments of Yoder and Tilley (1962), on the crystallization behaviour of alkalic basalt and hawaiite at various water-pressures and temperatures. A primary mica phase appeared at temperatures up to 650-900°C, depending on the pressure, and in the hawaiite biotite crystallized at 900°C at 200 bars pH_2O, or near the solidus. More recent work relating to the stability of phlogopite (Luth, 1967; Yoder and Kushiro, 1969) has shown that phlogopite is stable with forsterite and liquid at pressures of 1 kb or more at approximately 1180°C, in the presence of excess water, but stable at higher temperatures in conditions of water-deficiency (Yoder and

Kushiro, 1969, fig. 60).

Biotites in the Setberg alkalic series are typically a groundmass constituent, which may exhibit a subophitic relationship with groundmass plagioclase. Reaction features, such as rimming by iron-ore granules, have not been observed and we can only conclude that the biotites are near equilibrium in the magma at the time of crystallization. Some of the biotite flakes are up to 0.5 mm in diameter and are frequently found as inclusions in olivine and plagioclase phenocrysts (344, 384).

Similarly, the phlogopite crystals found in vugs of a mugearite lava are considered a product of low pressure crystallization. A build-up of pressure within vesicles in a semi-solid lava is, however, a possibility and may have favoured the growth of phlogopite, which is absent from the groundmass.

Flower (1969) suggests that the phlogopites found in vesicles of a Jan Mayen basalt are xenocrysts from a mantle phase. It is indeed difficult to envisage why such "xenocrysts" would be present in cavities only, while entirely absent from the body of the lava.

In view of the extended stability field of phlogopite at low pressures, we consider all the biotite and phlogopite occurrences described here as products of low pressure

and near-surface or surface crystallization from a water-rich magma. On vesiculation the crystallization of the hydrous groundmass minerals will be hindered and eventually terminated, but in quiet conditions of flow the formation of phlogopite and a hornblende could take place at the interphase between the volatile component and the silicate melt, i.e. on the vesicle walls as observed in the Setberg mugearite and Jan Mayen basalt.

The possibility of biotite and phlogopite crystallization from a melt at greater depths and the importance of the latter mineral as a possible minor mantle phase (Griffin and Murthy, 1969) is by no means dismissed here, but in the case of the Setberg trioctahedral micas, more tangible explanations are at hand to account for their occurrence in the Late-Quaternary alkalic series.

3. Apatite

The occurrence of apatite microphenocrysts in the mugearites and benmoreites of the Late-Quaternary alkalic series has been remarked upon (p.149) and their presence related to the high P_2O_5-content of these lavas. Similar phenocrysts are also present in some of the basaltic andesites and icelandites of Centre 2 (p.121). Few reports of similar nature have been encountered in the literature. Apatite microphenocrysts, 0.3 mm in size, are

reported from a Tasmanian basanite and Queensland hawaiites (Joplin, p. 83 and 52, 1964). I. Baker (1969) describes discrete microphenocrysts of apatite in St. Helena trachybasalts and trachyandesites, typically pink and weakly pleochroic, as are the Setberg apatites. Baker attributes their colour and pleochroism to minute oriented inclusions, possibly of rutile.

Two partial analyses of apatite phenocrysts are presented in Table 7. A notable feature is the presence of significant amounts of iron, while TiO_2 is present in very small amount only. The pleochroism of the Setberg apatites may be attributed to the presence of iron as an integral component, rather than foreign inclusions.

TABLE 8 MINERAL VARIATION IN THE SETBERG LAVAS, PHENOCRYSTS

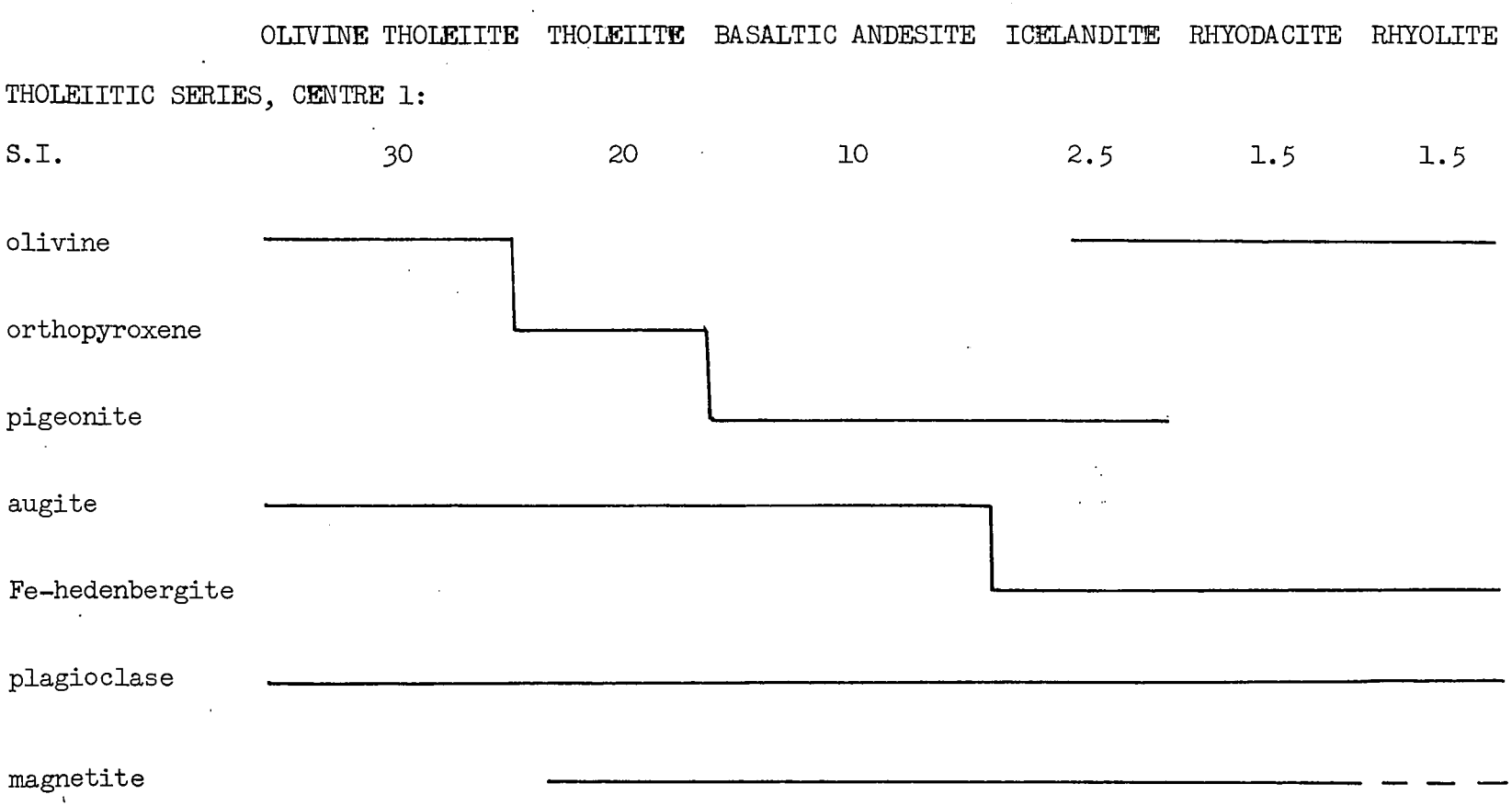

TABLE 8 (continued)

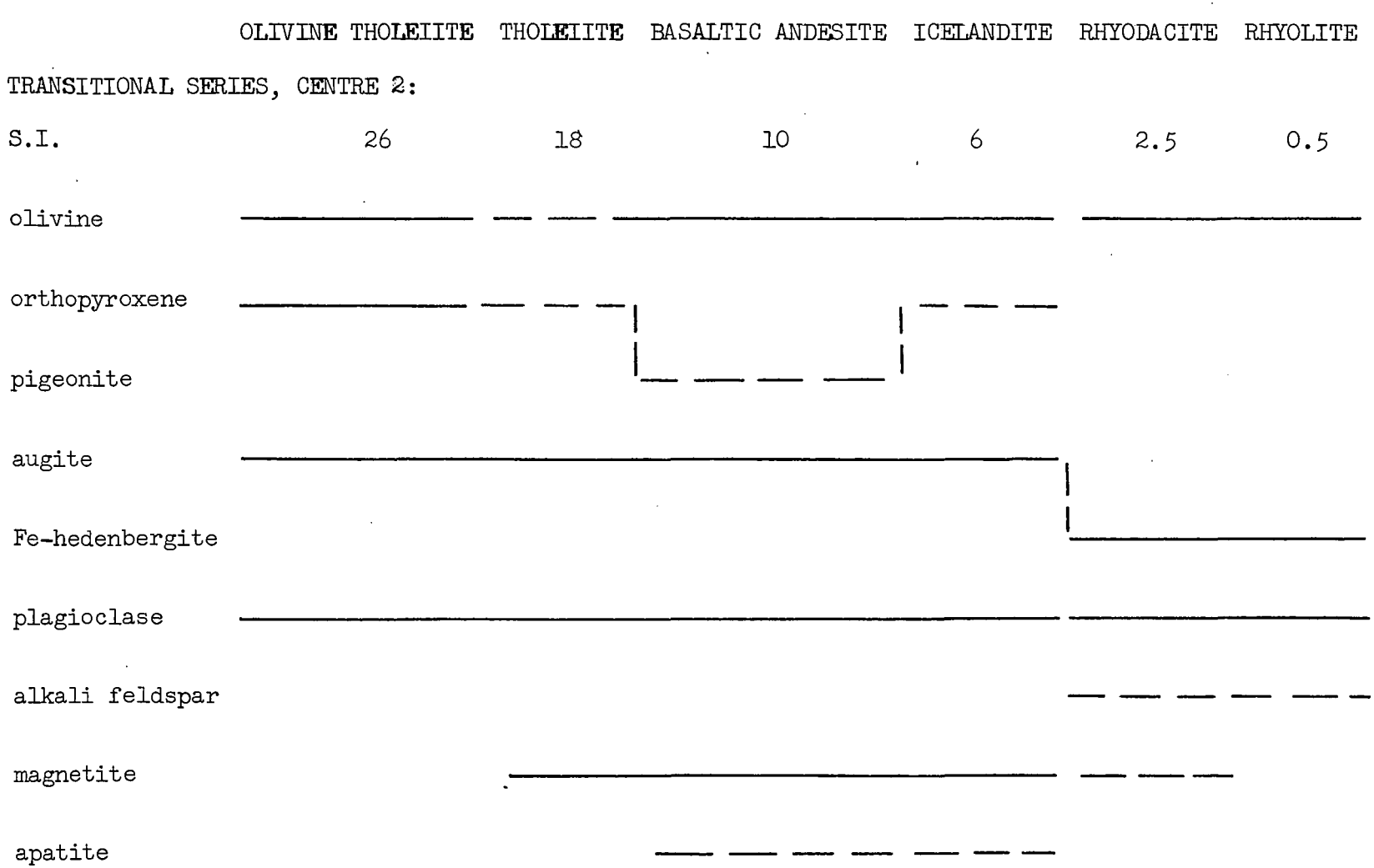

TABLE 8 (continued)

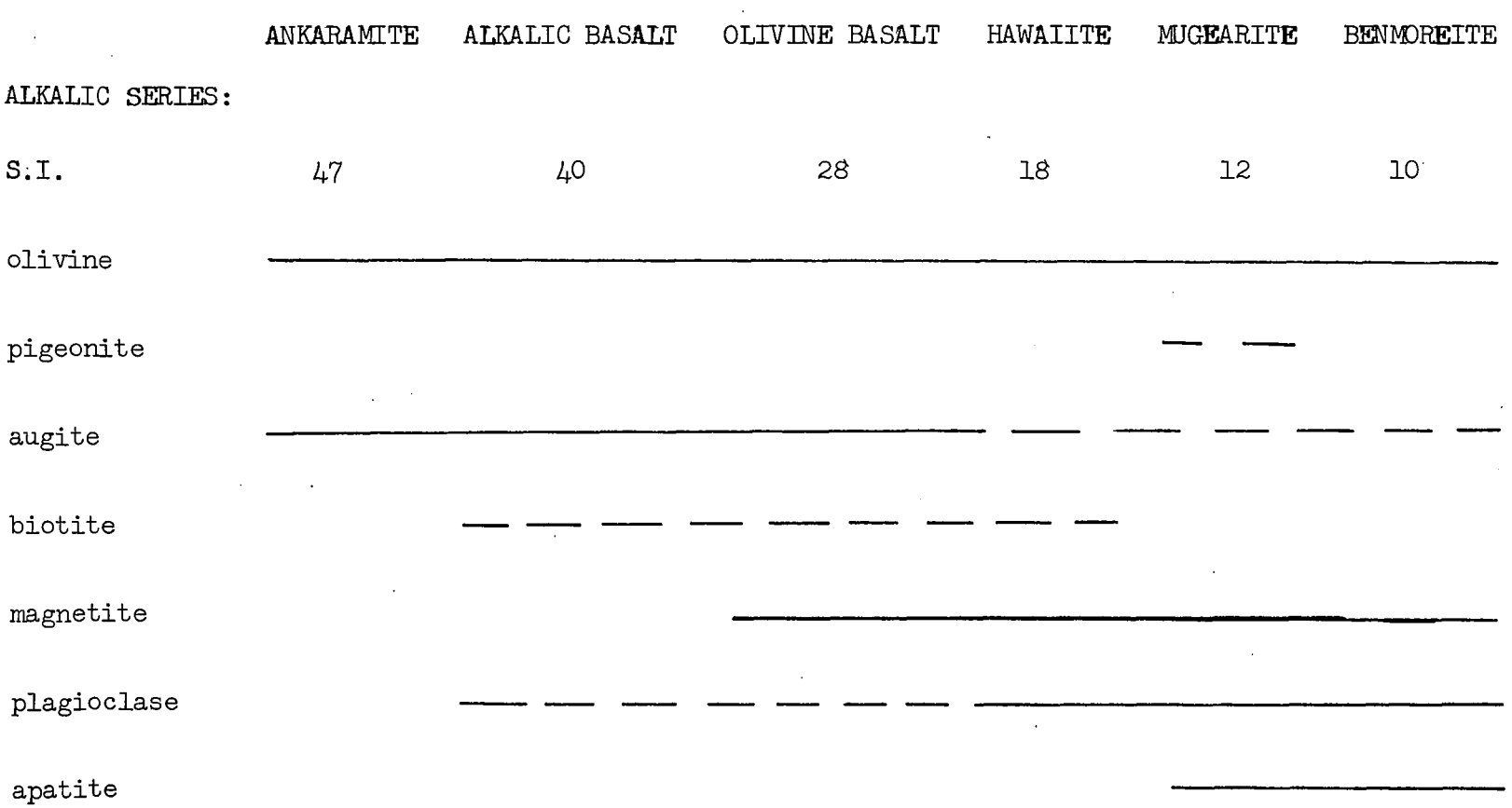

CHAPTER V: PETROCHEMISTRY

Introduction

The analyses carried out on rocks from the Setberg area are presented in Table 14 in the Appendix. From these data, averages of the chief rock types in the tholeiitic, transitional and alkalic series have been computed and are presented, along with their norms, in Tables 9 to 11. Norms of the 281 analyses included in this study have been computed, but the inclusion of all these data is not practicable. The following discussion will be confined chiefly to the variation diagrams, in which all the analyses have been plotted, and the average chemical analyses as presented in the tables.

Analyses chosen for inclusion in the averages were all of fresh rocks, of medium to fine grain-size, and the grouping falls within narrow limits of solidification and differentiation indices. Analytical methods employed in the determination of major and trace elements are discussed in the Appendix.

A. Oxide variations

The ten major oxides analysed in the Setberg rock series are plotted against solidification Index (MgO x 100/MgO+FeO+Fe_2O_3+Na_2O+K_2O) in Figures 44 to 46. This index has been

Fig. 44: Analyses of rocks from Centre 1 plotted in a variation diagram of solidification index versus oxides.

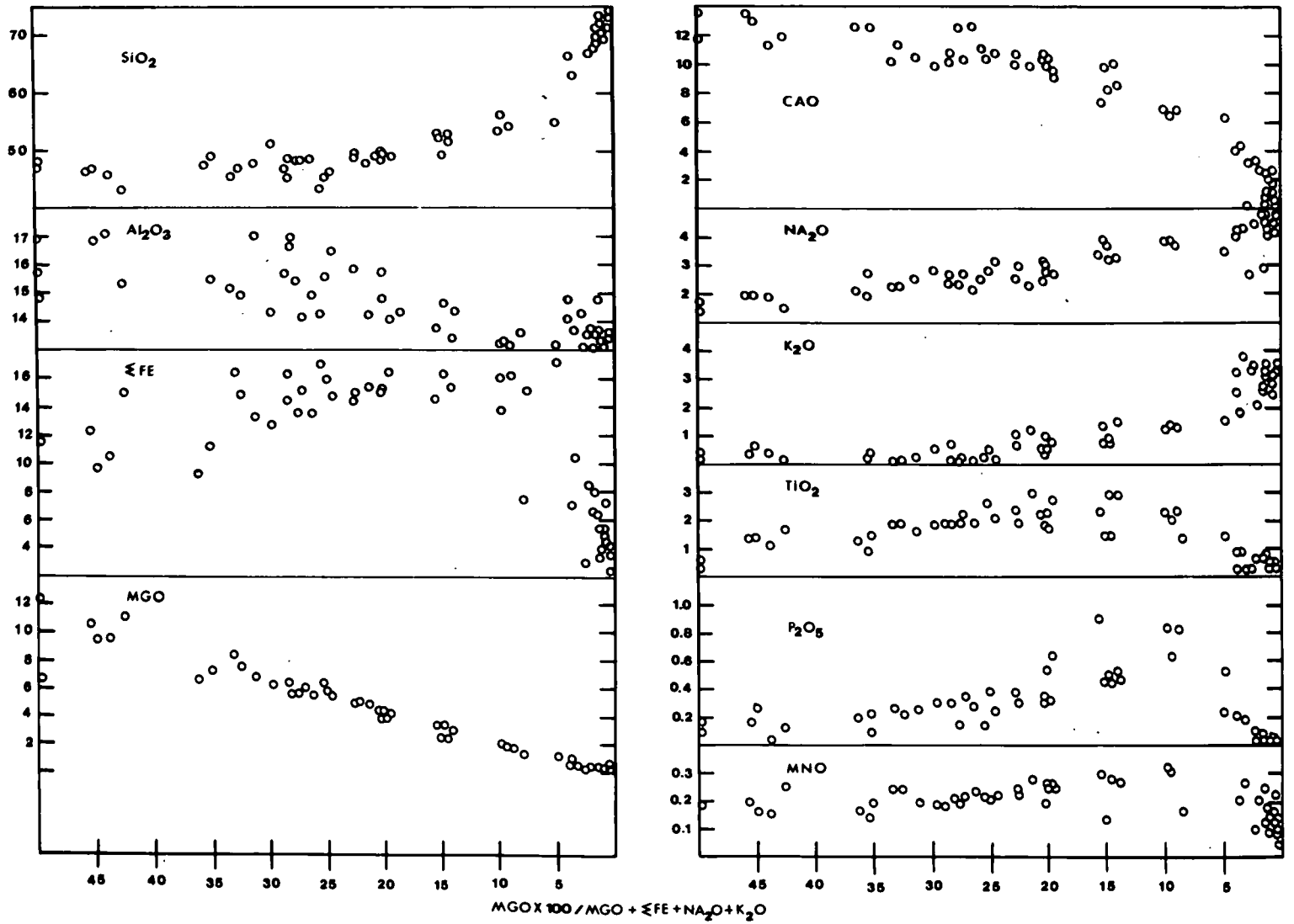
SiO2
Al2O3
ΣFE
MGO
CAO
NA2O
K2O
TIO2
P2O5
MNO
MGO X 100 / MGO + ΣFE + NA2O + K2O

TABLE 9 AVERAGE COMPOSITION OF ROCKTYPES OF THE TERTIARY THOLEIITIC SERIES, CENTRE 1

	OLIVINE THOLEIITE	THOLEIITE	BASALTIC ANDESITE	ICELAND-ITE	RHYO-DACITE	RHYO-LITE
SiO_2	47.00	49.50	55.54	63.90	71.22	74.35
Al_2O_3	15.80	14.70	13.28	13.90	13.47	13.77
Fe_2O_3	4.30	4.80	3.73	2.50	2.60	1.50
FeO	10.00	10.00	11.20	7.50	2.65	1.52
MgO	6.70	4.40	1.60	0.50	0.15	0.15
CaO	11.40	9.80	6.57	4.20	1.83	0.42
Na_2O	2.32	2.95	3.80	4.28	4.45	4.32
K_2O	0.14	0.75	1.32	1.82	2.97	3.55
TiO_2	1.91	2.53	1.94	0.97	0.46	0.26
MnO	0.21	0.25	0.36	0.26	0.17	0.10
P_2O_5	0.23	0.35	0.67	0.19	0.03	0.01
Trace elements (ppm):						
Ba	170	190	400	615	770	860
Sr	180	220	230	200	150	110
Rb	2	7	40	42	66	75
Zr	100	170	400	600	720	550
Zn	90	100	165	170	160	155
Ni	55	25	18	-	-	-
Cu	100	50	20	7	4	2

TABLE 9 (continued)

	OLIVINE THOLEIITE	THOLEIITE	BASALTIC ANDESITE	ICELAND-ITE	RHYO-DACITE	RHYO-LITE
			NORM:			
Qz	-	2.71	9.79	19.35	29.06	33.96
Or	0.83	4.43	7.80	10.75	17.55	20.99
Ab	19.63	24.95	32.14	36.21	37.65	36.57
An	32.28	24.64	15.27	13.34	8.01	2.02
Di	18.63	17.91	11.15	5.48	0.76	-
Hy	14.52	12.77	13.17	8.96	2.25	1.68
Fo	2.07	-	-	-	-	-
Fa	1.64	-	-	-	-	-
Mt	6.23	6.96	5.41	3.62	3.77	2.18
Il	3.63	4.80	3.68	1.84	0.87	0.49
Ap	0.54	0.83	1.59	0.45	0.07	0.02
D.I.	20.45	32.09	49.73	66.31	84.26	91.52
S.I.	28.5	19.2	7?.4	2.4	1.2	1.4

TABLE 10 AVERAGE COMPOSITION OF ROCKTYPES OF THE MID-QUATERNARY TRANSITIONAL SERIES OF CENTRE 2

	OLIVINE THOLEIITE	THOLEIITE	BASALTIC ANDESITE	ICELAND-ITE	LYSUSKARD GRANOPHYRE	RHYO-DACITE	RHYO-LITE
SiO_2	48.02	49.26	54.20	58.61	67.19	68.04	74.10
Al_2O_3	15.64	14.41	14.43	14.61	15.63	15.24	12.60
Fe_2O_3	3.33	3.70	3.29	4.00	2.20	2.50	2.10
FeO	9.97	11.08	9.88	7.69	2.70	2.58	1.40
MgO	5.87	4.04	2.34	1.10	0.39	0.34	0.01
CaO	11.09	9.20	6.91	5.07	1.90	1.50	0.10
Na_2O	2.65	3.34	4.15	4.30	5.10	4.68	4.78
K_2O	0.68	1.02	1.80	2.38	4.06	4.43	4.50
TiO_2	2.18	2.94	2.23	1.49	0.63	0.47	0.20
MnO	0.22	0.28	0.33	0.34	0.18	0.20	0.16
P_2O_5	0.31	0.65	0.72	0.43	0.11	0.04	0.01
			Trace elements (ppm):				
Ba	420	600	900	1040	1250	1100	100
Zr	120	170	310	500	565	750	1000
Sr	300	410	360	330	230	160	10
Rb	12	18	35	60	85	100	165
Zn	70	90	135	140	110	140	320
Cu	60	30	15	12	5	2	-
Ni	34	10	-	-	-	-	-

TABLE 10 (continued)

	OLIVINE THOLEIITE	THOLEIITE	BASALTIC ANDESITE	ICELAND-ITE	LYSUSKARD GRANOPHYRE	RHYO-DACITE	RHYO-LITE
			NORM:				
Qz	-	0.46	4.32	11.00	16.72	19.21	28.69
Or	4.02	6.03	10.60	14.06	23.97	26.17	26.60
Ab	22.43	28.28	35.01	36.37	43.11	39.59	39.77
An	28.78	21.32	15.38	13.53	7.76	7.18	-
Ac	-	-	-	-	-	-	0.61
Di	19.93	16.77	11.96	7.57	0.80	-	0.38
Hy	9.52	14.65	12.05	7.83	2.99	3.11	0.80
Fo	2.90	-	-	-	-	-	-
Fa	2.71	-	-	-	-	-	-
Mt	4.83	5.37	4.75	5.80	3.19	3.62	2.74
Il	4.14	5.59	4.22	2.83	1.20	0.89	0.38
Ap	0.73	1.54	1.70	1.02	0.26	0.09	0.02
D.I.	26.45	34.77	49.93	61.43	83.80	84.98	95.07
S.I.	26.1	17.5	10.9	5.7	2.7	2.3	0.1

TABLE 11 AVERAGE COMPOSITION OF ROCKTYPES OF THE LATE-QUATERNARY ALKALIC SERIES

	ANKARAMITE	ALKALIC BASALT	OLIVINE BASALT	HAWAIITE	MUGEARITE	BENMOREITE
SiO_2	47.40	47.22	47.83	49.92	53.30	58.30
Al_2O_3	14.84	16.28	16.57	16.22	16.90	16.70
Fe_2O_3	1.80	1.80	2.30	2.20	3.10	1.80
FeO	8.28	8.72	9.48	10.15	8.50	6.40
MgO	11.34	8.88	6.06	3.90	2.30	1.80
CaO	11.80	11.45	11.07	8.73	7.10	5.30
Na_2O	1.93	2.53	2.95	3.83	4.38	5.09
K_2O	0.62	0.75	0.89	1.36	1.95	2.45
TiO_2	1.46	1.81	2.17	2.71	2.19	1.49
MnO	0.18	0.18	0.20	0.24	0.29	0.26
P_2O_5	0.33	0.33	0.48	0.67	0.89	0.58
Trace elements (ppm):						
Ba	1600	400	490	650	880	1100
Zr	90	95	120	220	370	520
Sr	230	360	410	490	500	520
Rb	5	12	16	29	40	60
Zn	50	65	70	100	125	124
Cu	55	85	60	25	12	7
Ni	330	165	80	15	11	10

TABLE 11 (continued)

	ANKARAMITE	ALKALIC BASALT	OLIVINE BASALT	HAWAIITE	MUGEARITE	BENMOREITE
			NORM:			
Qz	-	-	-	-	1.55	4.64
Or	3.66	4.43	5.26	8.04	11.42	14.45
Ab	16.33	19.83	24.96	32.42	36.72	42.98
An	30.00	30.86	29.34	23.06	20.50	15.45
Ne	-	0.86	-	-	-	-
Di	21.25	19.31	18.44	13.27	7.28	5.92
Hy	4.28	-	0.01	5.86	11.88	9.75
Fo	12.59	11.23	7.07	3.03	-	-
Fa	5.72	6.64	6.35	4.40	-	-
Mt	2.61	2.61	3.33	3.19	4.45	2.60
Il	2.77	3.44	4.12	5.15	4.12	2.82
Ap	0.78	0.78	1.14	1.59	2.09	1.37
D.I.	20.00	25.12	30.21	40.46	49.68	62.08
S.I.	47.2	39.2	27.9	18.2	11.8	10.1

chosen because of its capacity to spread out the compositional range of basaltic rocks, but an inherent drawback is the deceptive linearity of the MgO plot where both ordinate and abscissa are interdependent. The oxides of the three series display fairly smooth compositional trends, particularly the Late-Quaternary alkalic series and the transitional lavas of Centre 2. Greater scatter in the Tertiary tholeiitic series of Centre 1 may be due to slight alteration of some samples, but the main feature of oxide variation in the Tertiary tholeiitic series (Figure 44) is the high total iron content, which persists in the basaltic andesites (S.I.$<$ 10).

The intermediate and acid rocks of Centre 2 (Figure 45) consist of two distinct groups, which display parallel but different trends. The basaltic rocks, including basaltic andesites and icelandites, form a smooth, continuous trend, here referred to as the "icelandite trend", in contrast to the "rhyodacite trend" of rhyolites and acid rocks from the Lysuskard cone sheet of Centre 2 (filled circles in Figure 45). The rhyodacite trend is characterized by high SiO_2, K_2O and, to a lesser extent, Na_2O, being lower in total Fe, CaO and MnO than the rocks of the icelandite trend. Most notable is the difference in K_2O and total Fe of these two trends. Rocks in

Fig. 45: A plot of oxides against solidification index for rocks of Centre 2. Felsites, granophyres and other rocks associated with the Lysuskard cone sheet are shown as filled circles.

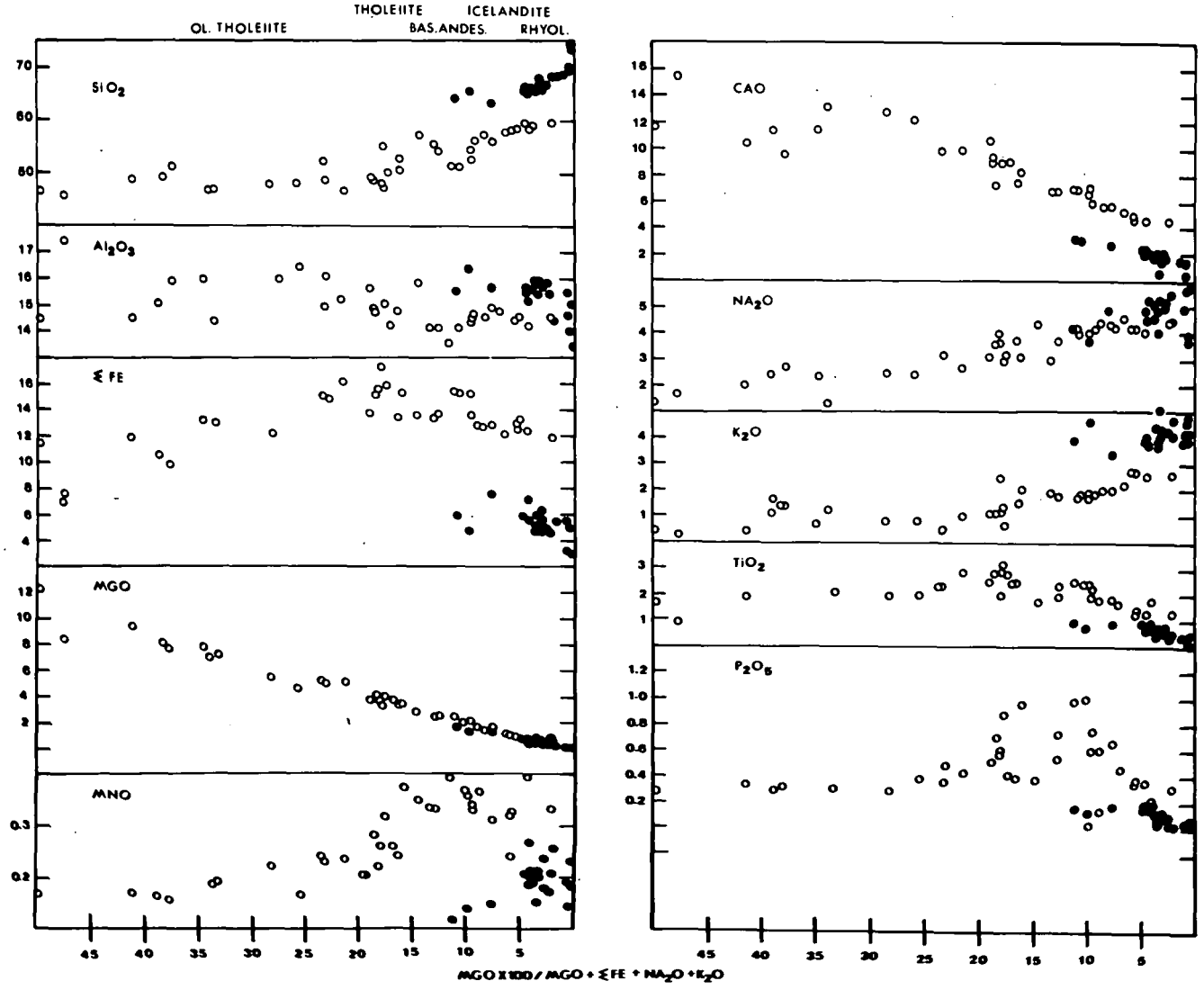
THOLEIITE
ICELANDITE
OL. THOLEIITE
BAS.ANDES.
RHYOL.
SiO2
Al2O3
ΣFE
MGO
MNO
CAO
Na2O
K2O
TiO2
P2O5
MGO X100 / MGO + ΣFE + Na2O + K2O

the rhyodacite group contain 4 to 5% K_2O on the whole, whereas icelandites of comparable S.I. show approx. 2.5% K_2O.

Mineralogical differences also exist between the two groups of Centre 2. Whereas the icelandites are plagioclase-augite-olivine-magnetite-bearing rocks, with rare hypersthene and apatite, the rhyodacitic group shows alkaline affinities in containing alkali feldspar and sodic pyroxene, as well as plagioclase and ferrohedenbergite. Although of the same age and geologically related, the more alkalic, rhyodacitic group of Centre 2 thus does not show chemical or mineralogical affinities with the contemporaneous transitional basalt series.

Iron and titanium reach a maximum in the tholeiites of the transitional series, after which a gradual fall-off occurs, coinciding with the appearance of titano-magnetite as a microphenocryst in the tholeiites and basaltic andesites. Similarly, the variation curve for P_2O_5 (Figure 45) shows a maximum in the basaltic andesites, where apatite phenocrysts appear and whose sinking is probably instrumental in the subsequent depletion of P_2O_5 in the icelandites.

Most notable features of the oxide variation in the alkalic series (Figure 46) are the abrupt changes of slope of the curves for CaO, Na_2O and K_2O at an S.I. of approximately

---

Fig. 46: A plot of oxides versus solidification index for rocks of the Late-Quaternary alkalic series.

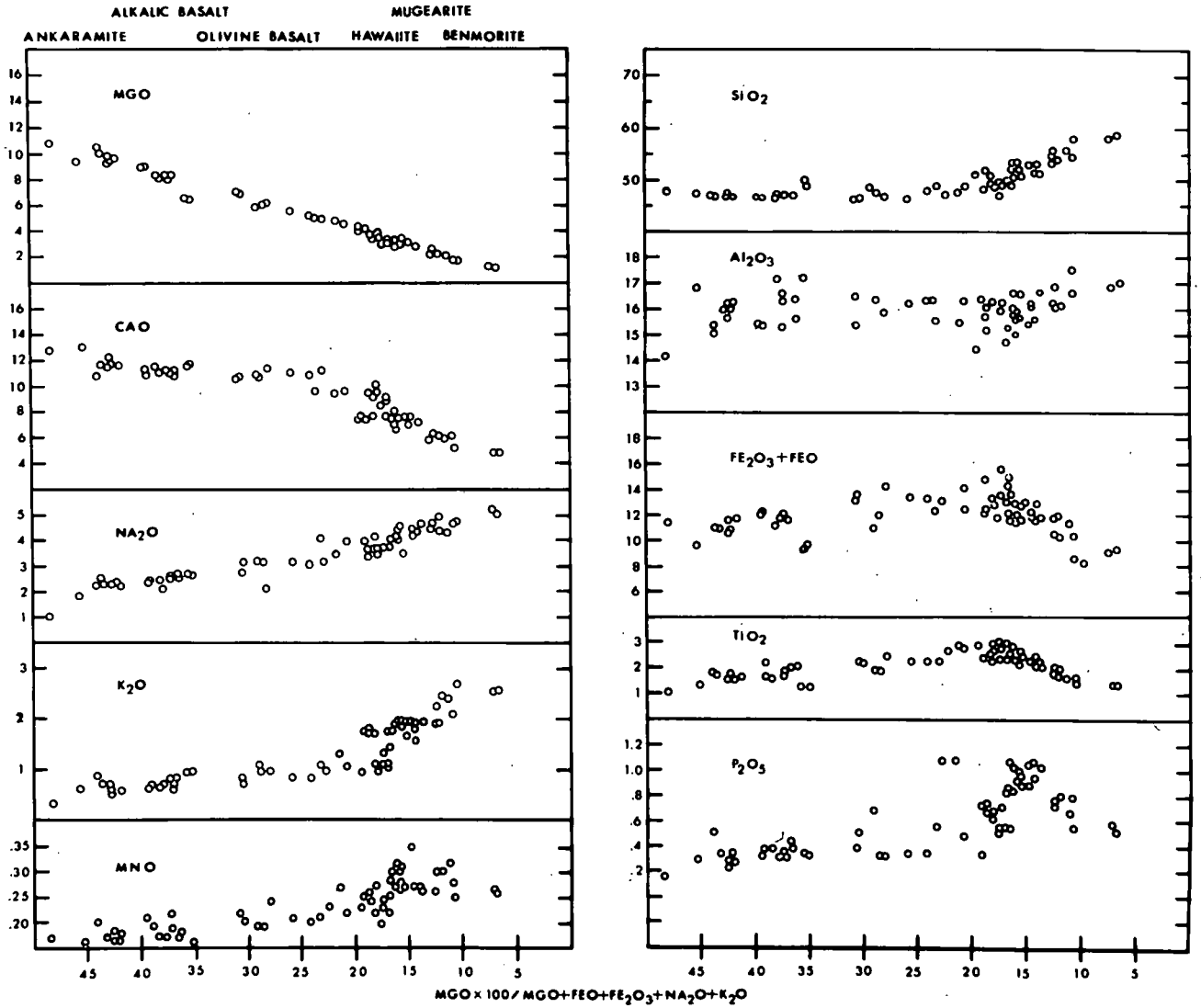
ALKALIC BASALT
MUGEARITE
ANKARAMITE
OLIVINE BASALT
HAWAIITE
BENMORITE
MGO
CAO
NA2O
K2O
MNO
SiO2
Al2O3
FE2O3+FEO
TiO2
P2O5
MGO x 100/ MGO+FEO+FE2O3+NA2O+K2O

20, i.e. in the hawaiites. Phenocrysts of plagioclase only become common in the hawaiites and the onset of extraction of a relatively calcic plagioclase from them accounts for the change of slope of the CaO and Na_2O curves. The relatively greater increase of K_2O over Na_2O in the mugearites and benmoreites is related to removal of some of the soda in plagioclase, whereas K_2O only becomes fixed in anorthoclase of the benmoreites.

Phosphorus reaches a maximum in the mugearites (S.I. 15), where apatite phenocrysts appear in the lavas, and the subsequent decrease in P_2O_5 content is analogous to the behaviour of this oxide in the transitional series of Centre 2. The solubility of phosphorus in the Setberg magmas was discussed on p.149.

The A-F-M diagram shows the predominant increase in iron content in all three series, before alkali-enrichment becomes dominant (Figure 47). Iron-enrichment of the intermediate rocks is greatest in the tholeiitic series of Centre 1, parallelling the Thingmuli trend, and progressively less in the transitional and alkalic series. The continuum of the tholeiitic trend from basic to acid is clearly demonstrated in the Tertiary series of Centre 1, but the A-F-M plot of lavas of Centre 2 re-emphasises the lack of affinity between the rhyodacitic group and the basaltic and intermediate lavas

(as pointed out above, in discussing the S.I. plot). The basaltic trend of Centre 2 maintains a high degree of iron enrichment relative to alkalis, and no rocks have been found which bridge the compositional gap between the icelandite and acid groups.

The early and close approach of the icelandite trend of Centre 2 lavas to the alkalis-iron oxides join on Figure 47 reflects a highly efficient Fe/Mg fractionation. This could be accounted for by removal of magnesian minerals, a suggestion supported by the observation that olivine forms a phenocryst phase in all the rock-types of the basaltic and icelandite group of Centre 2. The broken, rather than continuous path of the basaltic trend may suggest a two-stage fractionation process, initially controlled by the subtraction of olivine only (Fo_{80}), and later joined by plagioclase and augite.

The Setberg alkalic series displays a trend on the A-F-M diagram (Figure 47) similar to that of the alkalic rocks of

---

Fig. 47: The Setberg volcanic rocks plotted in terms of FeO+ Fe_2O_3, MgO and Na_2O+K_2O. Triangles 1, 2 and 3 show variations in the Centre 1, Centre 2 and alkalic series respectively. The crystallization trend of the Tholeiitic Thingmuli series is indicated (Carmichael, 1964) as well as that of the Hawaiian alkalic series (Macdonald and Katsura, 1964). Circle on the F-M join in the alkalic diagram (part 3) represents common composition of early-formed olivine phenocrysts in the alkalic basalts.

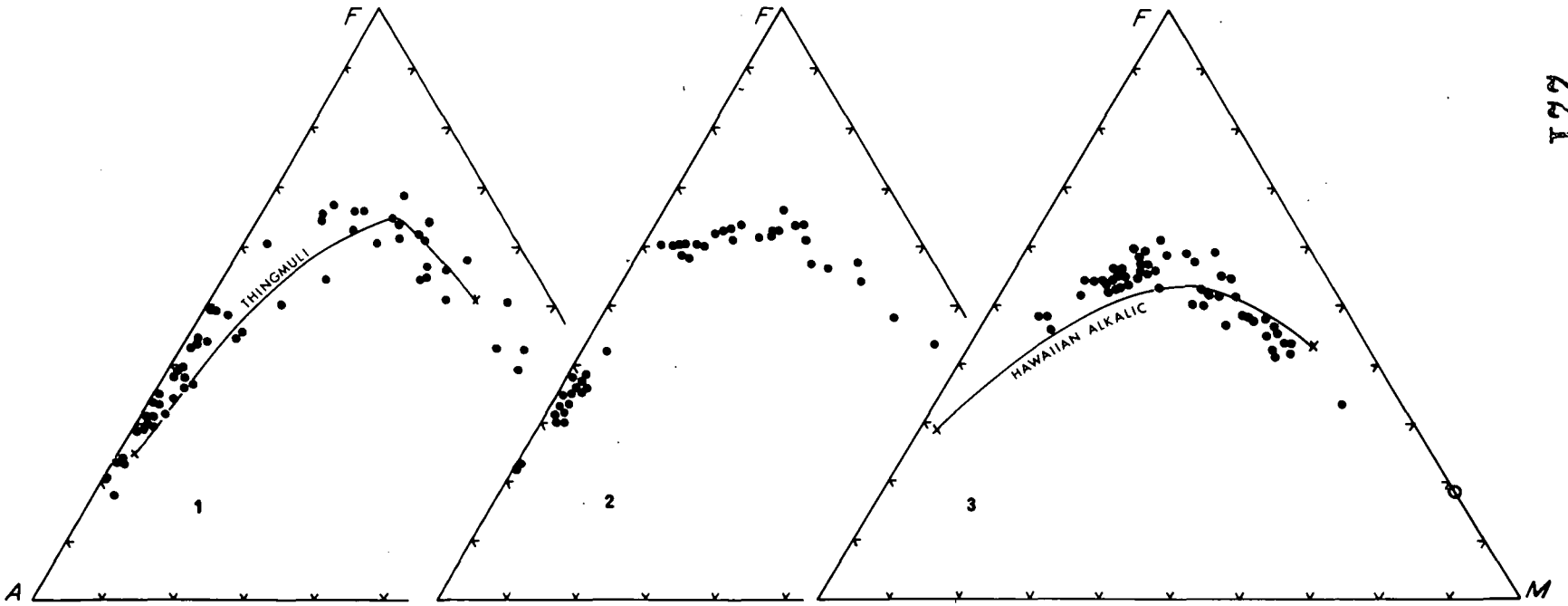
F
THINGMULI
1
A
F
2
F
HAWAIIAN ALKALIC
3
M

St. Helena (Baker, 1969), and showing considerably greater iron-enrichment in the differentiated basalts than do the Hawaiian alkalic series.

A plot relating total iron oxides to magnesia for the three series is shown in Figure 48. The tholeiitic and transitional series show a notable difference from the Thingmuli series in the maintenance of a high iron content in the more differentiated, magnesia-poor lavas. The depletion of iron and thus the deviation from the Skaergaard trend of the Thingmuli tholeiitic andesites and icelandites has been attributed to precipitation and removal of magnetite from the tholeiitic magma (Carmichael, 1964). Magnetite also appears as a microphenocryst in the basaltic andesites of Centre 1 and Centre 2 but the continued removal of olivine, and hence magnesium, in the transitional series is believed to be instrumental in producing the high iron oxides/magnesia ratio of the basaltic andesites, rather than delay in the precipitation of magnetite.

For comparative purposes, averages of the three Setberg

Fig. 48 : A plot relating total iron oxides and magnesia for Setberg volcanic rocks. Parts 1, 2 and 3 figure the rocks of Centre 1, Centre 2 and the alkalic series respectively. The Thingmuli tholeiitic trend (Carmichael, 1964) and the Hawaiian alkalic trend (Macdonald and Katsura, 1964) are indicated.

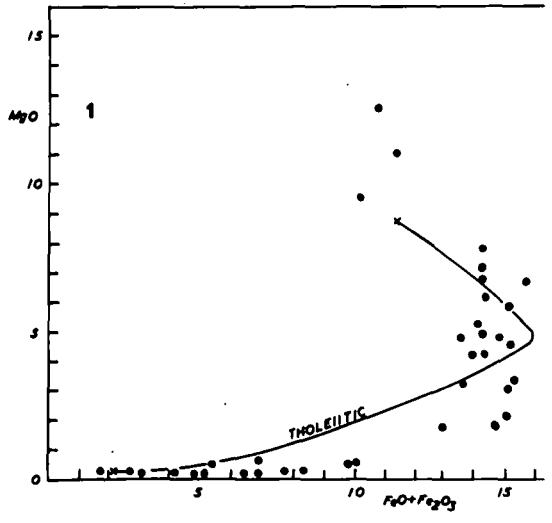
1
MgO
15
10
5
0
5
10
15
FeO+Fe2O3
THOLEIITIC

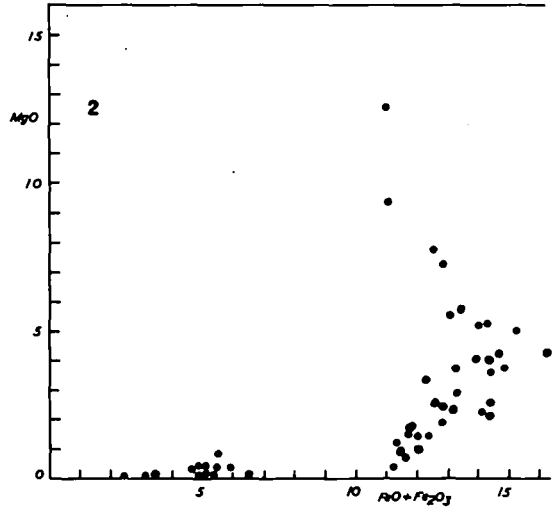
2
MgO
15
10
5
0
5
10
15
FeO+Fe2O3

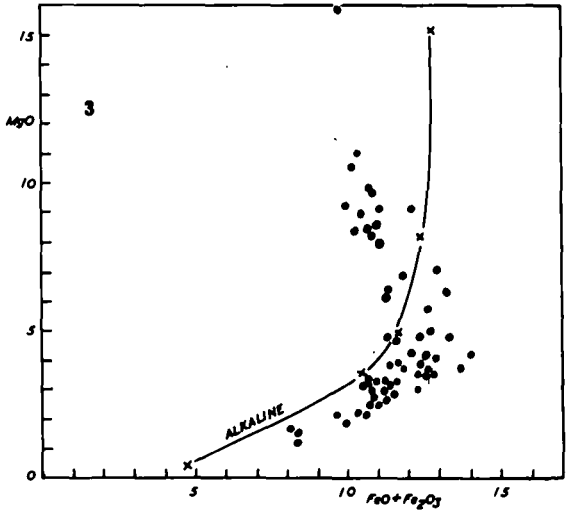
3
MgO
15
10
5
0
5
10
15
FeO+Fe2O3
ALKALINE

rock series are plotted on the alkalis/silica diagram (Figure 49), along with the Hawaiian alkalic series (Macdonald and Katsura, 1964) and the tholeiitic series of Thingmuli. The lavas of Centre 1 follow broadly this latter trend and form a continuous range from basic to acid. The basaltic and acid trends of lavas from Centre 2 have been tentatively connected, but a direct genetic relationship between these two groups is not inferred. A distinct compositional gap exists in the rock analyses from Centre 2 and the only analyses falling between 60 and 66% SiO_2 are those of composite rocks, such as the rhyodacite from Gjafakollur (p.105) with 64.69% SiO_2. When 3% of "basaltic" material (a conservative estimate of the basic clots in this rock) is subtracted from this composition, a silica percentage of 66.40 is arrived at, placing the original acid magma among the rhyodacites. Further sampling is unlikely to bridge the compositional gap in the rock series of Centre 2, and the evidence supports the notion that the immediate origin of the acid rocks of Centre 2 can hardly be sought among the contemporaneous basaltic series.

Fig. 49: A plot of Na_2O+K_2O versus SiO_2 of average Setberg rocks, with comparisons. The basaltic and rhyodacitic trends of Centre 2 are tentatively connected across the compositional gap from 60 to 66% SiO_2. The Hawaiian demarcation line between tholeiitic and alkalic basalts is after Macdonald and Katsura (1964).

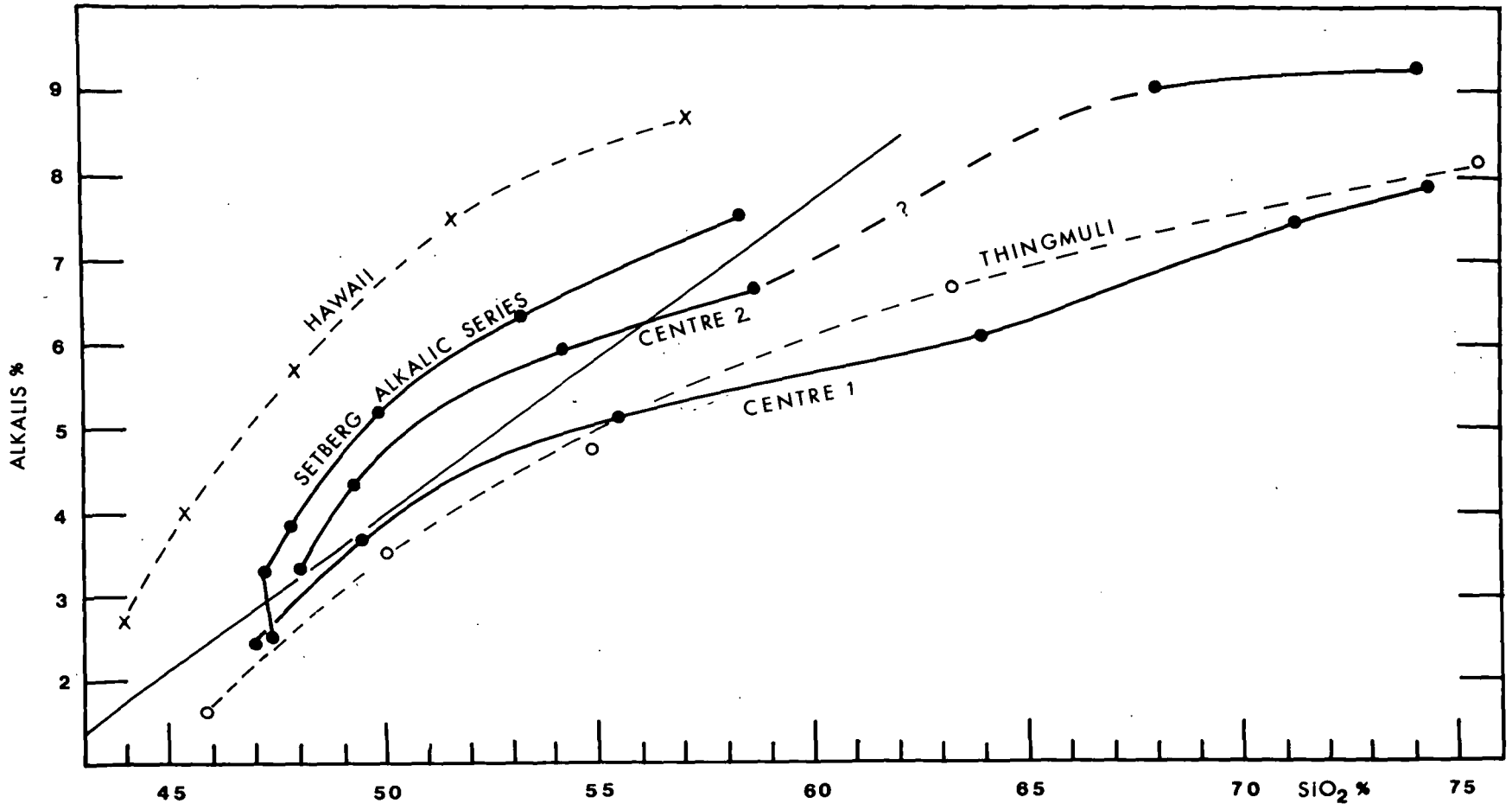
ALKALIS %
9
8
7
6
5
4
3
2
HAWAII
SETBERG ALKALIC SERIES
CENTRE 2
?
THINGMULI
CENTRE 1
45
50
55
60
65
70
SiO2 %
75

The compositional trends of the three Setberg series have been plotted in terms of total alkalis vs. iron enrichment (Fe_2O_3+FeO/Fe_2O_3+FeO+MgO). The Hawaiian alkalic series and the Kilauea tholeiitic trend are also presented (Tilley et al., 1967) to illustrate two extremes, along with the Hebridean alkalic series which parallels the Late-Quaternary alkalic series of Setberg, although somewhat more sodic (Figure 50). The field of rhyodacitic and rhyolitic rocks from Centre 2 is delineated, to point out the dissimilarity of the two groups from this Centre.

Fig. 50: Plot of total alkalis against iron enrichment for the three Setberg series. The ellipsoidal field represents compositional range found among acid rocks of Centre 2. Comparative trends of Hawaiian and Hebridean alkalic series and the Kilauea tholeiite trend are after Tilley et al. (1967).

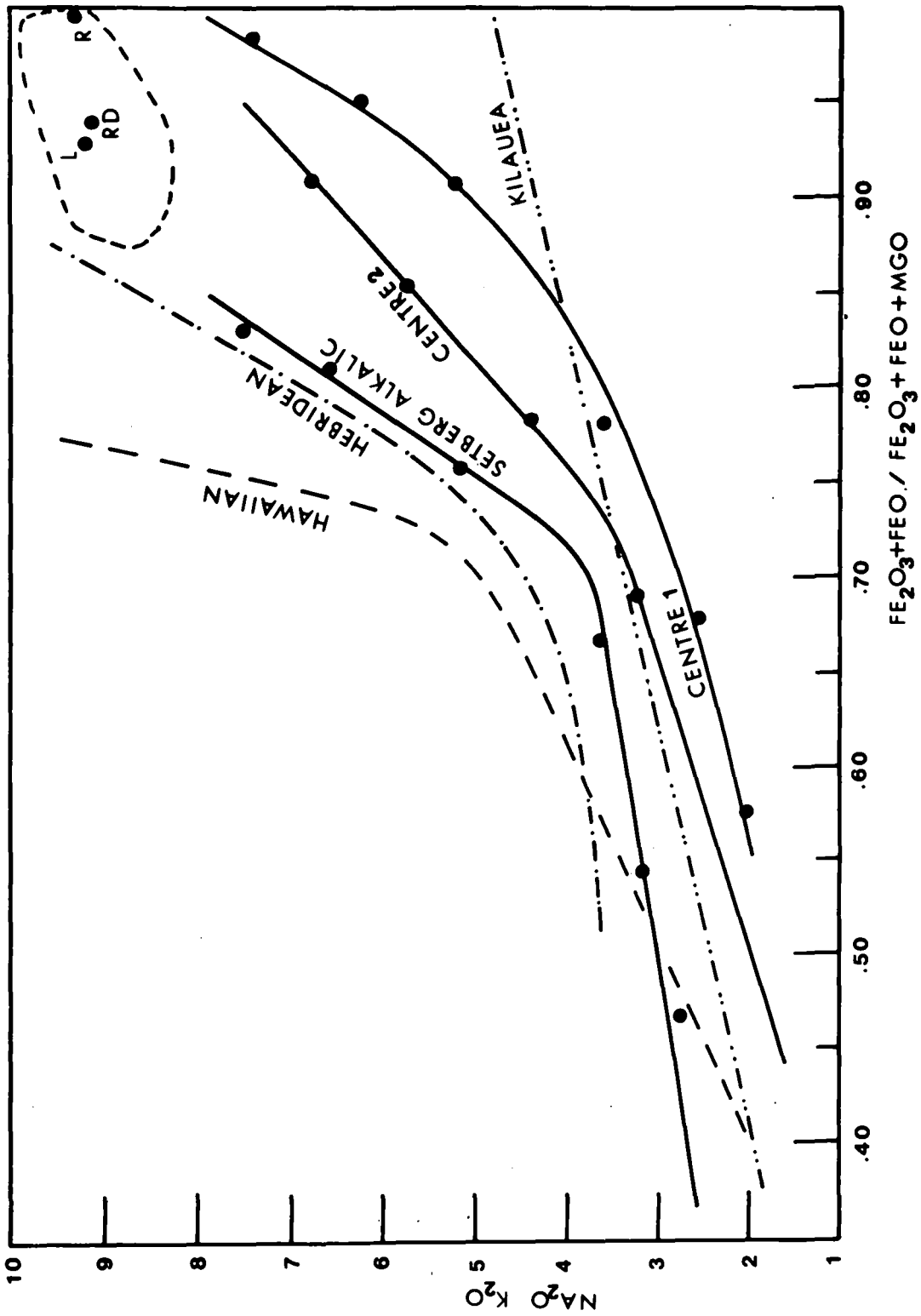
R
RD
L
KILAUEA
CENTRE 2
SETBERG ALKALIC
HEBRIDEAN
HAWAIIAN
CENTRE 1
10
9
8
7
6
5
4
3
2
1
Na_2O K_2O
.40
.50
.60
.70
.80
.90
FE_2O_3+FEO / FE_2O_3+FEO+MGO

B. Trace element variations

Ba, Sr, Rb, Zr, Zn, Cu and Ni were determined by X-ray fluorescence analysis (methods in Appendix).). Variations of these trace elements (parts per million) are shown graphically for all the analyzed rocks in Figures 51 to 57, but only average concentrations are given in Tables 9.to 11.

Barium is highly enriched in the differentiated rocks of the Setberg area (Figure 51), although the degree of enrichment varies with the rock series. The Ba/K x 100 ratio for the tholeiitic series is 3.3, but 6.0 in the alkalic series and 5.0 in the transitional series of Centre 2. The Ba/K ratio varies little or not at all with differentiation except in the very last stages, although the acid rocks of Centre 2 show a ratio of 3.7, again significantly different from the associated transitional basaltic rocks. The work of Berlin and Henderson (1969) shows that plagioclase does hardly or not at all incorporate Ba, which consequently becomes continuously enriched in the liquid. This is borne out by an analysis of plagioclase from the Klakkur ankaramite (p.162), where the bytownite phenocrysts and the whole rock contain 129 and 1600 ppm Ba, respectively. Berlin and Henderson further showed that crystallization of anorthoclase and sanidine depletes the liquid in Ba. This relationship is shown by some of the

anorthoclase or sanidine-bearing acid and peralkaline rocks of Centre 2 (295, 331, 311), containing as little as 39 ppm Ba.

The evidence on Ba is of interest with regard to acid rocks from eastern Iceland, which show a high but narrow range of Ba content, near 1100 ppm (Carmichael and McDonald, 1961), and have plagioclase as the sole precipitating feldspar phase. The Ba content of Icelandic rocks may thus be an effective indicator of the feldspar suite in equilibrium with the magma.

All Ba determinations on samples of the Klakkur ankaramite show a concentration near 1600 ppm, an increase by a factor of four over the associated alkalic lavas. As plagioclase, olivine and clinopyroxene phenocrysts from this formation each show Ba contents of less than 200 ppm, the high concentration must be attributed to the groundmass. Accidental contamination has been ruled out and the extreme Ba content of this formation remains an interesting geochemical problem.

Of the three Setberg series, the alkalic lavas show greatest Ba enrichment, as expressed by a Ba/D.I. ratio of

---

Figs. 51 to 57: Distribution of Ba, Sr, Rb, Ni, Zr, Cu and Zn in the three Setberg rock series. Parts A, B and C of figures refer to the rocks of Centre 1, Centre 2 and the alkalic series, respectively.

A
B
C
Ba
ppm
1500
1000
500
0
50
100%
Dr

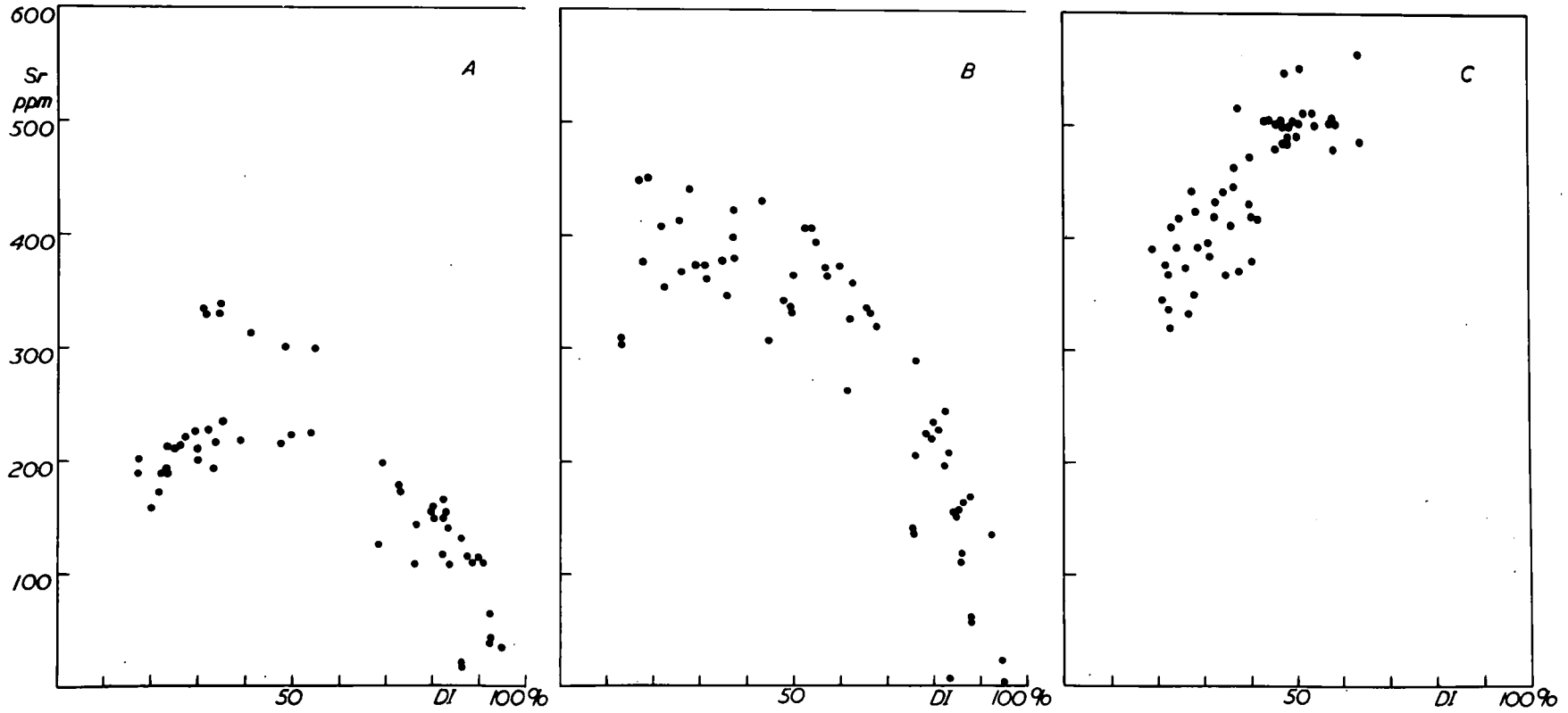

Fig 2

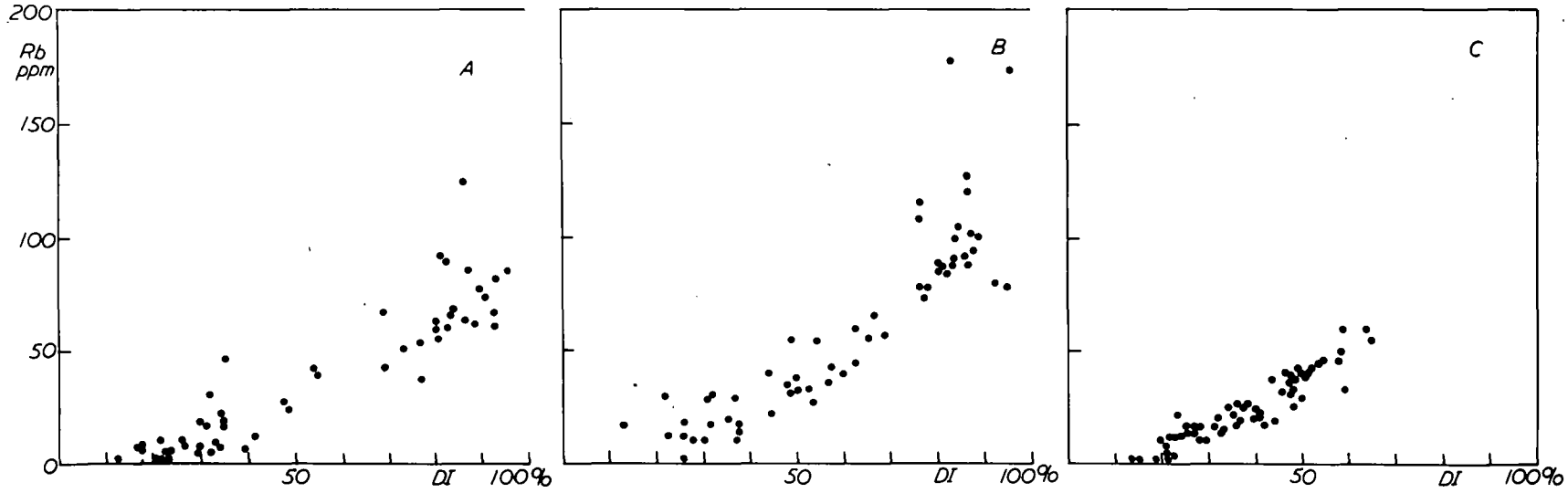
200
Rb
ppm
150
100
50
0
A
50
DI
100%
B
50
DI
100%
C
50
DI
100%

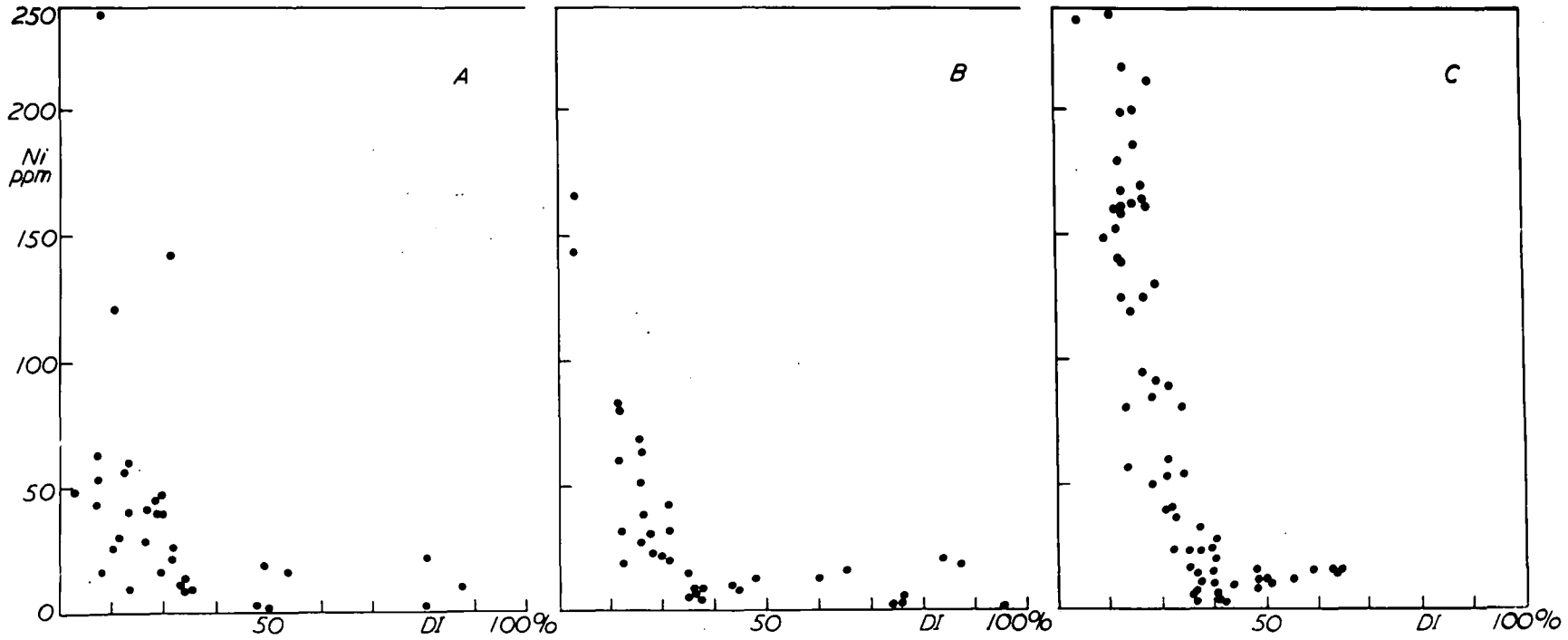
250
200
Ni
ppm
150
100
50
0
A
B
C
50
DI
100%
50
DI
100%
50
DI
100%

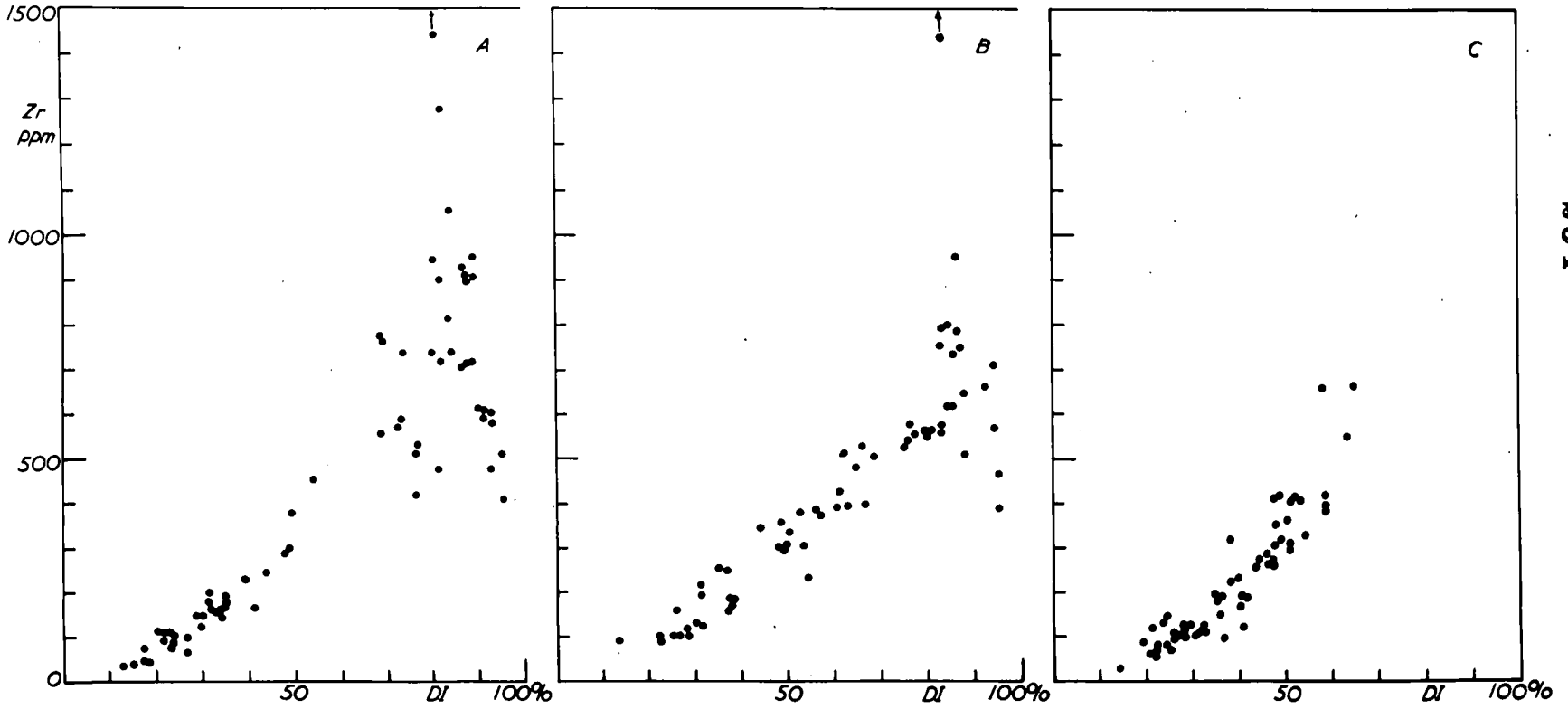
1500
Zr
ppm
1000
500
0
A
50
DI
100%
B
50
DI
100%
C
50
DI
100%

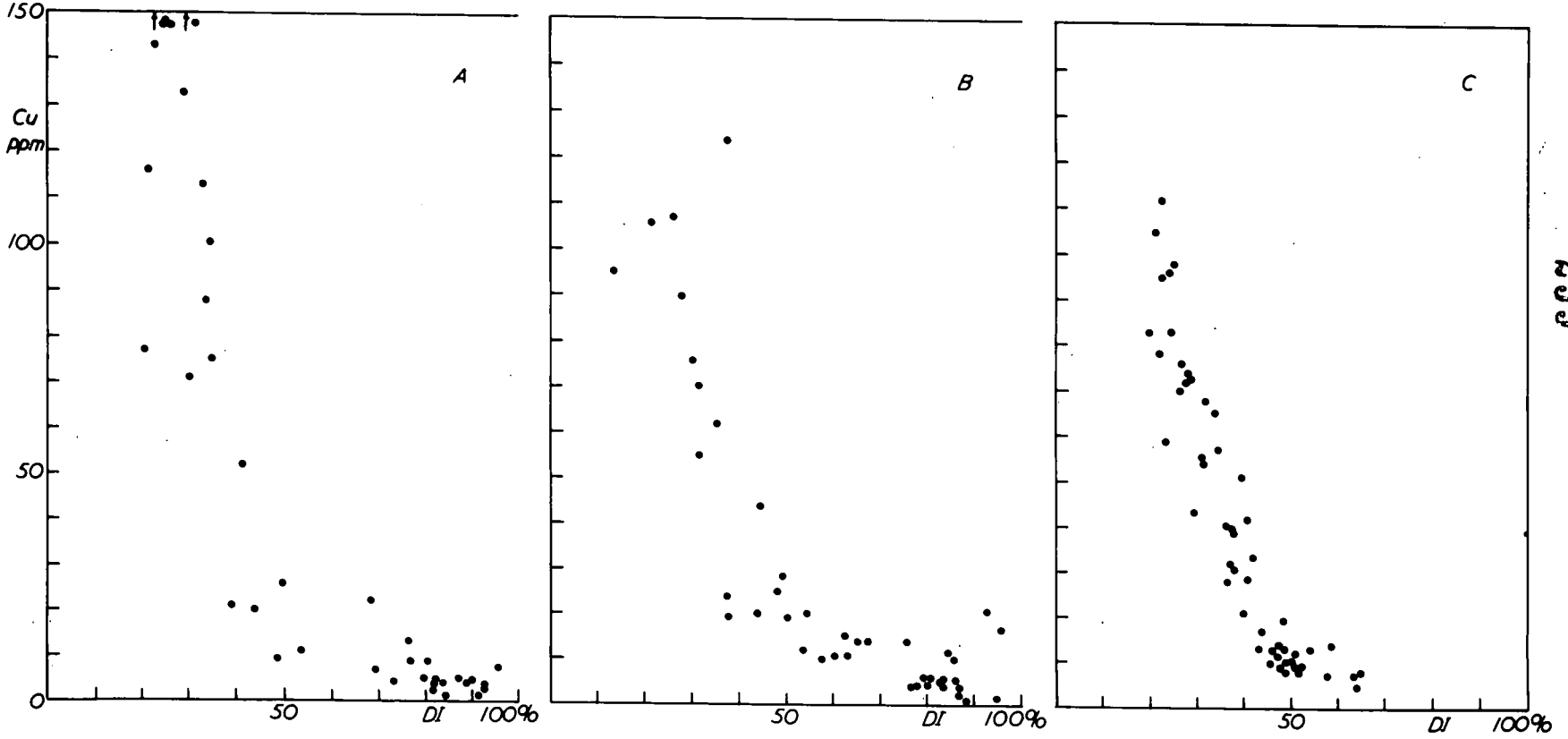
150
Cu
ppm
100
50
0
A
B
C
50
DI
100%
50
DI
100%
50
DI
100%

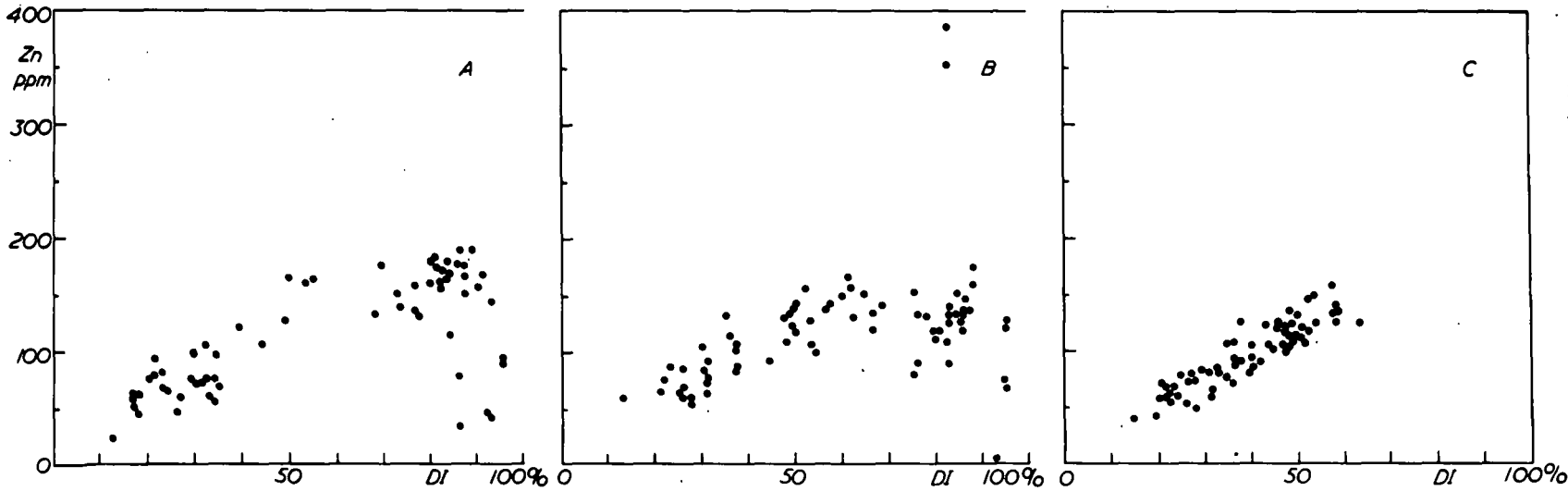
400
Zn
ppm
300
200
100
0
A
50
DI
100%
0
B
50
DI
100%
0
C
50
DI
100%

17. The rocks of Centre 1 and Centre 2 have a ratio of 10 and 14, respectively, the latter series being comparable to the alkalic lavas of St. Helena in terms of Ba-enrichment. The great enrichment in the alkalic series of Setberg may be accounted for by the absence of plagioclase as a precipitating phase, as borne out by the petrographic evidence, whereas plagioclase is an important phenocryst in the tholeiitic and transitional series. Thus plagioclase does have a significant effect on Ba concentration, although very slight.

Strontium variation in the Setberg rocks is illustrated in Figure 52. The great contrast of Sr variation between the three rock series, along with the fact that both the highest and lowest Sr concentrations are found among the acid rocks, makes this element perhaps the most illuminating geochemical indicator of this study.

While Sr shows a fairly continuous decrease with differentiation in the rocks of Centre 1 and Centre 2, the alkalic series shows a trend of Sr-enrichment. The similar enrichment of Sr in the alkalic lavas of St. Helena (Baker, 1969) is reversed in the trachytic rocks there, but comparable trachytic differentiates have not been found in the Setberg alkalic series.

Important recent work on the partition of Sr and Ca in

magmas has been carried out by Brooks (1969) and later Berlin and Henderson (1969) reached similar conclusions. The evidence shows that Sr enters more readily into the plagioclase structure than does Ca, contradicting earlier concepts. Thus in keeping with the Setberg petrographic evidence, and our conclusions on the distribution of Ba, the depletion of Sr from the tholeiitic and transitional series is accounted for by the presence of plagioclase as a major cumulate phase in the differentiation process. In the alkalic series, on the other hand (Figure 52), plagioclase phenocrysts are rare or absent in many of the lavas, and its absence from the liquidus has led to continuous enrichment of Sr in the liquid. We anticipate that Sr depletion would be shown in trachytic liquids of this alkalic series, when phenocrysts of alkali feldspar appear, in keeping with the evidence from St. Helena (Baker, op.cit.).

Rubidium displays a steady increase with differentiation in the Setberg rocks (Figure 53), ranging from approximately 10 ppm in the basalts to 100 ppm in the acid rocks. The highest Rb values are encountered in the two peralkaline obsidians of Centre 2 (331 and 295) which contain 178 and 174 ppm, respectively. The correlation between Rb and K is good in the three series (Figure 58) with a strong

grouping about a K/Rb ratio of 400, with the exception of highly porphyritic rocks and the above-mentioned obsidians, which have a K/Rb ratio of 200. The relative enrichment in Rb and the low K/Rb ratio in these highly fractionated obsidians is comparable with that shown by comendites and pantellerites (Nicholls and Carmichael, 1969), but significantly lower than the K/Rb ratios of all associated rocks of the Setberg area. Whether or not this fact tells us anything about the genetic process which gave rise to the peralkaline magma is another matter, but volatile transfer has been suggested as an important mechanism in the derivation of similar magmas (Ewart et al., 1968).

Nickel shows a sharp decrease in the initial stages of fractionation in the Setberg rock series; this is the normal trend found in fractionated basaltic magmas (Wager and Mitchell, 1951). The average Tertiary olivine tholeiite of Centre 1 contains 55 ppm (Table 9) and the alkalic basalts have an average Ni content of 165 ppm, while the olivine tholeiitic and tholeiitic transitional basalts of Centre 2 only contain 34 and 10 ppm respectively, and Ni is near or below detection limit in the rest of the rocks of Centre 2. The very low Ni sets the transitional series apart from other analyzed rock series in Iceland,

but may conceivably be accounted for by invoking a long process of olivine extraction in the formation of the parental magma of the series.

The great range of Ni content among the basaltic rocks of the alkalic series reflects the modal content of olivine in the porphyritic rocks to some extent. An analysis of olivine phenocrysts from the Klakkur ankaramite shows 760 ppm Ni.

Zirconium behaves in a similar manner in all three series and increases from approximately 100 ppm in the basalts to 700-800 ppm in the acid rocks (Figure 54). A wide scatter of Zr content is observed in the acid rocks of Centres 1 and 2. Zircon is a sporadic accessory in these rocks, but no correlation has been observed between Zr content and the occurrence of zircon. The peralkaline obsidian of Centre 2 (331) contains 1610 ppm Zr. High Zr is characteristic of peralkaline rocks, and generally attributed to the high solubility of that element in peralkaline liquids (Dietrich, 1968). Several of the metaluminous acid rocks of Centre 1 also show exceptionally high Zr concentrations (e.g. 509 and 476) of 1740 and 1280 ppm, respectively. The abundance in these two samples can

Fig. 58: Plot of K (wt. %) versus Rb (ppm) for the three Setberg series. A, B and C represent the Centre 1, Centre 2 and alkalic rocks, respectively. The diagonal line is drawn for a K/Rb ratio of 400.

A
B
C
%K
10
5
4
3
2
0.5
0.3
0.2
0.1
Rb
2
10
100
100ppm
3
10
100

be related to the unusual abundance of accessory zircon crystals. In both the Tertiary tholeiitic series and the transitional series a general trend towards Zr-enrichment reaches 600-700 ppm in the acid rocks. A number of acid rocks are significantly higher and lower than this value, and it is an interesting possibility that the above concentration range represents the level of solubility of Zr in the acid magmas, while Zr-rich and Zr-poor acid rocks have acquired their Zr-contents by accumulative addition and subtraction of zircon, respectively.

Copper shows a decrease with differentiation in the Setberg rock series, parallelling the trend of the St. Helena volcanic rocks (Baker, 1969) but unlike the variation trend of Cu in the Red Hill dolerite intrusion, in which the Cu-enrichment is only reversed in the fayalitic granophyre (McDougall and Lovering, 1963). The Setberg rocks (Figure 56) show a decrease from approximately 100 ppm Cu in the basalts to 10-15 ppm in the basaltic andesites and hawaiites. This rapid depletion of Cu is hard to account for in terms of the known petrographic features. Cu-content of olivine, plagioclase and clinopyroxene phenocrysts from the Klakkur ankaramite is 7, 6 and 14 ppm, respectively, whereas the whole rock contains 80 ppm. The extraction of Cu from the Setberg

liquids has thus in all probability not been effected by removal of the major precipitating phases, but more likely by the separation of sulphide or oxide phases, such as has been demonstrated for the St. Helena rocks (Baker, 1969). Zinc shows similar distribution in all three series, ranging from 60 ppm to 100 ppm in the basalts, up to 160 ppm in the acid rocks (Figure 55). Data on the phenocrysts from the Klakkur ankaramite indicate that Zn is not enriched in the plagioclase, clinopyroxene or olivine phases of the basaltic rocks (< 5, 14 and 57 ppm Zn, respectively). In the tholeiitic and transitional series Zn-enrichment levels off somewhat at a stage when magnetite becomes an important precipitating phase. The extreme enrichment of Zn (390 ppm) in the peralkaline obsidian of Centre 2 (331) is in keeping with evidence for peralkaline acid rocks in general (e.g. Nicholls and Carmichael, 1969).

The unusually high Zn content of the eastern Iceland pitchstones was pointed out by Carmichael and McDonald (1961), who gave an average of 125 ppm and suggested that a distinct regional variation existed among acid rocks, the Scottish Tertiary pitchstones being much poorer in Zn. The Setberg data supports this view, but Zn-depletion is shown by some of the acid rocks, notably those with very low iron content (311, 316 and 262).

The trace element contents of average Setberg basalts from the three series are compared with other basalts from the Iceland area and the average oceanic tholeiites and alkalic basalts (Engel et al., 1965) in Table 12. Of immediate interest is the close similarity of trace element abundance in the transitional basalts of Centre 2 and alkalic basalts in general, notably the high Ba and Sr. The Icelandic olivine tholeiites show a somewhat higher Ba and Sr content than do "primitive" oceanic tholeiites, but an interesting imtermediate type between the two extreme Ba and Sr concentrations in the tholeiites is the Reykjanes lava. The Ba and Sr content of inland tholeiites in Iceland is near 150 and 180 ppm, decreasing to 80 and 161 ppm respectively in the lava from Reykjanes, where the Mid-Atlantic Ridge strikes into Iceland. Oceanic tholeiite from the islet of Kolbeinsey (Sigurdsson and Brown, 1970) contains still lower Ba and Sr (34 and 65 ppm). Further work along the strike of the Mid-Atlantic Ridge and into the Icelandic volcanic zone may possibly substantiate our proposal of geochemical gradations in the olivine tholeiites along the Ridge and volcanic zone.

The Setberg alkalic and transitional basalts are compared with alkalic-type lavas from the eastern part of the volcanic zone in Table 12. The Ba and Sr contents of alkalic

TABLE 12

TRACE ELEMENTS IN SETBERG AVERAGE BASALTS AND COMPARISONS

	Ba	Sr	Rb	Zr	Zn	Ni	Cu
Olivine tholeiites:							
Basalts of Centre 1, Setberg area	170	180	2	100	90	55	100
Oceanic tholeiites (Engel et al., 1965)	14	130	<10	95		97	77
Kolbeinsey basalt (Sigurdsson and Brown, 1970)	34	65	2	27	50	106	124
Laki lava (Heier et al., 1966)	110	225	8	180		43	
Reykjanes lava (Heier et al., 1966)	80	161	4	120		70	
Transitional basalts, Centre 2, Setberg	420	300	12	120	70	34	60
Alkalic basalts:							
Alkalic basalts, Setberg area	400	360	12	95	65	165	85
Alkalic basalts (oceanic) (Engel et al., 1965)	498	815	33	333		51	36
Vestmann Islands basalts (Jakobsson, 1968)	50	175		165		235	85
Surtsey basalts (Steinthorsson, 1966)	65	300	15	100	75	125	77
Eldgja basalts (Robson and Spector, 1962)	200	500	10	100		40	

basalt from the Vestmann Islands (Jakobsson, 1968) and Surtsey (Steinthorsson, 1966) are surprisingly low, when compared to the Setberg lavas and alkalic basalts in general: so low, in fact, that their alkalic affinities are concealed. The low Ba/K ratio of the alkalic basalts from the Vestmann Islands and Surtsey, as compared with alkalic basalts in general, is an interesting geochemical problem.

Rb is considerably higher in the Icelandic alkalic basalts than in the tholeiitic rocks, whereas Cu is lower, by a factor of two. Zr is similar in both suites, and much lower than in alkalic basalts of Hawaii (Hubbard, 1969). No significant difference in Zn concentration is apparent between the alkalic and tholeiitic basalts, but more data are needed. Ni content in the Icelandic non-differentiated basalts is highly variable and a systematic difference between the two suites is not apparent, presumably due to the great sensitivity of Ni-concentration to olivine precipitation.

CHAPTER VI: DIVERSITY AND ORIGIN OF THE ACID ROCKS

Introduction

The distribution of acid rocks in Iceland and their association with central volcanoes has been dealt with in Chapter I and more fully in print (Sigurdsson, 1967). The chemical and petrographic diversity of these rocks has not been fully realized by previous workers and in the following account some new data are presented to illustrate this point.

The volume of acid rocks in the volcanic succession of Iceland as a whole has previously been estimated at about 10% (Sigurdsson, 1966). A reliable value of 9% for acid rocks in a restricted part of the succession in the Tertiary of eastern Iceland (Walker, 1966) and some new data on the post-glacial acid rocks (Thorarinsson, 1967) make more realistic calculations possible. Working from a wealth of detailed field measurements, Thorarinsson states that of the lava and tephra production in historic times (40 km^3 in 1100 years), 30% are acid and intermediate. This value includes, however, all the andesitic and basaltic andesite lavas of Hekla (8 km^3). If these are excluded, the volume of truly acid magma extruded in Iceland in the last 1100 years is 4 km^3 or 10% of the total magma production. We are therefore left with an astonishingly large volume of intermediate lavas from the very active Hekla

volcano, 8 km^3 or 20% of the Icelandic total erupted in historic time.

Thorarinsson (op.cit.) calculates that during all of post-glacial time, total extrusive activity produced 400 km^3, of which acid and intermediate rocks form 10% (again with intermediate rocks bulking high, making up 7%). The total volume of post-glacial magma production is difficult to assess, but Sigurdsson (1967) assumed that post-glacial lavas cover 12000 km^2, with an average thickness of 20-40 m, giving 300 to 500 km^3 as an independent estimate, closely comparable to that of Thorarinsson.

Excluding the intermediate rocks, we have 12 km^3 of acid rocks produced in the post-glacial period in Iceland, and assuming 400 km^3 as a fair estimate of the total magma production, the acid rocks make up only 3% of the entire post-glacial pile. Further fieldwork will, I believe, increase the known volume of the post-glacial acid rocks somewhat, but it seems likely that this figure cannot exceed 5%.

An independent, but rather qualitative approach to estimating the amount of acid rocks can be attempted by working from the number of known central volcanoes and acid centres throughout Iceland. In 1967, 42 central volcanoes were known (Sigurdsson, 1967). Since that time, another 10

acid centres can be added to the list, including Prestahnúkur, Geysir, Eyjafjallajökull, Myrdalsjökull, Hágöngur, Grímsvötn and Kverkfjöll. Whether all these areas merit the status of a central volcano remains to be seen after field work has been carried out, but their number already exceeds Walker's (1963) prophetic estimate of 50 central volcanoes in Iceland.

In the Torfajökull centre alone, some 450 km^2 of acid rocks are present, and it is a conservative estimate that in each silicic centre in Iceland some 50 km^2 of acid rocks occur, which would amount to approximately 2.5% of the area of Iceland. To this can be added a considerable quantity of rhyolitic tephra sandwiched between basalt lavas, and some hitherto undiscovered acid centres, but it seems very unlikely that the volume can be brought higher than 4% at the most.

The presence of only 3% acid rocks in the post-glacial pile, as compared with some 9% in the eastern Iceland Tertiary (Walker, 1966) may conceivably be related to petrographic differences between the Tertiary and Quaternary basalts. As noted earlier (p. 15), tholeiitic, saturated lavas are the chief basalt type in the eastern Iceland Tertiary, whereas alkalic, transitional and tholeiitic basalts are all present in the Quaternary and Recent succession. If the acid rocks are related to the basalts by a

process of differentiation, it is to be expected that saturated tholeiitic magma is a more efficient and productive source of the rhyolites than are undersaturated olivine basalts.

In summary, the evidence suggests that the volume of acid rocks in Iceland as a whole does not exceed 4%. Similarly, acid rocks make up some 3% of all the post-glacial volcanic pile alone (including historic eruptions), but the large volume of acid magmas erupted in historic time alone (10%) is hardly representative, due to the short duration of the period sampled (1100 years). We can conclude that the volume of acid magma present in the Icelandic succession as a whole is not in excess of the amount of acid liquid which can be derived from a tholeiitic or olivine tholeiitic parental magma, under conditions of extreme fractionation.

A. The 'Daly gap'

Largely because of collecting bias, the chemical composition of analysed volcanic rocks from Iceland shows a strong bimodal distribution, with intermediate rocks poorly represented. The Daly gap, as this condition is generally referred to, is a well-known phenomenon on oceanic islands (Chayes, 1963), but recent work on Saint Helena places its significance in doubt (I. Baker, 1968; Cann, 1968).

The relative scarcity of intermediate rocks in Iceland cannot be used as evidence against a continuum from basic to acid compositions. There are possibly some petrological grounds for claiming that during differentiation of a basaltic magma, a relatively small amount of liquid with intermediate composition is formed, in proportion to acid magma. Barth (1962), for example, points out that the shape of the melting curves for plagioclase is such that in the normal crystallization of plagioclase melts, calcic plagioclase will form in relatively great amount, followed by a small amount of intermediate plagioclase, and eventually ending with a large amount of sodic plagioclase. The effect is more pronounced in polycomponent systems, as shown by Wyllie (1963) for the system diopside-anorthite-albite. Wyllie points out changes of slope of the liquidus and solidus and the presence of thermal shelves where a small change in temperature causes great compositional change in the liquid.

An experimental verification of the concept of liquidus shelves comes in the work of Piwinskii and Wyllie (1968) who show that during fusion of tonalite and granodiorite, two thermal plateaux or shelves exist, separated by a temperature interval where considerable change in temperature causes very little melting. If this relation

holds equally well during crystallization, then a large amount of liquid would solidify at the high-temperature shelf (basaltic), followed by a large temperature interval during which very little crystallization takes place (intermediate liquid), and then by the lower thermal shelf where a small drop in temperature results in final solidification of the remaining acid melt.

There are a number of other criteria, some of which have been mentioned by Cann (1968), which go to show that acid rocks may be represented at the surface by a volume in excess of the proportions expected from fractional crystallization. An important concept is the recycling of acid magma; by virtue of the low melting temperature of rhyolite lavas, they may be remelted deep in the lava pile by rising basaltic magma and re-erupted to the surface.

B. Centres with alkaline affinities

The Ljosufjöll volcanic centre in eastern Snaefellsnes is petrographically similar to the contemporaneous alkalic series of the Setberg area. It is best described as a node on the Snaefellsnes volcanic zone (Figure 10) and its relationship to the eastern line of that zone is comparable to the relationship between the Setberg alkalic series and

the volcanic line in central Snaefellsnes (p. 63). Activity in the Ljosufjöll centre ranges from Late-Quaternary to Recent, giving rise to numerous basaltic lavas as well as rhyolitic domes. The area is characterized by faults and fissure eruptions of a small scale, trending WNW.

The basalts are Ne-normative alkalic basalts (480, 485) ranging to olivine basalts (483, 490), generally olivine-augite phyric and with interstitial biotite. Two mugearites have been encountered (479, 487), both of which are gradational to benmoreites and contain common xenocrysts of anorthoclase as well as sodic pyroxene, plagioclase, and rare apatite. Quartz xenocrysts are also present in one of the lavas.

A typical feature of the Ljosufjöll succession is the abundance and variety of acid rocks, so rare in the Setberg alkalic series. Three types can be distinguished: alkalic rhyolites (481, 491), quartz-trachytes (484, 486), and comendites (489). No intermediate lavas have been found so far in the area, leaving a compositional gap from 55 to 67% SiO_2. The acid rocks are invariably anorthoclase or sanidine-bearing and other phenocrysts include greenish pyroxene ($Wo_{41}En_{11}Fs_{48}$ to $Wo_{41}En_{5}Fs_{54}$) and fayalite ($Fo_{1.5}Fa_{88}Tp_{10}Ln_{0.5}$ to $Fo_{4}Fa_{86}Tp_{9}Ln_{1}$). Minor plagioclase

and biotite are present, while green, strongly pleochroic hornblende (arfvedsonite?) is very common in druses and segregation veins. Zircon is accessory in one obsidian (491). While only one of the analysed Ljosufjöll acid rocks is truly peralkaline (489), most of the others are close to peralkalinity.

Chemically they are very similar to the Quaternary acid rocks of the Setberg area and to other mildly alkalic provinces such as Easter Island (Bandy, 1937) and Tutuila (Macdonald, 1968), in all of which differentiation of undersaturated magmas has resulted in a trend towards oversaturated quartz-trachytes and alkalic rhyolites.

Eyjafjallajökull is situated in southern Iceland, near the eastern margin of the central volcanic zone. The volcano erupted in 1821-23 but was largely built up in the Late-Quaternary. Since only three samples have been investigated from this large central volcano, our knowledge is woefully inadequate. Two quartz-trachytes

---

Fig. 59: Alkalis/silica diagram of lavas from miscellaneous Icelandic centres. Closed circles, Drapuhlidarfjall (Mid-Quaternary of Snaefellsnes); T-symbols, Thjorsa at Fitjaskogar, central Iceland (Mid-Quaternary); crosses, Ljosufjöll on Snaefellsnes (Late-Quaternary to Recent); open circles, Torfajökull (Late-Quaternary to Recent); triangles, acid rocks from Myrdalsjökull, southern Iceland (Late-Quaternary).

The diagonal line is the dividing line between Hawaiian alkalic and tholeiitic basalts (Macdonald and Katsura, 1964).

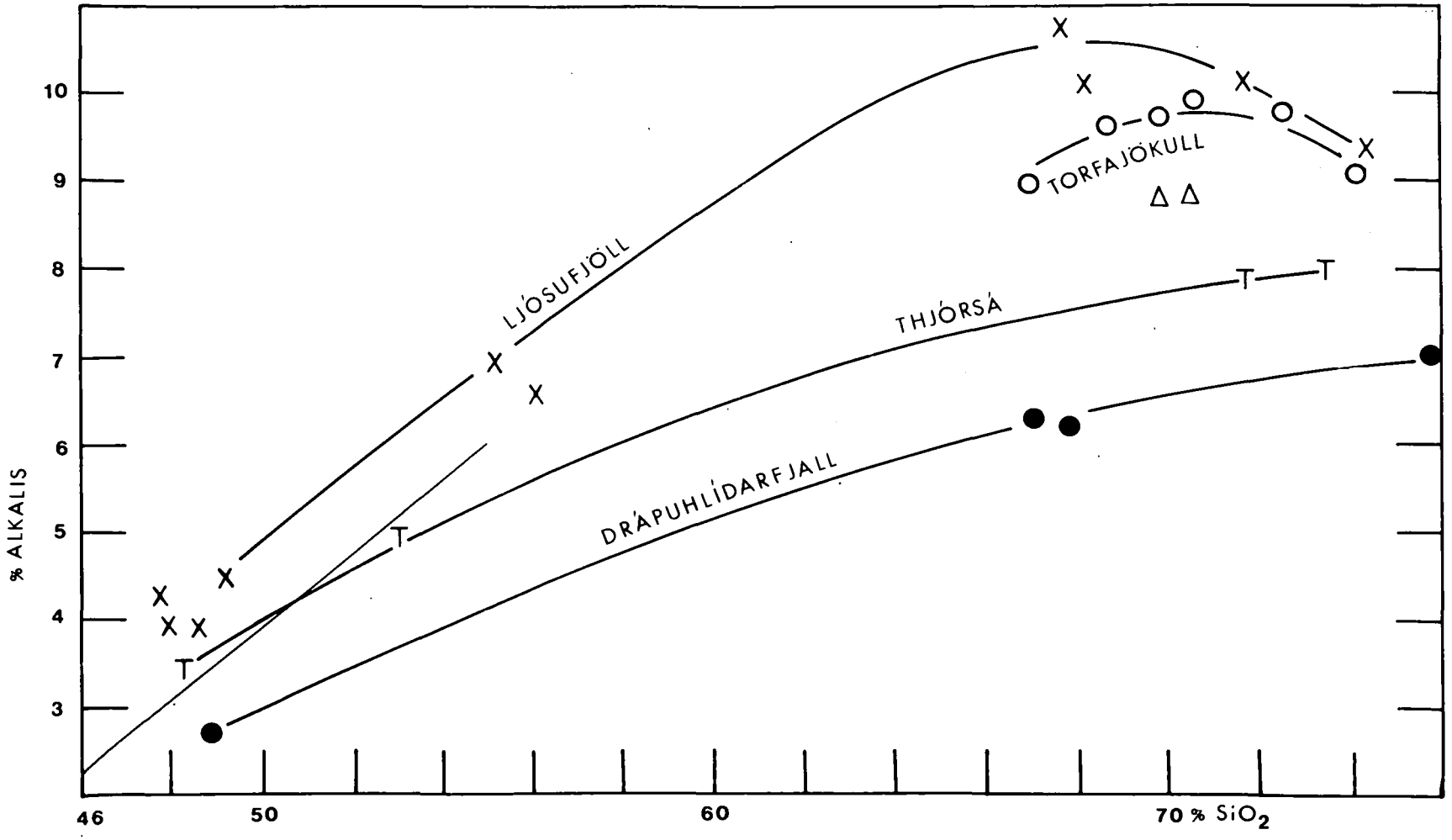
10
9
8
7
6
5
4
3
% ALKALIS
46
50
60
70 % SiO2
LJÓSUFJÖLL
THJÓRSÁ
DRÁPUHLÍÐARFJALL
TORFAJÖKULL

(470, 471) and a benmoreite (472) have been analysed from Eyjafjallajökull. They are typically olivine-phyric rocks, the trachytes containing a fayalitic olivine ranging in composition from $Fo_{11}Fa_{83}Tp_5Ln_1$ to $Fo_{16}Fa_{79}Tp_4Ln_1$.. Green, strongly pleochroic, sodic clinopyroxene, anorthoclase and (potassic?) oligoclase phenocrysts are also common in the quartz-trachytes, which are notably iron-rich rocks (Fe_2O_3+ FeO = 5.7 - 7.0%). The benmoreite contains large olivine phenocrysts, ranging from $Fo_{53}Fa_{45}Tp_2Ln_0$(margins) to $Fo_{86}Fa_{13}Tp_1Ln_0$ (cores). Hornblende is an important constituent of the interstitial groundmass. Chemically, the Eyjafjallajökull acid rocks correspond to the mildly alkalic differentiates of transitional or alkalic provinces.

Immediately north of the Eyjafjallajökull volcano lies another centre, Tindfjallajökull, but a Late-Quaternary welded tuff flow from this volcano outcrops in Thorsmörk. The tuff layer is highly porphyritic, containing 16% of feldspar ranging from potassic oligoclase to anorthoclase, greenish clinopyroxene and iron ore. The form of numerous basaltic inclusions is suggestive of a composite magma. Pyroxenes from the Thorsmörk tuff are ferro-hedenbergites, and the average of four microprobe analyses gave the composition $En_1Fs_{55}Wo_{40}Ac_4$. Chemically, this tuff (443) has affinities with the acid rocks of neighbouring centres,

e.g. in relatively high alkalis (8.86%) and only moderately high SiO_2 (69.3%).

Torfajökull. By far the largest concentration of acid volcanic rocks in Iceland is encountered in the Torfajökull area, where rhyolitic rocks cover some 490 km^2. Although predominantly of Late-Quaternary age, the centre has been active in post-glacial and possibly in historic time, and at least five post-glacial acid lavas are known: Laugahraun, Sudurnamshraun, Domadalshraun, Hrafntinnuhraun and Hrafntinnusker.

Older parts of the centre, e.g. the Late-Quaternary rocks of Brandsgil, are feldspar-phyric rhyolites (456, 463), rather low in silica (69.4%) and high in alkalis (9% K_2O+Na_2O). They contain phenocrysts of anorthoclase and a potassic oligoclase, along with ferrous augite and rare fayalitic olivine. A somewhat younger formation within this centre is the small volcano Blahnukur, formed by sub-glacial eruption of rhyolitic magma, probably during the last glacial period. The Blahnukur rhyolites rest on a basaltic pillow lava with alkalic affinities (459)1 followed by a voluminous glassy acid tuff (464, 458) and partly glassy rhyolite (450, 451, 452, 453, 454) with distinct pillow structures in a glassy, tuff matrix. At the summit of Blahnukur, a flow-banded rhyolitic dyke may

represent the feeder (455).

The Blahnukur rhyolites contain phenocrysts of greenish pyroxene, commonly near $En_{26}Fs_{26}Wo_{42}Ac_6$ but more sodic varieties are encountered, especially in the more crystalline varieties such as the feeder dyke, which contains aegirine-augite. Fayalitic olivine is common, as well as iron ore microphenocrysts, and zircon is a rare accessory. Two feldspar phenocryst types are present in most of the Blahnukur rocks: anorthoclase in large, slightly corroded grains, and euhedral laths of potassic oligoclase. Sanidine is found only in the summit dyke (455).

These rhyolites are chemically a very homogeneous type and clearly represent the product of a single eruption. SiO_2 varies from 70.5% to 70.7% in five analysed samples, and alkalis from 9.3% to 9.9%. An exception to this is the Graenagil tuff (458, 464), where leaching has probably been effective in removing alkalis, and the summit dyke (455), which is a comenditic rock with 1.5% acmite in the norm. All the Blahnukur rhyolites are near peralkalinity, and the somewhat stronger alumina undersaturation of the rhyolite dyke, presumably the last-erupted magma, does not set it significantly apart from other acid rocks of this small volcano.

A flow-banded, Quaternary comendite from Langasata (467) also belongs to the Torfajökull complex. This rock is peralkaline, with 2.6% acmite in the norm, and contains 73.9% SiO_2 and 8.8% alkalis. Pyroxenes unusual for Iceland occur in this rock, ranging in composition from nearly pure aegirine ($Fs_1Wo_7Ac_{92}$) to aegirine-augite ($En_2Fs_{28}Wo_5Ac_{65}$) and occurring as irregular, highly coloured, blue-green to lavender grains, both in the groundmass and projecting into vugs and vesicles.

The very interesting, post-glacial acid lavas of the Torfajökull centre cannot be done justice in this account, but some important features will be discussed. The obsidian lava of Laugahraun (457, 462) is a feldspar-phyric (30%) rock with scattered phenocrysts of greenish clinopyroxene, ranging from $En_{23}Fs_{37}Wo_{38}Ac_2$ to $En_{32}Fs_{18}Wo_{44}Ac_6$. Rare phenocrysts of amphibole are strongly pleochroic, from dark brown to yellowish brown. The feldspars are variable, and probably range from a potassic oligoclase type to anorthoclase with a rather small 2V, but this awaits microprobe confirmation. Mineralogically this lava is thus similar to Blahnukur, being comparable in total alkali content (9.7%), although somewhat lower in SiO_2 (69.9%).

Domadalshraun (424) is unique in being a post-glacial

example of a composite lava flow, having an acid interior with a basaltic carapace. The mix relations in this lava merit a special study, but the plagioclase-phyric component is reminiscent of the basalt lavas from Vatnaöldur, north-east of the Domadalshraun craters and possibly on the same fissure. The acid component is an oligoclase-ferroaugite-fayalite-magnetite-phyric rock, high in alkalis (9.63%) and relatively low in SiO_2 (69.5%). Compositionally, this lava is identical to Hrafntinnuhraun to the south and on the strike of the Sw-trending Domadalshraun fissure. Hrafntinnuhraun (426), with 69.8% SiO_2 and 9.6% alkalis, has comparable mineralogy but contains rare, euhedral grains of brown, pleochroic amphibole. The pyroxene phenocrysts are of two types. Brownish, more sodic grains have the composition $En_{33}Fs_{20}Wo_{23}Ac_{24}$, contrasted with greenish, somewhat elongate phenocrysts of $En_{35}Fs_{22}Wo_{38}Ac_{5}$. Clinopyroxenes intermediate in composition between these two types have not been found in a cursory microprobe investigation.

Sudurnamshraun (465) is the least siliceous of the Torfajökull obsidian flows, containing 67.1% SiO_2 and 8.8% alkalis. The rock is somewhat porphyritic, with phenocrysts of sodic plagioclase, olivine, and clinopyroxene ranging from $En_{45}Fs_{14}Wo_{39}Ac_{2}$ to $En_{34}Fs_{19}Wo_{40}Ac_{7}$.

The comenditic obsidian flow of Hrafntinnusker (423) is a beautifully homogeneous, non-porphyritic glass, with 72.6% SiO_2 and 9.8% alkalis. It contains 1.5% acmite in the norm and is thus the only known post-glacial peralkaline lava in Iceland.

At the present state of research, no known lavas of truly intermediate composition can be associated with the Torfajökull acid rocks. A post-glacial basaltic andesite lava in the vicinity (Nordurnamshraun (466)) has more tholeiitic affinities (54.4% SiO_2 and 4.5% alkalis), and is not a likely member of any differentiation sequence that would include the highly alkalic rhyolitic rocks of this complex.

The occurrence of alkalic rhyolites, comendites, and lavas with quartz-trachytic affinities (Sudurnamshraun) are ample evidence for the alkaline character of the Torfajökull complex as a whole. The possible association of these rocks with alkalic basalts is unknown, but it may be significant that the pillow lava underlying the Blahnukur rhyolites has distinct alkalic affinities, resembling the transitional basalts of Centre 2 of the Setberg area. Basalts of undoubted alkalic character are known to occur immediately east of the Torfajökull region, e.g. in the Eldgja-Katla fissure zone (Robson and Spector, 1962).

Myrdalsjökull. In addition to concealing Katla, one of Iceland's most active volcanoes, the ice cap of Myrdalsjökull covers an acid centre, parts of which outcrop in the nunataks of Huldufjöll, Kötlukollar and Kötlustigur, forming a circle of rhyolitic outcrops around the Katla vent. The area was visited by Robson (1956), who first described these Late-Quaternary acid lavas and on whose samples (stored in the Department of Geology, Durham) the following petrographic account is based.

The rocks are almost entirely glassy, and generally non-porphyritic or with sparse, small phenocrysts of oligoclase and ferroaugite. Six analyses of Myrdalsjökull acid rocks (434-439) show a remarkably small compositional range, with total alkalis ranging from 8.55% to 8.96% and SiO_2 from 70.0% to 70.4%. Robson (1956) shows the possible association of the somewhat alkalic rhyolites with the Sandfell "trachybasalts" (440, 442), a group of Late-Quaternary lavas east of Myrdalsjökull which are not unlike the basaltic andesites of Centre 2 of the Setberg area.

The Katla volcano consistently produces an alkalic olivine-basalt magma, invariably very high in TiO_2 (4-5%) and Ne-normative (Robson, op.cit.). A genetic relation

between the Katla magma and that of the Myrdalsjökull differentiated rocks is not apparent, and the association may purely be a geographical one.

Öraefajökull is Iceland's largest volcano, but the petrography of its products is almost totally unknown. The character of the acid tephra is distinctly alkalic (Tomasson, 1967), and an analysis of a comenditic obsidian from the summit of the volcano (Carmichael, 1967) shows 1.4% acmite in the norm (71.52% SiO_2 and 9.46% alkalis). Öraefajökull thus has affinities with alkalic centres like Ljosufjöll and Torfajökull. Recent eruptions, in 1362 and 1727 (Thorarinsson, 1958), produced rhyolitic and intermediate tephra respectively, and it is possible that further work on this volcano may reveal a chemically cyclic activity, akin to that of Hekla (Thorarinsson, op.cit.).

Thjorsa. Rhyolitic rocks of Quaternary age outcrop in Fitjaskogar, on either side of the river Thjorsa in south-central Iceland. They are associated with basaltic andesites with alkaline affinities (420), and with transitional basalts (421). The rhyolites (419, 422) are not distinctly alkalic, with 73.4% SiO_2 and 8.1% alkalis, and the whole Thjorsa series is aptly termed transitional in chemistry between the tholeiitic and alkalic centres (Figure 59).

C. . Centres with tholeiitic affinities

Acid rocks from the volcanic centres described in the preceding section have all possessed alkalic characters as borne out by the rock chemistries, the presence of anorthoclase (rarely sanidine) and sodic pyroxene in the rocks, and the association with alkalic or transitional basalts in the field. In strong contrast are certain silicic centres of Thingmuli type, where the acid rocks are low in alkalis, the feldspars are generally oligoclase or andesine, and the ferromagnesian assemblage is restricted to fayalitic olivine and ferroaugite - ferrohedenbergite. The field-associated basalts are invariably tholeiitic.

The Drapuhlidarfjall rhyolitic and intermediate lavas, erupted during the Mid-Quaternary, are of Thingmuli type and are particularly noteworthy for their low alkali content (Figure 59). A range of rock types from this volcano (325, 353, 354, 355) has been analysed. They include an aphyric quartz-tholeiite lava (48.8% SiO_2 and 2.7% alkalis), and two icelandites containing sparse phenocrysts of andesine and hedenbergite ($En_{0.3}Fs_{59}Wo_{39}Ac_{1.6}$), and microphenocrysts of fayalitic olivine.

The summit of Drapuhlidarfjall is capped by a rhyolitic lava, some 150 m thick, which is entirely aphyric and beautifully spherulitic in parts (325). The rhyolite

contains 76.4% SiO_2 and 7.0% alkalis, being even poorer in K_2O+Na_2O than the eastern Icelandic pitchstones (Carmichael and McDonald, 1961).

The acid rocks of Alftafjördur in north-eastern Snaefellsnes (Ulfarsfell) display similar features (477, 492, 494, 478, 493), and may be related to the adjacent Drapuhlidarfjall centre. An icelandite from Alftafjordur contains phenocrysts of plagioclase and pigeonite, as well as rare microphenocrysts of apatite. A striking feature is the low alkalis content of these rocks and a fresh-looking, plagioclase-augite-phyric obsidian contains only 5.1% alkalis with 70.0% SiO_2.

The acid and intermediate rocks of Drapuhlidarfjall and Alftafjördur are chemically similar to those of Centre 1 of the Setberg area. The presence, in the acid rocks of all three areas, of plagioclase as the only feldspar phase, the absence of quartz phenocrysts, and the occurrence of pigeonite, although rare, indicate their tholeiitic affinities.

D. Origin of the peralkaline acid rocks

Acid rocks showing the peculiar condition of alumina undersaturation (molecular Na_2O+K_2O greater than Al_2O_3) have now been discovered in four volcanic centres in

Iceland: Setberg, Ljosufjöll, Torfajökull and Öraefajökull. Their field association with alkalic-rhyolites, quartz-trachytes, and intermediate rocks of benmoreitic composition has been demonstrated in two centres, but the derivation of these peralkaline acid liquids from the metaluminous rhyolitic and trachytic magmas is an interesting problem.

Bowen (1945) pointed out the failure of pure albite to crystallize from a liquid containing lime, resulting in the precipitation of plagioclase rather than albite. Thus the "plagioclase effect" is the preferential incorporation of Ca and Al into feldspar, resulting in the formation of excess Na in the liquid and hence the creation of excess alkali silicates in the later differentiates. As pointed out by Carmichael and McKenzie (1963), the "plagioclase effect" ceases to operate once sodium silicate is present in significant amount in the liquid, because an alkali feldspar starts to precipitate. The peralkaline condition will, however, be maintained and even accentuated by the separation of alkali feldspar, as pointed out by Bailey and Schairer (1964), who coined the term "orthoclase effect" for the fractionation of alumina and potash by separation of alkali feldspar from a slightly alumina-deficient liquid, leading to strongly peralkaline

and sodic residual liquids.

A pre-requisite for the operation of the "plagioclase effect" is the presence of lime-bearing components in the norm of the parental liquid, such as diopside and/or wollastonite. Precipitation of calcium-bearing plagioclase from the liquid will, in effect, consume lime at the expense of potential diopside and wollastonite, and Al_2O_3 at the expense of the more sodic feldspars, leading to an excess of sodium silicate.

The alkali-rhyolites and quartz-trachytes associated with the Icelandic comendites are generally slightly diopside-normative rocks (1-3%) and typically contain abundant phenocrysts of potassic oligoclase and anorthoclase. The view was expressed above (p.170) that these rocks had acquired their feldspar relations through migration of the liquid into the thermal valley of the system $NaAlSi_3O_8$-$KAlSi_3O_8$-SiO_2, and were, in fact, one-feldspar liquids whose feldspars show a compositional range from oligoclase to anorthoclase. Continued separation of potassic oligoclase or calcic anorthoclase from these liquids, and operation of the "plagioclase effect", is a plausible mechanism for the derivation of the associated peralkaline acid magmas.

Some workers have looked to other processes, such as localisation of the alkali elements by volatile transfer, to account for the genesis of peralkaline acid magmas. However, in the words of Bowen (1928): "It is very easy to derive liquids by means of gaseous transfer, liquid immiscibility or the like, because these processes always do just what one may wish them to do." Another, more substantiated doubt on the feasibility of volatile transfer as an important mechanism is raised by the evidence for absence of water, or at the most a very low water content, in peralkaline acid lavas. Nicholls and Carmichael (1969) point out that for the retention of the high halides and sodium during crystallization, a very dry peralkaline liquid is required and, furthermore, they give evidence that the composition of the volatile phase is close to the low oxygen fugacity of an FMQ buffer.

E. Origin of the acid magmas by partial melting

The derivation of the Icelandic acid magmas from a direct mantle source, without an intervening basalt liquid phase, has been suggested as a possible mechanism for the origin of these rocks (Sigurdsson, 1967, p.42). The process might be akin to Green and Ringwood's (1968) model for the genesis of calc-alkaline rocks, being a

two-stage melting process with partial melting of sinking eclogite giving rise to andesites (dry melt) and rhyodacites (wet melt).

Gibson (1970), using the data of Carmichael (1962, 1963, 1964) and Carmichael and McDonald (1961), opposes the view that the pitchstones of eastern Iceland are derived from tholeiitic magmas by fractional crystallization and favours an origin by partial melting in the upper mantle or lower part of the Icelandic crust. He points out that the phyric pitchstones are always lower in silica than the aphyric ones, and that a roughly linear relationship holds between silica-content and the volume of phenocrysts. Furthermore, the higher content of P, Ni, Cu, Zr, Rb and S in the low-silica, porphyritic pitchstones prompts Gibson to conclude that these rocks are fractionated products of the "primitive" high-silica, aphyric pitchstones, which in turn are derived by partial melting at depth. He is aware of the difficulty in accounting for the lower silica and alkalis in the phyric rocks being the fractionation products of the more silica-rich glasses, but overcomes this by suggesting modification of the melts by vapour-phase leaching. Finally, Gibson considers the great similarity amongst the non-porphyritic pitchstones in Eastern Iceland as testimony for eutectoid melting in a similar pressure/

temperature regime.

The thesis of a parent-daughter relationship for the aphyric and porphyritic pitchstones, respectively, and an origin of the eastern Icelandic acid magmas by partial fusion does not gain support here. Gibson is dealing with and comparing bulk analyses of aphyric and phyric rocks and naturally the porphyritic ones will be poorer in silica, since phenocrysts of any lava (except, of course, quartz phenocrysts, which are unknown in eastern Iceland) are lower in silica than the liquid from which they precipitate. Thus subtraction of phenocrysts from a phyric pitchstone analysis leaves a liquid with a chemistry similar to that of the aphyric pitchstones, as shown by the work of Carmichael and McDonald (1961, Table 4b).

Thus the aphyric and phyric pitchstones of eastern Iceland are related by the simple rules of fractional crystallization, the phenocrysts bearing testimony to the fractionation process and the non-porphyritic rocks representing the residual liquids.

Gibson (op.cit.) indicates the gradual increase in P, Ni, Cu, Zr, Rb and S with decreasing silica content, or more significantly, with increasing content of phenocrysts, not only of plagioclase, but also of ferroaugite,

fayalitic olivine and iron oxides. All the above elements may be fractionated from a liquid during crystallization. That this is so also with the eastern Icelandic pitchstones is borne out by inspection of Table 4b of Carmichael and McDonald (op.cit.), where it is seen that the porphyritic pitchstones are generally higher in P, Ni, Cu, Zr and S than their residual glasses. Thus decrease in these elements in going from the porphyritic to aphyric pitchstones is the result of fractionation, and not the reverse as Gibson suggests.

Finally, if the eastern Iceland aphyric pitchstones were eutectoid partial melts from great depth, their composition would be expected to coincide with the cotectic silica-feldspar boundary curves for high water-pressures in the system $NaAlSi_3O_8$-$KAlSi_3O_8$-SiO_2-H_2O, i.e. in excess of 3000 kg/cm^2, having supposedly equilibrated at depth. The fact that, on Gibson's Figure 4, the aphyric pitchstones plot nearer to the 500 kg/cm^2 boundary curve in this system speaks against any immediate origin from great depth and rather supports fractionation in shallow-depth magma chambers, as proposed by Carmichael (1963, 1964).

The debate on the genesis of the Icelandic acid magmas has been largely centred around the relatively

large volume of rhyolites estimated present in the volcanic pile, but geologists have variously attributed their origin to crystal fractionation from a basaltic magma, melting of a sialic substratum or, thirdly, partial melting in the upper mantle or at the base of the Icelandic crust.

The presence of sial is without geological or geophysical support and furthermore, all granitic xenoliths found so far in the basalt lavas can be related to young intrusions, akin to those of south-eastern Iceland, rather than the presence of ancient crustal rocks at depth (Sigurdsson, 1968). In addition, the evidence from Sr and Pb isotope studies on Icelandic acid and basic rocks, as discussed on p.16, excludes sial as a probable source for the acid magmas.

While the process of partial fusion in the upper mantle or lower crust remains an attractive mechanism, conclusive evidence has yet to be presented to make it anything more than a tentative hypothesis. The chemical affinities between basaltic and rhyolitic rocks, observed in the central volcanoes described above (p.264), i.e. the association of alkali-rhyolites, peralkaline acid rocks and alkalic basalts on the one hand and low-alkali pitchstones and tholeiites on the other, speaks against

an independent origin of the acid rocks by partial melting, as the chemistry of such magmas would be governed by the source rock chemistry alone and not necessarily related to field-associated basalts.

The process of high-level basaltic fractionation has been shown to be capable of producing 5% of acid residuum from the Skaergaard initial magma (Wager and Brown, 1968) and from 7% to 12% in the case of Thingmuli tholeiites (Carmichael, 1964). Rather efficient fractionation and extraction is demanded, but the presence of some 3% to 4% of acid rocks in Iceland is well accounted for by such a process, keeping in mind the effect that re-cycling of the acid (low-melting) rocks will have on the volume relations between the acid and basic rocks.

CHAPTER VII: BASALT PETROGENESIS

A. Introduction

Of considerable petrological interest is the origin of the transitional basalt series of Centre 2 and its relation to the tholeiitic and alkalic series. The existence of a continuum between these two basalt types has been recognized for some time (Yoder and Tilley, 1962; Coombs, 1963) and an extensive literature is building up on transitional basalts, which may or may not be associated with alkali-rhyolites, quartz-trachytes and comendites (e.g. Wilkinson, 1968; Upton and Wadsworth, 1966; Aoki, 1966; Lipman, 1969; Green, 1968; Wise, 1969; Muir and Tilley, 1964).

Kuno (1968) placed high-alumina basalts as the transitional type between tholeiites and alkalic basalts, but examination of the literature reveals that only in certain cases does this hold true.

This chapter deals with petrogenesis of the Setberg transitional basalts and the presence of alkalic basalts, hitherto very rarely described in the volcanic succession of Iceland. A part of the basalt tetrahedron, the system Pl-Di-Fo-SiO_2, is illustrated in Figures 61 and 62, representing conditions at 1 atm. and 20 kb respectively. The Setberg basaltic rocks have been plotted on planes as

projections from the four apices of this system, in order to determine the relative position of these basalts and the phase boundaries of the system. The plots are not presented here, but Table 13 gives co-ordinates of the average Setberg basalt lavas in the basalt tetrahedron. Approximately 85 wt. % of the normative constituents are represented in this system, the notable exclusions being the iron oxides.

B. Relationship of the three basalt magma types

The occurrence in the Setberg area of tholeiitic, transitional and alkalic basalts in a defined age sequence can be viewed either as an accidental relationship, or the sequence may have some petrogenetic significance. The latter, more positive view, is adopted here and two alternative hypotheses are presented, which could conceivably account for the sequence of magma types in the Setberg area.

The effect of pressure on the evolution of basaltic liquids is known from the work of numerous authors, e.g. Kushiro's (1969) work on the system Fo-Di-SiO_2 at 20 kb, and the demonstration of congruent melting of enstatite above 5 kb (Boyd and England, 1961; Green and Ringwood, 1964). However, the replacement of olivine by orthopyroxene as the liquidus phase in an olivine tholeiite liquid at approximately 15 km depth, and subsequent fractionation by

orthopyroxene crystallization, will have the effect of sending the residual liquid toward more undersaturated compositions (Green and Ringwood, 1967).

An origin by orthopyroxene fractionation has been considered in order to account for the Setberg basalt spectrum, from tholeiitic to alkalic, by invoking solidication from above, in an olivine tholeiite magmatic reservoir of great vertical dimensions. The emplacement of this magma in Tertiary time initially led to outpouring of olivine

---

Fig. 60: A P/T diagram for dry and water-saturated olivine tholeiite magmas.

Saturated solidus and liquidus curves are those for an olivine tholeiite of the 1921 Kilauea eruption (Yoder and Tilley, 1962), while the curve for the dry liquidus of basalt (6°C/Kb or 1.7°C/km) is from Cohen et al. (1967). The replacement of olivine by orthopyroxene on the liquidus is based on dry melting experiments carried out on olivine tholeiite by Green and Ringwood (Figure 4, 1967). The adiabatic gradient of 0.3°C/km (Jeffreys, 1929) is that of a liquid magma body, assuming no convection. The diagram shows P/T conditions up to a level of zero km and kb, but realistically, the roof of the hypothetical magma body must lie at a minimum depth of 3 to 5 km.

During cooling of a dry melt, the adiabatic gradient will intersect the liquidus at depth and crystallization will proceed from below, upwards. On the other hand, in a wet magma the adiabatic gradient intersects the liquidus in the roof zone and gradual solidification from above restricts the remaining basaltic liquid to deeper levels. At approx. 5 kb (dry), orthopyroxene replaces olivine on the liquidus, and subsequent removal of orthopyroxene by sinking may thus give rise to a trend of undersaturation.

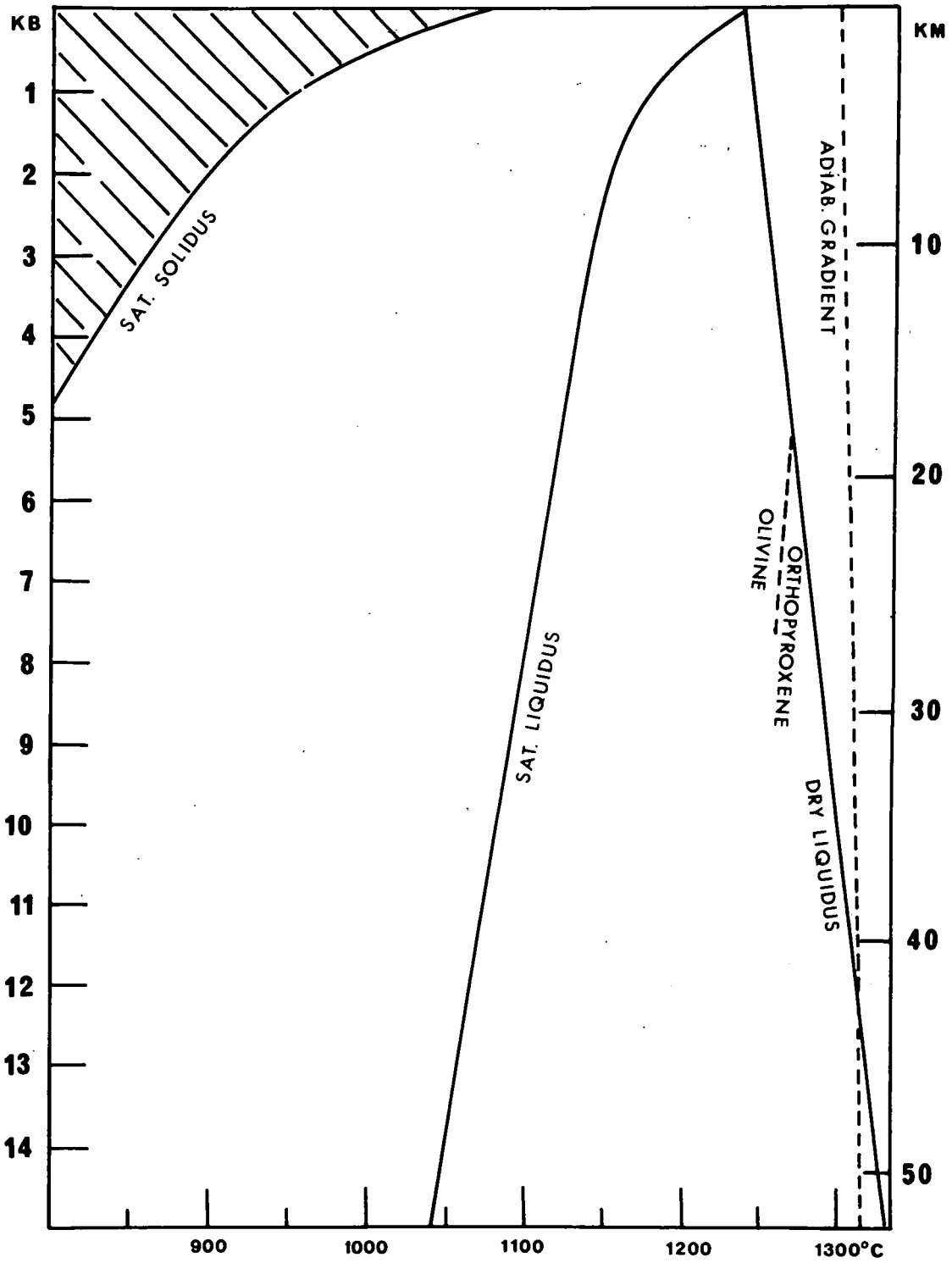
KB
1
2
3
4
5
6
7
8
9
10
11
12
13
14
KM
10
20
30
40
50
SAT. SOLIDUS
SAT. LIQUIDUS
ADIAB. GRADIENT
OLIVINE
ORTHOPYROXENE
DRY LIQUIDUS
900
1000
1100
1200
1300°C

tholeiites, and the formation of a near-surface subsidiary magma chamber in Centre 1.

Variation of factors controlling crystallization in a homogenous magmatic body, such as pressure and water content of the magma, is reflected in the slope of the liquidus as shown in Figure 60, which illustrates the two possible extremes of crystallization in a dyke-like magmatic reservoir of great vertical dimensions, in the absence of convection. In Figure 60 the cooling of a basaltic magma will result in the intersection of the adiabatic gradient with the liquidus. In the case of a dry melt, the adiabatic gradient intersects the liquidus at depth and hence crystallization will start at the base of the magma reservoir and proceed upwards, as Jackson (1961) has proposed for the Stillwater intrusion. In water-saturated basaltic liquids the liquidus slope is reversed (Figure 60), due to the effect of water and pressure on lowering the liquidus temperature. Cooling of a water-saturated basaltic melt will result in the intersection of the adiabatic gradient with the liquidus in the roof zone (under appreciable cover) and eventually in solidication from above, restricting the remaining magma to deeper parts of the column. Fractionation during crystallization will presumably have the effect of maintaining the condition of water-saturation, as volatile phases become enriched during

precipitation of the early crystalline phases.

In applying this concept to the Setberg basalts, we envisage the initial emplacement of a dyke-like tholeiitic magma body, of crustal dimensions, similar to those indicated under some of the Scottish Tertiary centres (Tuson, 1959). Initial volcanicity of olivine tholeiites was followed by the establishment of a high-level subsidiary magma chamber under Centre 1, giving rise to acid magmas, caldera formation and a cone-sheet swarm. Crystallization from above in the major, magmatic reservoir followed the pattern of a relatively water-rich magma (Figure 60), restricting the melt to successively deeper levels. This process may have taken place in the prolonged interval between the activity of Centres 1 and 2, during which time the cooling and some crystallization in the reservoir may have been responsible for the metamorphic aureole of Centre 1.

Restriction of the magma to deeper levels would eventually have the important petrological effect of orthopyroxene replacing olivine on the liquidus in the olivine tholeiite magma, once the liquid is confined to depths of the order of 15 km, or near the base of the Icelandic crust. The resulting precipitation of orthopyroxene would lead to a degree of undersaturation of the magma on removal of a mineral phase more silica-rich than the liquid, giving rise

to the transitional orthopyroxene- and olivine-bearing basalts of Centre 2. A degree of fractionation at depths sufficient to suppress the incongruent melting of enstatite has been proposed above (p.186) to account for the presence of orthopyroxene, together with olivine, in the transitional basalts. The composition of a transitional basalt liquid in equilibrium with orthopyroxene and olivine at high pressures, will be overtaken on ascent by the expanding olivine phase volume (Figure 62). Continuous precipitation of olivine takes place during rise of the magma, until the magma reaches the surface or until the removal of olivine has succeeded in shifting the composition of the liquid out of the olivine phase volume, whichever event occurs first. The presence of olivine phenocrysts and microphenocrysts in all rock-types of the transitional series of Centre 2 (olivine tholeiites to icelandites) and perhaps the very low Ni content of these rocks, is suggestive of such an olivine-fractionation process during ascent. Continued orthopyroxene fractionation would lead to critically undersaturated magmas, such as alkalic basalts.

After the emplacement of a transitional basalt magma in a shallow-level magma chamber, the character of subsequent fractionation high in the crust would be of a very different type, as orthopyroxene is now completely replaced by olivine

on the liquidus. Such high-level fractionation of the rather alkali-rich transitional basalt magma is believed to have given rise to the alkali-rhyolites and rhyodacites of the Lysuskard type.

The contrasted differentiation careers of the transitional basalt magmas at high pressure as opposed to fractionation in a near-surface magma chamber may explain the dichotomy of the rock-types in this series. Two compositional trends were noted above in the Centre 2 rocks (p.217), one encompassing basaltic to icelandite types, the other including rhyodacitic and rhyolitic rocks with alkaline affinities and typically associated with the ring-features of Centre 2 only. We suggest that the latter suite is the product of high-level, low pressure fractionation of transitional type magma in a chamber underlying Centre 2, but evidence for such a high-level magma chamber comes from the presence and disposition of cone sheets around the centre (p.49).

The above model is also capable of accounting for some other features of the transitional series, particularly the high content of Ba and Sr in the basalts which, together with the high alkali content, suggest a long history of fractionation or, alternatively, a very low degree of partial melting in the upper mantle (Gast, 1968). The high Ba and Sr and

depletion of Ni could be explained by extensive fractionation at depth in a major magma reservoir, where orthopyroxene and olivine are the principal precipitating phases, leading to enrichment in Ba and Sr in the absence of plagioclase-extraction and impoverishment of Ni due to olivine fractionation.

An alternative hypothesis, relating to the origin of the tholeiitic, transitional and alkalic basalt magmas, was hinted at in the discussion of Icelandic plate tectonics and the structure of the Snaefellsnes volcanic zone (p.63). Following the concept of crustal spreading in Iceland (Bodvarsson and Walker, 1964) we can assume that the Setberg region was in or near the central volcanic zone in Tertiary time, where tholeiitic basalts were being erupted. But by virtue of crustal spreading the Setberg area would be at least 100 km west of the active volcanic zone in Quaternary time. McBirney and Gass (1967) have related basalt chemistry to the distance of a volcano from the central ridge or rift zone of Mid-Oceanic Ridges and intensity of heat flow, and demonstrate that silica saturation of basalts decreases away from the rift zones. Similarly, Gast (1968), working with the thermal mantle model of Oxburgh and Turcotte (1968), suggests that olivine tholeiitic basalts are generated at shallower levels under the ridge crest region, but that the

zone of alkalic basalt formation lies further away from the crests and at greater depth. Heat flow pattern over oceanic ridges indicates that mantle isotherms dip steeply away from the crest region and consequently magma generation will be restricted to greater depths on the flanks of ocean ridges and rift zones. Hence the alkalic basalts would be generated there, whereas in the central regions, magmatic generation would take place at shallower levels, giving rise to olivine tholeiites.

Viewing basalt petrogenesis in the Setberg area in the light of such a model, the transition from tholeiitic to alkalic basalts would be attributed to gradual migration of the area away from the central volcanic zone, consequent fall-off in mantle isotherms, and restriction of magma generation to greater depths.

This latter hypothesis does not, however, account adequately for some of the geochemical features of the transitional basalts, notably the high content of Ba and Sr and low Ni, which were attributed to a two-stage fractionation process in the alternative hypothesis discussed above.

The occurrence of the alkalic basalts of the Late-Quaternary Snaefellsnes volcanic zone as a whole, is consistent with the concept of variation in basalt geochemistry with distance from the central zone. Although gradational to

the transitional series in terms of major elements, the alkalic basalts of Setberg do not show features which would be expected by an origin such as put forward in the hypothesis of downward crystallization of an elongate magma reservoir. Such an origin should be reflected in enrichment of certain trace elements in the alkalic basalts, being in effect residual, over that present in the transitional basalts, whereas in fact Ba and Sr concentrations are roughly equal in the two basalt types (Table 12).

In summary, we suggest that the origin of the transitional basalts of Centre 2 may be closely related to the olivine tholeiite magma of Centre 1, and we advocate an extensive reservoir under the Setberg area in Tertiary and Early-Quaternary time which, by solidification from above and the precipitation of orthopyroxene, gave rise ultimately to magma with alkaline affinities in Centre 2.

The Setberg Late-Quaternary series, on the other hand, along with contemporaneous alkalic basalts in the Snaefellsnes volcanic zone, are believed to owe their origin to the presence of a major tectonic feature in Snaefellsnes (p.63) and their alkalic character is related to the greater depth of generation. This in turn is necessitated by the relatively cool mantle outside the central Icelandic volcanic belt, and may thus be unrelated to the genesis of

the earlier transitional basalts of Centre 2.

Little consideration has been given to the question of water content in the Setberg basaltic magmas in the above discussion. The importance of water in the pressure/temperature system is obvious from Figure 60, and is particularly well dealt with by Harris et al. (1969). Addition of water to a silicate melt under pressure decreases the liquidus temperature, and in a water-saturated system the effect of increased depth (to moderate pressures) is to further diminish the liquidus temperature. Hamilton and Anderson (1967) suggest that basalts may contain at least 4% H_2O at some depth, and claim there is no reason to believe that basalts at depth are dry.

The presence of hornblende in cavities and vugs of some of the basalts and icelandites of Centre 2, along with the abundant biotite and hornblende of the Lysuskard gabbro, are only a qualitative indication of the amount of water in the transitional basalt magmas, but we can safely claim that they have been much "wetter" than the tholeiitic magma of Centre 1.

By a similar argument, the frequent presence of phlogopitic mica in the groundmass and phlogopite and hornblende in vugs and vesicles of lavas of the alkalic series may be a good indication of relatively high water content. Although

both the transitional and alkalic series show considerable iron enrichment, a feature usually associated with decreasing P_{O_2} and constant bulk composition, the P_{H_2O} and P_{O_2} conditions are not necessarily directly relatable.

Our hypothesis for the origin of the transitional basalts by a fractionation of orthopyroxene pre-supposes, and indeed requires, a saturated or wet magma. The solubility of water in a basaltic melt at 1100°C at 2kb is near 5 wt. % H_2O (Hamilton and Anderson, 1967), but the lack of quantitative data on the water content of natural magmas such as the Setberg transitional series leaves the validity of the hypothesis open to question.

C. The alkalic basalt series

Basalts of the alkalic series show a tendency to fractionate in or near the critical plane of silica undersaturation in the early stages, as borne out by the occurrence of just-Ne-normative olivine basalts and hawaiites (p.141). As pointed out by Schairer (1967), magmas generated in or near the Di-Ol-Pl plane (Figure 62) have the potential of fractionating either towards silica-saturated or undersaturated compositions. Schairer suggests that a basanitic trend from this plane is favoured only by an albite-rich system ($<An_{50}$).

The petrographic evidence indicates that the alkalic basalts in the Setberg area started from within the Ol volume (Figure 61) and, by precipitation of olivine, moved to the

---

Fig. 61: A diagrammatic representation of the quaternary system Di-Ol-Pl-SiO_2, part of the simplified basalt tetrahedron at 1 atm. pressure, based on published phase-equilibrium diagrams.

A: a quaternary invariant point (ol-en-pl-di-liq) at 1120°C, and a reaction point for olivine.

B: a quaternary invariant point (pl-di-en-qz-liq) at 1060°C, a quaternary eutectic.

c: a piercing point at 1386°C (ol-en-di-liq), also a reaction point, where olivine reacts with liquid to produce diopside and enstatite.

d: piercing point at 1374°C (en-di-qz-liq).

e: piercing point at 1150°C (ol-di-pl-liq).

f: piercing point at 1098°C (ol-en-pl-liq).

g: piercing point at 1058°C (pl-en-qz-liq).

h: piercing point at 1073°C (pl-di-qz-liq).

Phase-equilibrium diagrams from the following sources were used in construction of this tetrahedron: the system albite-forsterite-silica, Schairer and Yoder (1961); the system forsterite-diopside-silica, Kushiro and Schairer (1963); the system albite-diopside-silica, Schairer and Yoder (1960); the system albite-forsterite-diopside, Schairer and Morimoto (1959); the join albite-enstatite-diopside, Schairer and Morimoto (1958); the system anorthite-forsterite-silica, Anderson (1915); the volume forsterite-anorthite-diopside-silica, Hytonen and Schairer (1961).

Ol-Di boundary surface where augite and olivine precipitated together as in the olivine basalts, but nevertheless preserving their position near to the critical plane of silica undersaturation without crossing into the En-Pl-Di-SiO_2 compositional field (Figure 61). Petrographic and trace element evidence shows that plagioclase did not appear on the liquidus in any significant amount until in the hawaiites, at the stage when the fractionating liquid had followed a path down the ol-di boundary surface, onto the univariant line pl-ol-di-liquid (line e-A in Figure 61).

By virtue of their position within the Di-Fo-SiO_2 system, i.e. in the area between the Fo corner, the Fo-Di eutectic and the point of intersection of the En-Di join and the Di-Fo boundary surface, the Setberg alkalic and olivine basalts should behave as liquids which precipitate olivine which shows no reaction relationship with the liquid to give pyroxene (Yoder and Tilley, 1962), thus prohibiting the movement of such liquids across the Di-En join with fractionation at high or low pressure.[1)] It is unlikely, however, that this relation holds <u>within</u> the basalt tetrahedron (Figure 61), i.e. when plagioclase is included. Work by Schairer and

---

1) Kushiro (1969) has shown that this relationship does not hold for wet systems, as the forsterite-enstatite liquidus boundary shifts towards silica with increasing water pressure, and at 20 kb the join diopside-enstatite is not a thermal barrier.

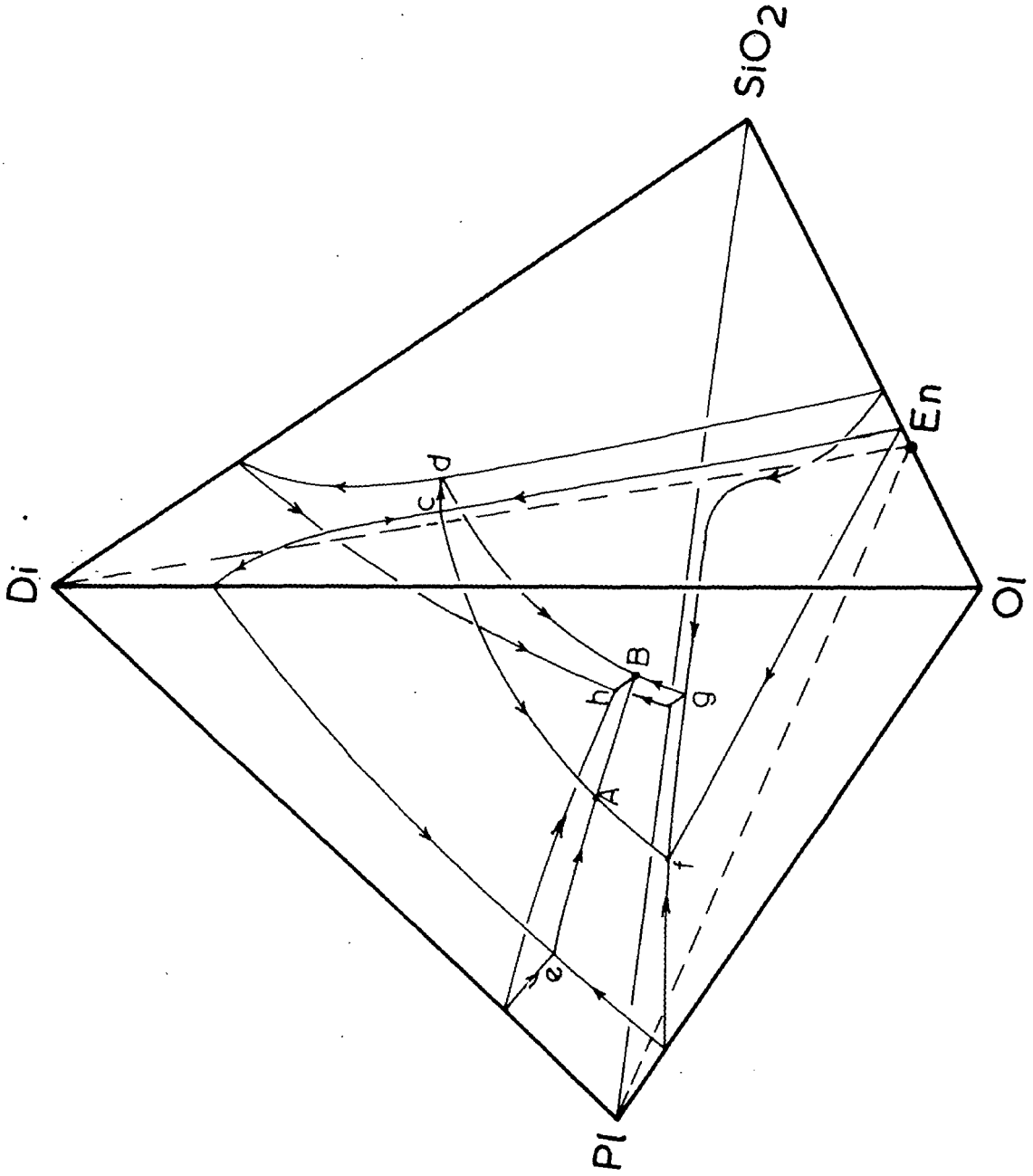
SiO2
En
Di
Ol
Pl
d
c
B
h
g
A
f
e

Morimoto (1958, 1959) and Schairer (1967) on the "plane of silica saturation" (the join albite-enstatite-diopside) shows the course of liquids on the univariant line pl-di-ol-liquid (line e-A, Figure 61). Point e is a piercing point at 1150°C (ol-di-ab-liquid), while A is a quaternary invariant point (ol-en-ab-di-liquid) with the temperature 1120°C. This line pierces the plane of silica-saturation at 1138°C (en-ab-di-liquid).

Fractionation along the line e-A of plagioclase-rich liquids in the olivine basalt field affords one means of producing silica-saturated derivatives from magmas originally in the critical plane of silica undersaturation. The proximity of the Setberg alkalic and olivine basalts to this univariant line is indicated by their composition, as shown by their co-ordinates in the basalt tetrahedron (Table 13).

The appearance of abundant plagioclase phenocrysts in the hawaiites, along with olivine and augite, is taken as evidence of the attainment by the Setberg alkalic basalt liquid of this univariant line. The subsequent precipitation of plagioclase is the main motivation of the course of the liquid along this line towards the quaternary invariant point (A), with the development of the quartz-normative mugearite and benmoreite magmas.

Fractionation of the alkalic series has chiefly taken place at low pressures. The expansion of the En-volume with

pressure, at the expense of olivine (Figures 61 and 62), would have resulted in the precipitation of olivine and orthopyroxene in the alkalic basalt magma at depth, leading to a trend of strong silica-undersaturation. There is no evidence of such a trend and we favour the ascent of an alkalic basalt liquid, whose composition is in or near the critical plane, to a position relatively high in the Iceland crust (<5 km), and the subsequent fractionation of the Setberg alkalic series in a shallow level reservoir.

Fig. 62: A diagrammatic view of the possible phase relations in the system Di-Ol-Pl-SiO_2 at 20 kb pressure. Symbols as in Figure 61.

Notable features of this system at high pressures are: the expansion of the orthopyroxene phase-volume at the expense of olivine, to intersect the critical plane of silica undersaturation (Di-Pl-Ol); the congruent melting of compositions on the Di-En join, which now appears as a thermal barrier between silica-saturated and undersaturated parts of the tetrahedron (forsterite-rich liquids cannot fractionate across this plane towards silica-saturated compositions). Point c is a reaction point at 1 atm. where the reaction is ol+liq=di+en (Figure 61), but at 20 kb the probable reaction is en+liq=fo+di (Kushiro, 1969), sending the liquid toward the Fo-Di join; B is a quaternary invariant point (pl-di-en-qz-liq).

Phase-equilibrium data for this quaternary system at 20 kb are still scanty. The following sources were used for the construction of this figure: the system forsterite-diopside-silica, Kushiro (1969); the system diopside-albite-anorthite, Lindsley and Emslie (1968); the system forsterite-albite-silica, Kushiro (1968); the system forsterite-anorthite-silica, Kushiro (1968).

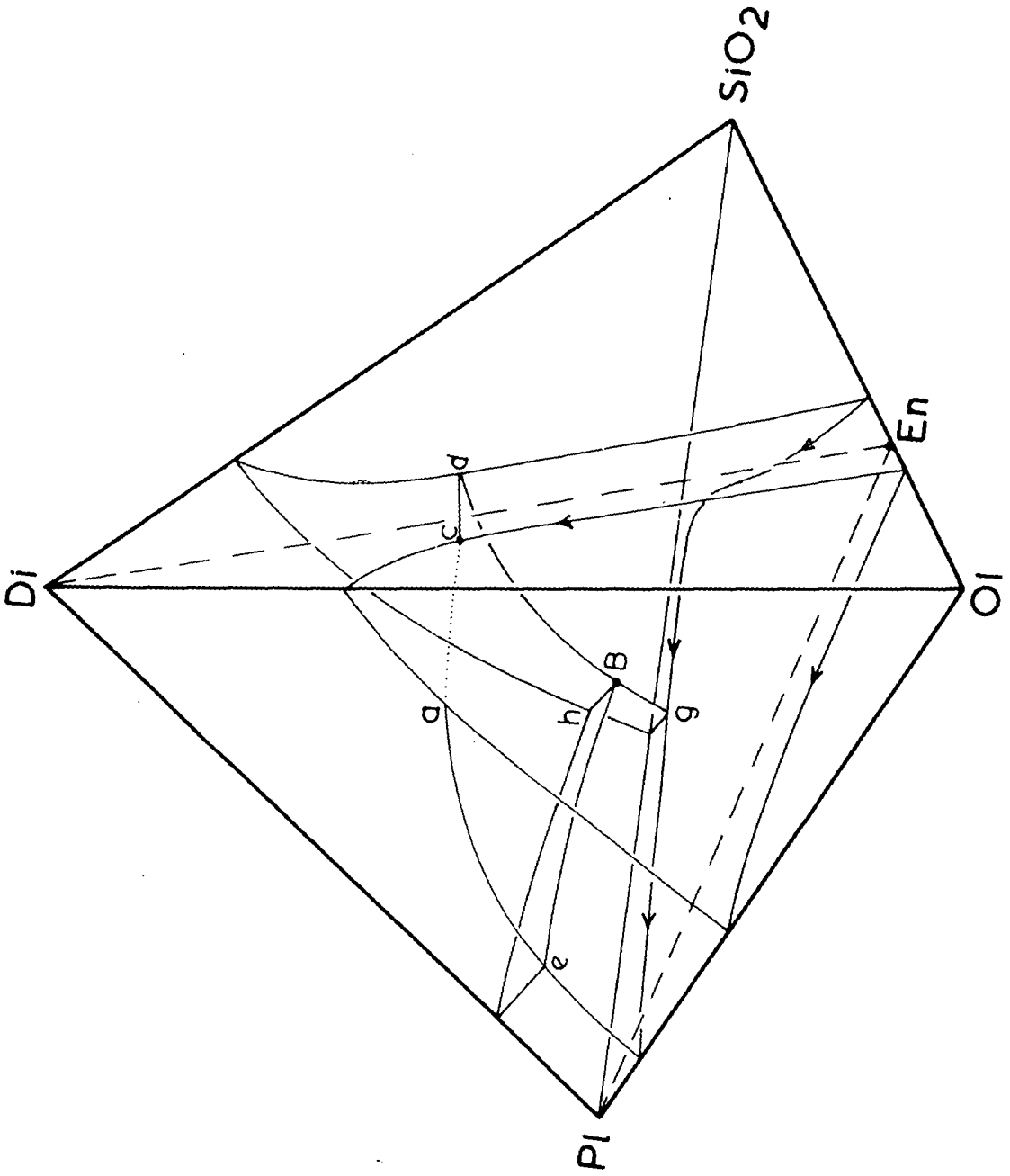
SiO2
En
Di
Ol
Pl
d
c
B
a
h
g
e

The abundance of highly zoned, magnesian olivine phenocrysts in the alkalic basalts was commented upon above (p.137) and is taken as evidence of the differentiated nature of these rocks, in spite of their "primary" role with respect to the Setberg alkalic series as a whole. O'Hara (1968) has emphasized that erupted magmas are not in general primary liquids, but must have undergone continuous fractionation, at least of olivine, during their ascent. We favour an origin of the Setberg alkalic basalts in a picritic liquid, such as would be produced by partial melting of a lherzolitic mantle (O'Hara, op.cit.). The magnesian phenocrysts of these lavas are an indirect evidence of a parental melt whose composition was within the olivine volume in the basalt tetrahedron at greater depth (Figure 62). Polybaric fractionation during ascent of such a liquid, combined with the expansion of the primary phase volume of olivine with decrease in pressure, must result in continuous precipitation of magnesian olivine, as the liquid strives to attain a cotectic state.

Variations in the polybaric and polythermal crystallization paths of ascending liquids, irrespective of composition of the original melt, can lead to a variety of compositions, diverse enough to account for the degree of non-conformity among erupted "primary" magmas in a volcanic region. In our view the diversity of chemical composition of tholeiitic

basalts among volcanic centres in the central volcanic zone of Iceland (Sigvaldason, 1969), or indeed in any large volcanic province, is to be expected in view of the complex events and many vicissitudes which lie in the paths of basaltic liquids, from mantle source to the earth's surface, and does not necessitate reference to other more obscure processes, such as differential batch melting.

TABLE 13

CO-ORDINATES OF AVERAGE SETBERG BASALTS IN THE SYSTEM PLAGIOCLASE-QUARTZ-OLIVINE-DIOPSIDE (wt. %)

	Plagioclase	Quartz	Olivine	Diopside	Represented by system (%)
Olivine tholeiite, Centre 1	58.5	4.4	16.1	21.0	88.77
Tholeiite, Centre 1	59.8	7.3	11.3	21.6	82.99
Olivine tholeiite, Centre 2	59.4	2.9	14.6	23.1	86.27
Tholeiite, Centre 2	60.9	5.2	13.3	20.6	81.47
Alkalic basalt	57.7	*	20.3	22.0	87.87
Olivine basalt	63.0	0	15.6	21.4	86.15
Hawaiite	67.6	1.9	14.4	16.1	82.03

*Contains 1% normative nepheline

KEY TO TABLE 14

List of analysed specimens and sample localities

104 Rhyolite, flow-banded, from Villingadalur, Setberg area, Centre 1.

107 Gabbro from Kolgrafamuli intrusion, Setberg area, Centre 1.

109 Dolerite cone sheet, Eyrarfjall, Setberg area, Centre 1.

110 Rhyolite, flow-banded, Villingadalur, Setberg area, Centre 1.

111 Ankaramitic basalt from palagonite breccia, Baelisdalur, alkalic series.

112 Rhyolite, Villingadalur, Setberg area, Centre 1.

114 Ankaramitic basalt, Steinahlidarhaus plug, Setberg area, alkalic series.

115 Gabbroic cone sheet, Eyrarfjall, Setberg area, Centre 1.

121 Olivine basalt, Eyraroddi, Setberg area, Tertiary.

202 Olivine basalt, Klakkur, Setberg alkalic series.

203 Basaltic dyke, altered, Grundarmon, Setberg area, Centre 2.

207 Hawaiite, Klakkur, Setberg alkalic series.

210 Dolerite sheet, Hop, Kolgrafir, Setberg Centre 1.

211 Composite plug (rhyodacite), Gjafakollur, Setberg Centre 2.

212 Tholeiite basalt, Grafarnes, Setberg Centre 1.

213 Cumulate gabbro xenolith, (Tertiary?), Axarhamar, Setberg Centre 1.

215 Granophyric cone sheet, Berserkseyri, Setberg Centre 1.

216 Dolerite cone sheet, Berserkseyri, Setberg Centre 1.

217 Granophyre, Laxa intrusion, Frodarhreppur, Snaefellsnes Tertiary.

218 Andesine-gabbro, Lysuskard intrusion, Setberg Centre 2.

220 Felsite, Lambahnukur, Setberg Centre 1.

221 Granophyre, Lysuskard acid cone sheet, Setberg Centre 2.

222 Felsite cone sheet, Eyrarbotn, Setberg Centre 2.

223 Felsite, chilled marginal facies of Lysuskard cone sheet, Centre 2.

226 Granophyre, Lysuskard cone sheet, Setberg Centre 2.

227 Granophyre, Lysuskard cone sheet, Setberg Centre 2, Hvitihnukur.

228 Granophyre, Lysuskard cone sheet, Setberg Centre 2, Svartihnukur.

229 Granophyre, Lysuskard cone sheet, Setberg Centre 2, Hvitihnukur.

230 Gabbro, Gunnungsfell, Setberg Centre 1.

231 Gabbro, Holahlid, Setberg Centre 1.

233 Gabbro, Kolgarafamuli, Setberg Centre 1.

234 Gabbro contact facies, Kolgrafamuli intrusion, Berserkseyri.

235 Gabbro, Kolgrafamuli, Setberg Centre 1.

236 Gabbro, Kolgrafamuli, Setberg Centre 1.

238 Gabbro, Kolgrafamuli, Setberg Centre 1.

242 Gabbro, Tradir, Stadarsveit, Setberg Centre 2.

248 Biotite-gabbro, Lysuskard, Setberg Centre 2.

249 Biotite-gabbro, Lysuskard, Setberg Centre 2.

251 Diorite, Smjorhnukur, Lysuskard intrusion, Setberg Centre 2.

252 Gabbro, Stekkholl, Stadarsveit, Setberg Centre 2.

254 Cumulate gabbro, Thorgeirsfell, Setberg Centre 2.

255 Rhyodacite cone sheet, Gerdishamrar, Setberg Centre 1.

257 Rhyolite dyke, Kalfa, Snaefellsnes Tertiary.

258 Rhyolite lava, Holtsa, Snaefellsnes Tertiary.

259 Rhyodacite facies, Lysuskard cone sheet, Tindar outcrop, Setberg Centre 2.

260 Rhyodacite facies, Lysuskard cone sheet, Tindar outcrop, Setberg Centre 2.

261 Rhyodacite facies, Lysuskard cone sheet, Tindar outcrop, Setberg Centre 2.

262 Felsite, Hrafnagil, Setberg Centre 1.

263 Rhyolite dyke, Lysuskard, Centre 2.

264 Rhyolite dyke, Slitandastadir, Tertiary of Snaefellsnes.

266 Felsite cone sheet, Berserkjadalur, Setberg Centre 1.

267 Basic component of composite dyke, Berserkjadalur, Setberg Centre 1.

268 Acid component of composite dyke.

269 Rhyolitic cone sheet, Grundarmon, Setberg Centre 1.

272 Obsidian cone sheet margin, Kolgrafamuli, Setberg Centre 1.

273 Basaltic dyke, Grundarmon, Setberg Centre 1.

275 Basaltic andesite cone sheet, Hamrar, Setberg Centre 1.

277 Tholeiite sill, Grundarmon, Setberg Centre 2.

278 Basalt sill, Kalfa, Stadarsveit, Snaefellsnes Quaternary, Non-porph. facies.

279 Basalt sill, Kalfa, Stadarsveit, Snaefellsnes Quaternary, Highly porphyritic lower facies.

280 Dolerite plug, Arnarholl, Snaefellsnes Tertiary.

281 Dolerite dyke, Glaumbaer, Stadarsveit, Snaefellsnes Tertiary.

282 Dolerite dyke, Lysuskard, Setberg Centre 1.

283 Gabbro xenolith, Kirkjuholl, Setberg Centre 1.

286 Olivine tholeiite, Arnarhyrna, Setberg Centre 1.

290 Olivine tholeiite (hypersthene-bearing), Straumhlid, Setberg Centre 1.

291 Tholeiite, Arnardalur, Setberg Centre 1.

292 Basaltic dyke, Grundarmon, Setberg Centre 1.

295 Obsidian from Midhyrna dome, Quaternary, Centre 2?

301 Olivine tholeiite, Grjota, Setberg Centre 1.

302 Granophyre cone sheet, Grjota, Setberg Centre 1.

303 Rhyodacitic cone sheet, Lambahnukur, Setberg Centre 1.

304 Rhyodacitic cone sheet, Skalardalur, Setberg Centre 1.

306 Icelandite, Grundarmon, Setberg Centre 2. Basal lava.

307 Icelandite, Grundarmon, Setberg Centre 2. Second lava.

308 Plagioclase-phyric basalt, Grundarmon, Setberg Centre 2.

309 Tholeiite dyke, Grundarmon, Setberg Centre 2.

311 Sanidine-bearing tuff (acid), Grundarmon, Setberg Centre 2.

316 Granite xenolith, Grenjadalur agglomerate, Setberg Centre 2.

318 Olivine basalt, Axarhamar, Setberg alkalic series.

319 Olivine basalt, Axarhamar, Setberg alkalic series.

320 Hawaiite, Grundarbotn, Setberg alkalic series.

321 Hawaiite, Grundarbotn, Setberg alkalic series.

322 Diorite boulder, Grundarmon conglomerate, Setberg Centre 2.

323 Rhyolite, Grundarmon, Setberg Centre 1.

325 Spherulitic rhyolite, Drapuhlidarfjall, Snaefellsnes Quaternary.

326 Rhyolite, Grundarbotn, Setberg Centre 1.

331 Peralkaline obsidian dyke, north of Lysuskard, Setberg Centre 2.

336 Basaltic andesite, Grundarmon, Setberg Centre 2.

337 Benmoreite, Torfahlid, Stadarsveit, Setberg alkalic series.

338 Basaltic andesite tuff, Grundarmon, Setberg Centre 2.

339 Olivine tholeiite, Grundarmon, Setberg Centre 2.

340 Basaltic andesite, Grundarmon, Setberg Centre 2.

341 Basaltic andesite breccia, Grundarmon, Setberg Centre 2.

342 Rhyodacite lava, Gjafakollur, Setberg Centre 2.

343 Mugearite, Barnalaekur, Stadarsveit, Setberg alkalic series.

344 Alkalic basalt, porphyritic, Torfahlid, Setberg alkalic series.

345 Hawaiite, Grundarfoss, Setberg alkalic series.

346 Olivine tholeiite, Grundarargil, Setberg Centre 2.

347 Basaltic andesite, Arnardalur, Setberg Centre 2.

348 Hawaiite, Grundarfoss, Setberg alkalic series.

349 Olivine tholeiite (hypersthene), Tindar, Setberg Centre 2.

350 Mugearite, Tindar, Setberg alkalic series.

352 Basaltic andesite breccia, Arnardalur, Setberg Centre 2.

353 Tholeiite, Drapuhlidarfjall, Snaefellsnes Quaternary.

354 Icelandite, Drapuhlidarfjall, Snaefellsnes Quaternary.

355 Icelandite, Drapuhlidarfjall, Snaefellsnes Quaternary.

356 Mugearite, Laxardalur, Setberg alkalic series.

357 Mugearite, Laxardalur, Setberg alkalic series.

358 Basaltic andesite, Smjorhnukur, Setberg Centre 2.

359 Mugearite, Lysuhyrna, Setberg alkalic series.

360 Tholeiite, Grundarmon, Setberg Centre 2.

361 Basaltic andesite, Grundarmon, Setberg Centre 2.

362 Basaltic andesite, Grundarmon, Setberg Centre 2.

363 Icelandite, Bjarnarhafnarfjall, Setberg Centre 1.

364 Icelandite, Grundarmon, Setberg Centre 2.

365 Icelandite, Holahlid, Setberg Centre 2.

366 Tholeiite, Bjarnarhafnarfjall, Setberg Centre 2.

367 Icelandite, Smjorhnukur, Setberg Centre 2.

368 Olivine basalt, Stadarsveit, Barnalaekur, Setberg alkalic series.

369 Mugearite, Midhyrna, Setberg alkalic series.

370 Mugearite, Midhyrna, Setberg alkalic series.

371 Olivine basalt, Kirkjuholl, Setberg alkalic series.

372 Alkalic basalt, Grisholsa, Snaefellsnes alkalic series, Quaternary.

373 Olivine basalt, Blafeldarkulur, Setberg alkalic series.

374 Basaltic sill, Kalfa, Snaefellsnes Quaternary.

375 Mugearite, Laxardalur, Setberg alkalic series.

376 Benmoreite, Stadarsveit, Setberg alkalic series.

377 Olivine-phyric basalt, Torfahlid, Setberg alkalic series.

378 Basaltic palagonite, Axarhamar, Setberg alkalic series.

379 Hawaiite, Lysuskard, Setberg alkalic series.

380 Mugearite, Midhyrna, Setberg alkalic series.

381 Mugearite, Lysuskard, Setberg alkalic series.

382 Olivine basalt, Blafeldarkulur, Setberg alkalic series.

383 Alkalic basalt, Blafeldarkulur, Setberg alkalic series.

384 Alkalic basalt, Blafeldarkulur, Setberg alkalic series.

385 Alkalic basalt, Barnalaekur, Setberg alkalic series.

387 Hawaiite, Klakkur, Stadarsveit, Setberg alkalic series.

389 Alkalic basalt, Lysuskard, Setberg alkalic series.

390 Plagioclase-phyric tholeiite, Gjafakollur, Setberg Centre 2.

391 Olivine basalt, Thorgeirsfell, Setberg alkalic series.

392 Hawaiite, Stadarsveit, Setberg alkalic series.

393 Porphyritic basalt, Grundarmon, Setberg Centre 2.

395 Basaltic palagonite, Klakkur, Setberg alkalic series.

396 Ankaramite, Steinahlidarhaus, Setberg alkalic series.

397 Hawaiite, Helgrindur crater, Setberg alkalic series.

398 Olivine basalt, Helgrindur dyke, Setberg alkalic series.

399 Alkalic basalt, Melrakkaey, Setberg alkalic series.

400 Alkalic basalt, Laxardalur, Setberg alkalic series.

401 Hawaiite, Grafarnes, Setberg alkalic series.

402 Alkalic basalt, Blafeldarkulur, Setberg alkalic series.

403 Hawaiite, Grundarbotn, (plug), Setberg alkalic series.

404 Hawaiite, Grundarbotn, Setberg alkalic series.

405 Mugearite, Eldhamrar, Setberg alkalic series.

406 Benmoreite, Midhyrna, Setberg alkalic series.

407 Rhyolite from Recent dome, Maelifell, Snaefellsnes Quaternary.

409 Porphyritic basalt, Grundarmon, Setberg Centre 2.

410 Hawaiite, Thorgeirsfell, Setberg alkalic series.

411 Olivine tholeiite, Kolbeinsey Island, Iceland Sea.

412 Basaltic andesite, Hraunsfjordur, Setberg Centre 1.

413 Basaltic andesite, Bjarnarhafnarfjall, Setberg Centre 1.

414 Rhyolite, Drapuhlidarfjall, Snaefellsnes Quaternary.

416 Mugearite, Lysuskard, Setberg alkalic series.

417 Gabbro, Thorgeirsfell, Setberg Centre 2.

418 Obsidian, Lodmundur, Kerlingafjoll, Central Iceland Quaternary.

419 Rhyolite, Fitjaskogar, Thjorsa, Central Iceland Quaternary.

420 Basaltic andesite, Fitjaskogar, Thjorsa, Central Iceland Quaternary.

421 Tholeiite, Fitjaskogar, Thjorsa, Central Iceland Quaternary.

422 Rhyolite, Fitjaskogar, Thjorsa, Central Iceland Quaternary.

423 Obsidian, Hrafntinnusker, southern Iceland, Recent.

424 Obsidian, Domadalshraun, southern Iceland, Recent.

425 Basalt, Domadalshraun (composite lava), southern Iceland, Recent.

426 Obsidian, Hrafntinnuhraun, southern Iceland, Recent.

427 Alkalic basalt, Lambafitarhraun, Recent lava, southern Iceland.

428 Basaltic andesite lava, Hekla eruption 1389/90.

429 Basaltic andesite lava, Hekla eruption 1300, Sudurhraun.

432 Amygdaloidal greenstone, Tradir, Setberg metamorphic aureole.

433 Amygdaloidal greenstone, Lysuskard, Setberg metamorphic aureole.

434 Rhyolite, Kotlukollar cliff, Myrdalsjokull, southern Iceland.

435 Obsidian, Kotlukollar cliff, Myrdalsjokull, southern Iceland.

436 Obsidian, Huldufjoll, Myrdalsjokull, southern Iceland.

437 Rhyolite, Huldufjoll, Myrdalsjokull, southern Iceland.

438 Obsidian, Huldufjoll, Myrdalsjokull, southern Iceland.

439 Rhyolitic tuff, Huldufjoll, Myrdalsjokull, southern Iceland.

440 Basaltic andesite, Sandfell, southern Iceland, Quaternary.

441 Rhyolitic tuff, Nunatak, Myrdalsjokull, southern Iceland.

442 Basaltic andesite, Sandfell, southern Iceland.

443 Rhyolitic ignimbrite, Thorsmork, southern Iceland.

444 Benmoreite, Hellnar, Snaefellsnes Quaternary.

445 Pitchstone, Drapuhlidarfjall, Snaefellsnes Quaternary.

446 Alkalic basalt, Thorgeirsfell, Setberg alkalic series.

447 Gabbro, Thorgeirsfell, Setberg Centre 2.

448 Olivine basalt lava, Berserkjahraun, Snaefellsnes alkalic series.

449 Rhyolite, Leirdalsheidi, Flateyjardalur, North Iceland Tertiary.

450 Obsidian, Blahnukur, Landmannalaugar, southern Iceland.

451 Rhyolite, Blahnukur, Landmannalaugar, southern Iceland, Quaternary.

452 Obsidian dyke, Blahnukur, Landmannalaugar, southern Iceland,

453 Rhyolite, Blahnukur, Landmannalaugar, southern Iceland.

454 Rhyolite, Blahnukur, Landmannalaugar, southern Iceland.

455 Rhyolite, Blahnukur, Landmannalaugar, southern Iceland.

456 Rhyolite, Brandsgil, Landmannalaugar, southern Iceland.

457 Obsidian lava, Laugahraun, Landmannalaugar, southern Iceland, Recent.

458 Acid tuff, Graenagil, Landmannalaugar, southern Iceland, Quaternary.

459 Basaltic pillow lava, Landmannalaugar, southern Iceland, Quaternary.

460 Rhyolite, Brennisteinsalda, Landmannalaugar, southern Iceland, Quaternary.

461 Rhyolite tuff, Brennisteinsalda, Landmannalaugar, southern Iceland, Quaternary.

462 Obsidian lava, Laugahraun, Landmannalaugar, southern Iceland, Recent.

463 Rhyolite, Brandsgil, Landmannalaugar, southern Iceland, Quaternary.

464 Rhyolite tuff, Graenagil, Landmannalaugar, southern Iceland, Quaternary.

465 Rhyodacite lava, Sudurnamshraun, southern Iceland, Recent.

466 Basaltic andesite lava, Nordurnamshraun, southern Iceland, Recent.

467 Peralkaline rhyolite, Langasata, southern Iceland, Quaternary.

468 Tholeiitic basalt, Burfellshals, southern Iceland, Quaternary.

469 Basalt cone sheet, Hrafnagil, Setberg Centre 2.

470 Trachytic lava, Eyjafjallajokull, southern Iceland, Quaternary.

471 Trachytic lava, Eyjafjallajokull, southern Iceland, Quaternary.

472 Benmoreite, Eyjafjallajokull, southern Iceland, Quaternary.

473 Olivine basalt, Dyrholaey, southern Iceland, late-Quaternary.

474 Pitchstone, Barnafoss, western Iceland, ?Quaternary.

475 Rhyodacite cone sheet, Kolgrafir, Setberg Centre 1.

476 Icelandite, Grundarmon, Setberg Centre 2.

477 Obsidian, Ulfarsfellsa, Snaefellsnes Tertiary.

478 Rhyolite from plug, Ulfarsfellsa, Snaefellsnes Quaternary.

479 Mugearite, Sandfell, Ljosufjoll alkalic series, Quaternary.

480 Olivine basalt, Sandfell, Ljosufjoll alkalic series, Quaternary.

481 Rhyolite, nr. Sydri-Raudakula, Ljosufjoll alkalic series.

482 Hawaiite, Kattarhryggur, Ljosufjoll alkalic series.

483 Olivine basalt, Kattarhryggur, Ljosufjoll alkalic series.

484 Alkalic rhyolite, Ljosufjoll alkalic series.

485 Olivine basalt, Ljosufjoll alkalic series.

486 Alkalic rhyolite, Ljosufjoll alkalic series.

487 Mugearite, Ljosufjoll alkalic series.

488 Rhyolite, Botna-Skyrtunna, Ljosufjoll alkalic series.

489 Rhyolite, Botna-Skyrtunna, Ljosufjoll alkalic series.

490 Alkalic basalt, Ljosufjoll alkalic series.

491 Obsidian, Ljosufjoll alkalic series.

492 Icelandite plug, Ulfarsfellsa, Snaefellsnes Tertiary.

493 Obsidian, Ulfarsfellsa, Snaefellsnes Tertiary.

494 Icelandite, Orlygsstadahnukar, Snaefellsnes Tertiary.

495 Olivine basalt lava, Kirkjufell, Snaefellsnes Quaternary.

496 Plagioclase-phyric basalt, Kirkjufell, Snaefellsnes Quaternary.

497 Tholeiite dyke, Kirkjufell, Snaefellsnes Tertiary.

498 Hawaiite, Kverna, Setberg alkalic series.

499 Hawaiite, Hrokshnukur, Setberg alkalic series.

500 Mugearite, Hrokshnukur, Setberg alkalic series.

501 Basaltic andesite plug, Arnardalur, Setberg Centre 2.

502 Olivine tholeiite, Arnardalur, Setberg Centre 2.

503 Mugearite, Arnardalsskard, Setberg alkalic series.

504 Benmoreite, Arnardalsskard, Setberg alkalic series.

505A Obsidian margin, intrusion in Arnardalsskard, Setberg alkalic series.

505B Felsite, intrusion in Arnardalsskard, Setberg alkalic series.

506 Icelandite, Smjorhnukur, Setberg Centre 2.

507 Mugearite, Hroksdalur, Setberg alkalic series.

508 Obsidian dyke, Kalfa, Snaefellsnes Tertiary.

509 Felsite cone sheet (composite), Kolgrafir, Setberg Centre 1.

510 Obsidian dyke, Kolgrafamuli, Setberg Centre 1.

517 Olivine basalt lava, Blafeldarhraun, Snaefellsnes, Recent.

518 Olivine basalt lava, Hraunsmulahraun, Snaefellsnes, Recent.

REFERENCES

Al-Rawi, Y., and Carmichael, I.S.E., 1967. Natural fusion of granite. Amer.Min. 52, p.1806-1814.

Anderson, O., 1915. The system anorthite-forsterite-silica. Am.J.Sci. 39, p.407-454.

Aoki, K.I., 1966. Petrography and petrochemistry of latest Pliocene olivine-tholeiites of Taos area, northern New Mexico, U.S.A. Contr. Mineral. and Petrol. 14, p.190-203.

Askelsson, J., 1938. Quartärgeologische Studien auf Island. Meddel. fra Dansk Geol.Foren., 9, p.300-319.

—— 1955. Thar var baerinn, sem nu er borgin. Natturufr. 25, p.122-132.

Bailey, D.K. and Schairer, J.F., 1964. Feldspar-liquid equilibria in peralkaline liquids - the orthoclase effect. Am.J.Sci. 262, p.1198-1206.

Baker, I., 1968. Intermediate oceanic volcanic rocks and the "Daly gap". Earth Planet. Sci.Letters 4, p.103-106.

—— 1969. Petrology of the volcanic rocks of Saint Helena Island, South Atlantic. Geol.Soc.Amer.Bull. 80, p.1283-1310.

Baker, P.E., Gass, I.G., Harris, P.G., and LeMaitre, R.W., 1964. The volcanological report of the Royal Society expedition to Tristan da Cunha, 1962. Roy.Soc.London Philos. Trans., Ser. A, no.256, p.439-578.

Bandy, M.C., 1937. Geology and petrology of Easter Island. Geol.Soc.Amer.Bull. 48, p.1589-1610.

Barth, T.F.W., 1962. Theoretical petrology. New York: Wiley & Sons, 416 pp.

Bemmelen, R.W. van, and Rutten, M.G., 1955. Tablemountains of northern Iceland. Leiden, 217 pp.

Berlin, R. and Henderson, C.M.B., 1968. A reinterpretation of Sr and Ca fractionation trends in plagioclases from basic rocks. Earth Planet.Sci. Letters, 4, p.79-83.

Bjornsson, S. (ed.), 1967. Iceland and Mid-Ocean Ridges, Report of a Symposium. Visindafelag Islendinga, 38, Reykjavik, 208 pp.

Blake, D.H., Elwell, R.W.D., Gibson, I., Skelhorn, R.R. and Walker, G.P.L., 1965. Some relationships resulting from the intimate association of acid and basic magmas. Quart. J.Geol.Soc.Lond., 121, p.31-50.

Bodvarsson, G. and Walker, G.P.L., 1964. Crustal drift in Iceland. Geophys.J.Roy.Astron.Soc. 8, p.285-300.

Bowen, N.L., 1928. The evolution of the igneous rocks. Princeton: Princeton Univ.Press, 332 pp.

—— 1945. Phase equilibria bearing on the origin and differentiation of alkaline rocks. Am.J.Sci., Daly vol. 243A, p.75-89.

Boyd, F.R. and England, J.L., 1961. Melting of silicates at high pressures. Carnegie Inst.Wash. Yearbook 60, p.116-125.

—— and England, J.L., 1963. Effect of pressure on the melting of diopside, $CaMgSi_2O_6$, and albite, $NaAlSi_3O_8$, in the range up to 50 kilobars. Jour.Geophys.Res. 68, p.311-323.

Brooks, K.C., 1968. On the interpretation of trends in element ratios in differentiated igneous rocks, with particular reference to strontium and calcium. Chem.Geol., 3, p.15-20.

Brown, G.M., 1957. Pyroxenes from the early and middle stages of fractionation of the Skaergaard intrusion, east Greenland. Miner.Mag. 31, p.511-543.

—— 1968. Mineralogy of basaltic rocks. In: Basalts, The Poldervaart treatise on rocks of basaltic composition, vol. 1, p.103-162. New York: Wiley & Sons.

—— and Vincent, E.A., 1963. Pyroxenes from the late stages of fractionation of the Skaergaard intrusion, east Greenland. J. Petrology 4, p.175-197.

Burri, C., Parker, R.L. and Wenk, E., 1965. Die optische Orientierung der Plagioklase. Unterlagen und Diagramme zur Plagioklasbestimmung nach der Drehtischmethode. Basel: Birkhäuser.

Cann, J.R., 1968. Bimodal distribution of rocks from volcanic islands. Earth Planet.Sci. Letters, 4, p.479-480.

Cargill, H.K., Hawkes, L. and Ledeboer, J.A., 1928. The major intrusions of south-east Iceland. Quart.J.Geol.Soc.London, 84, p.505-39.

Carmichael, I.S.E., 1960a. The pyroxenes and olivines from some Tertiary acid glasses. J. Petrology, 1, p.309-336.

—— 1960b. The feldspar phenocrysts of some Tertiary acid glasses. Mineralog.Mag., 32, p.587-608.

—— 1962. A note on the composition of some natural acid glasses. Geol.Mag., 99, p.253-264.

—— 1963. Crystallization of feldspar in volcanic acid liquids. Quart.J.Geol.Soc.London, 119, p.95-131.

—— 1964. The petrology of Thingmuli, a Tertiary volcano in eastern Iceland. J. Petrology, 5, p.435-460.

—— 1967. The mineralogy of Thingmuli, a Tertiary volcano in eastern Iceland. Amer.Min. 52, p.1815-1841.

—— 1967. The iron-titanium oxides of salic volcanic rocks and their associated ferromagnesian silicates. Contr. Mineral.Petrol. 14, p.36-64.

—— and McDonald, A., 1961. The geochemistry of some natural acid glasses from the North Atlantic Tertiary volcanic province. Geochim. et Cosmochim.Acta, 25, p.189-222.

—— and McKenzie, W.S., 1963. Feldspar-liquid equilibria in pantellerites: an experimental study. Am.J.Sci. 261, p.382-396.

Chayes, F., 1963. Relative abundance of intermediate members of the oceanic basalt-trachyte association. J. Geophys. Res., 68, p.1519-1534.

Cohen, L.H., Ito, K. and Kennedy, G.C., 1967. Melting and phase relations in an anhydrous basalt to 40 kilobars. Am.J.Sci. 265, p.475-518.

Coombs, D.S., 1963. Trends and affinities of basaltic magmas and pyroxenes as illustrated on the diopside-olivine-silica diagram. Min.Soc.America Special Paper 1, p.227-250.

Deer, W.A., Howie, R.A., and Zussman, J., 1963. Rock-forming minerals, Vol. 2, London: Longmans.

Dietrich, R.V., 1968. Behaviour of zirconium in certain artificial magmas under diverse P-T conditions, Lithos, 1, p.20-29.

Doell, R.R., Dalrymple, G.B. and Cox, A., 1966. Geomagnetic polarity epochs - Sierra Nevada data. J.Geophys.Res., 71, p.531-541.

Einarsson, Th., 1968. Jardfraedi, saga bergs og lands. Reykjavik: Mal og Menning, 335 pp.

Engel, A.E.J., Engel, C.G. and Havens, R.G., 1965. Chemical characteristics of oceanic basalts and the Upper Mantle. Geol.Soc.Amer.Bull., 76, p.719-734.

Ewart, A., Taylor, S.R. and Capp, A., 1968. Geochemistry of the pantellerites of Mayor Island, New Zealand. Contr. Mineral. and Petrol. 17, p.116-140.

Field, J.E., 1964. Fracture of solids. Times Science Review, 51, p.5-9.

Friedrich, W., 1966. Zur Geologie von Brjanslaekur (Nordwest-Island) unter besonderer Berücksichtigung der fossilen Flora. Sonderveröff. Geolog.Inst. der Universität Köln, 10, 108 pp.

Flower, M.F.J., 1969. Phlogopite from Jan Mayen Island (North Atlantic). Earth Planet.Sci. Letters, 6, p.461-466.

Gale, N.H., Moorbath, S., Simons, J. and Walker, G.P.L., 1966. K-Ar ages of acid intrusive rocks from Iceland. Earth Planet.Sci. Letters, 1, p.284.

Gast, P.W., 1968. Trace element fractionation and the origin of tholeiitic and alkaline magma types. Geochim. et Cosmochim. Acta. 32, p.1057-1086.

Gibson, I., 1970. Origin of some pitchstones from Iceland. (in press).

—— and Walker, G.P.L., 1963. Some composite rhyolite/basalt lavas and related composite dykes in eastern Iceland. Proc.Geol.Ass.London, 74, p.301-318.

Green, D.C., 1968. Further evidence for a continuum of basaltic compositions from southeast Queensland. J.Geol. Soc.Aust., 15, p.159.

Green, D.H. and Ringwood, A.E., 1964. Fractionation of basalt magmas at high pressures. Nature, 201, p.1276-1279.

—— and Ringwood, A.E., 1967. The genesis of basaltic magmas. Contr. Mineral. and Petrol. 15, p.103-190.

Green, T.H., and Ringwood, A.E., 1968. Genesis of the calc-alkaline igneous rock suite. Contr. Mineral. and Petrol. 18, p.105-162.

Griffin, W.L. and Murthy, V.R., 1969. Distribution of K, Rb, Sr and Ba in some minerals relevant to basalt genesis. Geochim. et Cosmochim. Acta, 33, p.1389-1414.

Guppy, E.M. and Hawkes, L., 1925. A composite dyke from eastern Iceland. Quart.J.Geol.Soc.Lond., 81, p.325-343.

Hamilton, D.L. and Anderson, G.M., 1967. Effects of water and oxygen pressures on the crystallization of basaltic magmas. In: Basalts, the Poldervaart treatise on rocks of basaltic composition. New York: Wiley, p.445-482.

Harris, P.G., Kennedy, W.Q. and Scarfe, C.M., 1969. Volcanism versus plutonism - the effect of chemical composition. Liverpool Geol.Soc. Symposium on "Mechanism of Igneous Intrusion".

Heier, K.S., Chappell, B.W., Arriens, P.A and Morgan, J.W., 1966. The geochemistry of four Icelandic basalts. Norsk Geol.Tidsskr., 46, p.427-437.

Holland, J.G. and Brindle, D.W., 1966. A self-consistent mass absorption correction for silicate analysis by X-ray fluorescence. Spectrochim.Acta, 22, p.2083-2093.

Holmes, A., 1918. The basaltic rocks of the Arctic region. Min.Mag. 85, p.180-223.

Hubbard, N.J., 1969. A chemical comparison of oceanic ridge, Hawaiian tholeiitic and Hawaiian alkalic basalts. Earth Planet.Sci. Letters, 5, p.346-352.

Hytönen, K. and Schairer, J.F., 1961. The plane enstatite-anorthite-diopside and its relation to basalts. Carnegie Inst.Wash. Yearbook 60, p.125-141.

Jackson, E.D., 1961. Primary textures and mineral associations in the Ultramafic Zone of the Stillwater Complex, Montana. U.S.Geol.Surv. Prof. Paper, 358, p.1-106.

Jakobsson, S., 1968. The geology and petrology of the Vestmann Islands - a preliminary report. In: Surtsey Research Progress Report IV, Reykjavik: Surtsey Research Society, p.113-131.

Jeffreys, H., 1929. The earth: its origin, history and physical constitution. Cambridge: Univ.Press. 420 pp.

Joplin, G.A., 1964. A petrography of Australian igneous rocks. Sydney: Angus and Robertson. 210 pp.

Kracek, F.C. and Neuvonen, K.J., 1952. Thermochemistry of the plagioclase and alkali feldspars. Amer.Journ.Sci. Bowen vol., p.293.

Kuno, H., 1968. Differentiation of basalt magmas. In: Basalts, the Poldervaart treatise on rocks of basaltic composition, vol. 2. New York: Wiley & Sons, 862 pp.

Kushiro, I., 1964. The system diopside-forsterite-enstatite at 20 kb. Carnegie Inst.Wash. Yearbook 63, p.101-108.

—— 1965. The liquidus relations in the systems forsterite-$CaAl_2SiO_6$-silica and forsterite-nepheline-silica at high pressures. Carnegie Inst.Wash. Yearbook 64, p.103-109.

—— 1968. Melting of a peridotite at high pressures and high water pressures. J.Geophys.Res. 73, p.6023-6029.

—— 1969. The system forsterite-diopside-silica with and without water at high pressures. Amer.Jour.Sci. 267-A, p.269-294.

—— and Schairer, J.F., 1963. New data on the system diopside-forsterite-silica. Carnegie Inst.Wash. Yearbook 62, p.95-103.

Lindsley, D.H. and Emslie, R.F., 1968. Effect of pressure on the boundary curve in the system diopside-albite-anorthite. Carnegie Inst.Wash. Yearbook 66, p.479-480.

Lipman, P.W., 1969. Alkalic and tholeiitic basaltic volcanism related to the Rio Grande depression, Southern Colorado and Northern New Mexico. Geol.Soc.Amer.Bull. 80, p.1343-1354.

Luth, W.C., 1967. Studies in the system $KAlSiO_4$-Mg_2SiO_4-SiO_2-H_2O: Inferred phase relations and petrologic applications. J.Petrology, 8, p.372-416.

Macdonald, G.A., 1968. A contribution to the petrology of Tutuila, American Samoa. Geol.Rundsch. 57, p.821-837.

—— and Katsura, T., 1964. Chemical composition of Hawaiian lavas. J.Petrology, 5, p.82-133.

McBirney, A.R. and Gass, I.G., 1967. Relations of oceanic volcanic rocks to Mid-Oceanic Rises and heat flow. Earth Planet. Sci. Letters, 2, p.265-276.

—— and Williams, H., 1969. A new look at the classification of calderas. I.A.V.C.E.I. symposium report, Oxford, England.

McDougall, I. and Lovering, J.F., 1963. Fractionation of chromium, nickel, cobalt and copper in a differentiated dolerite-granophyre sequence at Red Hill, Tasmania. Journ.Geol.Soc.Austr., 10, p.325-338.

Moorbath, S. and Walker, G.P.L., 1965. Strontium isotope investigation of igneous rocks from Iceland. Nature, 207, p.837.

—— Sigurdsson, H. and Goodwin, R., 1968. K-Ar ages of the oldest exposed rocks in Iceland. Earth Planet. Sci. Letters, 4, p.197-205.

Muir, I.D. and Tilley, C.E., 1963. Contributions to the petrology of Hawaiian basalts II, The tholeiitic basalts of Mauna Loa and Kilauea. Amer.Jour.Sci. 261, p.111-128.

—— and Tilley, C.E., 1964. Basalts from the northern part of the rift zone of the Mid-Atlantic Ridge. J.Petrology, 5, p.409-34.

Nash, W.P., Carmichael, I.S.E. and Johnson, R.W., 1969.. The mineralogy and petrology of Mount Suswa, Kenya. J.Petrology, 10, p.409-39.

Nicholls, J and Carmichael, I.S.E., 1969. Peralkaline acid liquids: a petrological study. Contr. Mineral. and Petrol., 20, p.268-294.

Noe-Nygaard, A., 1956. Some liparite dykes from Raudhellar in Morsardalur, Iceland. Medd.Dansk.Geol.Forening, 13,2.

—— 1966. Chemical composition of tholeiitic basalts from the Wyville-Thompson ridge belt. Nature, 212, p.272-273.

Norrish, K. and Hutton, J.T., 1969. An accurate X-ray spectrographic method for the analysis of a wide range of geological samples. Geochim. et Cosmochim.Acta, 33, p.431-453.

O'Hara, M.J., 1968. The bearing of phase equilibria studies in synthetic and natural systems on the origin and evolution of basic and ultrabasic rocks. Earth-Sci.Rev. 4, p.69-133.

Oxburgh, E.R. and Turcotte, D.L., 1968. Mid-Ocean Ridges and geotherm distribution during mantle convection. J.Geophys.Res. 73, p.2643-2662.

Peacock, M.A., 1925. A contribution to the petrography of Iceland. Trans.Geol.Soc.Glasgow, 17, p.271-333.

—— 1926. Petrology of Iceland, I. The basic tuffs. Trans. Roy.Soc.Edinburgh, 55, p.51-76.

—— 1931. Classification of igneous rock series. J.Geol. 39, p.54-67.

Piwinskii, A.J. and Wyllie, P.J., 1968. Experimental studies of igneous rock series: A zoned pluton in the Wallowa batholith, Oregon. J.Geol. 76, p.205-234.

Poldervaart, A., 1964. Chemical definition of alkali basalt and tholeiite. Geol.Soc.America Bull., 75, p.229-232.

Richey, J.E. and Thomas, H.H., 1930. The geology of Ardnamurchan, North-West Mull and Coll. Mem.Geol.Surv. U.K..

Roberts, B. and Hawkins, T.R.W., 1965. The geology of the area around Nordkapp, Jan Mayen. Norsk Polarinst. Arbok, 1963, p.25-48.

Robson, G.R., 1956. The volcanic geology of Vestur-Skaftafellssysla. PhD thesis, Durham University, 259 pp.

—— and Spector, J., 1962. Crystal fractionation of the Skaergaard type in modern Icelandic magmas. Nature, 193, p.1277-8.

Rutten, M.G., 1964. Formation of a plateau basalt series (from the example of Iceland). Bull.Volc. 27, p.1-19.

Schairer, J.F., 1967. Phase equilibria at one atmosphere related to tholeiitic and alkali basalts. In: Researches in Geochemistry, vol. 2, p.568-592.

—— and Morimoto, N., 1958. Systems of rock-forming olivines, pyroxenes and feldspars. Carnegie Inst.Wash Yearbook 57, p.212-213.

—— and Morimoto, N., 1959. The system forsterite-diopside-silica-albite. Carnegie Inst.Wash. Yearbook 58, p.113-118.

—— Smith, J.R. and Chayes, F., 1956. Refractive indices of plagioclase glasses. Carnegie Inst.Wash. Yearbook 55, p.195.

—— and Yoder, H.S., Jr., 1960. The nature of residual liquids from crystallization, with data on the system nepheline-diopside-silica. Am.J.Sci. Bradley vol. 258A, p.273-283.

—— and Yoder, H.S., Jr., 1961. Crystallization in the system nepheline-forsterite-silica at one atmosphere. Carnegie Inst.Wash. Yearbook 60, p.141-144.

Sigurdsson, H., 1966. Geology of the Setberg area, Snaefellsnes, western Iceland. Greinar IV, 2. Visindafelag Islendinga, p. 53-125.

—— 1967. The Icelandic basalt plateau and the question of sial. A review. In: Iceland and Mid-Ocean Ridges, Soc.Sci.Islandica, Rit 38, p.32-49.

—— 1967. Dykes, fractures and folds in the basalt plateau of western Iceland, In: Iceland and Mid-Ocean Ridges, Soc.Sci.Islandica, Rit 38, p.162-169.

—— 1968. Petrology of acid xenoliths from Surtsey. Geol. Mag., 105, p.440-453.

—— and Brown, G.M., 1970. Enstatite-forsterite basalt from the northern extremity of the Mid-Atlantic Ridge. J.Petrology (in press).

Sigvaldason, G.E., 1963. Epidote and related minerals in two deep geothermal drill holes, Reykjavik and Hveragerdi, Iceland. U.S.Geol. Survey Prof. Paper 450-E, p.77-79.

—— 1969. Chemistry of basalts from the Icelandic rift zone. Contr.Mineral. and Petrol. 20, p.357-370.

Smith, J.R. and Yoder, H.S., Jr., 1956. Variations in X-ray powder diffraction patterns of plagioclase feldspars. Amer.Min., 41, p.632.

Stearns, H.T. and Macdonald, G.A., 1946. Geology and ground-water resources of the island of Hawaii. Hawaii Div. Hydrogr.Bull. 6, 177 pp.

Steinthorsson, S., 1966. Surtsey: petrography and chemistry. In: Surtsey Research Progress Report II, Reykjavik: Surtsey Research Society, p.77-86.

—— 1967. Tvaer nyjar C^{14}-aldursakvardanir a ðskulðgum ur Snaefellsjðkli. Natturufraed. 37, p.236-238. (in Icelandic).

Streckeisen, A.L., 1967. Classification and nomenclature of igneous rocks. N.Jb.Miner.Abh. 107, p.144-240.

Thorarinsson, S., 1958. The Öraefajðkull eruption of 1362, Acta Nat. Isl. II, 2, p.1-99.

—— 1967. Hekla and Katla. The share of acid and intermediate lava and tephra in the volcanic products through the geological history of Iceland. In: Iceland and Mid-Ocean Ridges, Soc.Sci.Islandica, Rit 38, p.190-199.

—— 1967. The eruptions of Hekla in historical times. A tephrochronological study. The eruption of Hekla 1947-48. I, p.1-170.

—— and Sigvaldason, G.E., 1962. The eruption of Askja, 1961, a preliminary report. Am.Jour.Sci. 260, p.641-651.

Thornton, C.P. and Tuttle, O.F., 1960. Chemistry of igneous rocks I: Differentiation Index. Am.Jour.Sci., 258, p.664-684.

Tilley, C.E. and Muir, I.D., 1964. Intermediate members of the oceanic basalt-trachyte association. Geol. Fðren. Forh. 85, p.434-443.

—— Yoder, H.S., Jr. and Schairer, J.F., 1967. Melting relations of volcanic rock series. Carnegie Inst.Wash. Yearbook 65, p.260-269.

Tomasson, J., 1967. Mineralogical and petrographical characteristics of Icelandic tephra. The eruption of Hekla 1947-48. I, p.171-183.

Tryggvason, T., 1965. Petrographic studies on the eruption products of Hekla 1947-48. The eruption of Hekla 1947-48, IV, 6, p.1-13.

Turner, F.J. and Verhoogen, J., 1960. Igneous and Metamorphic petrology. New York: McGraw-Hill Inc., 694 pp.

Tuson, J., 1959. A geophysical investigation of the Tertiary volcanic districts of Western Scotland. Unpublished PhD thesis, University of Durham.

Tuttle, O.F. and Bowen, N.L., 1958. Origin of granite in light of experimental studies in the system $NaAlSi_3O_8$-$KAlSi_3O_8$-SiO_2-H_2O. Geol.Soc.Amer.Mem. 74, 153 pp.

Tyler, R.C. and King, B.C., 1967. The pyroxenes of the alkaline igneous complexes of eastern Uganda. Miner. Mag. 36, p.5-21.

Tyrrell, G.W., 1949. Petrography of igneous rocks from the Vatnajokull region, Iceland, collected by Mr. F.W. Anderson. Trans.Roy.Soc.Edinburgh, 61, p.793-801.

—— 1949. The Tertiary igneous geology of Scotland in relation to Iceland and Greenland. Meddel. fra Dansk Geolog.Foren. 11, p.413-40.

Upton, B.G.J. and Wadsworth, W.J., 1966. The basalts of Reunion Island, Indian Ocean. Bull.Volc. 29, p.7-24.

—— and Wright, J.B., 1961. Intrusions of gabbro and granophyre in the Snaefellsnes, western Iceland. Geol.Mag. 98, p.488-92.

Wager, L.R. and Brown, G.M., 1967. Layered igneous rocks. Edinburgh: Oliver & Boyd, 588 pp.

—— and Mitchell, 1951. The distribution of trace elements during strong fractionation of basic magma - a further study of the Skaergaard intrusion, East Greenland. Geochim. et Cosmochim. Acta, 1, p.129-208.

Walker, G.P.L., 1959. Geology of the Reydarfjordur area, eastern Iceland. Quart.J.Geol.Soc.London, 114, p.367-391.

—— 1960. Zeolite zones and dyke distribution in relation to the structure of the basalts of eastern Iceland. J.Geol., 68, p.515-28.

—— 1963. The Breiddalur central volcano, eastern Iceland. Quart.J.Geol.Soc.London, 119, p.23-63.

—— 1964. Geological Investigations in eastern Iceland. Bull.Volc. 27, p.3-15.

—— 1966. Acid volcanic rocks in Iceland. Bull.Volc. 29, p.375-406.

Ward, P.L., Palmason, G. and Drake, C., 1969. Micro-earthquake survey and the Mid-Atlantic Ridge in Iceland. J.Geophys.Res., 74, p.665-684.

Welke, H., Moorbath, S., Cumming, G.L. and Sigurdsson, H., 1968. Lead isotope studies on igneous rocks from Iceland. Earth Planet.Sci. Letters, 4, p.221-231.

Wilkinson, J.F.G., 1956. Clinopyroxenes of alkali olivine-basalt magma. Amer.Min. 41, p.724-743.

—— 1968. The magmatic affinities of some volcanic rocks from the Tweed Shield Volcano, S.E. Queensland, N.E. New South Wales. Geol.Mag. 105, p.275-289.

Wilson, J.T., 1965. Evidence from ocean islands suggesting movement in the earth. Phil.Trans.Roy.Soc.(London), 258, p.145.

Wise, W.S., 1969. Origin of basaltic magmas in the Mojave desert area, California, Contr. Mineral. and Petrol. 23, p.53-64.

Wyllie, P.J., 1963. Effects of the changes in slope occurring on liquidus and solidus paths in the system diopside-anorthite-albite. Min.Soc.Amer. Special Paper 1, p.204-212.

Yoder, H.S., Jr. and Eugster, H.P., 1954. Phlogopite synthesis and stability range. Geochim. et Cosmoch. Acta, 6, p.157-85.

—— and Kushiro, I., 1969. Melting of a hydrous phase: Phlogopite. Carnegie Inst.Wash. Yearbook 67, p.161-167.

—— and Tilley, C.E., 1962. Origin of basalt magmas: an experimental study of natural and synthetic rock systems. J.Petrology, 3, p.342-532.

APPENDIX

Analytical methods

1. Mineral analyses

An electron probe X-ray microanalyser (Cambridge Instruments Mk.II Geoscan), equipped with two spectrometers, was used for quantitative analysis of a number of elements in feldspars, pyroxenes and olivines, as well as some accessory minerals. The electron beam was focussed to about 1 micron diameter, giving a spot, or volume of analysis of 3 microns diameter. For the alkali feldspars and some plagioclases an accelerating voltage of 12 kV was used, but 15 kV for more calcic plagioclases and all mafic minerals. The specimen current was near 0.04 micro-amps in all runs. Analyses for two elements were always done simultaneously, using $K\alpha$ radiation. Operating conditions for the various elements are further specified in Table 1.

Although corrections for background are small in the analysis of major elements, background readings were always carried out on comparable mineral standards and one of the unknown minerals at the beginning and end of each run. Drift corrections were also derived from this data. All data was reduced using computer programmes and correction procedures developed by Dr. J.W. Aucott. Initial corrections for

instrument drift, dead-time (4 microseconds) and background were obtained by use of a computer programme, which provided crude element concentrations by straight ratioing against standards. Further computerized corrections for fluorescence effects, mass absorption, atomic number (electron backscattering and electron retardation), followed by iterations with reference to standards.

Detection limit is better than 0.1% for most of the elements analysed, but 0.2% in the case of Al and Ti. Precision of the method is at least $\pm$2% of the amount present for most elements; higher for Fe, Ca, Mg, and Mn but somewhat poorer for Ti, Na and Al.

2. Method of X-ray spectrographic analysis of rock samples

Rock samples were crushed in a jaw crusher, quartered and ground to less than 300 mesh in a swing-mill (approx. 5 min. per sample). A Mowiol solution was used as a binder during pelleting, four to five drops mixed thoroughly with the rock powder, before pressing under five tons ram pressure. Metal discs with a high polish were used as dies to give pellet a smooth surface, with Borax powder as backing.

In this work a Philips PW 1212 X-ray spectrograph was used and Table 2 gives the operating conditions for the various elements. In the analysis of major elements, three

samples were run simultaneously, along with a monitoring pellet or standard. The instrument was programmed for the accumulation of a fixed number of counts for each element on the monitoring pellet and corresponding elements in the unknown sample allocated equal counting time. The advantage of a standard monitor sample and the ratio method is the exclusion of instrumental errors and drift. Analysis time for the nine major elements in three unknown samples was approximately 35 minutes.

The absolute method was used in the analysis of trace elements and each element measured for a fixed counting period. Background measurements were made on both sides of the spectral peak when a significantly sloping background was present, and a geometric mean derived for the background correction. The interference of Sr $K\beta$ in the analysis of Zr was corrected for by subtracting 10% of Sr peak height from the Zr $K\alpha$ peak. Sensitivity, or the amount which is significant above the background noise for the trace elements is, in ppm: Ba 13, Cu 4, Ni 5, Zr 3, Sr 3, Rb 3, Zn 3. Trace element analyses were carried out on loose rock powders.

The major element analysis was performed following the method of Holland Brindle (1966), using a bank of comparable igneous rock standards. Mass absorption corrections were then made by an iterative process, giving a chemical

composition which subsequently is compared further to a set of standards by regression analysis. Heterogeneity, surface effects and other matrix effects are a possible source of error in non-fusion methods. We feel, however, that the fine grinding may have reduced these effects to a great extent, but the possible gain in accuracy by the fusion method would be at the sacrifice of the much greater speed of analysis of the pressed-pellet method. Rapid fusion methods, such as that recently developed by Norrish and Hutton (1969), combined with a self-consistent mass absorption computing technique, are an obvious advantage in future large-scale igneous geochemical investigations.

3. The determination of FeO by the metavanadate method

The finely ground rock powders were weighed into an 80 ml. polythene beaker, along with 0.05 g ammonium metavanadate (NH_4VO_3). Five ml. of hydrofluoric acid were added, beaker covered with Parafilm and left usually overnight. When rock powder had fully dissolved, the beaker was uncovered, 15 ml. of 10n H_2SO_4 added and gently mixed with contents by swirling. Five drops of 0.2% sodium diphenylamine indicator were added to a 400 ml. glass beaker and the solution of the polythene beaker transferred to the glass beaker, using 125 ml. of saturated boric acid solution to

wash out the polythene beaker. The solution is of a purplish colour at this stage and is titrated with a standardized ferrous ammonium sulphate solution to a clear end-point.

TABLE 1

OPERATING CONDITIONS FOR ELECTRON MICROPROBE

Element	line	2θ peak	2θ backgr.	crystal	counter	KV Felsics	KV Mafics	ΔE gate
Na	Kα	53°12'	+1°30'	KAP	flow	12	15	1.0
Mg	-	43°40'	-2°	-	-		15	1.0
Al	-	36°32'	±2°	-	-	12	15	1.5
Si	-	31°6'	+1°30'	-	-	12	15	2.0
K	-	68°3'	-2°	Qtz.	-	12		2.5
Ca	-	60°18'	-2°	-	-	12	15	1.5
Ti	-	48°33'	+2°	-	scint.		15	2.0
Mn	-	36°39'	+2°	-	-		15	2.0
Fe	-	33°40'	+2°	-	-	12	15	2.5

TABLE 2

OPERATING CONDITIONS FOR PHILIPS PW 1212 AUTOMATIC X-RAY SPECTROMETER IN THE ANALYSIS OF MAJOR AND TRACE ELEMENTS

Element		2θ	line	KV	mA	time (sec.)	counts	counter	radiation	crystal
Si	peak	108.96	Kα1	60	32		10^6	flow	Cr	P.E.
Al	-	144.62	-	50	40		300000	-	-	-
Fe	-	85.68	-	60	16		300000	-	-	LiF(110)
Mg	-	81.06	-	50	40		30000	-	-	ADP
Mg	backgr.	79.000		50	40		30000	-	-	-
Ca	peak	45.01	Kα1	60	8		10^6	-	-	P.E.
Na	-	103.08	-	50	40		10^4	-	-	ADP
Na	backgr.	105.00		50	40		10^4	-	-	-
K	peak	50.52	Kα1	60	16		300000	-	-	P.E.
Ti	-	36.53	-	60	8		300000	-	-	-
P	-	89.32	-	50	40		10^4	-	-	-
P	backgr.	87.00		50	40		10^4	-	-	-
Mn	peak	95.19	Kα1	70	30	20		-	W	LiF(110)
Mn	backgr.	93.50		70	30	20		-	-	-

TABLE 2 (continued)

Element		2θ	line	KV	mA	time (sec.)	counts	counter	radiation	crystal
Ba	peak	15.65	Kα1	80	24	20		scint.	W	LiF(110)
Ba	backgr.	16.80		80	24	20		-	-	-
Cu	-	64.80		60	32	100		scint. + flow	-	-
Cu	peak	65.67	Kα1	60	32	100		-	-	-
Cu	backgr.	66.50		60	32	100		-	-	-
Ni	-	70.00		60	32	100		-	-	-
Ni	peak	71.39	Kα1	60	32	100		-	-	-
Ni	backgr.	73.20		60	32	100		-	-	-
Sr	-	35.00		-	-	40		scint.	-	-
Sr	peak	35.85	Kα1	-	-	-		-	-	-
Sr	backgr.	36.90		-	-	-		-	-	-
Rb	-	36.90		-	-	-		-	-	-
Rb	peak	37.98	Kα1	-	-	-		-	-	-
Zn	backgr.	59.45		-	-	-		scint. + flow	-	-
Zn	peak	60.56	Kα1	-	-	-		-	-	-
Zn	backgr.	61.25		-	-	-		-	-	-
Zr	-	30.95		-	-	-		scint.	-	-
Zr	peak	32.08	Kα1	-	-	-		-	-	-